

LEONARDO DE PAULA CARVALHO

**Fault detection filter and fault accommodation
controller design for uncertain systems**

São Paulo
2022

LEONARDO DE PAULA CARVALHO

**Fault detection filter and fault accommodation
controller design for uncertain systems**

Revised Version

(The original version can be found in the unit that hosts the Graduate Program)

Thesis presented to the Escola Politécnica
da Universidade de São Paulo to obtain the
degree of Doctor of Science.

São Paulo
2022

LEONARDO DE PAULA CARVALHO

**Fault detection filter and fault accommodation
controller design for uncertain systems**

Revised Version

(The original version can be found in the unit that hosts the Graduate Program)

Thesis presented to the Escola Politécnica
da Universidade de São Paulo to obtain the
degree of Doctor of Science.

Concentration area:

3139 - System Engineering

Advisor:

Prof. Dr. Oswaldo Luiz do Valle
Costa

Co-Advisor:

Prof. Dr. Bayu Jayawardhana

São Paulo
2022

Autorizo a reprodução e divulgação total ou parcial deste trabalho, por qualquer meio convencional ou eletrônico, para fins de estudo e pesquisa, desde que citada a fonte.

Este exemplar foi revisado e corrigido em relação à versão original, sob responsabilidade única do autor e com a anuência de seu orientador.

São Paulo, 24 de março de 2022

Assinatura do autor: Leonardo de Paula Carvalho

Assinatura do orientador: Osvaldo Luiz do Valle Costa

Catálogo-na-publicação

Carvalho, Leonardo de Paula

Fault detection filter and fault accommodation controller design for uncertain systems / L. P. Carvalho -- versão corr. -- São Paulo, 2022.

160 p.

Tese (Doutorado) - Escola Politécnica da Universidade de São Paulo. Departamento de Engenharia de Telecomunicações e Controle.

1.TEORIA DE SISTEMAS E CONTROLE 2.SISTEMAS DINÂMICOS
3.MODELOS NÃO LINEARES I.Universidade de São Paulo. Escola Politécnica. Departamento de Engenharia de Telecomunicações e Controle II.t.

Name: CARVALHO, Leonardo de Paula

Title: Fault detection filter and fault accommodation controller design for uncertain systems

Thesis presented to the Escola Politécnica da Universidade de São Paulo to obtain the degree of Doctor of Science.

Aprovado em:

Banca Examinadora

Prof. Dr. Oswaldo Luiz do Valle Costa

Instituição: Escola Politécnica da Universidade de São Paulo (EP/USP)

Julgamento: _____

Prof. Dr. Rodolfo Reyes Báez

Instituição: University of Groningen (RUG)

Julgamento: _____

Prof. Dr. Grace Silva Deaecto

Instituição: Universidade Estadual de Campinas (UNICAMP)

Julgamento: _____

Prof. Caio César Graciani Rodrigues

Instituição: Laboratório Nacional de Computação Científica (LNCC)

Julgamento: _____

Prof. Dr. Fuad Kassab Junior

Instituição: Escola Politécnica da Universidade de São Paulo (EP/USP)

Julgamento: _____

ACKNOWLEDGMENTS

There are so many people that I need to say thank you, I hope that I will not forget anyone. Here we go. First and most important is my family, my mother Janete, my father Jorge, my brother João Gabriel, my sister-in-law Liliane my nephews Lorenzo and Vinicius. I would like to express all my gratitude for all the patience, understanding, and support you guys are my safe haven. I would like to thanks professor Oswaldo and professor Bayu for all the great advice they gave me, the knowledge they shared, and most important the patience and endurance they had to deal with my neurotic being. There are several friends and colleagues that help me on my academic journey, but these four people gave me the most support Matheus Souza, André Marcorin, Jonathan Palma, and Tabitha Rosa. They lent me a hand on key points in my academic life. Matheus helped me with the classes when I still had a full-time job during my masters. André is one of the wisest people that I know, I always go to him to get good advice. Jonathan is my best friend, encouraging me when I was down, making really bad jokes with his particular dark humor. And Tabitha, without her I wouldn't have the opportunity to go RUG and meet Professor Bayu. Always giving me support and listening when I was crying about a mean review that I received. My friend from USP, Gabriel, Guilherme, Matheus, Fabio, Arthur, Jorge, and Professor Bruno. I will always cherish the jokes, the anime and the gaming discussion, and the board game sessions. My friends Bruna, Renata and Karina. Bruna is the kindest, most reliable and hard-working person that I know. Renata is the most chill cat lady that I know, Bulba (the cat) is too scary. I'm glad that I could live with you two. And Karina is the craziest out-of-the-box mind ever, talking with you is always enlightening. My friends Obed, Carmen, Raphael, Hector, Amanda, Gabriel and Chico thank you for being great friends and average UNO players. I hope to play more board games with you all.

To CAPES for the grant number 88882.333365/2019-01 and Finance Code 001.

RESUMO

CARVALHO, L. P. **Fault detection filter and fault accommodation controller design for uncertain systems**. 2021. Tese (Doutorado) – Escola Politécnica. Universidade de São Paulo, São Paulo, 2021.

Nessa tese as abordagens de detecção de falhas baseadas em modelos matemático (FD) e de acomodação de falhas (FA) foram aplicadas em uma variedade de casos. Propomos várias técnicas para levar em conta a presença de incertezas durante a fase de projeto de controle. Primeiro, nos concentramos no projeto do Filtro de Detecção de Falhas (FDF) e do Controlador de Acomodação de Falhas (FAC) para Sistemas Lineares com Salto Markoviano¹ (MJLS). Tratar o problema no contexto MJLS nos permite incluir o comportamento da rede (perda de pacotes) durante o projeto do FDF e do FAC. Em segundo lugar, propomos um projeto FDF e FAC para o MJLS, partindo do pressuposto que o modo da cadeia de Markov não é diretamente acessível. Como estamos usando a estrutura MJLS para modelar o comportamento da rede, a suposição de que o estado da rede não é instantaneamente acessível é útil porque, do ponto de vista prático, essa suposição é verdadeira. Terceiro, a partir dos resultados apresentados para a estrutura MJLS, fornecemos resultados de acompanhamento usando o Sistema com Saltos Markovianos tipo Lur'e². Isso é convincente, pois em algumas ocasiões o comportamento não linear não pode ser ignorado. Portanto, a descrição do problema como Lur'e MJS nos permite considerar as mesmas suposições do MJLS, mas agora adicionando as não linearidades. Quarto, propomos o projeto Ganho-Escalonado³ FDF e FAC para sistemas com parâmetros linearmente variáveis⁴, partindo do pressuposto que o parâmetro de escalonamento não é adquirido diretamente. Assumimos que o parâmetro de escalonamento está sujeito a ruído aditivo. Esta imprecisão é incluída durante o projeto, usando a mudança de variáveis e técnicas multi-simplex. Finalmente, ao longo da tese, fornecemos alguns exemplos numéricos para ilustrar a viabilidade das abordagens propostas.

Palavras-Chave – Detecção de Falha, Controle Tolerante a Falta, Sistemas Sujeitos a Saltos Markovianos, Parâmetro Linearmente Variáveis, Desigualdade Matricial Linear.

¹do inglês: Markovian Jump Linear System

²do inglês: Lur'e Markov Jump System.

³do inglês: Gain-Scheduled

⁴do inglês: Linear Parameter Varying (LPV)

ABSTRACT

CARVALHO, L. P. **Fault detection filter and fault accommodation controller design for uncertain systems**. 2021. Tese (Doutorado) – Escola Politécnica. Universidade de São Paulo, São Paulo, 2021.

Model-based Fault Detection (FD) and Fault Accommodation (FA) approaches have been applied in a variety of cases. We propose several techniques to include uncertainties in the design process. First, we focus on the design of the Fault Detection Filter (FDF) and Fault Accommodation Controller (FAC) for Markovian Jump Linear Systems (MJLS). The MJLS framework allows us to include the network behavior (packet loss) during the design of the FDF and FAC. Second, we propose an FDF and FAC design for the MJLS, under the assumption that the Markov chain mode is not directly accessible. Since we are using the MJLS framework to model the network behavior, the assumption that the network state is not instantly accessible is useful because from a practical standpoint this is a truthful assumption. Third, from the results presented for the MJLS framework, we provided follow-up results using Lur'e Markov Jump System. This is compelling since on some occasions the nonlinear behavior cannot be ignored. Therefore, applying the Lur'e MJS framework allows us to consider the same assumptions from MJLS, but now adds the nonlinearities. Fourth, we propose the design Gain-Scheduled FDF and FAC for Linear Parameter Varying (LPV) systems, under the assumption that the schedule parameter is not directly acquired. We assume that the schedule parameter is subject to additive noise. This imprecision is included during the design, using change of variables and multi-simplex techniques. Finally, throughout the thesis, we provide some numerical examples to illustrate the viability of the proposed approaches.

Keywords – Fault-Detection, Fault-Tolerant Control, Markovian Jump Linear System, Linear Parameter Varying, Linear Matrix Inequality.

LIST OF FIGURES

1	Backlash, a normal behavior, image extracted from (NIIJAAWAN; NIIJ- JAAWAN, 2010).	17
2	Fatigue crack, a gear failure, image extracted from (RICHARD; SANDER, 2016).	17
3	Graphic representation of Supervisory Loop, and all the sub-processes that compose it. The standard controller is embedded in the "Control System" block. The Supervisory Loop is divided into two main processes the monitoring and management. The monitory part is responsible to acquire the information, and the management part deals with the decision- making and actions to keep the system working properly.	18
4	The placement of possible occurrence of fault in a generic system.	19
5	Classification of the FD approaches.	23
6	Classification of the FTC approaches.	25
7	Interaction between chapters.	26
8	Block diagram detailing the Fault Detection scheme, presenting the residue generation and residue evaluation steps.	33
9	Block diagram representing the topology used to design the Fault Detection Filter.	33
10	Mean and standard deviation for the residue signal obtained using FDF designed using the Theorems 1, 2, 3, 5. There are two graphics for each theorem, representing when the system is subjected to a fault and another graphic without fault.	48
11	Mean and standard deviation for the evaluation function obtained using FDF designed using the Theorems 1, 2, 3, 5. There are two graphics for each theorem, representing when the system is subjected to a fault and another graphic without fault.	49

12	Average value of the evaluation function signal for four distinct cases, where the blue curve represent the result using Theorem 1, the red curve represent the result obtained via Theorem 2, the magenta curve represent the results through Theorem 3, the black curve denote the result for Theorem 5, and the cyan line denotes the threshold TH.	50
13	Fault accommodation control scheme diagram used to design the controller.	51
14	Mean and standard deviation for the states and control signal for the FAC designed with Theorem 6 when the system is subjected to the fault. . . .	56
15	Mean and standard deviation for the states and control signal for the FAC designed with Theorem 6 when the system is in its nominal state (faultless).	57
16	Fault detection and isolation scheme diagram assuming that the network mode is not accessible.	62
17	Mean and standard deviation for residue signal obtained using FDF designed via Theorems 7, 8, and 9.	69
18	Mean and standard deviation for evaluation function obtained using FDF designed via Theorems 7, 8, and 9.	70
19	The mean value of the evaluation function signal for three distinct approaches, where the blue curve represents the results using Theorem 7, the red curve represents the results obtained via 8, the magenta curve represents the results through Theorem 9, and the cyan line denotes the threshold TH.	70
20	The Mean of the output signals obtained for SFDC designed via Theorem 10(blue curve), 11(red curve), and 12(magenta curve). All three curves were obtained when there is a fault, except for the green curve which represents the states without fault.	85
21	Mean and standard deviation for all control signals acquired using the SFDC designed via Theorems 10(blue curve), 11(red curve), and 12(magenta curve).	86
22	Mean and standard deviation for all residue signals acquired using the SFDC designed via Theorems 10(blue curve), 11(red curve), and 12(magenta curve).	87

23	The mean value of the evaluation function signal for three distinct cases, where the blue curve represent the results using Theorem 10, the red curve represent the results obtained via 11, the black curve represents the results through Theorem 12, the green curve portrays the evaluation function signal when there is no fault signal, and the indigo line denotes the threshold TH.	87
24	Fault accommodation control scheme diagram under the assumption that the network model is not accessible.	88
25	Mean and standard deviation for the states and control signal obtained using the FAC designed via Theorems 13, 14, 15, and the nominal control. These results were obtained via simulation where the system is subjected to an oscillatory fault.	99
26	Mean and standard deviation for the states and control signal obtained using the FAC designed via Theorems 13, 14, 15, and the nominal control. These results were obtained via simulation where the system is subjected to an abrupt fault.	100
27	Fault Detection Scheme for Lur'e systems.	105
28	The mean and standard deviation of the residue signal obtained using the FDF designed via Theorem 16.	110
29	The mean and standard deviation of the evaluation function obtained using the FDF designed via Theorem 16.	110
30	Feasible region for each pair $(\theta_i(k), \sigma_i(k))$, borrowed from (PALMA; MORAIS; OLIVEIRA, 2018).	115
31	Behavior for the Linear-Parameter variable $\theta(k)$ and $\sigma(k)$.	122
32	Upper bounds γ and λ behavior for Theorem 17 and 18 when scalar ξ varies. Rob denotes the results using the Robust structure, and Aff represents the results using Affine structure.	123
33	Behavior of the upper bound λ for Theorem 19 when ξ varies and $\gamma = 0.01$. Rob denotes the results using the Robust structure, and Af represents the results using Affine structure.	123
34	Mean and standard deviation for the residue signal (with and without fault) obtained using the FDI in the robust form designed via Theorem 17 (blue curve), 18 (red curve), and 19 (magenta curve).	126

35	Mean and standard deviation for the evaluation function (with and without fault) obtained using the FDI in the robust form designed via Theorem 17 (blue curve), 18 (red curve), and 19(magenta curve).	127
36	The mean value of the evaluation function signal for three distinct cases, where the blue curve represent the results using Theorem 17, the red curve represent the results obtained via 18, the magenta curve represents the results through Theorem 19, and the cyan line denotes the threshold TH. .	127
37	Mean and standard deviation for the residue signal (with and without fault) obtained using the FDI in the affine form designed via Theorem 17 (blue curve), 18 (red curve), and 19(magenta curve).	128
38	Mean and standard deviation for the evaluation function (with and without fault) obtained using the FDI in the affine form designed via Theorem 17 (blue curve), 18 (red curve), and 19(magenta curve).	129
39	The mean value of the evaluation function signal for three distinct cases, where the blue curve represent the results using Theorem 17, the red curve represent the results obtained via 18, the magenta curve represents the results through Theorem 19, and the indigo line denotes the threshold TH.	129
40	Upper bound behavior for Theorems 20 (\mathcal{H}_∞ norm) and 21 (\mathcal{H}_2 norm) when scalar ξ vary for the Robust, and Affine form.	136
41	Mean of the states signal obtained using FAC designed in the affine via Theorems 20 (black curve) and 21 (green curve), where the system is subjected to a fault.	138
42	Mean of the control signal obtained using FAC designed in the affine via Theorems 20 (black curve) and 21 (green curve), where the system is subjected to a fault.	138
43	Coupled tank model.	152
44	Mass-Spring model, (KHALIL, 2002).	154
45	Quarter vehicle model.	155
46	Diagram of the Markov chain for the Gilbert-Eliot model, for the Bernoulli model the variables ρ and β are equal.	156
47	Control loop example.	157

LIST OF TABLES

1	Numerical parameter of the coupled tank model.	154
2	Numerical parameter of the Spring-Mass model.	154

LIST OF SYMBOLS

\mathfrak{F}	σ -field.
Prob	Probability measure.
ρ_{ij}	Transition Probability from mode i to j .
Π	Transition probability matrix.
ϕ_{ij}	Conditional probability of obtaining Markov chain mode.
Γ	Conditional probability matrix.
$\mathbb{E}(\cdot)$	Expected value / mean value operator.
$\ w(k)\ $	Euclidean norm of the vector $w(k)$ at time k .
$\ \cdot\ _2$	l_2 -norm of the sequence w .
I	Identity matrix.
0	Null operator.
\bullet	Symmetric term in a symmetric matrix.
$Tr(\cdot)$	Trace operator.
$'$	Transpose of a matrix.
$\text{diag}(\cdot)$	Block diagonal matrix.
$x, x(k)$	State.
$w, w(k)$	Exogenous input
$u, u(k)$	Controller input.
$y, y(k)$	Measured output.

CONTENTS

1	Introduction	16
1.1	Fault Detection and Fault Tolerant state-of-the-art	19
1.1.0.1	Fault Detection	19
1.1.0.2	Fault Tolerant Control	23
1.2	Outline and Main contributions	25
2	FDF and FAC for Markov Jump Linear Systems	27
2.1	Notation	28
2.2	Preliminary for the Markovian Jump Linear System	28
2.2.1	Stability for Markovian Jump Linear Systems	28
2.2.2	\mathcal{H}_∞ norm for MJLS	29
2.2.3	\mathcal{H}_2 norm for MJLS	30
2.2.4	\mathcal{H}_- index for MJLS	31
2.3	Fault Detection Filter Formulation	32
2.3.1	Residue Generator using Fault Detection Filter	34
2.3.2	Evaluation Function	35
2.3.3	Theoretical Results	37
2.3.3.1	\mathcal{H}_∞ Fault Detection Filter Design for MJLS	37
2.3.3.2	\mathcal{H}_2 Fault Detection Filter Design for MJLS	39
2.3.3.3	Mixed $\mathcal{H}_2/\mathcal{H}_\infty$ Fault Detection Filter Design for MJLS	40
2.3.3.4	Mixed $\mathcal{H}_-/\mathcal{H}_\infty$ Fault Detection Filter Design for MJLS	41
2.3.4	Simulations Results	46
2.3.4.1	Monte Carlo Simulation	48
2.4	Fault Accommodation Formulation	49

2.4.1	Fault Accommodation Controller	50
2.4.2	Theoretical Results	52
2.4.2.1	\mathcal{H}_∞ Fault Accomodation Control Design for MJLS	52
2.4.3	Simulations Results	54
2.4.3.1	Monte Carlo Simulation	54
2.5	Concluding remarks	55
3	FDF and FAC for Markovian Jump Linear Systems with Parameter Estimation	58
3.1	Preliminary for Markovian Jump Linear Systems with Parameter Estimation	59
3.1.1	Stability for Hidden Markovian Jump Linear Systems	60
3.1.2	\mathcal{H}_∞ norm for Hidden MJLS	60
3.1.3	\mathcal{H}_2 norm for MJLS for Parameter Estimation	61
3.2	Fault Detection Filter Formulation for MJLS with Parameter Estimation .	62
3.2.1	\mathcal{H}_∞ Fault Detection Filter Design for MJLS with Parameter Estimation	63
3.2.2	\mathcal{H}_2 Fault Detection Filter Design for MJLS with Parameter Estimation	65
3.2.3	Mixed $\mathcal{H}_2/\mathcal{H}_\infty$ Fault Detection Filter Design for MJLS with Parameter Estimation	67
3.2.4	Simulations Results	68
3.2.4.1	Monte Carlo Simulation	69
3.3	Simultaneous Fault Detection and Control formulation for MJLS with Parameter Estimation	71
3.3.1	\mathcal{H}_∞ Simultaneous Fault Detection and Control Design for MJLS with parameter estimation	75
3.3.2	\mathcal{H}_2 Simultaneous Fault Detection and Control Design for MJLS with parameter estimation	78
3.3.3	Mixed $\mathcal{H}_2/\mathcal{H}_\infty$ Simultaneous Fault Detection and Control Design for MJLS with parameter estimation	82
3.3.4	Simulations Results	84

3.3.4.1	Monte Carlo Simulation	85
3.4	Fault Accommodation Formulation for MJLS with Parameter Estimation	88
3.4.1	\mathcal{H}_∞ Fault Accommodation Control Design for MJLS with Parameter Estimation	90
3.4.2	\mathcal{H}_2 Fault Accommodation Control Design for MJLS with Parameter Estimation	92
3.4.3	Mixed $\mathcal{H}_2/\mathcal{H}_\infty$ Fault Accommodation Control Design for MJLS with Parameter Estimation	95
3.4.4	Simulations Results	97
3.4.4.1	Monte Carlo Simulation	97
3.5	Concluding remarks	98
4	FDF for Markovian Jump Lur'e Systems	101
4.1	Preliminary for Markovian Jump Lur'e Systems	101
4.1.1	Candidate Lyapunov function	102
4.1.2	\mathcal{H}_∞ norm for Markovian Jump Lur'e Systems	103
4.2	Fault Detection Filter for Markov Jump Lur'e Systems	105
4.2.1	\mathcal{H}_∞ Fault Detection Design for MJS Lur'e Systems	107
4.2.2	Simulations Results	108
4.2.2.1	Monte Carlo Simulation	109
4.3	Concluding remarks	110
5	FDF and FAC for LPV Systems with Uncertain Parameters	111
5.1	Preliminary for LPV Systems	112
5.1.1	\mathcal{H}_∞ Guaranteed Cost Analysis	112
5.1.2	\mathcal{H}_2 Guaranteed Cost Analysis	113
5.2	Gain Scheduled Fault Detection Formulation	114
5.2.0.1	Parameter under additive uncertainty	114

5.2.0.2	Change of variables	116
5.2.1	Theoretical Results	117
5.2.1.1	\mathcal{H}_∞ Fault Detection Filter Design for LPV with uncertain parameter	117
5.2.1.2	\mathcal{H}_2 Fault Detection Filter Design for LPV with uncertain parameter	118
5.2.1.3	Mixed $\mathcal{H}_2 / \mathcal{H}_\infty$ Fault Detection Filter Design for LPV with uncertain parameter	120
5.2.2	Simulations Results	121
5.2.2.1	Monte Carlo Simulation	125
5.3	Gain Scheduled Fault Accommodation Formulation	128
5.3.1	Theoretical Results	131
5.3.1.1	\mathcal{H}_∞ Fault Accommodation Control Design	132
5.3.1.2	\mathcal{H}_2 Fault Accommodation Control Design	133
5.3.2	Simulations Results	135
5.3.2.1	Monte Carlo Simulation	137
5.4	Concluding remarks	138
6	Conclusions	139
6.1	Contribution	139
6.2	Further Research	140
	References	142
	Appendix A – Numerical Examples Modeling and Basic Results	152
A.1	Coupled tank model	152
A.2	Mass-Spring System	154
A.3	Quarter vehicle	155
A.4	Network Packet Loss Modeling	156

A.5 Schur Complement	157
A.6 Bounded Real Lemma	158
A.7 Finsler Lemma	158

1 INTRODUCTION

The presence of undesired behaviors is inherent in a multitude of systems in engineering (PATTON; CHEN, 1994). The source of these unwanted behaviors can vary for a plethora of reasons. Among these reasons are, for example, physical issues in the plant (PATTON; CHEN, 1997), communication problems (SRINIVASAN et al., 2006), imprecision on the identification procedure (JR; ADELI, 2012), missing dynamical behavior in the model, etc. All the listed reasons are aggravated as systems become more complex as technology advances. Since the occurrence of these undesired behaviors is innate to all types of systems, it is of utmost interest that a procedure to detect, isolate, or mitigate these behaviors be developed.

Before any remedial actions can be planned to deal with those behaviors, it is crucial to understand and classify them. As in the reference (ISERMANN; SCHWARZ; STOLZL, 2002), we use the following definitions of unwanted behaviors:

- **Fault.** A fault is an unwanted abnormal behavior of at least one characteristic of the nominal system. A fault can be characterized as follows *i*) a fault may cause a reduction of the nominal performance; *ii*) some sources of the fault are design fault; manufacturing fault, assembling fault, fault caused by wear, wrong operation (human error), hardware fault, software fault, and communication fault; *iii*) a fault may occur and the system may remain functional; *iv*) a fault is the first step to greater problems (malfunctions and failures); *v*) a fault can be abrupt, intermittent, oscillatory, or gradual.
- **Malfunction** A malfunction is a temporary interruption of the system capability to fulfill its nominal functions. A malfunction can be characterized as follows *i*) a malfunction is a temporary interruption that may or may not be intermittent; *ii*) a malfunction is commonly a result of wear or lack of maintenance; *iii*) a malfunction is the result of one or multiple faults; *iv*) a malfunction is an event;
- **Failure** A failure is the permanent interruption of the capability to fulfill its nominal

tasks. A failure can be characterized as follows *i)* a failure is the permanent loss of the system's ability to perform its functions; *ii)* a failure is a result of one or multiples faults; *iii)* a failure is classified by the number of failures, or predictability (random, deterministic, systematic); *iv)* a failure is an event;

In order to illustrate the above notions we provide the following example. Let us say the reader is driving a manual car with a regular clutch. Assuming the driver knows how to change gear, the clutch system will perform a smooth change of gears without any noise, which is the nominal behavior. A fault in this scenario would be the change in the clutch pedal "sensation", where the driver would need to change the force applied to the pedal to change gear, but the change of gear would still be smooth without any noise. A malfunction in this scenario would be the next step where sometimes the driver will not be able to change gears, the clutch would "slip", but after a few attempts, the driver would be able to change gear. Finally, a failure happens when the clutch system would stop working permanently.

To provide a visual representation, the following image in Fig.1 is a representation

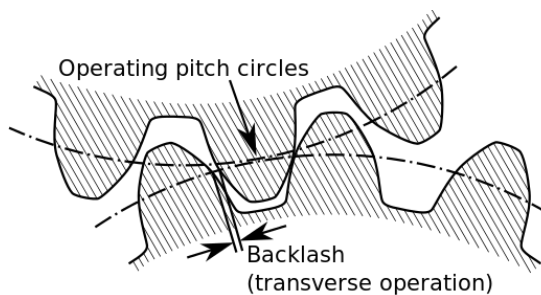


Figure 1: Backlash, a normal behavior, image extracted from (NIIJAAWAN; NIIJAAWAN, 2010).

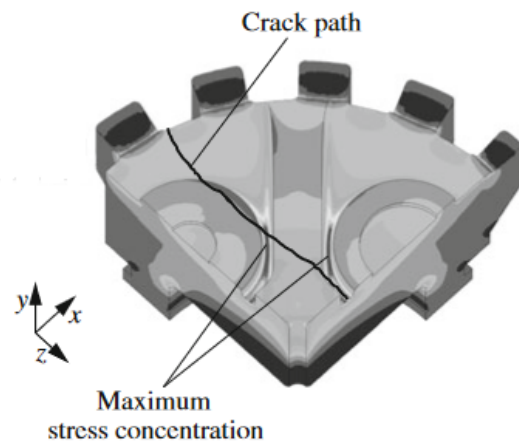


Figure 2: Fatigue crack, a gear failure, image extracted from (RICHARD; SANDER, 2016).

of the backlash, which is a typical physical phenomenon but can be gradually increased due to wear. Fig.2 exemplifies a failure caused by overload or other improper use of the equipment or caused by wear associated with the lack of maintenance.

Now that we understand the problem it is necessary to define what are the goals for a procedure that is responsible to detect, isolate, or mitigate a fault. The purpose of this procedure is to maintain three characteristics: reliability, availability, and safety.

Reliability can be defined as the ability to fulfill a task in a given time. Availability is the amount of time a system is able to fulfill its task properly. Safety is the ability to keep the people involved in the system's operation safe.

In industrial process control systems, fault detection and fault mitigation solutions are used simultaneously. This issue is dealt with using a supervisory loop. A supervisory loop is defined as a technical process that provides all the information regarding the system, to point out any unwanted behavior, and also helps with the decision-making process to solve these problems. The placement of each procedure in a supervisory loop is represented in Fig.3. As can be seen in Fig.3, Fault Detection (FD), Fault Isolation (FI), and Fault

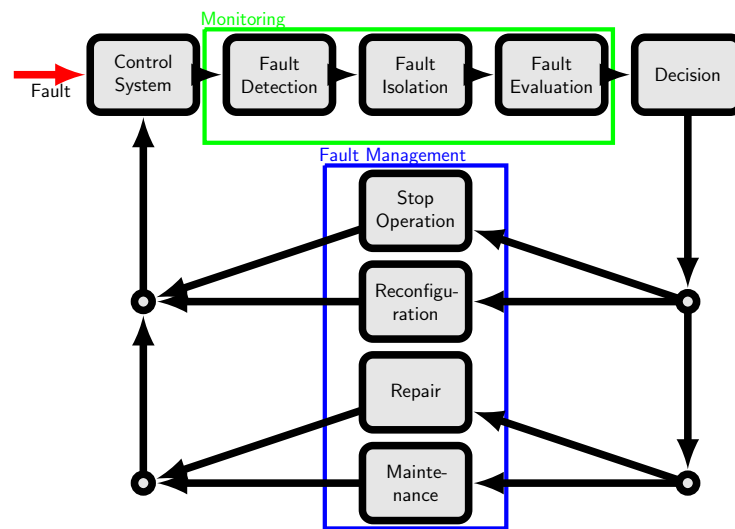


Figure 3: Graphic representation of Supervisory Loop, and all the sub-processes that compose it. The standard controller is embedded in the "Control System" block. The Supervisory Loop is divided into two main processes the monitoring and management. The monitoring part is responsible to acquire the information, and the management part deals with the decision-making and actions to keep the system working properly.

Evaluation (FE) are classified as monitoring procedures. The processes of reconfiguration, operational change, maintenance, and repairs are considered to be fault management procedures. The procedures of reconfiguration and change operation can be automated.

As seen in Fig.3 the monitoring process is divided into three main parts, the FD is the process that signals the presence of a fault, the FI points out where the fault is occurring, and the FE estimates the magnitude of the fault. Concerning the fault management procedures, the reconfiguration process refers to all procedures that keep the system working and manage to change some characteristics to mitigate the fault and the change in the operation block represents the action altering the entire process to keep the plant working (this is a more severe action compared to the reconfiguration). Repair is the action to send a team of workers to fix a piece of equipment that already failed and

maintenance is scheduled to send a team of workers to do preventive fixes in an equipment to prevent a failure caused by wear.

From the standpoint of the system itself, the faults can occur in every part of the process. From the diagram in Fig.4 we can observe that the faults can occur on an actuator,

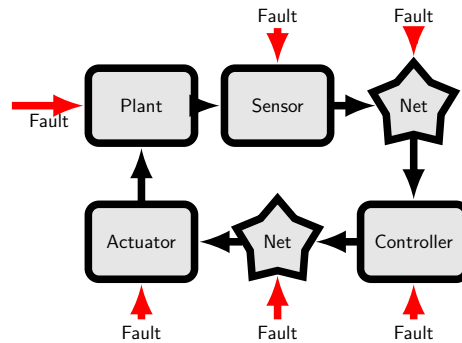


Figure 4: The placement of possible occurrence of fault in a generic system.

sensors, a structural problem, and/or during the signals transmissions. Therefore, to deal with the maximum amount of faults simultaneously, it is necessary to consider the different sources of the faults during the design procedure of fault detection systems.

1.1 Fault Detection and Fault Tolerant state-of-the-art

1.1.0.1 Fault Detection

The literature on the fault detection problem is extensive. Among all the literature, it is possible to classify the solutions related to the fault occurrence with two main branches, namely, the model-based solutions (ISERMANN; SCHWARZ; STOLZL, 2002; PATTON; FRANK; CLARK, 2013; ZHONG; XUE; DING, 2018; MARZAT et al., 2012) and the data-driven solutions (DING, 2014; SCHWABACHER, 2005; ALAUDDIN et al., 2018). Both classes have their pros and cons, as described in (ZHANG, March, 2014; DING et al., 2011; TIDRIRI et al., 2016; VENKATASUBRAMANIAN; RENGASWAMY; KAVURI, 2003). The main advantages of model-based approaches are:

- Guarantee on the performance when the model is precise and reliable,(ISERMANN; SCHWARZ; STOLZL, 2002; VENKATASUBRAMANIAN et al., 2003b).
- Easy to implement, and design. Since it is a well-established branch of research in control engineering, there are plenty of suitable results for many situations (ZHONG; XUE; DING, 2018).

One major disadvantage of this approach is its reliance on the veracity of the model being used. Thus the mathematical description or the identification process must be precise.

On the other hand, the main advantages of data-driven approaches are:

- They can directly be implemented using previously available data without needing an analytical model (DING et al., 2011).
- They do not demand a high level of computational effort, which enables their implementation in real time (TIDRIRI et al., 2016).

The main difficulty of the data-driven are the data preprocessing, and the dependency on data reliability, quality, and quantity (CHIANG; RUSSELL; BRAATZ, 2000).

Among the model-based branch of solutions, it is possible to categorize them into four main approaches: Observer-based, Parity space, Parameter estimation, and Bond Graph. All these approaches make some sort of comparison between the expected/predicted behavior and the real behavior, the discrepancy between behaviors indicates the occurrence of a fault. This comparison is made in two steps. The first one is the residue signal generation, which is generated using the aforementioned approaches. The second step is the evaluation process which uses the residue signal to distinguish if a fault occurred or not in the monitored processes.

Observer-based: This approach relies on the observability assumption where systems behavior can be obtained from the output. As it is true for all model-based approaches, the observer approach depends on a precise and reliable mathematical model of the system. Yet, a perfect mathematical model is not achievable in practice (PATTON; FRANK; CLARK, 2013). This inherent imprecision in the mathematical model is caused by simplifications (i.e. linearization process), or overlooking a particular behavior that at first glance seems irrelevant to the overall behavior. Bypassing those behaviors may ease the task describing the system mathematically. But for an FD procedure, this may cause bias or imprecision that leads to false alarms. Besides the model imprecision, another important aspect is that all systems are subjected to disturbances or noises, which can be interpreted as an unknown and uncontrollable input. A possible way to deal with this is proposed in (PATTON; CHEN, 1997), where an approach to decouple the control input from the fault signal is presented. Other approaches propose the decoupling of the unknown input (noise/disturbance) from the fault signal using the for example the Unknown Input Observer (UIO), as in (CHEN; SAIF, 2006; ALHELOU; GOLSHAN; ASKARI-MARNANI, 2018) or the Unknown Input

Filter (UIF) (PATTON; CHEN, 1997). Besides the aforementioned approaches, we can also point out the results based on observers that are derived in the following frameworks as the Markov Jump Linear Systems (ZHONG et al., 2005), Fuzzy logic (HAN et al., 2017; CHIBANI et al., 2016), \mathcal{H}_- index and \mathcal{H}_∞ norm (CHADLI; ABDO; DING, 2013; AOUAOUDA et al., 2015; RAMBEAUX; HAMELIN; SAUTER, 1999), and Kalman filter in (LUO; FANG, 2013; ZAREI; SHOKRI, 2014).

Parity space: The Parity space approach was first presented in (POTTER; SUMAN, 1977). Roughly, speaking a Parity space FD uses the transformation of the state-space model of the system to gather the parity relations by observing the system on a finite horizon, (GERTLER, 1991). The idea behind this approach is to generate the parity relation to acquire equations that only depends on known or measured parameters (inputs and outputs). The major main disadvantage of parity space based approaches is that they do not consider the uncertainties on the system. Consequently, they are mostly applied only on Linear Time-Invariant Systems. A few examples of FD approaches based on parity space are (DING; GUO; JEINSCH, 1999; GERTLER, 1997; ODENDAAL; JONES, 2014; PATTON; CHEN, 1994).

Parameter Estimation: The procedures based on parameter estimation are based on the premise that the state variables can be estimated given the access to the inputs and outputs of the system. A way to describe the FD based on the parameter estimation is that the fault is detected via a comparison between the estimated parameters of the nominal process and the online parameter estimation over a pre-set time horizon. In this procedure, we consider that a fault occurred when a discrepancy between these estimations appears (ISERMANN; SCHWARZ; STOLZL, 2002; VENKATASUBRAMANIAN et al., 2003a).

Bond Graph: A bond graph is another way to represent a system dynamic, its main advantage is the direct representation of the bidirectional energy exchange in the system. This characteristic allows to generate a residual signal based on the energy exchange. Some examples of the bond graph being applied to the FD problem are (SAMANTARAY et al., 2006; DJEZIRI et al., 2007; BENMOUSSA; BOUAMAMA; MERZOUKI, 2013; CAUFFRIEZ et al., 2016). An extension of the FD approach based in bond graphs is the signed bond graph, which uses the bond graph qualitative and quantitative structural properties to generate multiples behavior predictions, as cited in (TIDRIRI et al., 2016), and presented in (CHATTI et al., 2014).

We can classify the FD approaches based on data-driven with two main classes, namely,

the supervised and unsupervised approaches. A supervised approach can be sub-classified as Bayesian Networks, or Artificial Neural Networks. For the unsupervised ones, we can classify them as Control Charts, Principal Component Analysis or Partial Least Squares.

The supervised approach bases its function on the historical data to design a learning model that will be used as an FD to evaluate the new data.

Bayesian Networks: Bayesian networks are a type of acyclic graphs where a node represents a variable, which can be a discrete or a continuous variable (VERRON; LI; TIPLICA, 2010). Another similar approach is the Dynamic Bayesian Network, which besides the stochastic modeling also includes temporal information (YU; RASHID, 2013).

Artificial Neural Networks: An Artificial Neural Networks are models that imitate the learning process of a biological system. An artificial Neural Network is composed of a series of interconnected processes called nodes, those nodes are organized in layers, which form a complex network (PAYA; ESAT; BADI, 1997; SAMANTA; AL-BALUSHI; AL-ARAIMI, 2003).

The unsupervised approaches as opposed to the supervised approaches do not use any previously acquired knowledge of the system. Some examples of methods that can be classified as unsupervised are control charts, principal component analysis or partial least squares.

Control Charts: Among all the data-driven approach presented here, the Control Charts is the oldest, and is firstly presented in (SHEWHART, 1931). As described in (MONTGOMERY, 2007), the Control Chart approach is a statistical hypothesis testing, the design of a Control Chart is separated into two parts. The first one is the retrospective analysis, and the second one is the monitoring process.

Principal Component Analysis: The authors in (WOLD; ESBENSEN; GELADI, 1987) state, that a Principal Component Analysis is a multivariate data analysis method that is capable of simplifying the data to keep the important information and reduce the data set size.

Partial Least Squares: The Partial Least Squares method can be described as a projection of a data set with a high number of dimensions in a data set with lower dimension, this new data set is defined using latent variables. The purpose of those latent variables is to define the most important information on the original data set that should be retained (KOURTI; NOMIKOS; MACGREGOR, 1995).

It is important to mention that there are more types of FD approaches. The above

mentioned examples and classification are just a glimpse of how rich the FD literature is. Another critical piece of information that worth mentioning is that there are approaches that are based on both main branches of FD approaches, the model-based and the data-driven approaches, these types of approaches are called hybrid. The authors can refer to these works (FRANK et al., ; TIDRIRI et al., 2016) that are based on this premise.

A graphical representation of the aforementioned classification of the FD problem is given by Fig.5.

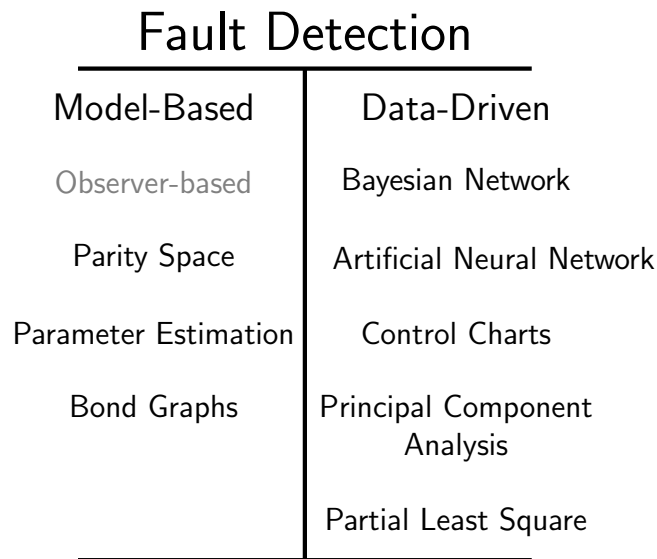


Figure 5: Classification of the FD approaches.

1.1.0.2 Fault Tolerant Control

For the Fault Tolerant Control (FTC) problem we may classify it into two distinct manners. The first one, similarly to the FD problem, the model-based (PATTON, 1997) and data-driven approaches (DING, 2014). The latter one is the classification based on whether the approach is active or passive. A Reconfigurable Control approach correspond to the solutions where the controller only acts (reconfigure) in the presence of a fault (ZHANG; PARISINI; POLYCARPOU, 2004). For the passive approach, the potential fault is taken into account during the controller design, which provides a Robust Control solution (LI et al., 2018).

Referring to the FTC problem based on the data-driven we may cite some procedures for the robust and reconfigurable approaches.

Markov parameter sequence: The Markov parameter sequence is a stochastic tool utilized to identify a system from its input and output as presented in (KIM, 2016; HAN;

FENG, 2019).

Subspace Predictive Control (SPC): the SPC uses subspace identification predictors associated with predictive control applied to an affine LPV system (KULCSÁR; DONG; VERHAEGEN, 2009).

Fault Tolerant Architecture: The FTA is an online fault tolerant control based on residue generation designed using Youla parametrization, (WANG; YANG, 2016).

Regarding the model-based FTC problem, we can point out a few approaches for the robust or reconfigurable approaches.

Gain Scheduled Control: A gain scheduled control is the type of control that depends on a parameter. This parameter vary in time, and the variation is dictated by the system (ROTONDO, 2017).

Adaptive Control: The basic idea of adaptive control is similar to the one presented for the gain scheduled control. There are plenty of approaches that fall into this category, as for example, Model Reference Adaptive Controller (MRAC) (CHAMSEDDINE et al., 2011), Model Identification Adaptive controller (MIAC) (ÖREG; SHIN; TSOURDOS, 2019). Some other examples can be seen in (ZHANG; PARISINI; POLYCARPOU, 2004; TOHIDI; SEDIGH; BUZORGNIA, 2016).

Fault Accommodation: The fault accommodation procedure is a method that changes the controller parameters or structure to mitigate the consequences of a fault. The input and output between plant and controller remain unchanged but the performance may decrease (BLANKE; STAROSWIECKI; WU, 2001).

Robust Fault tolerant Control: The robust approach can be implemented using any appropriate framework, such as, the Linear Parameter Varying (LPV), Markov Jump Linear System (MJLS), or any other framework. We consider that a controller is robust when during the design process the presence of a fault is considered, but the controller acquired is static (meaning that the controller is not gain-scheduled or mode-dependent) (CHADLI; ABDO; DING, 2013). Usually, these controllers are suboptimal since they are designed to work in multiple operational points.

As was mentioned for the FD, the same statement can be made here, where all the classes and parameters presented above are just an example of the rich literature of the Fault tolerant control.

Fault Tolerant Control	
Reconfigurable	Model-Based
	Gain Scheduled Control
	Adaptive Control
Robust	Fault Accommodation
	Robust Fault tolerant Control
	Markov parameter Sequence

Figure 6: Classification of the FTC approaches.

1.2 Outline and Main contributions

From the discussion and explanation presented in the previous section now we are prepared to describe the main contributions presented in this thesis, and also positioning of the results in the literature. As the title of the thesis says, we deal with the fault detection and fault accommodation problem.

From the classifications discussed in the first part of the introduction, all the results presented herein are model-based. Regarding the Fault Detection results, classifying them as shown in Fig.5, they are all based on residue generated using observers. For the FAC problems, we proposed a FAC under some frameworks and also a Gain-Scheduled FAC, as classified in Fig. 6.

Each chapter in this thesis is organized as follows. In the first two sections a preliminary discussion is introduced, presenting the theoretical background necessary to understand and implement the results in the respective chapter. They are followed by the proposed design, theoretical works, and illustrative examples for the respective frameworks. The chapter is concluded with simulations to exemplify the usability of the approaches.

The content for every chapter is as follows.

- **Chapter 2:** In Chapter 2 we propose the Fault Detection Filter (FDF) and FAC design under the Markov Jump Linear Systems framework. We derive the results under this framework intending to model the network communication loss. The results presented in Chapter 2 have been published in (CARVALHO; OLIVEIRA; COSTA,

2018b; CARVALHO; OLIVEIRA; COSTA, 2018a; CARVALHO; OLIVEIRA; COSTA, 2018; CARVALHO et al., May 2021; CARVALHO et al., 2020b).

- **Chapter 3:** In Chapter 3 we follow the same idea of the previous chapter, but including the assumption that the Markov chain is not directly accessible, instead, the FDF and FAC depends on an estimation of the Markov chain parameter. Chapter 3 contains the results from the following publications (CARVALHO; OLIVEIRA; COSTA, 2018c; CARVALHO; OLIVEIRA; COSTA, 2020; CARVALHO; OLIVEIRA; COSTA, 2020; CARVALHO et al., 2020a).
- **Chapter 4:** For Chapter 4, we follow the idea from Chapter 2, but instead of the MJLS framework, we implement the Markov Jump Lur'e Systems, in order to add the non-linear behavior during the FDF or FAC design. The results in Chapter 4 are presented in (CARVALHO; JAYAWARDHANA; COSTA, 2021).
- **Chapter 5:** In Chapter 5 we introduce the Gain-Scheduled FDF and FAC design for Linear Parameter Varying systems. Besides, we also use some techniques to include during the design process, the assumption that the schedule parameter is imprecise. The results in Chapter 5 are published in (CARVALHO et al., 2021a).

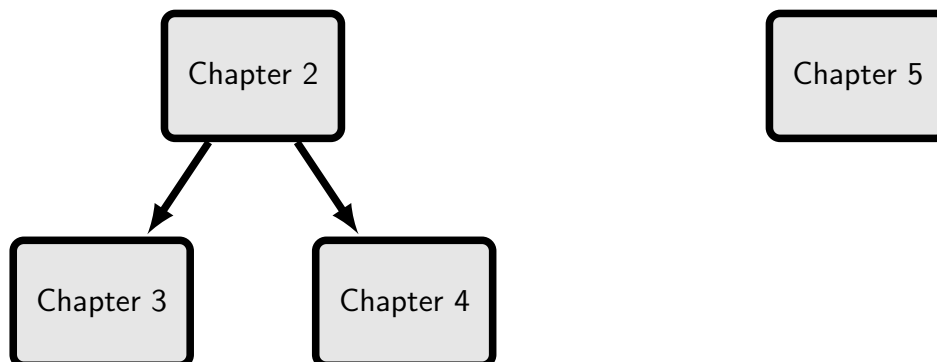


Figure 7: Interaction between chapters.

Finally, we wrap up the thesis with a conclusion chapter. For the sake of helping the reader, we present Appendix A. Appendix A, provides the modeling of the network using Markov chains, the modeling procedure of the illustrative models used throughout the thesis, and some useful lemmas.

2 FDF AND FAC FOR MARKOV JUMP LINEAR SYSTEMS

In this chapter we present the results for the Fault Detection Filter (FDF) and Fault Accommodation Controllers (FAC) under the Markov Jump Linear System (MJLS) framework. Herein, the MJLS is implemented as a tool to model the communication loss among system components, which allows us to draw results for the design of the FDF and FAC assuming that the communication is subjected to packet loss. This assumption is important since packet loss is inherent to any communication channel. The usual workaround to the communication loss is the retransmission of the information, however, this type of method burdens the network infrastructure. Hence, design an FDF or an FAC under the communication loss provides robust solutions against this type of problem and at the same time does not increase the load imposed on the network infrastructure.

The results presented in this chapter were published in the following conferences and journals

- Subsection 2.3.3.1 presented the \mathcal{H}_∞ Fault Detection Filter for Markovian Jump Linear Systems, which was presented in the European Control Conference 2018 (CARVALHO; OLIVEIRA; COSTA, 2018b).
- Subsection 2.3.3.2 presented the \mathcal{H}_2 Fault Detection Filter for Markovian Jump Linear Systems, which was presented in the Congresso Brasileiro de Automática 2018 (CARVALHO; OLIVEIRA; COSTA, 2018a).
- Subsection 2.3.3.3 presented the Mixed $\mathcal{H}_2/\mathcal{H}_\infty$ Fault Detection Filter for Markovian Jump Linear Systems, which was published in Mathematical Problems in Engineering (CARVALHO; OLIVEIRA; COSTA, 2018).
- Subsection 2.3.3.4 presented the Mixed $\mathcal{H}_-/\mathcal{H}_\infty$ Fault Detection Filter for Markovian Jump Linear Systems, which was published in European Journal of Control (CARVALHO et al., May 2021).

- Subsection 2.4.2.1 presented the \mathcal{H}_∞ Fault Accommodation Control for Markovian Jump Linear Systems, which was presented in the IFAC 2020, Berlin (CARVALHO et al., 2020b).

2.1 Notation

The real Euclidian space is presented by \mathbb{R}^n where n denotes its dimension, and $n \times m$ represents the real matrices dimension, for example $A(\mathbb{R}^n, \mathbb{R}^m)$. The symbol $(\cdot)'$ denotes the transpose of a matrix, I indicate the identity matrix. The operator $\text{Her}(\cdot)$ represents the symmetric sum $(X) = X + X'$. A diagonal matrix is represented by the operator $\text{diag}(\cdot)$. The symbol \bullet represents a symmetric block in a partitioned symmetric matrix. On a probability space $(\Omega, \mathcal{F}, \mathcal{P})$ with filtration $\{\mathcal{F}_k\}$, the expected value operator is represented by $\mathbb{E}(\cdot)$, the conditional expected operator, by $\mathbb{E}(\cdot | \cdot)$, and the space of all discrete-time sequences of dimension r , \mathcal{F}_k -adapted processes, such that $\|z\|_2^2 \triangleq \sum_{k=0}^{\infty} \mathbb{E}(\|z(k)\|^2) < \infty$, by \mathcal{L}_2^{r2} . We set $\mathfrak{W}_i \triangleq \{w \in \mathcal{L}_2^r : \|\tilde{w}\|_{2i} > 0\}$, and the operator $\mathbb{E}_i(X) = \sum_{j=1}^N \rho_{ij} X_j$.

2.2 Preliminary for the Markovian Jump Linear System

We consider the following general discrete-time Markovian Jump Linear System (MJLS)

$$\mathcal{G} : \begin{cases} x(k+1) = A_{\theta(k)}x(k) + J_{\theta(k)}w(k), \\ z(k) = C_{\theta(k)}x(k) + D_{\theta(k)}w(k), \end{cases} \quad (2.1)$$

where $x(k) \in \mathbb{R}^{n_x}$ is the state, $y(k) \in \mathbb{R}^{n_y}$ is the measured output, $z(k) \in \mathbb{R}^{n_z}$ is the estimated output, $w(k) \in \mathbb{R}^{n_w}$ is the exogenous input. We also consider that $w(k) \in \mathcal{L}_2^{r2}$. The index $\theta(k)$ is a random variable such that $\{\theta(k) : k \in \mathbb{N}\}$, denotes a Markov chain.

With $\theta_k \in \mathbb{K} = \{1, \dots, N\}$, where N represents the number of modes in which (2.1) may operate. The transition matrix is represented by $\mathbb{P} = [\rho_{ij}]$ where $\rho_{ij} = \text{Prob}[\theta_{k+1} = j | \theta_k = i]$ and $\sum_{j=1}^N \rho_{ij} = 1$ for all $i \in \mathbb{K}$.

2.2.1 Stability for Markovian Jump Linear Systems

Definition 1. Consider system (2.1), with null exogenous input $w(k) = 0 \forall k \in \mathbb{N}$, and initial conditions $x(0) = x_0 \in \mathbb{R}^n$, $\theta_0 \in \mathbb{K}$. The system is

- *Mean Square Stable (MSS)* $\forall (x_0, \theta_0)$ if

$$\lim_{k \rightarrow \infty} \mathbb{E}\{x(k)'x(k)|x_0, \theta_0\} = 0. \quad (2.2)$$

- *Stochastically stable (SS)* $\forall (x_0, \theta_0)$ if

$$\mathbb{E}\left\{\sum_{k=0}^{\infty} x(k)'x(k)|x_0, \theta_0\right\} < \infty. \quad (2.3)$$

As in (COSTA; FRAGOSO, 1993), the definition (2.2) and definition (2.3) are equivalent, and are known as Second Moment Stability (SMS).

2.2.2 \mathcal{H}_∞ norm for MJLS

Assuming that (2.1) is MSS with $x_0 = 0$, the \mathcal{H}_∞ norm of \mathcal{G} is given by (see (FRAGOSO; COSTA, 2005; SEILER; SENGUPTA, 2003))

$$\|\mathcal{G}\|_\infty = \sup_{0 \neq w \in \mathcal{L}_2, \theta_0 \in \mathbb{K}} \frac{\|z\|_2}{\|w\|_2}. \quad (2.4)$$

Notice that the case $\mathbb{K} = \{1\}$ corresponds to the deterministic case, that is, the case without jumps.

It is possible to calculate the H_∞ norm using the so-called Bounded Real Lemma for Markovian Jump Linear Systems, first presented in (SEILER; SENGUPTA, 2003), and stated below.

Lemma 1. *System (2.1) is MSS and satisfies the norm constraint $\|\mathcal{G}\|_\infty^2 < \gamma$ if and only if there exist matrices $P_i = P_i' > 0$ such that*

$$\begin{bmatrix} A_i & J_i \\ C_i & D_i \end{bmatrix}' \begin{bmatrix} \mathbb{E}_i(P) & 0 \\ 0 & I \end{bmatrix} \begin{bmatrix} A_i & J_i \\ C_i & D_i \end{bmatrix} - \begin{bmatrix} P_i & 0 \\ 0 & \gamma I \end{bmatrix} < 0, \forall i \in \mathbb{K}. \quad (2.5)$$

Proof: See (SEILER; SENGUPTA, 2003).

Applying the Schur complement to (2.5) we get that

$$\begin{bmatrix} P_i & \bullet & \bullet & \bullet \\ 0 & \gamma I & \bullet & \bullet \\ \mathbb{E}_i(P)A_i & \mathbb{E}_i(P)J_i & \mathbb{E}_i(P) & \bullet \\ C_i & D_i & 0 & I \end{bmatrix} > 0, \quad (2.6)$$

and the LMI constraint (2.6) can also be described by the inequality below

$$\begin{bmatrix} P_i & \bullet & \bullet & \bullet \\ 0 & \gamma I & \bullet & \bullet \\ A_i & J_i & \mathbb{E}_i(P)^{-1} & \bullet \\ C_i & D_i & 0 & I \end{bmatrix} > 0. \quad (2.7)$$

2.2.3 \mathcal{H}_2 norm for MJLS

Assuming that (2.1) is MSS with $x_0 = 0$, the \mathcal{H}_2 norm is given by

$$\|\mathcal{G}\|_2^2 = \sum_{s=1}^{n_w} \sum_{i=1}^N \mu_i \|z^{i,s}\|_2^2, \quad (2.8)$$

where z represents the output $z(0), z(1), \dots$ obtained when

- the input is given by $w(k) = e_s \delta(k)$, where $e_s \in \mathbb{R}^{n_m}$ is the s -th column of the $m \times m$ identity matrix and $\delta(k)$ is the unitary impulse, see (COSTA; VAL; GEROMEL, 1997).
- $\theta_0 = i \in \mathbb{K}$ with probability $\mu_i = P(\theta_0 = i)$

In (COSTA; FRAGOSO; MARQUES, 2006) it is shown that, if the Markov chain is ergodic, and taking $\mu_i = \rho_i$, where $\rho_i = \lim_{k \rightarrow \infty} P(\theta(k) = i)$, the norm defined in (2.8) can also be written as

$$\|G\|_2^2 = \lim_{k \rightarrow \infty} \mathbb{E}[z(k)'z(k)], \quad (2.9)$$

where $z(k)$ is the controlled output and $w(k)$ represents a wide-sense white-noise with covariance given by the identity matrix that is independent of the initial condition x_0 , and the Markov chain $\{\theta_k\}$. From the above, we have the following lemma.

Lemma 2. *System (2.1) is MSS and satisfies the norm constraint $\|\mathcal{G}\|_2^2 < \lambda$ if and only if there exist matrices $P_i = P_i' > 0$ and $S_i = S_i' > 0$ such that*

$$\sum_{i=1}^N \mu_i \text{Tr}(S_i) < \lambda, \quad (2.10)$$

$$\begin{bmatrix} S_i & \bullet & \bullet \\ \mathbb{E}_i(P)J_i & \mathbb{E}_i(P) & \bullet \\ D_i & 0 & I \end{bmatrix} > 0, \quad (2.11)$$

$$\begin{bmatrix} P_i & \bullet & \bullet \\ \mathbb{E}_i(P)A_i & \mathbb{E}_i(P) & \bullet \\ C_i & 0 & I \end{bmatrix} > 0, \quad \forall i \in \mathbb{K}. \quad (2.12)$$

Proof: See (FIORAVANTI; GONÇALVES; GEROMEL, 2008) or (COSTA; VAL; GEROMEL, 1997).

Pre- and post- multiplying (2.11) and (2.12) by $\text{diag}(I, \mathbb{E}_i(P)^{-1}, I)$ we obtain that if the inequalities

$$\begin{bmatrix} S_i & \bullet & \bullet \\ J_i & \mathbb{E}_i(P)^{-1} & \bullet \\ D_i & 0 & I \end{bmatrix} > 0, \quad (2.13)$$

$$\begin{bmatrix} P_i & \bullet & \bullet \\ A_i & \mathbb{E}_i(P)^{-1} & \bullet \\ C_i & 0 & I \end{bmatrix} > 0, \quad (2.14)$$

are satisfied then $\|\mathcal{G}\|_2^2 < \lambda$.

2.2.4 \mathcal{H}_- index for MJLS

Assuming that (2.1) is MSS and $x_0 = 0$, the H_- sensitivity index is defined as

$$\|G\|_-^2 = \inf_{0 \neq w \in \mathcal{L}_2, \theta_0 \in \mathbb{K}} \frac{\|z\|_2}{\|w\|_2}. \quad (2.15)$$

Lemma 3. : *Assuming that (2.1) is MSS we have that $\|G\|_- > \xi$ for $\xi > 0$ if there exist matrices $P_i > 0$, $i \in \mathbb{K}$ such that*

$$\begin{bmatrix} A_i & J_i \\ C_i & 0 \end{bmatrix}' \begin{bmatrix} \mathbb{E}_i(P) & 0 \\ 0 & -I \end{bmatrix} \begin{bmatrix} A_i & J_i \\ C_i & 0 \end{bmatrix} - \begin{bmatrix} P_i & C_i' D_i \\ D_i' C_i & D_i' D_i - \xi I \end{bmatrix} < 0, \forall i \in \mathbb{K}, \quad (2.16)$$

is satisfied.

Moreover for $P_i > 0$ we have that (2.16) is satisfied if and only if

$$\begin{bmatrix} P_i + C_i' C_i & \bullet & \bullet \\ D_i' C_i & D_i' D_i - \xi I & \bullet \\ A_i & J_i & \mathbb{E}_i(P)^{-1} \end{bmatrix} > 0, \forall i \in \mathbb{K}, \quad (2.17)$$

holds.

Proof: Let us show first that if there exist matrices $P_i > 0$ such that (2.16) is satisfied then $\|G\|_- > \xi$. Pre and post multiplying (2.16) by $[x(k)' \ w(k)']$ and its transpose we get that

$$\begin{bmatrix} x(k) \\ w(k) \end{bmatrix}' \begin{bmatrix} A_{\theta(k)}' \mathbb{E}_{\theta(k)}(P) A_{\theta(k)} - P_{\theta(k)} - C_{\theta(k)}' C_{\theta(k)} & A_{\theta(k)}' \mathbb{E}_{\theta(k)}(P) J_{\theta(k)} - C_{\theta(k)}' D_{\theta(k)} \\ J_{\theta(k)}' \mathbb{E}_{\theta(k)}(P) A_{\theta(k)} - D_{\theta(k)}' C_{\theta(k)} & J_{\theta(k)}' \mathbb{E}_{\theta(k)}(P) J_{\theta(k)} - D_{\theta(k)}' D_{\theta(k)} + \xi I \end{bmatrix} \begin{bmatrix} x(k) \\ w(k) \end{bmatrix} < 0. \quad (2.18)$$

From (2.18) and (2.1) we get that

$$x(k+1)' \mathbb{E}_{\theta(k)}(P) x(k+1) - x(k)' P_{\theta(k)} x(k) - z(k)' z(k) + \xi w(k)' w(k) < 0. \quad (2.19)$$

Denoting by \mathfrak{F}_k the σ -field generated by the variables $\{x(l), w(l), \theta(l); l = 0, \dots, k\}$ we get that $x(k+1)' \mathbb{E}_{\theta(k)}(P) x(k+1) = \mathbb{E}(x(k+1)' P_{\theta(k+1)} x(k+1) | \mathfrak{F}_k)$, and thus $\mathbb{E}(x(k+1)' \mathbb{E}_{\theta(k)}(P) x(k+1)) = \mathbb{E}(x(k+1)' P_{\theta(k+1)} x(k+1))$. Recalling that $x_0 = 0$ we get from (2.19) after taking the sum over k from 0 to T that

$$\sum_{k=0}^T \mathbb{E} \left[x(k+1)' P_{\theta(k+1)} x(k+1) - x(k)' P_{\theta(k)} x(k) - \|z(k)\|^2 + \xi \|w(k)\|^2 \right] =$$

$$\mathbb{E}(x(T+1)'P_{\theta(T+1)}x(T+1)) - \sum_{k=0}^T \mathbb{E}(\|z(k)\|^2) + \xi \sum_{k=0}^T \mathbb{E}(\|w(k)\|^2) < 0. \quad (2.20)$$

Taking the limit as $T \rightarrow \infty$ in (2.20) and recalling that (2.1) is MSS, we obtain that $\lim_{T \rightarrow \infty} \mathbb{E}(x(T+1)'P_{\theta(T+1)}x(T+1)) = 0$, and we conclude that

$$\|z\|_2^2 - \xi \|w\|_2^2 > 0,$$

showing the first part of the proof. Let us show now the equivalence between (2.16) and (2.17). Suppose that there exists $P_i > 0$ satisfying the constraints in (2.16). For any $\alpha > 0$ we may rewrite (2.16) as

$$\begin{bmatrix} P_i & \bullet \\ D_i' C_i & D_i' D_i - \xi I \end{bmatrix} - \begin{bmatrix} A_i & J_i \\ C_i & 0 \end{bmatrix}' \left\{ \begin{bmatrix} \mathbb{E}_i(P) & 0 \\ 0 & \alpha I \end{bmatrix} - \begin{bmatrix} 0 & 0 \\ 0 & (1+\alpha)I \end{bmatrix} \right\} \begin{bmatrix} A_i & J_i \\ C_i & 0 \end{bmatrix} > 0. \quad (2.21)$$

Reorganizing (2.21) we get that

$$\underbrace{\begin{bmatrix} P_i + (1+\alpha)C_i' C_i & C_i' D_i \\ D_i' C_i & D_i' D_i - \xi I \end{bmatrix}}_{>0} - \underbrace{\begin{bmatrix} A_i & J_i \\ C_i & 0 \end{bmatrix}' \begin{bmatrix} \mathbb{E}_i(P) & 0 \\ 0 & \alpha I \end{bmatrix} \begin{bmatrix} A_i & J_i \\ C_i & 0 \end{bmatrix}}_{\geq 0} > 0. \quad (2.22)$$

From Schur's complement we obtain that (2.22) is equivalent to

$$\begin{bmatrix} P_i + (1+\alpha)C_i' C_i & \bullet & \bullet & \bullet \\ D_i' C_i & D_i' D_i - \xi I & \bullet & \bullet \\ A_i & J_i & \mathbb{E}_i(P)^{-1} & \bullet \\ C_i & 0 & 0 & \alpha^{-1} I \end{bmatrix} > 0, \quad (2.23)$$

and from the Schur's complement again we get that (2.23) is equivalent to

$$\begin{bmatrix} P_i + (1+\alpha)C_i' C_i & \bullet & \bullet \\ D_i' C_i & D_i' D_i - \xi I & \bullet \\ A_i & J_i & \mathbb{E}_i(P)^{-1} \end{bmatrix} - \alpha \begin{bmatrix} C_i' \\ 0 \\ 0 \end{bmatrix} \begin{bmatrix} C_i & 0 & 0 \end{bmatrix} > 0,$$

showing (2.17). On the other hand, suppose that (2.17) holds. By taking the reverse steps as before we get that (2.16) is satisfied, completing the proof. ■

Remark 1. Notice that, unlike Lemma 1, we cannot guarantee from (2.16) that (2.1) is MSS.

2.3 Fault Detection Filter Formulation

Let us consider the FD scheme in Fig. 8. As shown in Fig.8, the main points for a model-based FD to perform properly are the *i*) accurate model for the plant; *ii*) a reliable network communication; *iii*) a well-designed residue generator filter; and *iv*) a proper residue evaluation. In this work, we concentrate our endeavors on providing residue generator filter designs that contemplate some common issues as imprecise modeling,

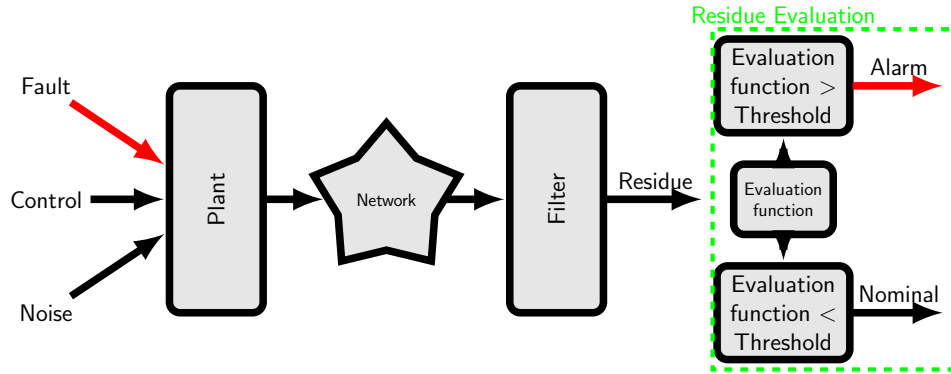


Figure 8: Block diagram detailing the Fault Detection scheme, presenting the residue generation and residue evaluation steps.

unreliable network connections, and unknown network behavior.

It is important to state that the design of a residue evaluation procedure is not in the scope of this work. However, a proper residue evaluation is required to guarantee the FD procedure overall performance. The block diagram representing the FD topology is presented in Fig.9. We assume that the MJLS subject to faults is defined as

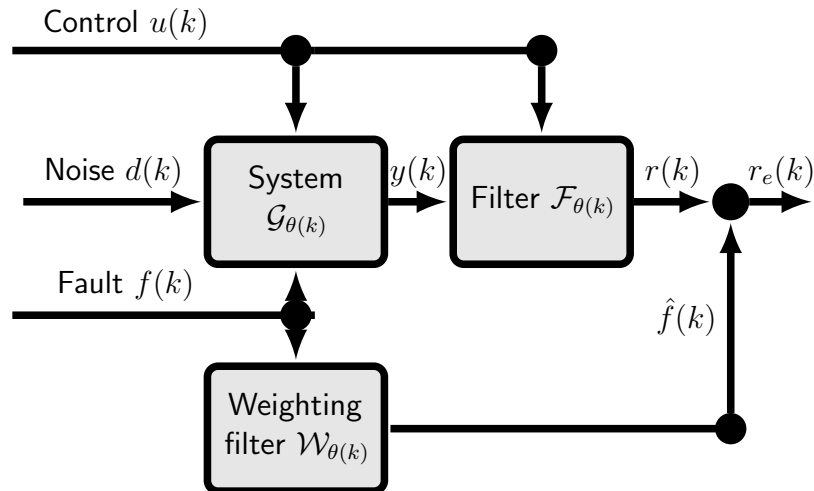


Figure 9: Block diagram representing the topology used to design the Fault Detection Filter.

$$\mathcal{G} : \begin{cases} x(k+1) = A_{\theta(k)}x(k) + B_{\theta(k)}u(k) + J_{\theta(k)}w(k) + F_{\theta(k)}f(k), \\ y(k) = C_{\theta(k)}x(k) + D_{\theta(k)}w(k) + E_{\theta(k)}f(k), \\ x(0) = x_0, \quad \theta(0) = \theta_0, \end{cases} \quad (2.24)$$

where $x(k) \in \mathbb{R}^{n_x}$, $y(k) \in \mathbb{R}^{n_y}$, $u(k) \in \mathbb{R}^{n_u}$, $w(k) \in \mathbb{R}^{n_w}$, $f(k) \in \mathbb{R}^{n_f}$, represent the state, measurements, control, exogenous, and fault signals respectively.

2.3.1 Residue Generator using Fault Detection Filter

The goal here is to design a FDF, which is responsible to generate the residue signal $r(k)$. The FDF is defined as

$$\mathcal{F} : \begin{cases} \eta(k+1) = \mathcal{A}_{\eta\theta(k)}\eta(k) + \mathcal{M}_{\eta\theta(k)}u(k) + \mathcal{B}_{\eta\theta(k)}y(k), \\ r(k) = \mathcal{C}_{\eta\theta(k)}\eta(k) + \mathcal{D}_{\eta\theta(k)}y(k), \\ \eta(0) = \eta_0, \end{cases} \quad (2.25)$$

where $\eta(k) \in \mathbb{R}^{n_x}$, $r(k) \in \mathbb{R}^{n_r}$ representing filter state, and residue signals, respectively.

A possible way to improve the FDF performance is to consider a weight system during the design process, as used in (CHEN; PATTON, 2000; ZHONG et al., 2005; ZHONG et al., 2003). As described in (CHEN; PATTON, 2000), the weight system improves the FDF performance for a specific frequency range. Herein, the weight system \mathcal{W} is denoted by

$$\mathcal{W} : \begin{cases} x_f(k+1) = A_{\mathcal{W}}x_f(k) + B_{\mathcal{W}}f(k), \\ \hat{f}(k) = C_{\mathcal{W}}x_f(k) + D_{\mathcal{W}}f(k), \\ x_f(0) = 0, \end{cases} \quad (2.26)$$

where $x_f(k) \in \mathbb{R}^{n_r}$ is the weight matrix state, $f(k)$ is the same signal as in (2.24), and $\hat{f}(k) \in \mathbb{R}^{n_r}$ is the weighted fault signal.

Remark 2. In (CHEN; PATTON, 2000), a non-minimal phase FDI system is presented, using the H_∞ criterion. It is important to state that the weighting system (2.26) is given, and its sole purpose is to be used as a tuning tool during the design process. In (CHEN; PATTON, 2000; NIEMANN; STOUSTRUP, 2001), this technique is implemented for the continuous-time domain, and in (ZHONG et al., 2005) the same approach is used for the discrete-time domain. As described in (NIEMANN; STOUSTRUP, 2001), the presence of (2.26) allows us to choose between a fault detection or a fault isolation problem, depending solely on the structure of (2.26). If the designer decides to solve a fault estimation problem with the same framework, the only action would be to set the values of (2.26) as $B_{\mathcal{W}} = 0$, $C_{\mathcal{W}} = 0$, and $D_{\mathcal{W}} = I$. It is important to make it clear that the filter \mathcal{W} is not present in the implementation, it is just a part of the design procedure.

The difference between the fault detection and fault isolation approaches is that fault detection needs only a single residue signal, and for the fault isolation case it is necessary to generate a set of residue signals, called structured residual set, as described in (CHEN; PATTON, 2012). In our case, for the fault detection approach, we can set $A_{\mathcal{W}}$, $B_{\mathcal{W}}$, $C_{\mathcal{W}}$,

and $D_{\mathcal{W}}$ as fixed matrices to generate a single residue signal $r(k)$. On the other hand, for the fault isolation approach, the matrices $A_{\mathcal{W}f}$, $B_{\mathcal{W}}$, $C_{\mathcal{W}}$, and $D_{\mathcal{W}}$ would need to be designed differently in a way to generate an appropriate number of residue signals to reach the fault isolability. The size of the residue set should be similar to the number of known recurring faults so that to isolate these specific faults. It is important to mention that a complete fault isolability is not always achievable since complete knowledge of all possible faults may be unreasonable for some practical situations.

The major goal in here is to design the matrices $\mathcal{A}_{\eta i}$, $\mathcal{B}_{\eta i}$, $\mathcal{C}_{\eta i}$, $\mathcal{D}_{\eta i}$, $\mathcal{M}_{\eta i}$ so that the Fault Detection Filter (2.25) is mean square stable when $x(0) = 0$, $u(0) = 0$, $d(0) = 0$ and $f(0) = 0$ and minimizes the value of γ in for the \mathcal{H}_{∞} norm cases as in

$$\sup_{w \neq 0, w \in \mathcal{L}_2, \theta_0 \in \mathbb{N}} \frac{\|r_e\|_2}{\|w\|_2} < \gamma, \quad (2.27)$$

where $r_e(k) = r(k) - \hat{f}(k)$. For the \mathcal{H}_2 norm the goal in the problem formulations is

$$\sum_{s=1}^m \sum_{i=1}^N \mu_i \|r_e\|_2^2 < \lambda. \quad (2.28)$$

From the above, the equivalent system can be written in the augmented form as

$$\mathcal{G}_{aug} : \begin{cases} \bar{x}(k+1) = \tilde{A}_{\theta(k)} \bar{x}(k) + \tilde{B}_{\theta(k)} \bar{w}(k), \\ r_e(k) = \tilde{C}_{\theta(k)} \bar{x}(k) + \tilde{D}_{\theta(k)} \bar{w}(k), \end{cases} \quad (2.29)$$

where the augmented state and the input signal are $\bar{x}(k) = [x(k)' \ \eta(k)' \ x_f(k)']'$ and $\bar{w} = [u(k)' \ w(k)' \ f(k)']'$ with

$$\left[\begin{array}{c|c} \tilde{A}_i & \tilde{B}_i \\ \hline \tilde{C}_i & \tilde{D}_i \end{array} \right] = \left[\begin{array}{ccc|ccc} A_i & 0 & 0 & B_i & J_i & F_i \\ \mathcal{B}_{\eta i} C_i & \mathcal{A}_{\eta i} & 0 & \mathcal{M}_{\eta i} & \mathcal{B}_{\eta i} D_i & \mathcal{B}_{\eta i} E_i \\ 0 & 0 & A_{\mathcal{W}} & 0 & 0 & B_{\mathcal{W}} \\ \hline \mathcal{D}_{\eta i} C_i & \mathcal{C}_{\eta i} & -C_{\mathcal{W}} & 0 & \mathcal{D}_{\eta i} D_i & \mathcal{D}_{\eta i} E_i - D_{\mathcal{W}} \end{array} \right]. \quad (2.30)$$

2.3.2 Evaluation Function

In the evaluation stage, it is necessary to set an evaluation function $\text{EVAL}(k)$ and also a threshold TH, both as defined in (ZHONG et al., 2005). We consider L as the evaluation time, and with that, we can separate the evaluation process into two distinct cases, the first one is defined by $k - L \geq 0$ and the second one, $k - L < 0$. Thus, we define the

auxiliary vectors for each case as

$$\begin{cases} \text{for } k - L \geq 0, \bar{r}(k) = [r(k) \ r(k-1) \ \dots \ r(k-L)]' \\ \text{for } k - L < 0, \bar{r}(k) = [r(k) \ r(k-1) \ \dots \ r(0)]' \end{cases} \quad (2.31)$$

and, given the discrepancy between the intervals, the evaluation functions for each case are set as

$$\begin{cases} \text{for } k - L \geq 0, \text{ EVAL}(k) = \left\{ \sum_{\sigma=k}^{\sigma=k-L} \bar{r}'(\sigma) \bar{r}(\sigma) \right\}^{\frac{1}{2}}, \\ \text{for } k - L < 0, \text{ EVAL}(k) = \left\{ \sum_{\sigma=k}^{\sigma=0} \bar{r}'(\sigma) \bar{r}(\sigma) \right\}^{\frac{1}{2}}. \end{cases} \quad (2.32)$$

Remark 3. *It is important to highlight that the choice of a suitable L is deeply linked with the Fault Detection Identification (FDI) performance, since if L is not large enough, the faults may not be detected since the evaluation signal will not have enough time to reach the threshold. On the other hand, if L is too large, the number of false alarms will drastically increase.*

Another part of the evaluation process is the definition of a threshold, denoted by TH. We refer to (CHEN; PATTON, 2012) or (FRANK; DING, 1997) for an in-depth discussion on how to choose one among the different types of thresholds. In our case, we implement a fixed threshold, which is obtained after performing a Monte Carlo simulation when there is no fault. After this simulation being performed, we obtain a curve that represents the mean and standard deviation of the evaluation function (2.32) for the evaluation window L . We assume that TH is the peak value of the curve that represents the mean summed with the standard deviation of $\text{EVAL}(k)$ in the period $(0, L)$. For a more detailed description of this subject, see (CHEN; PATTON, 2012),(FRANK; DING, 1997).

Considering the aforementioned discussion, the decision for the fault detection is as follows:

$$\begin{aligned} \text{EVAL}(k) > \text{TH} &\implies \text{fault occurrence} \implies \text{alarm}, \\ \text{EVAL}(k) \leq \text{TH} &\implies \text{absence of fault}. \end{aligned}$$

Remark 4. *For simplicity suppose in (2.24) and (2.25) that $u(k) = v$ is a constant input set-point and that $w(k)$ is a white noise sequence with null mean and constant covariance matrix. It is also important to mention that the system is not subjected to fault at this moment, meaning that $f = 0$. By combining equations (2.24) and (2.25) we obtain, for*

appropriate matrices $\tilde{A}_i, \tilde{B}_i, \tilde{C}_i$, (see (2.52)) the system

$$\mathcal{G}_{nh} = \begin{cases} \tilde{x}(k+1) = \tilde{A}_{\theta(k)}\tilde{x}(k) + \tilde{B}_{\theta(k)}\tilde{w}(k), \\ r(k) = \tilde{C}_{\theta(k)}\tilde{x}(k), \end{cases} \quad (2.33)$$

where

$$\tilde{x}(k) = \begin{bmatrix} x(k) \\ \eta(k) \end{bmatrix}, \quad \tilde{w}(k) = \begin{bmatrix} v \\ w(k) \end{bmatrix}.$$

Suppose that system (2.33) is MSS and that the Markov chain $\{\theta(k)\}$ is ergodic. Then it was shown in Theorem 3.33 and Proposition 3.36 of (COSTA; FRAGOSO; MARQUES, 2006) that $\mathbb{E}(\tilde{x}(k)1_{\{\theta(k)=j\}}) \rightarrow \mu_j$ and that $U_j(k) = \mathbb{E}(\tilde{x}(k)\tilde{x}(k)'1_{\{\theta(k)=j\}}) \rightarrow U_j$ as $k \rightarrow \infty$ for some vectors μ_j and positive semi-definite matrices U_j , $j = 1, \dots, N$. By noticing from (2.33) that $r(k) = \sum_{i=1}^N \tilde{C}_i \tilde{x}(k) 1_{\{\theta(k)=i\}}$ it follows that $\mathbb{E}(r(k)r(k)') = \sum_{i=1}^N \tilde{C}_i U_i(k) \tilde{C}_i'$. From this one can see that $\mathbb{E}(r(k)r(k)') \rightarrow R$ as $k \rightarrow \infty$ where $R = \sum_{i=1}^N \tilde{C}_i U_i \tilde{C}_i'$. Since

$$\mathbb{E}(EVAL(k)^2) = \sum_{i=k-L}^k \text{Tr}(\mathbb{E}(r(i)r(i)')),$$

it follows that $\mathbb{E}(EVAL(r, k)^2) \rightarrow (L+1)\text{Tr}(R)$ as $k \rightarrow \infty$ and also, from Jensen's inequality, that $0 \leq \limsup_{k \rightarrow \infty} \mathbb{E}(J(r, k)) \leq ((L+1)\text{Tr}(R))^{1/2}$. In the numerical simulation we can observe this kind of limit behavior for the evaluation function.

2.3.3 Theoretical Results

In this subsection we present the design of the FDF under the MJLS framework using the following performance indexes \mathcal{H}_∞ , \mathcal{H}_2 norms, and \mathcal{H}_- sensibility index, also the design for the mixed $\mathcal{H}_2/\mathcal{H}_\infty$ and $\mathcal{H}_-/\mathcal{H}_\infty$.

2.3.3.1 \mathcal{H}_∞ Fault Detection Filter Design for MJLS

Theorem 1. *There exists a mode-dependent FD Filter as in (2.25) satisfying $\|\mathcal{G}_{aug}\|_\infty^2 < \gamma$ if there exist symmetric matrices Z_i, X_i, W_i , and matrices $O_i, \nabla_i, \Gamma_i, \mathcal{C}_{\eta_i}, \mathcal{D}_{\eta_i}$ with compatible dimensions that satisfy the following LMI constraint*

$$\begin{bmatrix} Z_i & \bullet & \bullet & \bullet & \bullet & \bullet & \bullet & \bullet & \bullet & \bullet \\ Z_i & X_i & \bullet & \bullet & \bullet & \bullet & \bullet & \bullet & \bullet & \bullet \\ 0 & 0 & W_i & \bullet & \bullet & \bullet & \bullet & \bullet & \bullet & \bullet \\ 0 & 0 & 0 & \gamma I & \bullet & \bullet & \bullet & \bullet & \bullet & \bullet \\ 0 & 0 & 0 & 0 & \gamma I & \bullet & \bullet & \bullet & \bullet & \bullet \\ 0 & 0 & 0 & 0 & 0 & \gamma I & \bullet & \bullet & \bullet & \bullet \\ \mathbb{E}_i(Z)A_i & \mathbb{E}_i(Z)A_i & 0 & \mathbb{E}_i(Z)B_i & \mathbb{E}_i(Z)B_{di} & \mathbb{E}_i(Z)F_i & \mathbb{E}_i(Z) & \bullet & \bullet & \bullet \\ \Pi_{8,1} & \Pi_{8,2} & 0 & \Pi_{8,4} & \Pi_{8,5} & \Pi_{8,6} & \mathbb{E}_i(Z) & \mathbb{E}_i(X) & \bullet & \bullet \\ 0 & 0 & \mathbb{E}_i(W)A_W & 0 & 0 & \mathbb{E}_i(W)B_W & 0 & 0 & \mathbb{E}_i(W) & \bullet \\ \mathcal{D}_{\eta_i}C_i & -C_W & 0 & \mathcal{D}_{\eta_i}D_i & \bullet & \bullet & 0 & 0 & 0 & I \end{bmatrix} > 0, \quad (2.34)$$

where

$$\begin{aligned}\Pi_{8,1} &= \mathbb{E}_i(X)A_i + \nabla_i C_i + O_i, & \Pi_{8,2} &= \mathbb{E}_i(X)A_i + \nabla_i C_i, & \Pi_{8,4} &= \mathbb{E}_i(X)B_i + \Gamma_i, \\ \Pi_{8,5} &= \mathbb{E}_i(X)J_i + \nabla_i D_i, & \Pi_{8,6} &= \mathbb{E}_i(X)F_i + \nabla_i E_i, & \Pi_{10,1} &= \mathcal{D}_{\eta i}C_i + \mathcal{C}_{\eta i}, \\ \Pi_{10,6} &= \mathcal{D}_{\eta i}E_i - D_{\mathcal{W}},\end{aligned}$$

for all $i \in \mathbb{K}$. If a feasible solution for (2.34) is obtained, then a suitable FD Filter is given by $\mathcal{A}_{\eta i} = (\mathbb{E}_i(Z) - \mathbb{E}_i(X))^{-1}O_i$, $\mathcal{B}_{\eta i} = (\mathbb{E}_i(Z) - \mathbb{E}_i(X))^{-1}\nabla_i$, $\mathcal{M}_{\eta i} = (\mathbb{E}_i(Z) - \mathbb{E}_i(X))^{-1}\Gamma_i$, $\mathcal{C}_{\eta i}$, $\mathcal{D}_{\eta i}$, for all $i \in \mathbb{K}$.

Proof: The first step to derive the result is to impose the following structure, similar to the structure in (GONÇALVES; FIORAVANTI; GEROMEL, 2011), for the matrices P_i and P_i^{-1} :

$$P_i = \begin{bmatrix} X_i & U_i & 0 \\ U_i' & \hat{X}_i & 0 \\ 0 & 0 & W_i \end{bmatrix}, \quad P_i^{-1} = \begin{bmatrix} Y_i & V_i & 0 \\ V_i' & \hat{Y}_i & 0 \\ 0 & 0 & H_i \end{bmatrix}, \quad (2.35)$$

and also consider the following structure for the matrices $\mathbb{E}_i(P)$ and $\mathbb{E}_i(P)^{-1}$:

$$\mathbb{E}_i(P) = \begin{bmatrix} \mathbb{E}_i(X) & \mathbb{E}_i(U) & 0 \\ \mathbb{E}_i(U)' & \mathbb{E}_i(X) & 0 \\ 0 & 0 & \mathbb{E}_i(W) \end{bmatrix}, \quad \mathbb{E}_i(P)^{-1} = \begin{bmatrix} R_{1i} & R_{2i} & 0 \\ R_{2i}' & R_{3i} & 0 \\ 0 & 0 & \mathbb{E}_i(W)^{-1} \end{bmatrix}. \quad (2.36)$$

We define the matrices π and ζ by

$$\pi = \begin{bmatrix} I & I & 0 \\ V_i' Y_i^{-1} & 0 & 0 \\ 0 & 0 & I \end{bmatrix}, \quad \zeta = \begin{bmatrix} R_{1i}^{-1} \mathbb{E}_i(X) & 0 \\ 0 & \mathbb{E}_i(U)' \\ 0 & 0 & \mathbb{E}_i(G) \end{bmatrix}. \quad (2.37)$$

Since $U_i = Z_i - X_i$ in (2.35), we get from (2.35), and (2.37) that $Y_i = V_i'$ and $Y_i = Z_i^{-1}$. Also considering $U_i = -\hat{X}_i$ we get $R_{1i}^{-1} = \mathbb{E}_i(X + U) = \mathbb{E}_i(Z)$. Moreover, and so we have that

$$\begin{aligned}\pi' P_i \pi &= \begin{bmatrix} Y_i^{-1} & Y_i^{-1} & 0 \\ Y_i^{-1} & X_i & 0 \\ 0 & 0 & W_i \end{bmatrix}, & \zeta' \tilde{A}_i \pi &= \begin{bmatrix} R_{1i}^{-1} A_i & R_{1i}^{-1} A_i & 0 \\ \tilde{\Pi}_{2,1} & \mathbb{E}_i(X)A_i + \mathbb{E}_i(U)\mathcal{B}_{\eta i}C_i & 0 \\ 0 & 0 & \mathbb{E}_i(W)A_{\mathcal{W}} \end{bmatrix}, \\ \tilde{\Pi}_{2,1} &= \mathbb{E}_i(X)A_i + \mathbb{E}_i(U)\mathcal{B}_{\eta i}C_i + \mathbb{E}_i(U)\mathcal{A}_{\eta i}V_i'Y_i^{-1}, \\ \zeta' \tilde{B}_i &= \begin{bmatrix} R_{1i}^{-1} B_i & R_{1i}^{-1} J_i & R_{1i}^{-1} F_i \\ \tilde{\Pi}_{2,1} & \mathbb{E}_i(X)J_i + \mathbb{E}_i(U)\mathcal{B}_{\eta i}D_i & \mathbb{E}_i(X)F_i + \mathbb{E}_i(U)\mathcal{B}_{\eta i}E_i \\ 0 & 0 & \mathbb{E}_i(W)B_{\mathcal{W}} \end{bmatrix}, \\ \bar{\Pi}_{2,1} &= \mathbb{E}_i(X)B_i + \mathbb{E}_i(U)\mathcal{M}_{\eta i}, \\ \zeta' \mathbb{E}_i(P)^{-1} \zeta &= \begin{bmatrix} R_{1i}^{-1} \mathbb{E}_i(Z) & 0 \\ \mathbb{E}_i(Z) & \mathbb{E}_i(X) \\ 0 & 0 & \mathbb{E}_i(W) \end{bmatrix}, & \tilde{C}_i \pi &= [\mathcal{D}_{\eta i}C_i + \mathcal{C}_{\eta i}V_i'Z_i \quad \mathcal{D}_{\eta i}C_i \quad -C_{\mathcal{W}}], \\ \tilde{D}_i &= [0 \quad \mathcal{D}_{\eta i}D_i \quad \mathcal{D}_{\eta i}D_i - D_{\mathcal{W}}].\end{aligned}$$

Applying the change of variables $\mathbb{E}_i(U)\mathcal{A}_{\eta i}V_i'Z_i = O_i$, $\mathbb{E}_i(U)\mathcal{B}_{\eta i} = \nabla_i$, $\mathbb{E}_i(U)\mathcal{M}_{\eta i} = \Gamma_i$, $\mathcal{C}_{\eta i}V_i'Z_i = \mathcal{C}_{\eta i}$, $\mathcal{D}_{\eta i}$ and also substituting $\mathbb{E}_i(Z) = R_{1i}^{-1}$ in (2.34), we get the following

inequality

$$\begin{bmatrix} \pi' P_i \pi & \bullet & \bullet & \bullet \\ 0 & \delta I & \bullet & \bullet \\ \zeta' \tilde{A}_i \pi & \zeta' \tilde{B}_i & \zeta' \mathbb{E}_i(P)^{-1} \zeta & \bullet \\ \tilde{C}_i \pi & \tilde{D}_i & 0 & I \end{bmatrix} > 0, \quad (2.38)$$

and it is easy to see that inequality (2.38) is equivalent to the inequality (2.34). Multiplying to the right by $\text{diag}[\pi^{-1}, I, \zeta^{-1}, I]$ and to the left by its transpose, we get the inequality (2.7) and with that we can guarantee that $\|\mathcal{G}\|_\infty^2 < \gamma$. ■

2.3.3.2 \mathcal{H}_2 Fault Detection Filter Design for MJLS

Theorem 2. *There exists a mode-dependent FD Filter in the form of (2.25) satisfying the $\|\mathcal{G}_{aug}\|_2^2 < \lambda$ if there exist symmetric matrices Z_i, X_i, S_i, T_i and matrices $O_i, \nabla_i, \Gamma_i, \mathcal{C}_{\eta_i}, \mathcal{D}_{\eta_i}$, with compatible dimensions that satisfy the following LMI constraints*

$$\sum_{i=1}^N \mu_i \text{Tr}(S_i) < \lambda, \quad (2.39)$$

$$\begin{bmatrix} [S_i] & \bullet & \bullet & \bullet & \bullet \\ \mathbb{E}_i(Z)B_i & \mathbb{E}_i(Z)J_i & \mathbb{E}_i(Z)F_i & \mathbb{E}_i(Z) & \bullet \\ \mathbb{E}_i(X)B_i + \Gamma_i & \mathbb{E}_i(X)J_i + \nabla_i D_i & \mathbb{E}_i(X)F_i + \nabla_i E_i & \mathbb{E}_i(Z) & \mathbb{E}_i(X) \\ 0 & 0 & \mathbb{E}_i(T)B_{\mathcal{W}} & 0 & 0 \\ 0 & \mathcal{D}_{\eta_i} D_i & \mathcal{D}_{\eta_i} E_i - D_{\mathcal{W}} & 0 & 0 \end{bmatrix} > 0, \quad (2.40)$$

$$\begin{bmatrix} Z_i & \bullet & \bullet & \bullet & \bullet & \bullet \\ Z_i & X_i & \bullet & \bullet & \bullet & \bullet \\ 0 & 0 & T_i & \bullet & \bullet & \bullet \\ \mathbb{E}_i(Z)A_i & \mathbb{E}_i(Z)A_i & 0 & \mathbb{E}_i(Z) & \bullet & \bullet \\ \mathbb{E}_i(X)A_i + \nabla_i C_i + O_i & \mathbb{E}_i(X)A_i + \nabla_i C_i & 0 & \mathbb{E}_i(Z) & \mathbb{E}_i(X) & \bullet \\ 0 & 0 & \mathbb{E}_i(T)A_{\mathcal{W}} & 0 & 0 & \mathbb{E}_i(T) \\ \mathcal{D}_{\eta_i} C_i + \mathcal{C}_{\eta_i} & \mathcal{D}_{\eta_i} C_i & -C_{\mathcal{W}} & 0 & 0 & I \end{bmatrix} > 0, \quad (2.41)$$

for all $i \in \mathbb{K}$. If a feasible solution for (2.39), (2.40), (2.41) is obtained, then a suitable FD Filter is given by $\mathcal{A}_{\eta_i} = (\mathbb{E}_i(Z) - \mathbb{E}_i(X))^{-1} O_i$, $\mathcal{B}_{\eta_i} = (\mathbb{E}_i(Z) - \mathbb{E}_i(X))^{-1} \nabla_i$, $\mathcal{M}_{\eta_i} = (\mathbb{E}_i(Z) - \mathbb{E}_i(X))^{-1} \Gamma_i$, \mathcal{C}_{η_i} , \mathcal{D}_{η_i} , for all $i \in \mathbb{K}$.

Proof: In the same way as presented for the H_∞ case, the structures for the matrices T_i and T_i^{-1} are as shown in the equation (2.35) for, respectively, P_i and P_i^{-1} . For the matrices $\mathbb{E}_i(T)$ and $\mathbb{E}_i(T)^{-1}$ the structure are equal to the one in equation (2.36) for, respectively, $\mathbb{E}_i(P)$ and $\mathbb{E}_i(P)^{-1}$. Furthermore, the matrices π and ζ are as shown in equation (2.37). Applying the change of variables $\mathbb{E}_i(U)\mathcal{A}_{\eta_i}V_i'Z_i = O_i$, $\mathbb{E}_i(U)\mathcal{B}_{\eta_i} = \nabla_i$, $\mathbb{E}_i(U)\mathcal{M}_{\eta_i} = \Gamma_i$, $\mathcal{C}_{\eta_i}V_i'Z_i = \mathcal{C}_{\eta_i}$, $\mathcal{D}_{\eta_i} = \mathcal{D}_{\eta_i}$ and also substituting $\mathbb{E}_i(Z) = R_{1l}^{-1}$ in (2.40), (2.41), we get the following inequalities

$$\sum_{i=1}^N \mu_i \text{Tr}(S_i) < \lambda, \quad (2.42)$$

$$\begin{bmatrix} S_i & \bullet & \bullet \\ \zeta' \tilde{B}_i & \zeta' \mathbb{E}_i(P)^{-1} \zeta & \bullet \\ \tilde{D}_i & 0 & I \end{bmatrix} > 0, \quad (2.43)$$

$$\begin{bmatrix} \pi' P_i \pi & \bullet & \bullet \\ \zeta' \tilde{A}_i \pi & \zeta' \mathbb{E}_i(P)^{-1} \zeta & \bullet \\ \tilde{C}_i \pi & 0 & I \end{bmatrix} > 0. \quad (2.44)$$

Multiplying (2.43) to the right by $\text{diag}[I, \zeta^{-1}, I]$ (respectively (2.44) by $\text{diag}[\pi^{-1}, \zeta^{-1}, I]$) and to the left by its transpose we get the inequalities (2.13), (2.14) which, combined with (2.42), yields that $\|\mathcal{G}_{\text{aug}}\|_2^2 < \lambda$. ■

2.3.3.3 Mixed $\mathcal{H}_2/\mathcal{H}_\infty$ Fault Detection Filter Design for MJLS

Note that the structure of the FDF for the \mathcal{H}_2 and \mathcal{H}_∞ , allows us to reformulate the problem mixing $\mathcal{H}_2/\mathcal{H}_\infty$ norms, in order to attain a better performance in some cases. Therefore, it is necessary to rewrite the problem as mixed problem by setting the objective function as

$$\inf\{g(\lambda, \gamma), \text{ such that } \|\mathcal{G}_{\text{aug}}\|_2^2 < \lambda \text{ and } \|G_{\text{aug}}\|_\infty^2 < \gamma\}, \quad (2.45)$$

which considers the restrictions as defined in (2.27) and (2.28). By inspection it is possible to note that there are three possible ways to define the objective function in (2.45), as described below.

First Case: Find a minimum guaranteed cost λ for the \mathcal{H}_2 norm of system (2.29), subject to a given upper bound $\gamma > 0$ on the \mathcal{H}_∞ norm. In this case, we have

$$g(\gamma, \lambda) = \gamma. \quad (2.46)$$

Second Case: Find a minimum guaranteed cost γ for the \mathcal{H}_∞ norm of system (2.29), subject to a given upper bound $\lambda > 0$ on the \mathcal{H}_2 . In this case, we have

$$g(\gamma, \lambda) = \lambda. \quad (2.47)$$

Third Case: Find a minimum for a weighted combination of the guaranteed cost for both \mathcal{H}_2 and \mathcal{H}_∞ norms of system (2.29). Thus, for given scalars $\beta^{(\infty)} \geq 0$ and $\beta^{(2)} \geq 0$, we set

$$g(\gamma, \lambda) = \gamma\beta^{(\infty)} + \lambda\beta^{(2)}, \quad (2.48)$$

where $\beta^{(\cdot)}$ represents the weight for each upper bound. A similar approach is presented in (OLIVEIRA; COSTA, 2018).

In this subsection we consider the mixed $\mathcal{H}_2/\mathcal{H}_\infty$ case. The set of variables is defined as

$$\psi = \{Z_i > 0, X_i > 0, W_i > 0, T_i > 0, S_i > 0, O_i, \nabla_i, \Gamma_i, \mathcal{C}_{\eta_i}, \mathcal{D}_{\eta_i}\} \cup \zeta \quad (2.49)$$

where ζ represents a set that contains λ, γ or both, depending if these parameters λ, γ are assumed to be given or a variable of the problem. Hence, we also define

$$\Psi = \{\psi \text{ as in (2.49) such that the LMIs (2.34),(2.39),(2.40),(2.41) are simultaneously feasible}\}. \quad (2.50)$$

The next theorem provides a sufficient condition for the FD Filter design for the mixed $\mathcal{H}_2/\mathcal{H}_\infty$ case.

Theorem 3. *There exists a mode-dependent FD Filter as in (2.25) such that $\|G_{aug}\|_2^2 < \lambda$ and $\|G_{aug}\|_\infty^2 < \gamma$ if there exists $\psi \in \Psi$, where ψ is defined as in (2.50). If a feasible solution is obtained then a suitable FD Filter is given by $\mathcal{A}_{\eta_i} = (\mathbb{E}_i(Z) - \mathbb{E}_i(X))^{-1}O_i$, $\mathcal{B}_{\eta_i} = (\mathbb{E}_i(Z) - \mathbb{E}_i(X))^{-1}\nabla_i$, $\mathcal{M}_{\eta_i} = (\mathbb{E}_i(Z) - \mathbb{E}_i(X))^{-1}\Gamma_i$, \mathcal{C}_{η_i} , \mathcal{D}_{η_i} , for all $i \in \mathbb{K}$.*

Proof: The proof follows directly from the proofs for Theorems 1 and 2. ■

2.3.3.4 Mixed $\mathcal{H}_-/\mathcal{H}_\infty$ Fault Detection Filter Design for MJLS

For the mixed $\mathcal{H}_-/\mathcal{H}_\infty$ FDF design we rewrite (2.24) in a particular manner where (2.24) is rewritten into two forms: one for the \mathcal{H}_∞ norm design and another for the \mathcal{H}_- sensibility index. In the \mathcal{H}_∞ norm design we rewrite the system as

$$\mathcal{G}_\infty : \begin{cases} x(k+1) = A_{\theta(k)}x(k) + B_{\theta(k)}u(k) + J_{\theta(k)}w(k), \\ y(k) = C_{\theta(k)}x(k) + D_{\theta(k)}w(k), \\ x(0) = x_0, \quad \theta(0) = \theta_0, \end{cases} \quad (2.51)$$

One can observe that comparing (2.24) with (2.51) it is noticeable that the fault signal $f(k)$ is ignored. We choose this particular structure for the mixed $\mathcal{H}_-/\mathcal{H}_\infty$ FDF approach due to two major factors. The first one is that we need to guarantee the stability of the filter, and the latter one is that we want to minimize the effects of the exogenous and control input in the FDF residue signal. The idea supporting this choice is that two factors will reduce the presence of false alarms in the FDI scheme. Since there is no fault signal $f(k)$ we also ignore (2.26).

The augmented system under these considerations is

$$\mathcal{G}_{aug}^{\infty} : \begin{cases} \tilde{x}(k+1) = \tilde{A}_{\theta(k)}\tilde{x}(k) + \tilde{B}_{\theta(k)}\tilde{w}(k), \\ r(k) = \tilde{C}_{\theta(k)}\tilde{x}(k) + \tilde{D}_{\theta(k)}\tilde{w}(k), \end{cases} \quad (2.52)$$

where the augmented state is $\tilde{x}(k) = [x(k)' \ \eta(k)']'$ and $\tilde{w}(k) = [u(k)' \ w(k)']'$ and

$$\tilde{A}_i = \begin{bmatrix} A_i & 0 \\ \mathcal{B}_{\eta_i} C_i & \mathcal{A}_{\eta_i} \end{bmatrix}, \quad \tilde{B}_i = \begin{bmatrix} B_i & J_i \\ \mathcal{M}_{\eta_i} & \mathcal{B}_{\eta_i} D_i \end{bmatrix}, \quad \tilde{C}_i = [0 \ c_{\eta_i}], \quad \tilde{D}_i = [0 \ 0].$$

The fault detection problem for the \mathcal{H}_{∞} case may be represented by the optimization problem to derive the matrices that compose the FDF (2.25) in such a way that system (2.52) is MSS and minimizes the value γ in

$$\sup_{\|w\|_2 \neq 0, w \in \mathcal{L}_2} \frac{\|r\|_2}{\|w\|_2} < \gamma, \quad (2.53)$$

where $\gamma > 0$.

Using the augmented system (2.52), and the Bounded Real Lemma (BRL) constraints (2.7), the following theorem is proposed:

Lemma 4. *There exists a mode-dependent FDF in the form of (2.25) satisfying the constraint (2.53) for some $\gamma > 0$ if there exist symmetric matrices Z_i , X_i , and matrices O_i , ∇_i , Γ_i , C_{η_i} with compatible dimensions that satisfy the following LMI constraint*

$$\begin{bmatrix} Z_i & \bullet & \bullet & \bullet & \bullet & \bullet & \bullet \\ Z_i & X_i & \bullet & \bullet & \bullet & \bullet & \bullet \\ 0 & 0 & \gamma I & \bullet & \bullet & \bullet & \bullet \\ 0 & 0 & 0 & \gamma I & \bullet & \bullet & \bullet \\ \mathbb{E}_i(Z)A_i & \mathbb{E}_i(Z)A_i & \mathbb{E}_i(Z)B_i & \mathbb{E}_i(Z)J_i & \mathbb{E}_i(Z) & \bullet & \bullet \\ \Pi_i^{6,1} & \Pi_i^{6,2} & \mathbb{E}_i(X)B_i + H_i & \Pi_i^{6,4} & \mathbb{E}_i(Z) & \mathbb{E}_i(X) & \bullet \\ C_{\eta_i} & 0 & 0 & 0 & 0 & 0 & I \end{bmatrix} > 0, \quad (2.54)$$

where $\Pi_i^{6,1} = \mathbb{E}_i(X)A_i + \nabla_i C_i + O_i$, $\Pi_i^{6,2} = \mathbb{E}_i(X)A_i + \nabla_i C_i$, and $\Pi_i^{6,4} = \mathbb{E}_i(X)J_i + \nabla_i D_i$. If a feasible solution for (2.54) is obtained, then a suitable FDF is given by $\mathcal{A}_{\eta_i} = (\mathbb{E}_i(Z) - \mathbb{E}_i(X))^{-1}O_i$, $\mathcal{B}_{\eta_i} = (\mathbb{E}_i(Z) - \mathbb{E}_i(X))^{-1}\nabla_i$, $\mathcal{M}_{\eta_i} = (\mathbb{E}_i(Z) - \mathbb{E}_i(X))^{-1}\Gamma_i$, C_{η_i} , for all $i \in \mathbb{K}$.

Proof: The proof of Lemma 4 is similar to the proof presented in (GONÇALVES; FIORAVANTI; GEROMEL, 2011) and for this reason it will be omitted. ■

Now to design the \mathcal{H}_- side we rewrite (2.24) as follows

$$\mathcal{G} : \begin{cases} x(k+1) = A_{\theta(k)}x(k) + F_{\theta(k)}f(k), \\ y(k) = C_{\theta(k)}x(k) + E_{\theta(k)}f(k), \\ x(0) = x_0, \quad \theta(0) = \theta_0, \end{cases} \quad (2.55)$$

where $x(k) \in \mathbb{R}^{n_x}$, $y(k) \in \mathbb{R}^{n_y}$, $f(k) \in \mathbb{R}^{n_f}$, that represents the state, measurements, and fault signals, respectively. Therefore, the augmented system for the \mathcal{H}_- case is

$$\mathcal{G}_{aug}^- : \begin{cases} \bar{x}(k+1) = \bar{A}_{\theta(k)}\bar{x}(k) + \bar{B}_{\theta(k)}\bar{w}(k) \\ r_e(k) = \bar{C}_{\theta(k)}\bar{x}(k) + \bar{D}_{\theta(k)}\bar{w}(k) \end{cases}, \quad (2.56)$$

where the augmented state is $\bar{x}(k) = [x(k)' \ \eta(k)' \ x_f(k)']'$, $\bar{w}(k) = f(k)'$, and considering the equation $r_e(k) = r(k) - \hat{f}(k)$

$$\bar{A}_i = \begin{bmatrix} A_i & 0 & 0 \\ \mathcal{B}_{\eta_i} C_i & \mathcal{A}_{\eta_i} & 0 \\ 0 & 0 & A_{\mathcal{W}} \end{bmatrix}, \quad \bar{B}_i = \begin{bmatrix} F_i \\ \mathcal{B}_{\eta_i} E_i \\ B_{\mathcal{W}} \end{bmatrix}, \quad \bar{C}_i = [0 \ \mathcal{B}_{\eta_i} \ -C_{\mathcal{W}}], \quad \bar{D}_i = -D_{\mathcal{W}}.$$

For the \mathcal{H}_- case, the purpose of this sensibility index in the fault detection problem is to maximize the FDF (2.25) sensitivity against the fault signal, recalling that $\hat{f}(k) \in \mathcal{L}_2$. Therefore, the definition is somewhat inverse of the usual H_∞ norm since the H_- is defined as

$$\inf_{\hat{f} \in \mathcal{L}_2} \frac{\|r_e\|_2}{\|\hat{f}\|_2} > \xi, \quad (2.57)$$

$\xi > 0$, with the intention of increasing the sensibility of the output $r_e(k)$ against the weighted fault signal $\hat{f}(k)$.

Considering the augmented system (2.56) and Lemma 2 and the constraint in (2.17), we can propose the following theorem.

Theorem 4. *If there exist symmetric matrices Z_i , X_i , W_i and matrices O_i , \bar{V}_i , \bar{C}_{η_i} , with compatible dimensions that satisfy the following Bilinear Matrix Inequality (BMI) constraints*

$$\begin{bmatrix} Z_i + \bar{C}'_{\eta_i} \bar{C}_{\eta_i} & \bullet & \bullet & \bullet & \bullet & \bullet & \bullet \\ Z_i & X_i & \bullet & \bullet & \bullet & \bullet & \bullet \\ -C'_{\mathcal{W}} \bar{C}_{\eta_i} & 0 & C'_{\mathcal{W}} C_{\mathcal{W}} + W_i & \bullet & \bullet & \bullet & \bullet \\ -D'_{\mathcal{W}} \bar{C}_{\eta_i} & 0 & D'_{\mathcal{W}} C_{\mathcal{W}} & D'_{\mathcal{W}} D_{\mathcal{W}} - \xi I & \bullet & \bullet & \bullet \\ \mathbb{E}_i(Z) A_i & \mathbb{E}_i(Z) A_i & 0 & \mathbb{E}_i(Z) F_i & \mathbb{E}_i(Z) & \bullet & \bullet \\ \Xi_i^{6,1} & \Xi_i^{6,2} & 0 & \Xi_i^{6,4} & \mathbb{E}_i(Z) & \mathbb{E}_i(X) & \bullet \\ 0 & 0 & \mathbb{E}_i(W_i) A_{\mathcal{W}} & \mathbb{E}_i(W_i) B_{\mathcal{W}} & 0 & 0 & \mathbb{E}_i(W) \end{bmatrix} > 0, \quad (2.58)$$

where $\Xi_i^{6,1} = \mathbb{E}_i(X) A_i + \bar{V}_i C_i + O_i$, $\Xi_i^{6,2} = \mathbb{E}_i(X) A_i + \bar{V}_i C_i$, and $\Xi_i^{6,4} = \mathbb{E}_i(X) F_i + \hat{V}_i E_i$, and the following LMI constraints

$$\begin{bmatrix} Z_i & \bullet \\ Z_i & X_i \end{bmatrix} > 0, \quad (2.59)$$

then there exists $P_i > 0$ for all $i \in \mathbb{K}$ such that (2.17), replacing A_i , J_i , C_i , D_i by respectively \bar{A}_i , \bar{B}_i , \bar{C}_i , \bar{D}_i as in (2.56), and taking

$$\mathcal{A}_{\eta_i} = (\mathbb{E}_i(Z) - \mathbb{E}_i(X))^{-1} O_i, \quad \mathcal{B}_{\eta_i} = (\mathbb{E}_i(Z) - \mathbb{E}_i(X))^{-1} \bar{V}_i, \quad C_{\eta_i}, \quad (2.60)$$

will hold.

Remark 5. Notice that, as pointed out in Remark 1, we cannot guarantee from (2.17) that system (2.56) will be MSS. Therefore we cannot guarantee that a suitable FDF will be derived. However, since the goal is to combine the \mathcal{H}_- index with the \mathcal{H}_∞ filter, we will obtain MSS from the conditions for the \mathcal{H}_∞ filter (see Remark 1).

Proof: Consider that (2.58) and (2.59) hold and set the matrices $\mathcal{A}_{\eta i}$, $\mathcal{B}_{\eta i}$, $\bar{\mathcal{C}}_{\eta i}$ as in (2.60), and the matrices \bar{A}_i , \bar{B}_i , \bar{C}_i , \bar{D}_i as in (2.56). Notice that from (2.59) we have that $X_i - Z_i > 0$, which implies that $\mathbb{E}_i(\mathbf{X}) - \mathbb{E}_i(\mathbf{Z}) > 0$. Partitionate \mathbf{P}_i , \mathbf{P}_i^{-1} , $\mathbb{E}_i(\mathbf{P})$, $\mathbb{E}_i(\mathbf{P})^{-1}$ as

$$\mathbf{P}_i = \begin{bmatrix} X_i & U_i & 0 \\ U_i' & \hat{X}_i & 0 \\ 0 & 0 & W_i \end{bmatrix}, \quad \mathbf{P}_i^{-1} = \begin{bmatrix} Y_i & V_i & 0 \\ V_i' & \hat{Y}_i & 0 \\ 0 & 0 & W_i^{-1} \end{bmatrix},$$

$$\mathbb{E}_i(\mathbf{P}) = \begin{bmatrix} \mathbb{E}_i(\mathbf{X}) & \mathbb{E}_i(\mathbf{U}) & 0 \\ \mathbb{E}_i(\mathbf{U}') & \mathbb{E}_i(\hat{\mathbf{X}}) & 0 \\ 0 & 0 & \mathbb{E}_i(\mathbf{W}) \end{bmatrix}, \quad \mathbb{E}_i(\mathbf{P})^{-1} = \begin{bmatrix} R_{1i} & R_{2i} & 0 \\ R_{2i}' & R_{3i} & 0 \\ 0 & 0 & \mathbb{E}_i(\mathbf{W})^{-1} \end{bmatrix},$$

where $Y_i = Z_i^{-1}$, $-\hat{X}_i = U_i = Z_i - X_i$, $V_i = Z_i^{-1}$, $\forall i \in \mathbb{K}$, which yields to $R_{1i}^{-1} = \mathbb{E}_i(Z)$.

Defining the matrices ϱ_i and ς_i as

$$\varrho_i = \begin{bmatrix} I & I & 0 \\ I & 0 & 0 \\ 0 & 0 & I \end{bmatrix}, \quad \varsigma_i = \begin{bmatrix} \mathbb{E}_i(\mathbf{Z}) & \mathbb{E}_i(\mathbf{X}) & 0 \\ 0 & \mathbb{E}_i(\mathbf{Z}) - \mathbb{E}_i(\mathbf{X}) & 0 \\ 0 & 0 & \mathbb{E}_i(\mathbf{W}) \end{bmatrix},$$

and noticing that

$$\varrho_i' \mathbf{P}_i \varrho_i = \begin{bmatrix} Z_i & Z_i & 0 \\ Z_i & \hat{X}_i & 0 \\ 0 & 0 & W_i \end{bmatrix}, \quad \varrho_i' \bar{\mathcal{C}}_i' \bar{\mathcal{C}}_i \varrho_i = \begin{bmatrix} \bar{\mathcal{C}}_{\eta i}' \bar{\mathcal{C}}_{\eta i} & 0 & -\bar{\mathcal{C}}_{\eta i}' C_{\mathcal{W}} \\ 0 & 0 & 0 \\ -C_{\mathcal{W}}' \bar{\mathcal{C}}_{\eta i} & 0 & C_{\mathcal{W}}' C_{\mathcal{W}} \end{bmatrix},$$

$$\bar{D}_i' \bar{\mathcal{C}}_i \varrho_i = [-D_{\mathcal{W}}' \bar{\mathcal{C}}_{\eta i} \ 0 \ D_{\mathcal{W}}' C_{\mathcal{W}}], \quad \varsigma_i' \bar{A}_i \varrho_i = \begin{bmatrix} \mathbb{E}_i(\mathbf{Z}) A_i & \mathbb{E}_i(\mathbf{Z}) A_i & 0 \\ \mathbb{E}_i(\mathbf{X}) A_i + 0_i + \bar{\nabla}_i C_i & \mathbb{E}_i(\mathbf{X}) A_i + \bar{\nabla}_i C_i & 0 \\ 0 & 0 & \mathbb{E}_i(\mathbf{W}) A_{\mathcal{W}} \end{bmatrix},$$

$$\bar{C}_i \varrho_i = [c_{\eta i} \ 0 \ -c_{\mathcal{W}}], \quad \bar{D}_i' \bar{D}_i = D_{\mathcal{W}}' D_{\mathcal{W}},$$

$$\varsigma_i' \bar{B}_i = \begin{bmatrix} \mathbb{E}_i(\mathbf{Z}) B_i \\ \mathbb{E}_i(\mathbf{X}) F_i + \bar{\nabla}_i E_i \\ \mathbb{E}_i(\mathbf{W}) B_{\mathcal{W}} \end{bmatrix}, \quad \varrho_i' \mathbb{E}_i(\mathbf{P})^{-1} \varrho_i = \begin{bmatrix} \mathbb{E}_i(\mathbf{Z}) & \mathbb{E}_i(\mathbf{Z}) & 0 \\ \mathbb{E}_i(\mathbf{Z}) & \mathbb{E}_i(\mathbf{X}) & 0 \\ 0 & 0 & \mathbb{E}_i(\mathbf{W}) \end{bmatrix},$$

we conclude that the inequality in (2.58) can be re-written as

$$\begin{bmatrix} \varrho_i' \mathbf{P}_i \varrho_i + \varrho_i' \bar{\mathcal{C}}_i' \bar{\mathcal{C}}_i \varrho_i & \bullet & \bullet \\ \bar{D}_i' \bar{\mathcal{C}}_i \varrho_i & \bar{D}_i' \bar{D}_i - \xi I & \bullet \\ \varsigma_i' \bar{A}_i \varrho_i & \varsigma_i' \bar{B}_i & \varsigma_i' \mathbb{E}_i(\mathbf{P})^{-1} \varsigma_i \end{bmatrix} > 0. \quad (2.61)$$

Pre and post multiplying (2.61) by $\text{diag}(\varrho_i^{-1}, I, \varsigma_i^{-1})$, we obtain that (2.17) holds, showing the result. ■

Coordinate Descent Algorithm

Note that the constraint (2.58) is a BMI since the term $\bar{\mathcal{C}}_{\eta i}' \bar{\mathcal{C}}_{\eta i}$ is quadratic. Hence, it is necessary to use an appropriate method to solve this type of problem. A possible procedure to solve this BMI is to implement a Coordinate Descent Algorithm, as in

(CARVALHO et al., 2020a; CARVALHO; OLIVEIRA; COSTA, 2020). For this define $\bar{\psi} = \{Z_i, X_i, \bar{\nabla}_i, O_i, \bar{C}_{\eta_i}, i \in \mathbb{K}\}$, $\mathbf{T} = \{T_i, i \in \mathbb{K}\}$, and $\mathcal{S}_i(\bar{\psi}, \xi, \mathbf{T})$ the inequality in (2.58) with the variables $\bar{\psi}$, ξ and replacing the block (1,1) in (2.58) by $Z_i + T_i$ (that is replacing $F_i'F_i$ by T_i in the block (1,1)). For $\mathbf{T}^k = \{T_i^k, i \in \mathbb{K}\}$, with $T_i^k \geq 0$ fixed, solve the following LMI optimization problem, denoted by $Pr(\mathbf{T}^k)$: $\max \xi$ subject to the following LMIs: $\mathcal{S}_i(\bar{\psi}, \xi, \mathbf{T}^k) > 0$, (2.58) and

$$\begin{bmatrix} T_i^k & \bullet \\ \bar{C}_{\eta_i} & I \end{bmatrix} \geq 0. \quad (2.62)$$

Suppose that there is a solution $\bar{\psi}^k, \xi^k$ for this problem. Set now $\mathbf{T}_i^{k+1} = \bar{C}_{\eta_i}^{k'} \bar{C}_{\eta_i}^k$ and solve the problem $Pr(\mathbf{T}^{k+1})$. Consider that the solution for this problem is $\bar{\psi}^{k+1}, \xi^{k+1}$. From (2.62) we have that $T_i^k \geq \bar{C}_{\eta_i}^{k'} \bar{C}_{\eta_i}^k = T_i^{k+1} \geq \bar{C}_{\eta_i}^{k+1'} \bar{C}_{\eta_i}^{k+1}$, and $\mathcal{S}_i(\bar{\psi}^{k+1}, \xi^{k+1}, \mathbf{T}^k) \geq \mathcal{S}_i(\bar{\psi}^{k+1}, \xi^{k+1}, \mathbf{T}^{k+1}) > 0$, that is, $\bar{\psi}^{k+1}, \xi^{k+1}$ is feasible for problem $Pr(\mathbf{T}^k)$, so that $\xi^{k+1} \leq \xi^k$. Based on that, we propose the following algorithm.

Algorithm 1: Coordinate Descent Algorithm

Input: $\mathbf{T}^0, t_{\max}, \epsilon$

Output: $\mathcal{A}_{\eta_i}, \mathcal{A}_{\eta_i}, \bar{C}_{\eta_i}$ as in Theorem 3.

- 1 At iteration k use \mathbf{T}^k to solve the LMI optimization problem $Pr(\mathbf{T}^k)$ posed above. Obtain a solution $\bar{\psi}^k, \xi^k$.
 - 2 If $\frac{\xi^{k-1} - \xi^k}{\xi^{k-1}} \geq \epsilon$ and $k \leq t_{\max}$, go back to step 1 using $\mathbf{T}_i^{k+1} = \bar{C}_{\eta_i}^{k'} \bar{C}_{\eta_i}^k$. Otherwise stop the algorithm.
-

Since the sequence $\xi^k > 0$ is decreasing, it will converge and the algorithm will stop at some iteration.

Remark 6. *Observe that in Algorithm 1, the initial condition has impact on the feasibility or convergence speed of the algorithm. Note that, the first iteration finds a feasible solution the CDA convergence is guaranteed, meaning that the final results will be equal or better than the initial condition. A possible way to define the $\mathbf{T}_i^0 = \bar{C}_{\eta_i}^{0'} \bar{C}_{\eta_i}^0$, where $\bar{C}_{\eta_i}^0$ is obtained using Lemma 4.*

It is important to point out that the FDFs obtained using Lemma 4 and Theorem 3 have a similar structure, thus, this key aspect allows us to solve both problems simultaneously. Based on this property, we present an approach to solve the mixed H_∞/H_- problem, in a similar way as presented in (OLIVEIRA; COSTA, 2018). We need to impose the following constraints

$$\psi = \{\gamma, \xi, Z_i = Z_i, X_i = X_i, \nabla_i = \bar{\nabla}_i, O_i = O_i, C_{\eta_i} = \bar{C}_{\eta_i}\}. \quad (2.63)$$

Set

$$\Psi = \{\psi \text{ as in (2.63) such that the LMIs (2.54), and the BMIs (2.58),} \\ \text{are simultaneously feasible}\}. \quad (2.64)$$

Theorem 5. *There exists a mode-dependent FDF as in (2.24) such that $\|G_{aug}\|_\infty^2 < \gamma$ and $\|G_{aug}\|_-^2 > \xi$ if there exists $\psi \in \Psi$, where Ψ is defined as in (2.64). If a feasible solution is obtained then a suitable FDF is given by $\mathcal{A}_{\eta i} = (\mathbb{E}_i(Z) - \mathbb{E}_i(X))^{-1}O_i$, $\mathcal{B}_{\eta i} = (\mathbb{E}_i(Z) - \mathbb{E}_i(X))^{-1}\nabla_i$, $\mathcal{C}_{\eta i}$, $\mathcal{M}_{\eta i} = (\mathbb{E}_i(Z) - \mathbb{E}_i(X))^{-1}\Gamma_i$, $\forall i \in \mathbb{K}$.*

Proof: The proof follows directly from the proofs of Theorems 4 and 3. ■

Remark 7. *Observe that is not necessary to mention the LMI constraint (2.59) in (2.64), since (2.58) already has this constraints within.*

We define the mixed objective function

$$g(\gamma, \xi) = \sigma\gamma - (1 - \sigma)\xi, \quad (2.65)$$

where $\|G\|_\infty^2 < \gamma$, $\|G\|_-^2 > \xi$, and $\sigma > 0$ is a weighting scalar.

The goal is to minimize (2.65) subject to $\psi \in \Psi$. If one of the bounds is fixed the problem will be to minimize the objective function under the constraint $\|G\|_\infty^2 < \gamma$ or $\|G\|_-^2 > \xi$.

2.3.4 Simulations Results

As an illustrative example we use a coupled-tank, the modeling is described in the Appendix A. The matrices that compose the state-space system are

$$\begin{aligned} A_{1,2} &= \begin{bmatrix} -0.0239 & -0.0127 \\ 0.0127 & -0.0285 \end{bmatrix}, & B_{1,2} &= \begin{bmatrix} 0.7100 & 0 \\ 0 & 0.7100 \end{bmatrix}, \\ J_{1,2} &= \begin{bmatrix} 0.0071 & 0 \\ 0 & 0.0071 \end{bmatrix}, & F_{1,2} &= 0.1 \begin{bmatrix} 0.7100 \\ 0 \end{bmatrix}, & D_{1,2} &= \begin{bmatrix} 0.0100 & 0 \\ 0 & 0.0100 \end{bmatrix}, \\ E_{1,2} &= \begin{bmatrix} 0 \\ 0 \end{bmatrix}, & A_{\mathcal{W}} &= 0.25, & B_{\mathcal{W}} &= 0.5, & C_{\mathcal{W}} &= 0.75, & D_{\mathcal{W}} &= 0.5, \end{aligned}$$

As seen above, the matrix that represents the fault in the actuator (F) is a 10% ratio of the input matrices B . This choice of value represents the eventual fault in the actuator. Another aspect is that (F) should not be switched since the fault has no direct relationship with the network behavior. Regarding the sensor fault matrix (E) we consider it to be null since we are only considering an actuator fault and not a sensor fault. To model the

communication loss between the FDF and plant sensors, the matrices C_i are defined as

$$C_1 = \begin{bmatrix} 1 & 0 \\ 0 & 1 \end{bmatrix}, \quad C_2 = \begin{bmatrix} 0 & 0 \\ 0 & 0 \end{bmatrix}.$$

The transition matrix is defined as $\mathbb{P} = \begin{bmatrix} 0.80 & 0.2 \\ 0.575 & 0.425 \end{bmatrix}$, which represents a network with a packet loss rate of 25%.

Remark 8. *It is important to clarify the distinction between the concept of communication loss and sensor fault. The first one represents the information lost during the transmission, which is a network problem. The latter represents an equipment (sensor) problem where data gathering is compromised.*

Remark 9. *It is possible to implement more complex network models by changing the number of modes, and imposing different structures in the transition matrix \mathbb{P} . However, this is not the main goal of this work. Some works that tackle this subject are (BOLCH et al., 2006).*

Using Theorem 1 and the aforementioned systems we get,

$$\begin{aligned} \mathcal{A}_{\eta_1} &= \begin{bmatrix} 0.0021 & -0.0020 \\ 0.0021 & -0.0020 \end{bmatrix}, & \mathcal{A}_{\eta_2} &= \begin{bmatrix} 0.0058 & -0.0375 \\ 0.0478 & -0.0669 \end{bmatrix}, & \mathcal{M}_{\eta_1} &= \begin{bmatrix} 0.1342 & 0.0698 \\ -0.5776 & 0.7818 \end{bmatrix}, \\ \mathcal{M}_{\eta_2} &= \begin{bmatrix} 1.1986 & 0.0922 \\ 0.3684 & 0.9221 \end{bmatrix}, & \mathcal{B}_{\eta_1} &= \begin{bmatrix} -0.0259 & -0.0107 \\ 0.0106 & -0.0265 \end{bmatrix}, & \mathcal{B}_{\eta_2} &= \begin{bmatrix} 0 & 0 \\ 0 & 0 \end{bmatrix}, \\ \mathcal{C}_{\eta_1} &= \begin{bmatrix} -0.0489 & 0.0469 \end{bmatrix}, & \mathcal{C}_{\eta_2} &= \begin{bmatrix} 0 & 0 \end{bmatrix}, & \mathcal{D}_{\eta_1} &= \begin{bmatrix} 0.0523 & -0.1963 \end{bmatrix}, & \mathcal{D}_{\eta_2} &= \begin{bmatrix} 0 & 0 \end{bmatrix}, \end{aligned} \quad (2.66)$$

and the upper bound obtained was $\gamma = 1.4142$. Now considering Theorem 2 we obtained

$$\begin{aligned} \mathcal{A}_{\eta_1} &= \begin{bmatrix} -0.2535 & 0.2444 \\ 0.2540 & -0.2621 \end{bmatrix}, & \mathcal{A}_{\eta_2} &= \begin{bmatrix} -0.0132 & -0.0070 \\ 0.0070 & -0.0157 \end{bmatrix}, & \mathcal{M}_{\eta_1} &= \begin{bmatrix} 0.6814 & -0.2061 \\ -0.2060 & 0.6814 \end{bmatrix}, \\ \mathcal{M}_{\eta_2} &= \begin{bmatrix} 0.7100 & 0.0000 \\ 0.0000 & 0.7100 \end{bmatrix}, & \mathcal{B}_{\eta_1} &= \begin{bmatrix} 0.4334 & -0.4475 \\ -0.4419 & 0.4521 \end{bmatrix}, & \mathcal{B}_{\eta_2} &= \begin{bmatrix} 0 & 0 \\ 0 & 0 \end{bmatrix}, \\ \mathcal{C}_{\eta_1} &= \begin{bmatrix} -0.1239 & -0.1239 \end{bmatrix}, & \mathcal{C}_{\eta_2} &= \begin{bmatrix} 0 & 0 \end{bmatrix}, & \mathcal{D}_{\eta_1} &= \begin{bmatrix} -0.3259 & -0.3259 \end{bmatrix}, & \mathcal{D}_{\eta_2} &= \begin{bmatrix} 0 & 0 \end{bmatrix}, \end{aligned} \quad (2.67)$$

and the upper bound obtained was $\lambda = 5.6378$. For the Theorem 3 the FDF obtained was

$$\begin{aligned} \mathcal{A}_{\eta_1} &= \begin{bmatrix} -0.2534 & 0.2617 \\ 0.2605 & -0.2383 \end{bmatrix}, & \mathcal{A}_{\eta_2} &= \begin{bmatrix} -0.01298 & -0.0077 \\ 0.0069 & -0.01668 \end{bmatrix}, & \mathcal{M}_{\eta_1} &= \begin{bmatrix} 0.7399 & -0.1475 \\ -0.1475 & 0.7399 \end{bmatrix}, \\ \mathcal{M}_{\eta_2} &= \begin{bmatrix} 0.7572 & 0.04728 \\ 0.0472 & 0.7573 \end{bmatrix}, & \mathcal{B}_{\eta_1} &= \begin{bmatrix} 0.4330 & -0.4802 \\ -0.4544 & 0.4071 \end{bmatrix}, & \mathcal{B}_{\eta_2} &= \begin{bmatrix} 0 & 0 \\ 0 & 0 \end{bmatrix}, \\ \mathcal{C}_{\eta_1} &= \begin{bmatrix} -0.0379 & -0.1094 \end{bmatrix}, & \mathcal{C}_{\eta_2} &= \begin{bmatrix} -0.0061 & -0.0370 \end{bmatrix}, \\ \mathcal{D}_{\eta_1} &= \begin{bmatrix} 0.0036 & 0.0096 \end{bmatrix}, & \mathcal{D}_{\eta_2} &= \begin{bmatrix} 0 & 0 \end{bmatrix}, \end{aligned} \quad (2.68)$$

the upper bound $\gamma = 5$ and $\lambda = 5.8224$. At last, the FDF obtained using Theorem 5,

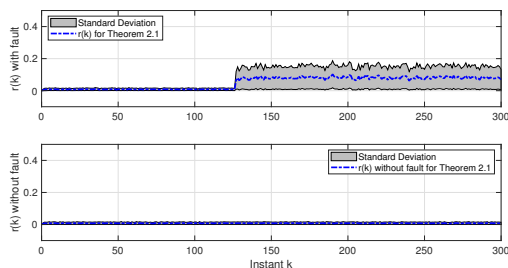
$$\begin{aligned} \mathcal{A}_{\eta_1} &= \begin{bmatrix} -0.2979 & -0.0109 \\ -0.0008 & -0.3017 \end{bmatrix}, & \mathcal{A}_{\eta_2} &= \begin{bmatrix} -0.0239 & -0.0127 \\ 0.0127 & -0.0285 \end{bmatrix}, & \mathcal{M}_{\eta_1} &= \begin{bmatrix} 0.7100 & -0.0000 \\ -0.0000 & 0.7100 \end{bmatrix}, \\ \mathcal{M}_{\eta_2} &= \begin{bmatrix} 0.7101 & -0.0000 \\ -0.0000 & 0.7101 \end{bmatrix}, & \mathcal{B}_{\eta_1} &= \begin{bmatrix} 0.2740 & -0.0018 \\ 0.0135 & 0.2732 \end{bmatrix}, & \mathcal{B}_{\eta_2} &= \begin{bmatrix} 0 & 0 \\ 0 & 0 \end{bmatrix}, \end{aligned}$$

$$\mathcal{C}_{\eta_1} = [0.4896 \ 0.1075], \quad \mathcal{C}_{\eta_2} = [3.1892 \ -2.0479], \quad (2.69)$$

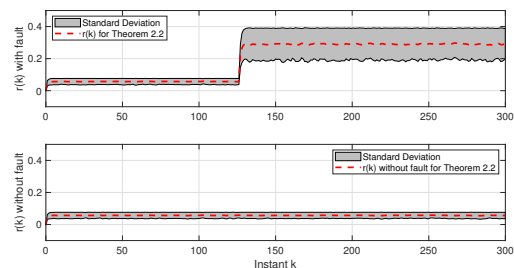
with the upper and lower bounds $\gamma = 1.2270$ and $\xi = 1.01$.

2.3.4.1 Monte Carlo Simulation

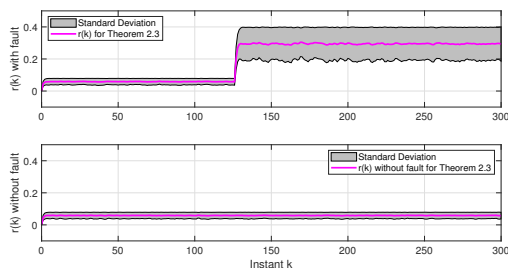
As previously discussed, the system is a coupled tank, the fault signal implemented in this simulation is an abnormal input on the first tank at $k = 125$. The intensity of this input is equal to 10% of the regular input. Also considering the threshold $\text{TH} = 0.3$. Under this specific situation, we present five graphical results from the simulation. The first four results are shown in Figs. 10a, 10b, 10c, 10d where the mean and standard deviation of the residue signal for each theorem are given, and the fifth result is the evaluation signal $\text{EVAL}(k)$ obtained for all three cases and shown in Fig. 12



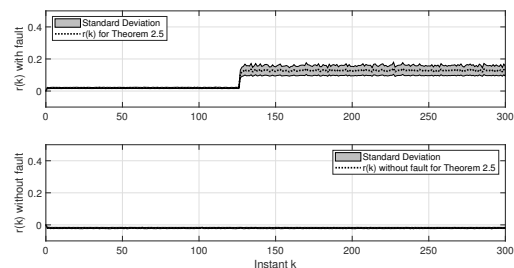
(a) Mean and standard deviation for residue signal obtained using Theorem 1.



(b) Mean and standard deviation for residue signal obtained using Theorem 2



(c) Mean and standard deviation for residue signal obtained using Theorem 3

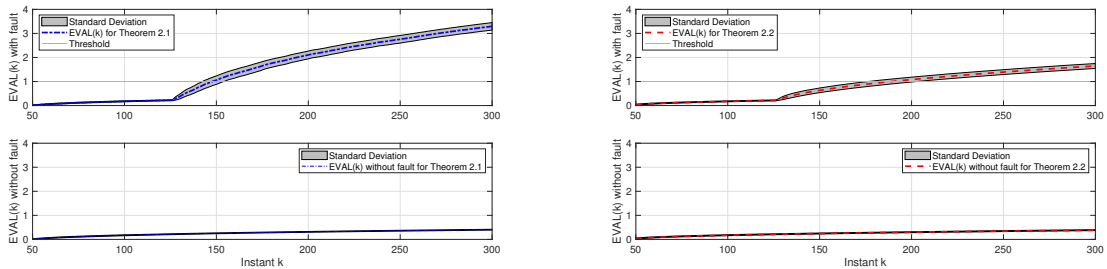


(d) Mean and standard deviation for residue signal obtained using Theorem 5

Figure 10: Mean and standard deviation for the residue signal obtained using FDF designed using the Theorems 1, 2, 3, 5. There are two graphics for each theorem, representing when the system is subjected to a fault and another graphic without fault.

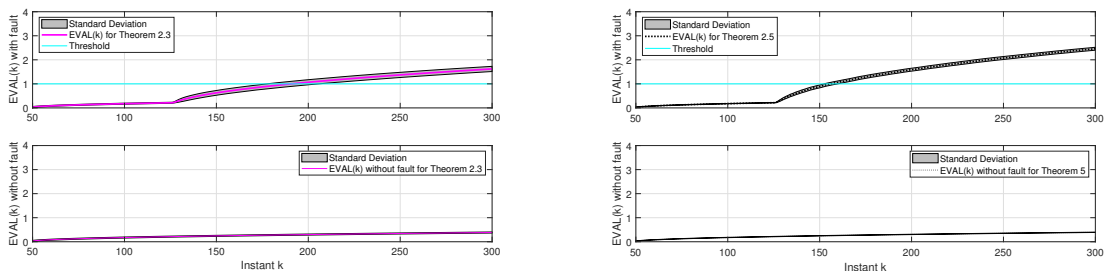
Examining Figs. 10a, 10b, 10c, 10d it is possible to observe that the lower value of standard deviation is obtained using Theorem 5, and the results obtained using Theorem 1 provided the higher value. Note that, the higher standard deviation is directly connected with the number of false alarms. Therefore, the results obtained via Theorem 5 will present a lower chance of false alarms. Another important piece of information is that all the

residue signals obtained with the presence of fault were close to zero, which is the expected behavior.



(a) Mean and standard deviation for evaluation function obtained using Theorem 1.

(b) Mean and standard deviation for evaluation function obtained using Theorem 2



(c) Mean and standard deviation for evaluation function obtained using Theorem 3

(d) Mean and standard deviation for evaluation function obtained using Theorem 5

Figure 11: Mean and standard deviation for the evaluation function obtained using FDF designed using the Theorems 1, 2, 3, 5. There are two graphics for each theorem, representing when the system is subjected to a fault and another graphic without fault.

Inspecting Figs. 11a, 11b, 11c, 11d we may state that all four approaches properly detected the fault. However, there is a performance discrepancy between the approaches, the fastest detection was obtained using Theorem 1, detecting the fault in the interval of $k = [143 \ 155]$ (12 range). However, the result obtained using Theorem 5 presented the most reliable results since the detection interval was $k = [153 \ 160]$ (7 range).

In Fig. 12 a comparison with all the four approaches is presented, where solely the mean value of the evaluation function is provided. It is clear that the results for Theorem 1 is faster, but the difference to the result obtained using Theorem 5 is equal to 6, and also there is an overlap in those intervals. Therefore, we may conclude that all four results are viable solution Fault Detection and Isolation problem for the MJLS framework.

2.4 Fault Accommodation Formulation

IN this section, we present the Fault Accommodation problem formulation and propose some theoretical approaches to solve such a problem. The formulation we present here

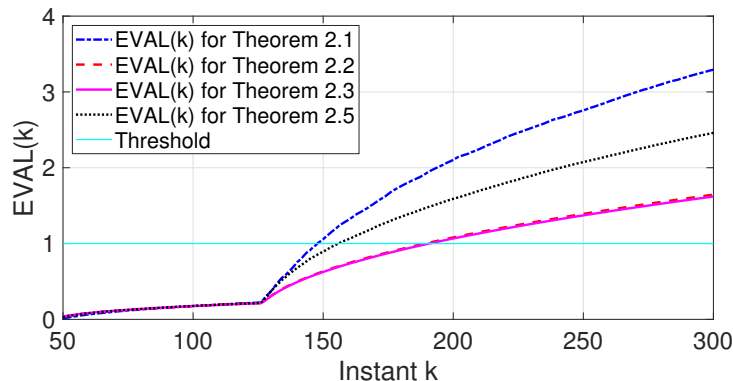


Figure 12: Average value of the evaluation function signal for four distinct cases, where the blue curve represent the result using Theorem 1, the red curve represent the result obtained via Theorem 2, the magenta curve represent the results through Theorem 3, the black curve denote the result for Theorem 5, and the cyan line denotes the threshold TH.

is a particular case of a model-based Active Fault Accommodation Control (FAC) problem, where an auxiliary controller is designed with the only purpose of mitigating the fault effect on the system performance.

The MJLS for the fault-compensation problem is described as

$$\mathcal{G} : \begin{cases} x(k+1) = A_{\theta(k)}x(k) + B_{\theta(k)}u(k) + B_{\theta(k)}h(k) + J_{\theta(k)}w(k) + F_{\theta(k)}f(k), \\ y(k) = C_{\theta(k)}x(k) + D_{\theta(k)}w(k), \\ x(0) = x_0, \theta(0) = \theta_0, \end{cases} \quad (2.70)$$

where the system states are denoted by $x(k) \in \mathbb{R}^{n_x}$, the control input is represented by $u(k) \in \mathbb{R}^{n_u}$, the exogenous input is $w(k) \in \mathbb{R}^{n_d}$, the fault signal is denoted by $f(k) \in \mathbb{R}^{n_f}$ and the measured output is represented by $y(k) \in \mathbb{R}^{n_y}$.

2.4.1 Fault Accommodation Controller

The Fault Compensation Controller scheme is presented in Fig. 13. We see from this scheme that our main goal is to provide an FAC (\mathcal{K}_{c_i}) that generates the control signal $h(k)$ with the sole purpose of compensating the fault signal $f(k)$. The control signal $h(k)$ should be close to zero when the system is working properly.

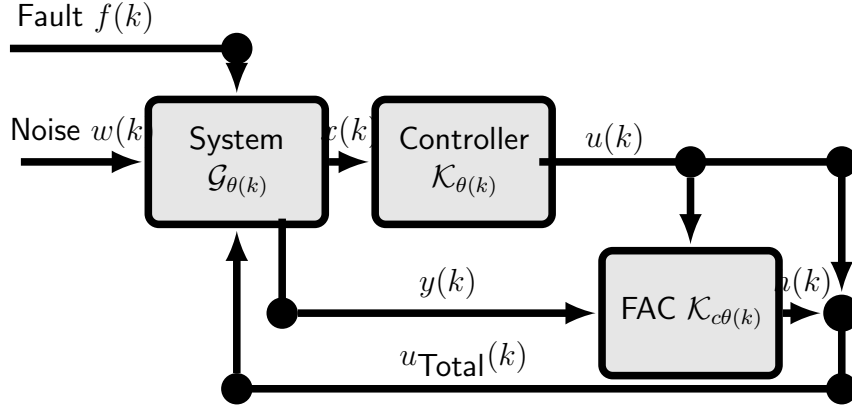


Figure 13: Fault accommodation control scheme diagram used to design the controller.

The FAC can be described as

$$\mathcal{K}_c : \begin{cases} \eta(k+1) = \mathfrak{A}_{\theta(k)}\eta(k) + \mathfrak{M}_{\theta(k)}u(k) + \mathfrak{B}_{\theta(k)}y(k), \\ h(k) = \mathfrak{C}_{\theta(k)}\eta(k), \\ \eta(0) = \eta_0, \theta(0) = \theta_0, \end{cases} \quad (2.71)$$

where $\eta \in \mathbb{K}^q$ represents the FAC, $u(k)$ and $y(k)$, are respectively, the control signal from the regular controller and the measured signal from the system.

The mode-dependent state-feedback controller is

$$u(k) = -K_{\theta(k)}x(k), \quad (2.72)$$

where $x(k) \in \mathbb{R}^n$ represents the states in (2.70). From that, we define $u_{\text{Total}}(k)$ as

$$u_{\text{Total}}(k) = u(k) + h(k). \quad (2.73)$$

Considering system (2.70), the state feedback control law (2.72), and the FAC (2.71), as presented in Fig.13, the augmented system is given by

$$\mathcal{G}_{\text{aug}} : \begin{cases} \bar{x}(k+1) = \bar{A}_{\theta(k)}\bar{x}(k) + \bar{B}_{\theta(k)}\bar{w}(k), \\ \bar{z}(k) = \bar{C}_{\theta(k)}\bar{x}(k) + \bar{D}_{\theta(k)}\bar{w}(k), \\ \bar{x}(0) = \eta_0, \end{cases}$$

where $\bar{x}(k) = [x(k)' \ \eta(k)']'$ and $\bar{w}(k) = [w(k)' \ f(k)']'$, with the following augmented

matrices are

$$\begin{aligned}\bar{A}_i &= \begin{bmatrix} A_i - B_i K_i & B_i \mathfrak{C}_i \\ \mathfrak{B}_i C_i - \mathfrak{M}_i K_i & \mathfrak{A}_i \end{bmatrix}, \quad \bar{B}_i = \begin{bmatrix} J_i & F_i \\ \mathfrak{B}_i D_i & 0 \end{bmatrix}, \\ \bar{C}_i &= [0 \quad -B_i \mathfrak{C}_i], \quad \bar{D}_i = [0 \quad F_i].\end{aligned}\tag{2.74}$$

The main goal of this paper is to design a FAC as presented in (2.71) where the difference $o(k) = F_i f(k) - B_i h(k)$ is close to zero. Therefore, the optimization problem is described as

$$\sup_{w \neq 0, w \in \mathcal{L}_2, \theta_0 \in \mathbb{N}} \frac{\|o\|_2}{\|w\|_2} < \gamma.\tag{2.75}$$

2.4.2 Theoretical Results

2.4.2.1 \mathcal{H}_∞ Fault Accomodation Control Design for MJLS

Theorem 6. *There exists a mode-dependent FAC as described in (2.71) satisfying the constraint (2.75) for some $\gamma > 0$ if there exist symmetric matrices Z_i , X_i , and the matrices Δ_i , ∇_i , Ω_i , and Θ_i with compatible dimensions such that*

$$\begin{bmatrix} Z_i & \bullet & \bullet & \bullet & \bullet & \bullet & \bullet \\ Z_i & X_i & \bullet & \bullet & \bullet & \bullet & \bullet \\ 0 & 0 & \gamma I & \bullet & \bullet & \bullet & \bullet \\ 0 & 0 & 0 & \gamma I & \bullet & \bullet & \bullet \\ \Pi_i^{5,1} & \Pi_i^{5,2} & \mathbb{E}_i(X)J_i & \mathbb{E}_i(X)F_i & \Pi_i^{5,5} & \bullet & \bullet \\ \Pi_i^{6,1} & \Pi_i^{6,2} & \mathbb{E}_i(X)J_i + \Theta_i D_i & \mathbb{E}_i(X)F_i & \mathbb{E}_i(X) & \mathbb{E}_i(X) & \bullet \\ -\Delta_i & 0 & 0 & \mathbb{E}_i(X) & 0 & 0 & \text{Her}(\mathbb{E}_i(X)) - I \end{bmatrix} > 0,\tag{2.76}$$

with

$$\begin{aligned}\Pi_i^{5,1} &= \mathbb{E}_i(X)A_i - \mathbb{E}_i(X)B_i K_i + \Delta_i, \\ \Pi_i^{6,1} &= \mathbb{E}_i(X)A_i - \mathbb{E}_i(X)B_i K_i + \Theta_i C_i + \nabla_i K_i + \Delta_i + \Omega_i, \\ \Pi_i^{6,2} &= \mathbb{E}_i(X)A_i - \mathbb{E}_i(X)B_i K_i + \Theta_i C_i + \nabla_i K_i, \\ \Pi_i^{5,2} &= \mathbb{E}_i(X)A_i - \mathbb{E}_i(X)B_i K_i, \quad \Pi_i^{5,5} = \text{Her}(\mathbb{E}_i(X)) - \mathbb{E}_i(Z),\end{aligned}$$

holds for all $i \in \mathbb{K}$. If a feasible solution is obtained, a suitable fault-compensation controller is given by $\mathfrak{A}_i = (\mathbb{E}_i(Z) - \mathbb{E}_i(X))^{-1} \Omega_i$, $\mathfrak{M}_i = (\mathbb{E}_i(Z) - \mathbb{E}_i(X))^{-1} \nabla_i$, $\mathfrak{B}_i = (\mathbb{E}_i(Z) - \mathbb{E}_i(X))^{-1} \Theta_i$, and $\mathfrak{C}_i = (\mathbb{E}_i(Z) - \mathbb{E}_i(X))^{-1} B_i^{-1} \Omega_i$.

Proof: The goal of the proof is to show that if the inequality (2.76) holds, then (2.5) is also satisfied. First, consider the following structures for the matrices

$$\begin{aligned}P_i &= \begin{bmatrix} X_i & U_i \\ U_i' & \hat{X}_i \end{bmatrix}, \quad P_i^{-1} = \begin{bmatrix} Y_i & V_i \\ V_i' & \hat{Y}_i \end{bmatrix}, \\ \mathbb{E}_i(P) &= \begin{bmatrix} \mathbb{E}_i(X) & \mathbb{E}_i(U) \\ \mathbb{E}_i(U)' & \mathbb{E}_i(\hat{X}) \end{bmatrix}, \quad \mathbb{E}_i(P)^{-1} = \begin{bmatrix} R_{1i} & R_{2i} \\ R_{2i}' & R_{3i} \end{bmatrix},\end{aligned}\tag{2.77}$$

and define the matrices Q_i and T_i as

$$T_i = \begin{bmatrix} I & I \\ V_i' Y_i^{-1} & 0 \end{bmatrix}, \quad Q_i = \begin{bmatrix} \mathbb{E}_i(X) & \mathbb{E}_i(X) \\ 0 & \mathbb{E}_i(U) \end{bmatrix}'.$$

As demonstrated in (GONÇALVES; FIORAVANTI; GEROMEL, 2010), by imposing that $U_i = Z_i - X_i$, it follows from (2.77) that $Y_i = V_i'$, $V_i = Z_i^{-1}$. Setting the following matrices

$$\begin{aligned} T_i' P_i T_i &= \begin{bmatrix} Y_i^{-1} & Y_i^{-1} \\ Y_i^{-1} & X_i \end{bmatrix}, \quad Q_i' \bar{A}_i T_i = \begin{bmatrix} \nu_i^{11} & \mathbb{E}_i(X) A_i - \mathbb{E}_i(X) B_i K_i \\ \nu_i^{21} & \nu_i^{22} \end{bmatrix}, \\ \nu_i^{11} &= \mathbb{E}_i(X) A_i - \mathbb{E}_i(X) B_i K_i + \mathbb{E}_i(X) B_i \mathfrak{C}_i, \\ \nu_i^{21} &= \mathbb{E}_i(X) A_i - \mathbb{E}_i(X) B_i K_i + \mathbb{E}_i(U) \mathfrak{B}_i C_i - \mathbb{E}_i(U) \mathfrak{M}_i K_i - \mathbb{E}_i(X) B_i \mathfrak{C}_i, \\ \nu_i^{22} &= \mathbb{E}_i(X) A_i - \mathbb{E}_i(X) B_i K_i + \mathbb{E}_i(U) \mathfrak{B}_i C_i - \mathbb{E}_i(U) \mathfrak{M}_i K_i \\ Q_i' \bar{B}_i &= \begin{bmatrix} \mathbb{E}_i(X) J_i & \mathbb{E}_i(X) F_i \\ \mathbb{E}_i(X) J_i + \mathbb{E}_i(U) \mathfrak{B}_i D_i & \mathbb{E}_i(X) F_i \end{bmatrix}, \\ \bar{C}_i T_i &= [-B_i \mathfrak{C}_i \ 0], \quad \bar{D}_i = [0 \ F_i]. \end{aligned}$$

as presented in (OLIVEIRA; BERNUSSOU; GEROMEL, 1999), it is possible to write

$$\text{Her}(\mathbb{E}_i(X)) - \mathbb{E}_i(Z) \leq \mathbb{E}_i(X)' \mathbb{E}_i(Z)^{-1} \mathbb{E}_i(X).$$

This step allow us to write

$$Q_i' \mathbb{E}_i(P)^{-1} Q_i = \begin{bmatrix} \text{Her}(\mathbb{E}_i(X)) - \mathbb{E}_i(Z) & \mathbb{E}_i(X) \\ \mathbb{E}_i(X) & \mathbb{E}_i(X) \end{bmatrix}.$$

Therefore the inequality given in (2.76) can be written as

$$\begin{bmatrix} T_i' P_i T_i & \bullet & \bullet & \bullet \\ 0 & \gamma I & \bullet & \bullet \\ Q_i' \bar{A}_i T_i & Q_i' \bar{B}_i & Q_i' \mathbb{E}_i(P)^{-1} Q_i & \bullet \\ \mathbb{E}_i(X) \bar{C}_i T_i & \mathbb{E}_i(X) \bar{D}_i & 0 & \text{Her}(\mathbb{E}_i(X)) - I \end{bmatrix} > 0.$$

Applying the congruence transform

$$\text{diag}(T_i^{-1}, I, Q_i^{-1}, \mathbb{E}_i(X)^{-1}),$$

in this last inequality, the following constraint is obtained

$$\begin{bmatrix} P_i & \bullet & \bullet & \bullet \\ 0 & \gamma I & \bullet & \bullet \\ \bar{A}_i & \bar{B}_i & \mathbb{E}_i(P)^{-1} & \bullet \\ \bar{C}_i & \bar{D}_i & 0 & I \end{bmatrix} > 0,$$

which, by applying a Schur complement, can be recognized as the BRL (2.5), concluding the proof. ■

Remark 10. Note that, from (2.76), matrix B_i in (2.70) should be invertible. However, by requiring it only to be square, we can obtain the matrix \mathfrak{C}_i using a Penrose inverse.

2.4.3 Simulations Results

To disclose the usability of the proposed approach we use the same coupled tank model example used in the previous section. A proper discussion of the modeling process is presented in Appendix A. The matrices that compose the coupled-tank system are:

$$A_{1,2} = \begin{bmatrix} -0.024 & -0.013 \\ 0.013 & -0.029 \end{bmatrix}, \quad B_{1,2} = \begin{bmatrix} 0.71 & 0 \\ 0 & 0.71 \end{bmatrix}, \quad J_{1,2} = 0.1B_{1,2}, \quad F_{1,2} = \text{diag}(I_1, 0_1), \\ C_1 = I_2, \quad C_2 = 0_2, \quad D_{1,2} = 0.1I_2.$$

Additionally, consider that the transition matrix is given by

$$\mathbb{P} = \begin{bmatrix} 0.8 & 0.2 \\ 0.8 & 0.2 \end{bmatrix}, \quad (2.78)$$

The nominal controller obtained using the results in (GONÇALVES; FIORAVANTI; GEROMEL, 2012) is

$$K_1 = \begin{bmatrix} -1.3456 & 0.0154 \\ -0.0154 & -1.3398 \end{bmatrix}, \quad K_2 = \begin{bmatrix} -0.0315 & 0.0167 \\ -0.0167 & -0.0375 \end{bmatrix},$$

and the \mathcal{H}_∞ norm value is $\gamma = 0.1276$. The fault-compensation controller obtained designed using Theorem 6 is

$$\mathfrak{A}_{c1} = \begin{bmatrix} 0.2233 & -0.0080 \\ -0.0059 & 0.2731 \end{bmatrix}, \quad \mathfrak{A}_{c2} = \begin{bmatrix} 0.0488 & -0.003 \\ -0.0013 & 0.0651 \end{bmatrix}, \\ \mathfrak{B}_{c1} = \begin{bmatrix} -0.1745 & 0.0041 \\ 0.0045 & -0.2079 \end{bmatrix}, \quad \mathfrak{B}_{c2} = \begin{bmatrix} -0.1745 & 0.0041 \\ 0.0045 & -0.2079 \end{bmatrix}, \\ \mathfrak{M}_{c1} = \begin{bmatrix} -0.1701 & 0.0063 \\ 0.0016 & -0.2018 \end{bmatrix}, \quad \mathfrak{M}_{c2} = \begin{bmatrix} -0.1701 & 0.0063 \\ 0.0016 & -0.2018 \end{bmatrix}, \\ \mathfrak{C}_{c1} = \begin{bmatrix} -0.4597 & 0.0239 \\ -0.0006 & -0.5075 \end{bmatrix}, \quad \mathfrak{C}_{c2} = \begin{bmatrix} -0.4596 & 0.0239 \\ -0.0006 & -0.5075 \end{bmatrix}.$$

and the \mathcal{H}_∞ norm value is $\gamma = 1.9002$.

2.4.3.1 Monte Carlo Simulation

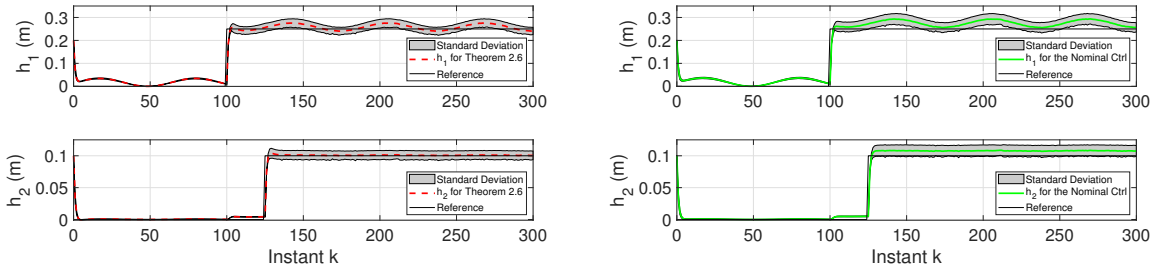
The fault signal implemented is a sinusoidal wave as $0.025\sin(k)$. The noise signal is a white noise with zero mean and deviation equal to 0.01. The results presented herein were obtained via Monte Carlo simulations with 300 rounds. In all the simulations we made a comparison between the proposed approach (Theorem 6), and a regular solution using only the controller designed using (GONÇALVES; FIORAVANTI; GEROMEL, 2012). The simulation results are organized in two sets of six subfigures, where the first set contains the results when there is a fault and the second set shows the results for the case without fault. Each set is organized as follows: the first graphic represents the mean and standard deviation for both tank levels h_1 and h_2 obtained using Theorem 6,

the second graphic represents the mean and standard deviation for both tank levels h_1 and h_2 obtained using solely the nominal controller, and the third graphic compares the mean of both previous graphics. The fourth graphic is the mean and standard deviation of the control signal obtained using Theorem 6, the fifth graphic is the mean and standard deviation of the control signal obtained using the nominal controller and the sixth graphic is the comparison of the fourth and fifth graphics. In Fig. 14c it is possible to observe that the fault is compensated for both levels, which can be seen by comparing the mean value of the system states using the accommodation and the nominal controller. In both graphics the compensation is noticeable, the sinusoidal behavior is mitigated in both levels. Fig. 14a, and 14b show that the standard deviation for both the plant states are slightly higher, approximately 0.05 meter. Additionally, note that the control signals for both actuators, which are shown in Fig. 14f, minimize the fault behavior while keeping the level near the linearization points, that is, 0.25m and 0.1m for the first and second tanks, respectively.

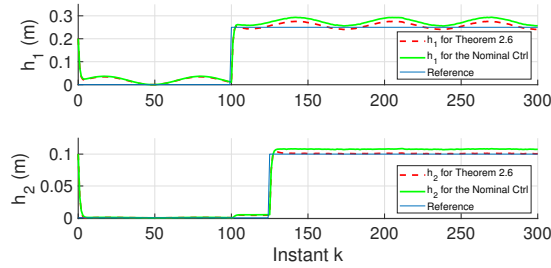
The analyzes of the simulation without fault is important since it shows that the proposed approach in Theorem 6 will not drastically change the nominal behavior of the plant. In Fig. 15c, we can observe that there is not a significant change when comparing it with the nominal results, which is desirable. The step response for the compensated approach is closer to the step signal. As seen in Fig. 15d, Fig. 15e also shows a distinct difference between the graphics, however, this difference is around 0.001, which is acceptable. For the control signal presented in Fig. 15f, there is a difference between the control signals for both actuators. Based on the aforementioned results, we see that the FAC approach proposed in this section indeed mitigates the fault signal as intended. However, there is a slight difference between the FAC and the nominal controller, which was not desired. This phenomenon can be explained due to the step input, as the FAC detects this abrupt change as a fault.

2.5 Concluding remarks

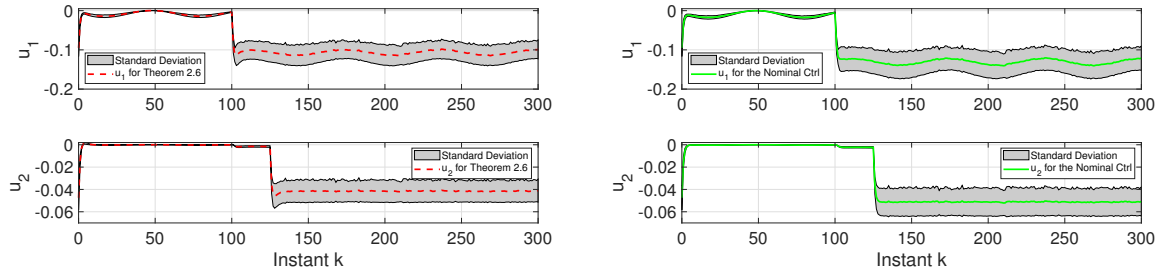
In this chapter, we presented the theoretical results obtained for the design of a FDF and FAC under the MJLS framework, additionally we also presented examples to illustrate the viability of the proposed methods. Analyzing the simulation results allows us to state that all approaches fulfilled the intended purpose. The next chapter presents the design of FDF and FAC with the additional assumption that the Markov mode is not accessible.



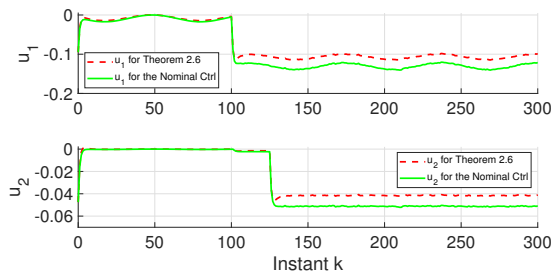
(a) Mean and standard deviation for states signal obtained using Theorem 6. (b) Mean and standard deviation for states signal obtained with the nominal controller.



(c) Mean for state signal obtained using Theorem 6 and the nominal controller.

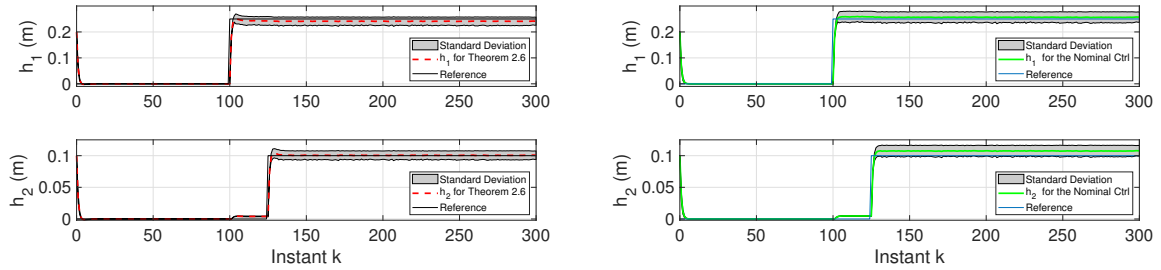


(d) Mean and standard deviation for control signal obtained using Theorem 6. (e) Mean and standard deviation for control signal obtained with the nominal controller.

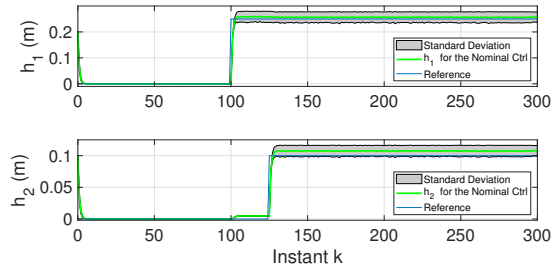


(f) Mean for control signal obtained using Theorem 6 and the nominal controller.

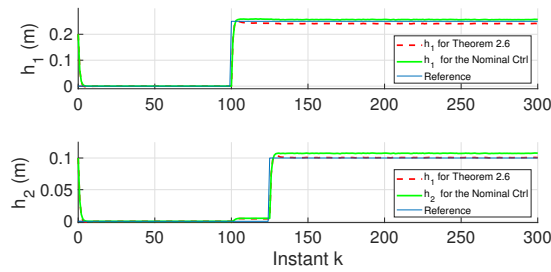
Figure 14: Mean and standard deviation for the states and control signal for the FAC designed with Theorem 6 when the system is subjected to the fault.



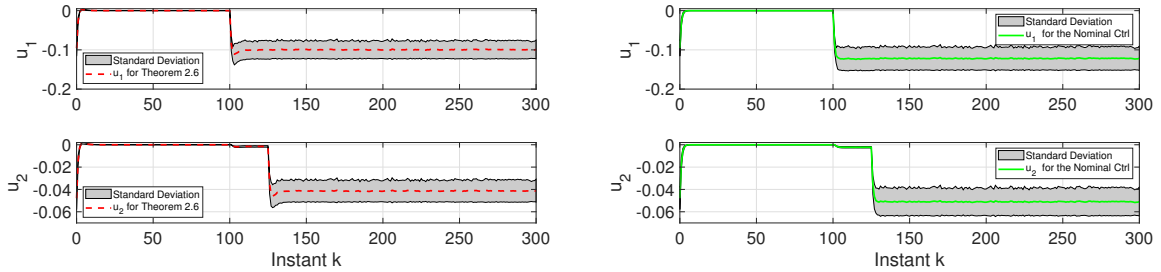
(a) Mean and standard deviation for states signal obtained using Theorem 6.



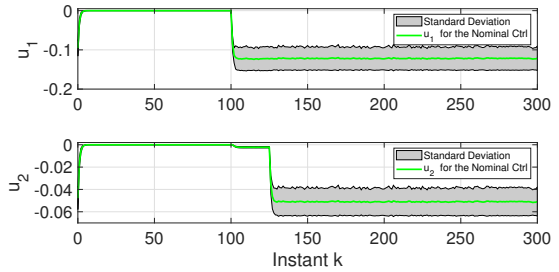
(b) Mean and standard deviation for states signal obtained with the nominal controller.



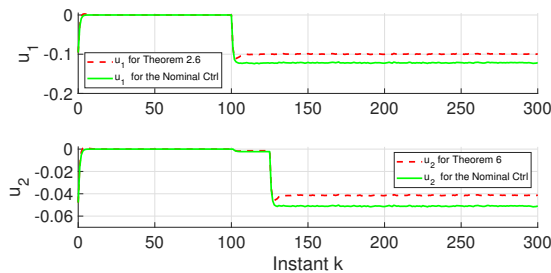
(c) Mean for state signal obtained using Theorem 6 and the nominal controller.



(d) Mean and standard deviation for control signal obtained using Theorem 6.



(e) Mean and standard deviation for control signal obtained with the nominal controller.



(f) Mean for control signal obtained using Theorem 6 and the nominal controller.

Figure 15: Mean and standard deviation for the states and control signal for the FAC designed with Theorem 6 when the system is in its nominal state (faultless).

3 FDF AND FAC FOR MARKOVIAN JUMP LINEAR SYSTEMS WITH PARAMETER ESTIMATION

In this chapter we present the theoretical background necessary to understand the results obtained for the FDF and FAC design herein. The major novelty in this chapter is the assumption that the Markov chain mode is not directly accessible. For that reason the FDF and FAC designed under this assumption do not depend on the Markov chain parameter $\theta(k)$, but instead, the FDF and FAC depend only on an estimation of the Markov chain mode denoted by $\hat{\theta}(k)$. From the practical point of view, the assumption of the Markov mode in our case is interesting, since we are using the Markov chain to model the network behavior, and the hypothesis that the network state is instantaneously acquired might be unrealistic. Therefore, the design methods presented here can circumvent this issue and guarantee the performance simultaneously.

The results presented in this chapter were published in the following journals and conferences:

- Subsection 3.2.1 presented the \mathcal{H}_∞ Fault Detection Filter for Markovian Jump Linear Systems with Estimation Parameter, which was presented in the 9th IFAC Symposium on Robust Control Design (ROCOND'18) (CARVALHO; OLIVEIRA; COSTA, 2018c).
- Subsection 3.2.2 presented the \mathcal{H}_2 Fault Detection Filter for Markovian Jump Linear Systems with Estimation Parameter, which was presented in the Congresso Brasileiro de Automatica 2020 (CARVALHO; OLIVEIRA; COSTA, 2020).
- Section 3.3 presented the Simultaneous Fault Detection and Control for Markovian Jump Linear Systems with Estimation Parameter, which was published in IEEE ACCESS (CARVALHO; OLIVEIRA; COSTA, 2020).
- Section 3.4 presented the Fault Accommodation controller under Markovian jump linear systems with asynchronous modes, which was published in International

3.1 Preliminary for Markovian Jump Linear Systems with Parameter Estimation

Consider the following hidden discrete-time MJLS in the stochastic space $(\Omega, \mathcal{F}, \mathcal{P})$ with filtration \mathcal{F}_k

$$\mathcal{G} : \begin{cases} x(k+1) = A_{\theta(k)\hat{\theta}(k)}x(k) + J_{\theta(k)\hat{\theta}(k)}w(k), \\ z(k) = C_{\theta(k)\hat{\theta}(k)}x(k) + D_{\theta(k)\hat{\theta}(k)}w(k), \end{cases} \quad (3.1)$$

where $x(k) \in \mathbb{R}^{n_x}$ is the state, $y(k) \in \mathbb{R}^{n_y}$ is the measured output, $z(k) \in \mathbb{R}^{n_z}$ is the estimated output, $w(k) \in \mathbb{R}^{n_w}$ is the exogenous input. We also consider that $w(k) \in \mathcal{L}_2$.

Observe that (3.1) depends on two distinct stochastic processes $\theta(k)$ and $\hat{\theta}(k)$. The first one represents a homogeneous Markov chain, with values are in the set \mathbb{N} . Considering that \mathcal{F}_k is a σ -field generated by

$$x(0), w(0), \theta(0), \hat{\theta}(0), \dots, x(k), w(k), \theta(k), \hat{\theta}(k), \quad (3.2)$$

we assume that

$$\text{Prob}(\theta(k+1) = j | \mathcal{F}_k) = \text{Prob}(\theta(k+1) = j | i) = \rho_{ij}, \quad i \in \mathbb{N}. \quad (3.3)$$

It is assumed that $\theta(k)$ is unaccessible and that $\hat{\theta}(k)$ is observable and takes values in the set \mathbb{M} . From the above, we consider the sigma field $\hat{\mathcal{F}}_0$, generated via $x(0), w(0), \theta(0)$, and $\hat{\mathcal{F}}_k$, by $x(0), w(0), \theta(0), \hat{\theta}(0), \dots, x(k), w(k), \theta(k), \hat{\theta}(k)$, $k > 0$, and assume that

$$\text{Prob}(\hat{\theta}(k+1) = \ell | \mathcal{F}_k) = \text{Prob}(\hat{\theta}(k+1) = \ell | i) = \phi_{i\ell}, \quad \ell \in \mathbb{M}. \quad (3.4)$$

We have that $\phi_{i\ell} \geq 0, \forall i \in \mathbb{N}$ is such that $\sum_{\ell \in \mathbb{M}} \phi_{i\ell} = 1$, where the set $\mathbb{M}_i, i \in \mathbb{M}$ is defined as in

$$\mathbb{M}_i \triangleq \{\ell \in \mathbb{M} : \phi_{ij} > 0\}, \cup_{i \in \mathbb{N}} \mathbb{M}_i = \mathbb{M}. \quad (3.5)$$

The detection probability matrix is denoted by $\Upsilon = [\phi_{i\ell}]$, $i \in \mathbb{N}, \ell \in \mathbb{M}_i$. This process is known as a Hidden Markov Model, as in (ROSS, 2014).

We define the transition probability matrix by $\Psi = [\rho_{ij}]$ where $\rho_{ij} = \text{Pr}[\theta_{k+1} = j | \theta_k = i]$

and $\sum_{j=1}^N \rho_{ij} = 1$ for all $i \in \mathbb{K}$. Observe that system (3.1) depends on the index $\theta(k)$, but also depends on the index $\hat{\theta}(k)$, which represents an estimation for the index $\theta(k)$.

3.1.1 Stability for Hidden Markovian Jump Linear Systems

Consider the hidden MJLS (3.1) with $w(k) = 0$ defined on the probability space $(\Omega, \mathfrak{F}, \text{Prob})$ with filtration $\{\mathfrak{F}_k\}$. As presented in (COSTA; FRAGOSO; TODOROV, 2014), the definition of stochastic stability is described as below.

Definition 2. *Considering (3.1) with $w(k) = 0$, system (3.1) is said to be stochastically stable if for any initial condition $\theta(0 = \theta_0)$, and for all second moment x_0 ,*

$$\|x\|_2^2 = \sum_{k=0}^{\infty} \mathbb{E}(\|x(k)\|^2) < \infty. \quad (3.6)$$

For $V = (V_1, \dots, V_n) \in \mathbb{H}^n$ consider the following linear operators $\mathcal{E}_i, \mathcal{L}_i, \mathcal{T}_i \in \mathbb{H}^{n_x}$, which allow us to draw the stability conditions for (3.1) as

$$\mathcal{E}_i(V) \triangleq \sum_{j \in \mathbb{N}} \rho_{ij} V_j, \quad (3.7)$$

$$\mathcal{L}_i(V) \triangleq \sum_{\ell \in \mathbb{M}_i} \phi_{i\ell} A'_{i\ell} \mathcal{E}_i(V) A_{i\ell}, \quad (3.8)$$

$$\mathcal{T}_j(V) \triangleq \sum_{i \in \mathbb{N}} \sum_{\ell \in \mathbb{M}_i} \rho_{ij} \phi_{ij} A_{i\ell} V_i A'_{i\ell}, \quad \forall i, j, \in \mathbb{N}. \quad (3.9)$$

3.1.2 \mathcal{H}_∞ norm for Hidden MJLS

Definition 3. *Assuming that (3.1) is MSS, the \mathcal{H}_∞ norm is given by*

$$\|\mathcal{G}\|_\infty \triangleq \sup_{0 \neq w \in \mathcal{L}_2, \theta_0 \in \mathbb{K}} \frac{\|z\|_2}{\|w\|_2}.$$

The next lemma is known as Bounded Real Lemma for the detector approach, which was first introduced in (TODOROV; FRAGOSO; COSTA, 2018).

Lemma 5. *If there exists $P_i > 0$, $M_{i\ell} > 0$, $S_{i\ell} > 0$, and $N_{i\ell}$ such that (3.10), (3.11), hold*

$$\begin{bmatrix} P_i & 0 \\ 0 & \gamma^2 I \end{bmatrix} > \sum_{\ell \in \mathbb{M}_i} \phi_{i\ell} \begin{bmatrix} M_{i\ell} & \bullet \\ N_{i\ell} & S_{i\ell} \end{bmatrix}, \quad (3.10)$$

$$\begin{bmatrix} M_{i\ell} & \bullet \\ N_{i\ell} & S_{i\ell} \end{bmatrix} > \begin{bmatrix} A_{i\ell} & J_{i\ell} \\ C_{i\ell} & D_{i\ell} \end{bmatrix}' \begin{bmatrix} \mathbb{E}_i(P) & 0 \\ 0 & I \end{bmatrix} \begin{bmatrix} A_{i\ell} & J_{i\ell} \\ C_{i\ell} & D_{i\ell} \end{bmatrix}, \quad (3.11)$$

for all $i \in \mathbb{N}$ and $\ell \in \mathbb{M}_i$ then $\|\mathcal{G}\|_\infty < \gamma$.

Proof: See (TODOROV; FRAGOSO; COSTA, 2018). ■

Applying the Schur complement in (3.11) we obtain the following inequality,

$$\begin{bmatrix} M_{i\ell} & \bullet & \bullet & \bullet \\ N_{i\ell} & S_{i\ell} & \bullet & \bullet \\ A_{i\ell} & J_{i\ell} & \mathbb{E}_i(P)^{-1} & \bullet \\ C_{i\ell} & D_{i\ell} & 0 & I \end{bmatrix} > 0. \quad (3.12)$$

3.1.3 \mathcal{H}_2 norm for MJLS for Parameter Estimation

Assuming that (3.1) is MSS, the \mathcal{H}_2 norm is given by

$$\|\mathcal{G}\|_2 = \sqrt{\sum_{s=1}^{n_w} \sum_{i=1}^N \mu_i \|z^{i,s}\|_2^2} \quad (3.13)$$

where the initial Markov chain state distribution is given by $\text{Prob}(\theta(0) = i) = \mu_i \geq 0$ for all $i \in \mathbb{N}$. Considering the strict inequalities,

$$Q_i > \sum_{\ell \in \mathbb{M}_i} \phi_{i\ell} (A'_{i\ell} \mathbb{E}_i(Q) A_{i\ell} + C'_{i\ell} C_{i\ell}), \quad i \in \mathbb{N}, \quad \ell \in \mathbb{M}_i, \quad (3.14)$$

for $Q_i > 0$, we have that

$$(\|\mathcal{G}\|_2)^2 < \sum_{i=1}^N \sum_{\ell \in \mathbb{M}_i} \phi_{i\ell} \mu_i \text{Tr}(J'_{i\ell} \mathbb{E}_i(Q) J_{i\ell}), \quad (3.15)$$

Lemma 6. *If there exists $W_{i\ell} > 0$, $R_{i\ell} > 0$, and $Q_i > 0$, such that (3.16), (3.17), (3.18), (3.19), hold*

$$\sum_{i=1}^N \sum_{\ell \in \mathbb{M}_i} \mu_i \phi_{i\ell} \text{Tr}(W_{i\ell}) < \lambda^2, \quad (3.16)$$

$$\begin{bmatrix} W_{i\ell} & \bullet & \bullet \\ J_{i\ell} & \mathbb{E}_i(Q)^{-1} & \bullet \\ D_{i\ell} & 0 & I \end{bmatrix} > 0, \quad (3.17)$$

$$Q_i > \sum_{\ell \in \mathbb{M}_i} \phi_{i\ell} R_{i\ell}, \quad (3.18)$$

$$\begin{bmatrix} R_{i\ell} & \bullet & \bullet \\ A_{i\ell} & \mathbb{E}_i(Q)^{-1} & \bullet \\ C_{i\ell} & 0 & I \end{bmatrix} > 0. \quad (3.19)$$

for all $i \in \mathbb{N}$ and $\ell \in \mathbb{M}_i$ then $\|\mathcal{G}\|_2 < \lambda$.

Proof: See (COSTA; FRAGOSO; TODOROV, 2014) or (OLIVEIRA; COSTA, 2017a).

3.2 Fault Detection Filter Formulation for MJLS with Parameter Estimation

In this section, we provide FDF design under the assumption that the Markov Chain mode is not accessible. From the discussion made at the beginning of this chapter, we may provide a block diagram of the system as in Fig.16 We assume that the MJLS subject to

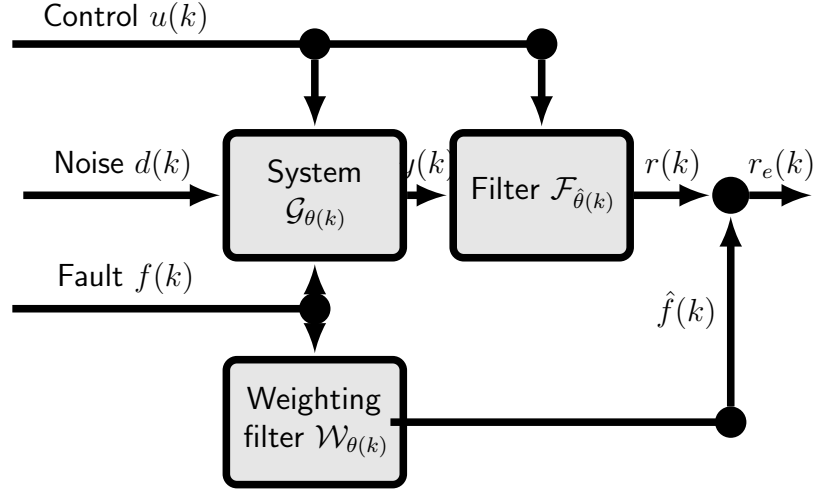


Figure 16: Fault detection and isolation scheme diagram assuming that the network mode is not accessible.

faults is defined as

$$\mathcal{G} : \begin{cases} x(k+1) = A_{\theta(k)}x(k) + B_{\theta(k)}u(k) + J_{\theta(k)}w(k) + F_{\theta(k)}f(k), \\ y(k) = C_{\theta(k)}x(k) + D_{\theta(k)}w(k) + E_{\theta(k)}f(k), \\ x(0) = x_0, \quad \theta(0) = \theta_0, \end{cases} \quad (3.20)$$

where $x(k) \in \mathbb{R}^{n_x}$, $y(k) \in \mathbb{R}^{n_y}$, $u(k) \in \mathbb{R}^{n_u}$, $w(k) \in \mathbb{R}^{n_w}$, $f(k) \in \mathbb{R}^{n_f}$, represent the state, measurements, control, exogenous, and fault signals respectively.

Using the same idea of the FDF in the previous chapter, we also implement a system \mathcal{W} given by (3.21), which is described as

$$\mathcal{W} : \begin{cases} x_f(k+1) = A_{\mathcal{W}}x_f(k) + B_{\mathcal{W}}f(k), \\ \hat{f}(k) = C_{\mathcal{W}}x_f(k) + D_{\mathcal{W}}f(k), \\ x_f(0) = 0, \end{cases} \quad (3.21)$$

where $x_f(k) \in \mathbb{R}^{n_r}$ is the weight matrix state, $f(k)$ is the same signal as in (2.24), and $\hat{f}(k) \in \mathbb{R}^{n_r}$ is the weighted fault signal.

We assume that the FDF depends only on the detected variable $\hat{\theta}(k)$ as in

$$\mathcal{F} : \begin{cases} \eta(k+1) = \mathcal{A}_{\eta\hat{\theta}(k)}\eta(k) + \mathcal{M}_{\eta\hat{\theta}(k)}u(k) + \mathcal{B}_{\eta\hat{\theta}(k)}y(k), \\ r(k) = \mathcal{C}_{\eta\hat{\theta}(k)}\eta(k) + \mathcal{D}_{\eta\hat{\theta}(k)}y(k), \\ \eta(0) = \eta_0, \end{cases} \quad (3.22)$$

whereby $\eta(k) \in \mathbb{R}_x^n$ represents the filter states, and $r(k) \in \mathbb{R}_n^n$ is the filter residual. We point out that this filter structure depends exclusively on the detector mode $\hat{\theta}(k)$.

With the intention of designing an FDF in the form of (3.22) to be mean square stable when $x(0) = 0$, $u(0) = 0$, $d(0) = 0$ and $f(0) = 0$ and minimizes the value of γ considering the \mathcal{H}_∞ norm case, we define criterion to be minimized in the optimization problem as

$$\sup_{w \neq 0, w \in \mathcal{L}_2, \theta_0 \in \mathbb{N}} \frac{\|r_e\|_2}{\|w\|_2} < \gamma, \quad (3.23)$$

where $r_e(k) = r(k) - \hat{f}(k)$. The definition of the criterion to be minimized in optimization problem for the \mathcal{H}_2 norm case is

$$\sum_{s=1}^m \sum_{i=1}^N \mu_i \|r_e\|_2^2 < \lambda. \quad (3.24)$$

Considering system (3.20), weighting system (3.21) the two different criteria (3.23), (3.24), allow us to describe augmented state and the input signal as $\bar{x}(k) = [x(k)' \ \eta(k)' \ x_f(k)']'$ and $\bar{w} = [u(k)' \ w(k)' \ \hat{f}(k)']'$,

$$\mathcal{G}_{aug} : \begin{cases} \bar{x}(k+1) = \tilde{A}_{\theta(k)\hat{\theta}(k)}\bar{x}(k) + \tilde{B}_{\theta(k)\hat{\theta}(k)}\bar{w}(k), \\ r_e(k) = \tilde{C}_{\theta(k)\hat{\theta}(k)}\bar{x}(k) + \tilde{D}_{\theta(k)\hat{\theta}(k)}\bar{w}(k), \end{cases} \quad (3.25)$$

where each matrix is described as

$$\left[\begin{array}{cc|ccc} \tilde{A}_{il} & \tilde{B}_{il} & & & \\ \tilde{C}_{il} & \tilde{D}_{il} & & & \end{array} \right] = \left[\begin{array}{ccc|ccc} A_i & 0 & 0 & B_i & J_i & F_i \\ \mathcal{B}_{\eta\ell}C_i & \mathcal{A}_{\eta\ell} & 0 & \mathcal{M}_{\eta\ell} & \mathcal{B}_{\eta\ell}D_i & \mathcal{B}_{\eta\ell}E_i \\ 0 & 0 & A_{\mathcal{W}} & 0 & 0 & B_{\mathcal{W}} \\ \hline \mathcal{D}_{\eta\ell}C_i & \mathcal{C}_{\eta\ell} & -C_{\mathcal{W}} & 0 & \mathcal{D}_{\eta\ell}D_i & \mathcal{D}_{\eta\ell}E_i - D_{\mathcal{W}} \end{array} \right]. \quad (3.26)$$

3.2.1 \mathcal{H}_∞ Fault Detection Filter Design for MJLS with Parameter Estimation

Theorem 7. *There exists a filter in the form of (3.22) such that $\|G_{aug}\|_\infty^2 < \gamma$ if there exist symmetric matrices \mathcal{Z}_i , \mathcal{X}_i , $\mathcal{H}_{i\ell}$, $\mathcal{N}_{i\ell}$, $\mathcal{S}_{i\ell}$, \mathcal{W}_i , and matrices \mathcal{R}_ℓ , \mathcal{O}_ℓ , ∇_ℓ , Γ_ℓ , $\mathcal{C}_{\eta\ell}$, $\mathcal{D}_{\eta\ell}$,*

with compatible dimensions that satisfy the following LMI constraints

$$\begin{bmatrix} Z_i & \bullet & \bullet & \bullet \\ Z_i & X_i & \bullet & \bullet \\ 0 & 0 & W_i & \bullet \\ 0 & 0 & 0 & \gamma^2 I \end{bmatrix} > \sum_{\ell \in \mathbb{M}_i} \phi_{i\ell} \begin{bmatrix} \mathcal{H}_{i\ell} & \bullet \\ \mathcal{N}_{i\ell} & \mathcal{S}_{i\ell} \end{bmatrix}, \quad (3.27)$$

$$\begin{bmatrix} & \begin{bmatrix} \mathcal{H}_{i\ell} \\ \mathcal{N}_{i\ell} \end{bmatrix} & & & \bullet & \bullet & \bullet & \bullet \\ & & \begin{bmatrix} \mathcal{S}_{i\ell} \end{bmatrix} & \Pi^{3,4} & \bullet & \bullet & \bullet & \bullet \\ \mathbb{E}_i(\mathcal{Z})A_i & \mathbb{E}_i(\mathcal{Z})A_i & 0 & \mathbb{E}_i(\mathcal{Z})J_i & \mathbb{E}_i(\mathcal{Z})F_i & \mathbb{E}_i(\mathcal{Z}) & \bullet & \bullet \\ \Pi^{4,1} & \Pi^{4,2} & 0 & \Pi^{4,3} & \Pi^{4,5} & \Pi^{4,6} & 0 & \Pi^{4,7} \\ 0 & 0 & \mathbb{E}_i(\mathcal{W})A_w & 0 & 0 & \mathbb{E}_i(\mathcal{W})B_w & 0 & 0 \\ \mathcal{D}_{\eta\ell}C_i + C_{\eta\ell} & \mathcal{D}_{\eta\ell}C_i & -C_w & 0 & \mathcal{D}_{\eta\ell}D_i & \Pi^{6,6} & 0 & 0 \\ & & & & & & 0 & I \end{bmatrix} > 0, \quad (3.28)$$

where

$$\begin{aligned} \Pi^{3,4} &= \mathbb{E}_i(\mathcal{Z})B_i, & \Pi^{4,1} &= \mathcal{R}_\ell A_i + \nabla_\ell C_i + \mathcal{O}_\ell, & \Pi^{4,2} &= \mathcal{R}_\ell A_i + \nabla_\ell C_i, \\ \Pi^{4,3} &= \mathcal{R}_\ell B_i + \Gamma_\ell, & \Pi^{4,5} &= \mathcal{R}_\ell J_i + \nabla_\ell D_i, & \Pi^{4,6} &= \mathcal{R}_\ell F_i + \nabla_\ell E_i, \\ \Pi^{4,7} &= \text{Her}(\mathcal{R}_\ell) + \mathbb{E}_i(\mathcal{Z}) - \mathbb{E}_i(\mathcal{X}), & \Pi^{6,6} &= \mathcal{D}_{\eta\ell}E_i - D_w. \end{aligned}$$

If a feasible solution is found a suitable FDF is given by $\mathcal{A}_{\eta\ell} = -\mathcal{R}_\ell^{-1}\mathcal{O}_\ell$, $\mathcal{B}_{\eta\ell} = -\mathcal{R}_\ell^{-1}\nabla_\ell$, $\mathcal{M}_{\eta\ell} = -\mathcal{R}_\ell^{-1}\Gamma_\ell$, $\mathcal{C}_{\eta\ell}$, $\mathcal{D}_{\eta\ell}$.

Proof: Consider the structure for the matrices

$$\tilde{P}_i = \begin{bmatrix} X_i & \bullet & \bullet \\ U_i' & \hat{X}_i & \bullet \\ 0 & 0 & P_i^{33} \end{bmatrix}, \quad \tilde{P}_i^{-1} = \begin{bmatrix} Y_i & \bullet & \bullet \\ V_i' & \hat{Y}_i & \bullet \\ 0 & 0 & P_i^{33} - 1 \end{bmatrix}, \quad \mathbb{E}_i(\tilde{P})^{-1} = \begin{bmatrix} \hat{T}_{1i} & \bullet & \bullet \\ \hat{T}_{2i}' & \hat{T}_{3i} & \bullet \\ 0 & 0 & \mathbb{E}_i(P_i^{33})^{-1} \end{bmatrix} \quad (3.29)$$

and the linearization matrices

$$\tau_i = \begin{bmatrix} I & I & 0 \\ V_i' Y_i^{-1} & 0 & 0 \\ 0 & 0 & I \end{bmatrix}, \quad \iota = \begin{bmatrix} \hat{T}_{1i}^{-1} \mathbb{E}_i(X) & 0 \\ 0 & \mathbb{E}_i(U)' & 0 \\ 0 & 0 & \mathbb{E}_i(P_i^{33}) \end{bmatrix}, \quad (3.30)$$

that leads to

$$\tau_i' \tilde{P}_i \tau_i = \begin{bmatrix} Y_i^{-1} & Y_i^{-1} & 0 \\ Y_i^{-1} & X_i & 0 \\ 0 & 0 & P_i^{33} \end{bmatrix}, \quad \iota' \mathbb{E}_i(\tilde{P})^{-1} \iota_i = \begin{bmatrix} \mathbb{E}_i(\mathcal{Z}) & \bullet & \bullet \\ \mathbb{E}_i(\mathcal{Z}) & \mathbb{E}_i(X) & \bullet \\ 0 & 0 & \mathbb{E}_i(P_i^{33}) \end{bmatrix}. \quad (3.31)$$

Considering the constraint (3.28), and $U_i = Z_i - X_i$, $\hat{X}_i = -U_i$, $V_i' Y_i^{-1}$ and from (3.27) we can say that $\mathbb{E}_i(X) - \mathbb{E}_i(Z)$ is invertible since $X_i > Z_i$. This observation also allows us to write $R_\ell(\mathbb{E}_i(X) - \mathbb{E}_i(Z))^{-1}R_\ell' > R_\ell + R_\ell' + \mathbb{E}_i(Z) - \mathbb{E}_i(X)$, (see (OLIVEIRA; BERNUSSOU; GEROMEL, 1999)), in such a way that the term $\text{Her}(R_\ell) + \mathbb{E}_i(Z) - \mathbb{E}_i(X)$ can be changed by $R_\ell(\mathbb{E}_i(X) - \mathbb{E}_i(Z))^{-1}R_\ell'$ in the constraint (3.28). Define the matrix $Q_{i\ell}$ as,

$$Q_{i\ell} = \begin{bmatrix} I_n & I_n & 0 \\ 0 & (R_\ell^{-1})'(\mathbb{E}_i(X) - \mathbb{E}_i(Z)) & 0 \\ 0 & 0 & I \end{bmatrix}. \quad (3.32)$$

Applying the congruence transformation $\text{diag}(I, Q_{i\ell}, I, I)$ in (3.28), and from that we acquire the term $R_\ell(\mathbb{E}_i(X) - \mathbb{E}_i(Z))^{-1}R_\ell'$. By consequence we can make the variable trans-

formation $\mathcal{O}_\ell = R_\ell \mathcal{A}_{\eta\ell}$, $\nabla_\ell = R_\ell \mathcal{B}_{\eta\ell}$, $\Gamma_\ell = R_\ell \mathcal{M}_{\eta\ell}$, $\mathcal{C}_{\eta\ell}$, $\mathcal{D}_{\eta\ell}$. As presented in (OLIVEIRA; COSTA, 2017b) and the references therein, $\hat{T}_{1i}^{-1} = \mathbb{E}_i(X) - \mathbb{E}_i(U)\mathbb{E}_i(\hat{X})^{-1}\mathbb{E}_i(U)$, and we also have that $\mathbb{E}_i(U) = -\mathbb{E}_i(\hat{X})$. Therefore, $\hat{T}_{1i}^{-1} = \mathbb{E}_i(Z) = \mathbb{E}_i(X) + \mathbb{E}_i(U)$, and so the constraint (3.27) and (3.28) can be also described as

$$\begin{bmatrix} \tau_i' \tilde{P} \tau_i & 0 \\ 0 & \gamma^2 I \end{bmatrix} > \sum_{\ell \in \mathbb{M}_i} \begin{bmatrix} \tau_i' \tilde{H}_{i\ell} \tau_i & \bullet \\ \tilde{N}_{i\ell} \tau_i & \tilde{S}_{i\ell} \end{bmatrix}, \quad (3.33)$$

$$\begin{bmatrix} \tau_i' \tilde{H}_{i\ell} \tau_i & \bullet & \bullet & \bullet \\ \tilde{N}_{i\ell} \tau_i & \tilde{S}_{i\ell} & \bullet & \bullet \\ \iota_i' \tilde{A}_{i\ell} \tau_i & \iota_i' \tilde{J}_{i\ell} & \iota_i' \mathbb{E}_i(\tilde{P})^{-1} \iota_i & \bullet \\ \tilde{C}_{i\ell} \tau_i & \tilde{D}_{i\ell} & 0 & I \end{bmatrix} > 0. \quad (3.34)$$

Using the congruence transformations $\text{diag}(\tau_i^{-1}, I)$ in (3.33) and $\text{diag}(\tau_i^{-1}, I, \iota_i^{-1}, I)$ in (3.34) we get the constraints in Lemma 5, concluding the proof. ■

3.2.2 \mathcal{H}_2 Fault Detection Filter Design for MJLS with Parameter Estimation

Theorem 8. *There exists a filter in the form of (3.22) such that $\|\mathcal{G}_{aug}\|_2^2 < \lambda$ if there exist symmetric matrices Z_i , X_i , $V_{i\ell}$, G_i , and matrices R_ℓ , \mathcal{O}_ℓ , ∇_ℓ , Γ_ℓ , $\mathcal{C}_{\eta\ell}$, $\mathcal{D}_{\eta\ell}$, with compatible dimensions that satisfy the following LMI constraints*

$$\sum_{i=1}^N \sum_{\ell \in \mathbb{M}_i} \mu_i \phi_{i\ell} \text{Tr}(W_{i\ell}) < \lambda, \quad (3.35)$$

$$\begin{bmatrix} Z_i & \bullet & \bullet \\ Z_i & X_i & \bullet \\ 0 & 0 & G_i \end{bmatrix} > \sum_{\ell \in \mathbb{M}_i} \phi_{i\ell} [V_{i\ell}], \quad (3.36)$$

$$\begin{bmatrix} [W_{i\ell}] & \bullet & \bullet & \bullet & \bullet \\ \mathbb{E}_i(Z)B_i & \mathbb{E}_i(Z)J_i & \mathbb{E}_i(Z)F_i & \mathbb{E}_i(Z) & \bullet \\ R_\ell B_i + \Gamma_\ell & R_\ell J_i + \nabla_\ell D_i & R_\ell F_i + \nabla_\ell E_i & \text{Her}(R_\ell) + \mathbb{E}_i(Z) - \mathbb{E}_i(X) & \bullet \\ 0 & 0 & \mathbb{E}_i(G)B_w & 0 & 0 \mathbb{E}_i(E) \\ 0 & \mathcal{D}_{\eta\ell} D_i & \mathcal{D}_{\eta\ell} E_i - D_w & 0 & 0 \quad I \end{bmatrix} > 0, \quad (3.37)$$

$$\begin{bmatrix} [V_{i\ell}] & \bullet & \bullet & \bullet & \bullet \\ \mathbb{E}_i(Z)A_i & \mathbb{E}_i(Z)A_i & 0 & \mathbb{E}_i(Z) & \bullet \\ \tilde{\Pi}^{3,1} & R_\ell A_i + \nabla_\ell C_i & 0 & 0 & \text{Her}(R_\ell) + \mathbb{E}_i(Z) - \mathbb{E}_i(X) \\ 0 & 0 & \mathbb{E}_i(G)A_w & 0 & 0 \mathbb{E}_i(G) \\ \mathcal{D}_{\eta\ell} C_i + \mathcal{C}_{\eta\ell} & \mathcal{D}_{\eta\ell} C_i & -C_w & 0 & 0 \quad I \end{bmatrix} > 0, \quad (3.38)$$

where $\tilde{\Pi}^{3,1} = R_\ell A_i + \nabla_\ell C_i + O_\ell$. If a feasible solution is obtained the matrices that compose the filter are $\mathcal{A}_{\eta\ell} = -R_\ell^{-1} \mathcal{O}_\ell$, $\mathcal{B}_{\eta\ell} = -R_\ell^{-1} \nabla_\ell$, $\mathcal{M}_{\eta\ell} = -R_\ell^{-1} \Gamma_\ell$, $\mathcal{C}_{\eta\ell}$, $\mathcal{D}_{\eta\ell}$.

Proof: Fixing the following structure for the matrices

$$\tilde{P}_i = \begin{bmatrix} X_i & \bullet & \bullet \\ U_i^T & \hat{X}_i & \bullet \\ 0 & 0 & P_i^{33} \end{bmatrix}, \quad \tilde{P}_i^{-1} = \begin{bmatrix} Y_i & \bullet & \bullet \\ V_i^T & \hat{Y}_i & \bullet \\ 0 & 0 & P_i^{33} \quad -1 \end{bmatrix}, \quad \mathbb{E}_i(\tilde{P})^{-1} = \begin{bmatrix} \hat{T}_{1i} & \bullet & \bullet \\ \hat{T}_{2i}^T & \hat{T}_{3i} & \bullet \\ 0 & 0 & \hat{T}_{4i} \end{bmatrix}, \quad (3.39)$$

and the linearization matrices

$$\tau_i = \begin{bmatrix} I & I & 0 \\ V_i^T Y_i^{-1} & 0 & 0 \\ 0 & 0 & I \end{bmatrix}, \quad \iota_i = \begin{bmatrix} \hat{T}_{1i}^{-1} \mathbb{E}_i(X) & 0 \\ 0 & \mathbb{E}_i(U)^T & 0 \\ 0 & 0 & \mathbb{E}_i(P^{33}) \end{bmatrix}, \quad (3.40)$$

we get that

$$\tau_i^T \tilde{P}_i \tau_i = \begin{bmatrix} Y_i^{-1} & Y_i^{-1} & 0 \\ Y_i^{-1} & X_i & 0 \\ 0 & 0 & P_i^{33} \end{bmatrix}, \quad \iota_i^T \mathbb{E}_i(\tilde{P})^{-1} \iota_i = \begin{bmatrix} \hat{T}_{1i}^{-1} & \bullet & \bullet \\ \hat{T}_{1i}^{-1} \mathbb{E}_i(X) & \bullet & \bullet \\ 0 & 0 & \mathbb{E}_i(P^{33}) \end{bmatrix}. \quad (3.41)$$

The matrix $\mathbb{E}_i(\tilde{P})^{-1}$, as explained in (GONÇALVES; FIORAVANTI; GEROMEL, 2010), depends nonlinearly on $\mathbb{E}_i(\tilde{P})$. Assuming that $U_i = -\hat{X}_i$, additionally from the structure of \tilde{P}_i and \tilde{P}_i^{-1} provides $U_i = -\hat{X}_i = Y_i^{-1} - X_i = Z_i - X_i$, which enable us to rewrite $\iota_i^T \mathbb{E}_i(\tilde{P})^{-1} \iota_i$ as

$$\iota_i^T \mathbb{E}_i(\tilde{P})^{-1} \iota_i = \begin{bmatrix} \mathbb{E}_i(Z) & \bullet & \bullet \\ \mathbb{E}_i(Z) \mathbb{E}_i(X) & \bullet & \bullet \\ 0 & 0 & \mathbb{E}_i(P^{33}) \end{bmatrix}. \quad (3.42)$$

Considering the constraints (3.37), (3.36) and (3.38), and $U_i = Z_i - X_i$, $\hat{X}_i = -U_i$, $V_i^T Y_i^{-1}$ and from (3.36) we are able to say that $\mathbb{E}_i(X) - \mathbb{E}_i(Z)$ is invertible due to $X_i > Z_i$. This observation also allows us to write $R_\ell(\mathbb{E}_i(X) - \mathbb{E}_i(Z))^{-1} R_\ell^T \geq \text{Her}(R_\ell) + \mathbb{E}_i(Z) - \mathbb{E}_i(X)$, (see (OLIVEIRA; BERNUSSOU; GEROMEL, 1999)), such that

$$\begin{bmatrix} \begin{bmatrix} W_{i\ell} \\ \mathbb{E}_i(Z)B_i & \mathbb{E}_i(Z)J_i & \mathbb{E}_i(Z)F_i & \mathbb{E}_i(Z) & \bullet & \bullet & \bullet & \bullet \\ R_\ell B_i + \Gamma_\ell & R_\ell J_i + \nabla_\ell D_i & R_\ell F_i + \Delta_\ell E_i & 0 & \Pi^{3,5} & \bullet & \bullet & \bullet \\ 0 & 0 & \mathbb{E}_i(E)B_w & 0 & 0 & \mathbb{E}_i(G) & \bullet & \bullet \\ 0 & \mathcal{D}_{\eta\ell} D_i & \mathcal{D}_{\eta\ell} E_i - D_w & 0 & 0 & 0 & I & \bullet \end{bmatrix} > 0, \quad (3.43)$$

$$\begin{bmatrix} \begin{bmatrix} V_{i\ell} \\ \mathbb{E}_i(Z)A_i & \mathbb{E}_i(Z)A_i & 0 & \mathbb{E}_i(Z) & \bullet & \bullet & \bullet & \bullet \\ R_\ell A_i + \nabla_\ell C_i + \mathcal{O}_\ell & R_\ell A_i + \nabla_\ell C_i & 0 & 0 & \Pi^{3,5} & \bullet & \bullet & \bullet \\ 0 & 0 & \mathbb{E}_i(G)A_w & 0 & 0 & \mathbb{E}_i(G) & \bullet & \bullet \\ \mathcal{D}_{\eta\ell} C_i + \mathcal{C}_{\eta\ell} & \mathcal{D}_{\eta\ell} C_i & -C_w & 0 & 0 & 0 & I & \bullet \end{bmatrix} > 0, \quad (3.44)$$

where $\Pi^{3,5} = R_\ell(\mathbb{E}_i(Z) - \mathbb{E}_i(X))^{-1} R_\ell^T$. Recall that $\mathcal{O}_\ell = -R_\ell \mathcal{A}_{\eta\ell}$, $\nabla_\ell = -R_\ell \mathcal{B}_{\eta\ell}$, $\Gamma_\ell = -R_\ell \mathcal{M}_{\eta\ell}$, $\mathcal{C}_{\eta\ell}$, $\mathcal{D}_{\eta\ell}$. As in (OLIVEIRA; COSTA, 2017b), $\hat{T}_{1i}^{-1} = \mathbb{E}_i(X) - \mathbb{E}_i(U) \mathbb{E}_i(\hat{X})^{-1} \mathbb{E}_i(U)^T$, and since $\mathbb{E}_i(U) = -\mathbb{E}_i(\hat{X})$ we get that $\hat{T}_{1i}^{-1} = \mathbb{E}_i(Z) = \mathbb{E}_i(X) + \mathbb{E}_i(U)$. Define the matrix $Q_{i\ell}$ as,

$$Q_{i\ell} = \begin{bmatrix} I & & & 0 \\ 0 & (R_\ell^{-1})^T (\mathbb{E}_i(X) - \mathbb{E}_i(Z)) & & 0 \\ 0 & 0 & & I \end{bmatrix}. \quad (3.45)$$

Applying congruence transformations $\text{diag}(I, Q_{i\ell}, I)$ and $\text{diag}(I, I, I, Q_{i\ell}, I)$, respectively, in (3.43) and (3.44) we obtain the constraints below (similarly as presented in (GONÇALVES;

FIORAVANTI; GEROMEL, 2010))

$$\begin{bmatrix} \begin{bmatrix} W_{i\ell} \\ \mathbb{E}_i(Z)B_i \\ \mathbb{E}_i(U)B_i + \mathbb{E}_i(U)\mathcal{M}_{\eta\ell} \\ 0 \\ 0 \end{bmatrix} & \begin{bmatrix} \mathbb{E}_i(Z)J_i \\ \mathbb{E}_i(U)J_i + \mathbb{E}_i(U)\mathcal{B}_{\eta\ell}D_i \\ 0 \\ \mathcal{D}_{\eta\ell}D_i \end{bmatrix} & \begin{bmatrix} \mathbb{E}_i(Z)F_i \\ \mathbb{E}_i(U)F_i + \mathbb{E}_i(U)\mathcal{B}_{\eta\ell}E_i \\ \mathbb{E}_i(G)B_w \\ \mathcal{D}_{\eta\ell}E_i - D_w \end{bmatrix} & \begin{bmatrix} \mathbb{E}_i(Z) \\ 0 \\ 0 \\ 0 \end{bmatrix} & \begin{bmatrix} \bullet \\ \bullet \\ 0 \\ 0 \end{bmatrix} & \begin{bmatrix} \bullet \\ \bullet \\ \mathbb{E}_i(X) \\ 0 \end{bmatrix} & \begin{bmatrix} \bullet \\ \bullet \\ \bullet \\ \mathbb{E}_i(G) \\ 0 \\ I \end{bmatrix} \end{bmatrix} > 0, \quad (3.46)$$

$$\begin{bmatrix} \begin{bmatrix} V_{i\ell} \\ \mathbb{E}_i(Z)A_i \\ \mathbb{E}_i(U)A_i + \mathbb{E}_i(U)\mathcal{B}_{\eta\ell}C_i \\ 0 \\ \mathcal{D}_{\eta\ell}C_i + C_{\eta\ell} \end{bmatrix} & \begin{bmatrix} \mathbb{E}_i(Z)A_i \\ \mathbb{E}_i(U)A_i + \mathbb{E}_i(U)\mathcal{B}_{\eta\ell}C_i + \mathbb{E}_i(U)\mathcal{A}_{\eta\ell} \\ 0 \\ \mathcal{D}_{\eta\ell}C_i \end{bmatrix} & \begin{bmatrix} 0 \\ 0 \\ \mathbb{E}_i(G)A_w \\ -C_w \end{bmatrix} & \begin{bmatrix} \mathbb{E}_i(Z) \\ \mathbb{E}_i(Z) \\ 0 \\ 0 \end{bmatrix} & \begin{bmatrix} \bullet \\ \bullet \\ 0 \\ 0 \end{bmatrix} & \begin{bmatrix} \bullet \\ \bullet \\ \mathbb{E}_i(X) \\ \mathbb{E}_i(G) \\ 0 \\ I \end{bmatrix} \end{bmatrix} > 0. \quad (3.47)$$

The constraints (3.36), (3.46) and (3.47) can also be described as

$$\tau_i^T \tilde{P}_i \tau_i > \sum_{\ell \in \mathbb{M}_i} \phi_{i\ell} \tau_i^T \tilde{R}_{i\ell} \tau_i, \quad (3.48)$$

$$\begin{bmatrix} W_{i\ell} & \bullet & \bullet \\ \iota_i^T \tilde{B}_{i\ell} \tau_i & \iota_i^T \mathbb{E}_i(\tilde{P})^{-1} \iota_i & \bullet \\ \tilde{D}_{i\ell} & 0 & I \end{bmatrix} > 0, \quad (3.49)$$

$$\begin{bmatrix} \tau_i^T \tilde{R}_{i\ell} \tau_i & \bullet & \bullet \\ \iota_i^T \tilde{A}_{i\ell} \tau_i & \iota_i^T \mathbb{E}_i(\tilde{P})^{-1} \iota_i & \bullet \\ \tilde{C}_{i\ell} & 0 & I \end{bmatrix} > 0. \quad (3.50)$$

Applying the congruence transformations τ_i^{-1} , $\text{diag}(I, \iota_i^{-1})$ and $\text{diag}(\tau_i^{-1}, \iota_i^{-1}, I)$ in (3.48), we end up with the equivalent LMI constraints as in (OLIVEIRA; COSTA, 2017a), concluding the proof. ■

3.2.3 Mixed $\mathcal{H}_2/\mathcal{H}_\infty$ Fault Detection Filter Design for MJLS with Parameter Estimation

Similarly to the mixed problem in Chapter 2 the mixed $\mathcal{H}_2/\mathcal{H}_\infty$ optimization problem may be defined as

$$\inf\{g(\lambda, \gamma), \text{ such that } \|G_{aug}\|_2^2 < \lambda \text{ and } \|G_{aug}\|_\infty^2 < \gamma\}, \quad (3.51)$$

so that (3.51) considers both (3.23) and (3.24) simultaneously. Observing (3.51), there are several different ways to solve it. We here choose to solve (3.51) finding a weighted combination of the guaranteed cost for both \mathcal{H}_2 and \mathcal{H}_∞ norms. Therefore, the objective function can be defined as in (2.46), or (2.47), or (2.48).

In order to solve the LMIs in Theorem (7) and (8), it is necessary to define

$$\psi = \{R_\ell, O_\ell, \nabla_\ell, \mathcal{C}_{\eta\ell}, \mathcal{D}_{\eta\ell}\}. \quad (3.52)$$

We set

$$\Psi = \{\psi \text{ as in (3.52), such that the LMIs (3.27), (3.28), (3.35), (3.37), (3.38) are simultaneously feasible}\}, \quad (3.53)$$

and,

$$\inf_{\psi \in \Psi} \{g(\lambda, \gamma)\}. \quad (3.54)$$

Theorem 9. *There exists a mode-dependent FDF as in (3.22) such that $\|G_{aug}\|_\infty^2 < \gamma$ and $\|G_{aug}\|_2^2 < \lambda$ if there exists $\psi \in \Psi$, where Ψ is defined as in (3.53). If a feasible solution is obtained then a suitable FDF is given by $\mathcal{A}_{\eta\ell} = -R_\ell^{-1}\mathcal{O}_\ell$, $\mathcal{B}_{\eta\ell} = -R_\ell^{-1}\nabla_\ell$, $\mathcal{M}_{\eta\ell} = -R_\ell^{-1}\Gamma_\ell$, $\mathcal{C}_{\eta\ell}$, $\mathcal{D}_{\eta\ell}$.*

Proof: The proof follows directly from the proofs for Theorems 7 and 8. ■

3.2.4 Simulations Results

For the illustrative example we used the same model as presented in Appendix A, which is a coupled tank where the fault is an abnormal input on the first tank. However, it is necessary to add the detector matrix information as in

$$\Gamma = \begin{bmatrix} 0.65 & 0.35 \\ 0.75 & 0.25 \end{bmatrix}. \quad (3.55)$$

Using this information and solving Theorem 7 we obtain the FDF in the form of (3.22) as

$$\begin{aligned} \mathcal{A}_{\eta 1} &= \begin{bmatrix} 0.0021 & -0.0020 \\ 0.0021 & -0.0020 \end{bmatrix}, & \mathcal{A}_{\eta 2} &= \begin{bmatrix} 0.0058 & -0.0375 \\ 0.0478 & -0.0669 \end{bmatrix}, & \mathcal{M}_{\eta 1} &= \begin{bmatrix} 0.1342 & 0.0698 \\ -0.5776 & 0.7818 \end{bmatrix}, \\ \mathcal{M}_{\eta 2} &= \begin{bmatrix} 1.1986 & 0.0922 \\ 0.3684 & 0.9221 \end{bmatrix}, & \mathcal{B}_{\eta 1} &= \begin{bmatrix} -0.0259 & -0.0107 \\ 0.0106 & -0.0265 \end{bmatrix}, & \mathcal{B}_{\eta 2} &= \begin{bmatrix} 0 & 0 \\ 0 & 0 \end{bmatrix}, \\ \mathcal{C}_{\eta 1} &= \begin{bmatrix} -0.0489 & 0.0469 \end{bmatrix}, & \mathcal{C}_{\eta 2} &= \begin{bmatrix} -2.1824 & 1.7279 \end{bmatrix}, & \mathcal{D}_{\eta 1} &= \begin{bmatrix} 0.0523 & -0.1963 \end{bmatrix}, \\ \mathcal{D}_{\eta 2} &= \begin{bmatrix} 0 & 0 \end{bmatrix}, \end{aligned} \quad (3.56)$$

and the upper bound obtained was $\gamma = 1.4142$. Now considering Theorem 8 we obtained

$$\begin{aligned} \mathcal{A}_{\eta 1} &= \begin{bmatrix} -0.2535 & 0.2444 \\ 0.2540 & -0.2621 \end{bmatrix}, & \mathcal{A}_{\eta 2} &= \begin{bmatrix} -0.0132 & -0.0070 \\ 0.0070 & -0.0157 \end{bmatrix}, & \mathcal{M}_{\eta 1} &= \begin{bmatrix} 0.6814 & -0.2061 \\ -0.2060 & 0.6814 \end{bmatrix}, \\ \mathcal{M}_{\eta 2} &= \begin{bmatrix} 0.7100 & 0.0000 \\ 0.0000 & 0.7100 \end{bmatrix}, & \mathcal{B}_{\eta 1} &= \begin{bmatrix} 0.4334 & -0.4475 \\ -0.4419 & 0.4521 \end{bmatrix}, & \mathcal{B}_{\eta 2} &= \begin{bmatrix} 0 & 0 \\ 0 & 0 \end{bmatrix}, \\ \mathcal{C}_{\eta 1} &= \begin{bmatrix} -0.1239 & -0.1239 \end{bmatrix}, & \mathcal{C}_{\eta 2} &= \begin{bmatrix} 0 & 0 \end{bmatrix}, & \mathcal{D}_{\eta 1} &= \begin{bmatrix} -0.3259 & -0.3259 \end{bmatrix}, & \mathcal{D}_{\eta 2} &= \begin{bmatrix} 0 & 0 \end{bmatrix}, \end{aligned} \quad (3.57)$$

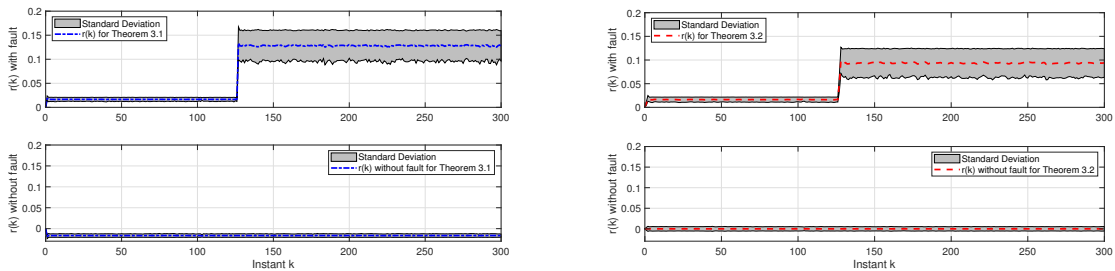
and the upper bound obtained was $\lambda = 5.6378$. For the Mixed problem presented in Theorem 9 the results are

$$\begin{aligned} \mathcal{A}_{\eta 1} &= \begin{bmatrix} -0.0034 & 0.0107 \\ 0.0018 & -0.0222 \end{bmatrix}, \quad \mathcal{A}_{\eta 2} = \begin{bmatrix} -0.0037 & 0.0110 \\ 0.0021 & -0.0242 \end{bmatrix}, \quad \mathcal{M}_{\eta 1} = \begin{bmatrix} 1.5849 & -0.3285 \\ -0.0001 & 0.7664 \end{bmatrix}, \\ \mathcal{M}_{\eta 2} &= \begin{bmatrix} 1.1125 & -0.1271 \\ -0.0000 & 0.7110 \end{bmatrix}, \quad \mathcal{B}_{\eta 1} = \begin{bmatrix} -0.0215 & -0.0227 \\ 0.0110 & -0.0064 \end{bmatrix}, \quad \mathcal{B}_{\eta 2} = \begin{bmatrix} 0 & 0 \\ 0 & 0 \end{bmatrix}, \\ \mathcal{C}_{\eta 1} &= [-1.3640 \quad -1.2157], \quad \mathcal{C}_{\eta 2} = [0 \quad 0], \quad \mathcal{D}_{\eta 1} = [0.1416 \quad 0.1841], \quad \mathcal{D}_{\eta 2} = [0 \quad 0], \end{aligned} \quad (3.58)$$

and the upper bounds obtained are $\lambda = 5.8733$ and $\gamma = 1.8795$.

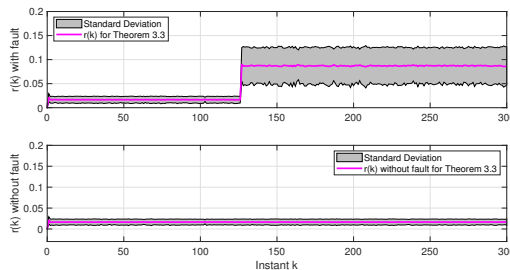
3.2.4.1 Monte Carlo Simulation

The simulations were made using the same setup from the previous section. Remembering that the system used in this simulation is a coupled tank and the fault signal represents an abnormal input on the first tank at the time of $t = 125$ s. We consider that the threshold is $\text{TH} = 1$. Performing the simulation under these particular circumstances the results obtained are the residue signal $r(k)$ using Theorems 7, 8, and 9. The second result is shown in Fig.19 with the evaluation function for all cases in this section. Examining



(a) Mean and standard deviation for residue signal obtained using Theorem 7.

(b) Mean and standard deviation for residue signal obtained using Theorem 8

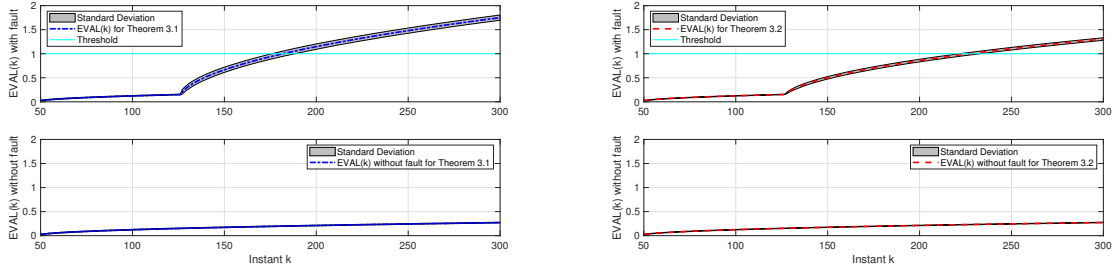


(c) Mean and standard deviation for residue signal obtained using Theorem 9

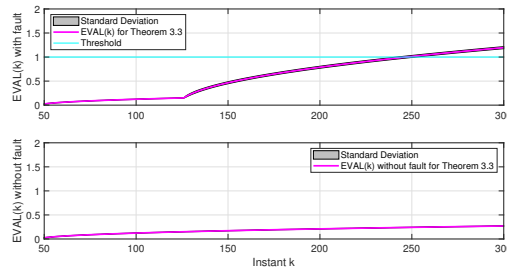
Figure 17: Mean and standard deviation for residue signal obtained using FDF designed via Theorems 7, 8, and 9.

Figs. 17a, 17b, 17c it is possible to observe that the residue signal for all three approaches behaved as intended, where they reacted to the fault properly when it occurs. There were

no changes on the residue signal when there was no fault. Figs. 18a, 18b, 18c show the



(a) Mean and standard deviation for evaluation function obtained using Theorem 7. (b) Mean and standard deviation for evaluation function obtained using Theorem 8



(c) Mean and standard deviation for evaluation function obtained using Theorem 9

Figure 18: Mean and standard deviation for evaluation function obtained using FDF designed via Theorems 7, 8, and 9.

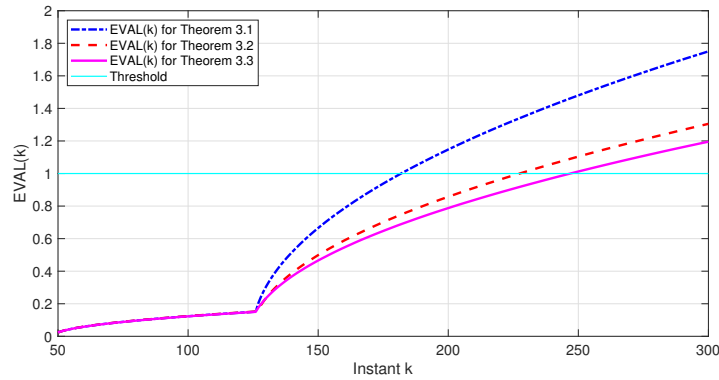


Figure 19: The mean value of the evaluation function signal for three distinct approaches, where the blue curve represents the results using Theorem 7, the red curve represents the results obtained via 8, the magenta curve represents the results through Theorem 9, and the cyan line denotes the threshold TH.

evaluation function obtained using all three theorems in this section. It is noteworthy that the fastest detection was provided by Theorem 7 with the detection range of [176 186]s, the detection range obtained using Theorem 8 was [223 236]s, and for Theorem 9 was [242 253]s. All approaches detected the fault properly, therefore, all can be considered a suitable solution for the FDI problem.

3.3 Simultaneous Fault Detection and Control formulation for MJLS with Parameter Estimation

In this section, we present the design of simultaneous fault detection and control for MJLS with parameter estimation. In this particular problem, we design an FDF and a state feedback controller at the same time. The major advantage provided by this topology is that a single element in the system is capable of detect a fault, and perform the regular controller task. The formulation presented here considers that the Hidden Markov mode as in Section 3.2. However, it is necessary to redefine the BRLs for the \mathcal{H}_∞ and \mathcal{H}_2 cases, and also rewrite the system for this specific design. Consider the following MJLS in the stochastic space $(\Omega, \mathcal{F}, \mathcal{P})$ with filtration $\{\mathcal{F}_k\}$,

$$\mathcal{G} : \begin{cases} x(k+1) = A_{\theta(k)}x(k) + B_{\theta(k)}u(k) + J_{\theta(k)}w(k) + F_{f\theta(k)}f(k) \\ y(k) = L_{\theta(k)}x(k) + H_{w\theta(k)}w(k) + H_{f\theta(k)}f(k) \\ z(k) = C_{\theta(k)}x(k) + D_{\theta(k)}u(k), \end{cases} \quad (3.59)$$

where $x(k) \in \mathbb{R}^{n_x}$ is the state, $u(k) \in \mathbb{R}^{n_u}$ is the control input, $w(k) \in \mathbb{R}^{n_r}$ is the disturbance, $f(k) \in \mathbb{R}^{n_f}$ is the signature of the failure, $y(k) \in \mathbb{R}^{n_y}$ is the measured output, and $z(k) \in \mathbb{R}^{n_z}$ is the controlled output. As we described in Section 3.2, the index $\theta(k)$ represents a homogeneous Markov chain.

We would like to design a type of stabilizing controller that simultaneously can act as a residual filter as well as a controller. The controller/filter structure is given by

$$\mathcal{C} : \begin{cases} x_c(k+1) = \mathcal{A}_{c\hat{\theta}(k)}x_c(k) + \mathcal{B}_{c\hat{\theta}(k)}y(k) \\ u(k) = \mathcal{C}_{c\hat{\theta}(k)}x_c(k) \\ \hat{f}(k) = \mathcal{C}_{f\hat{\theta}(k)}x_c(k) + \mathcal{D}_{f\hat{\theta}(k)}y(k), \end{cases} \quad (3.60)$$

where $x_c \in \mathbb{R}^{n_x}$ is the controller state and $\hat{f}(k) \in \mathbb{R}^{n_f}$ is an estimate of the signature signal $f(k)$.

The goal is to stabilize (3.59) through (3.60) whilst at the same time the controller acts also as supervisory filter providing estimates of $\hat{f}(k)$ through the residual signal

$$r(k) \triangleq f(k) - \hat{f}(k).$$

By connecting (3.59) and (3.60) and defining $\tilde{x}(k)' \triangleq [x(k)' \quad x_c(k)']'$ and, $\tilde{w}(k)' \triangleq$

$\begin{bmatrix} w(k)' & f(k)' \end{bmatrix}'$, we get the closed-loop dynamics

$$\mathcal{G}_c : \begin{cases} \tilde{x}(k+1) &= \tilde{A}_{\theta(k)\hat{\theta}(k)}\tilde{x}(k) + \tilde{J}_{\theta(k)\hat{\theta}(k)}\tilde{w}(k) \\ z(k) &= \tilde{C}_{c\theta(k)\hat{\theta}(k)}\tilde{x}(k), \\ r(k) &= \tilde{C}_{f\theta(k)\hat{\theta}(k)}\tilde{x}(k) + \tilde{E}_{f\theta(k)\hat{\theta}(k)}\tilde{w}(k), \end{cases} \quad (3.61)$$

where

$$\begin{aligned} \tilde{A}_{i\ell} &\triangleq \begin{bmatrix} A_i & B_i C_{cl} \\ \mathcal{B}_{cl} L_i & \mathcal{A}_{cl} \end{bmatrix}, & \tilde{J}_{i\ell} &\triangleq \begin{bmatrix} J_i & F_i \\ \mathcal{B}_{cl} H_{wi} & \mathcal{B}_{cl} H_{fi} \end{bmatrix}, \\ \tilde{C}_{ci\ell} &\triangleq [C_i \ D_i C_{cl}], & \tilde{C}_{fi\ell} &\triangleq [-\mathcal{D}_{f\ell} L_i \ -C_{f\ell}], \\ \tilde{E}_{fi\ell} &\triangleq [-\mathcal{D}_{f\ell} H_{wi} \ I_f - \mathcal{D}_{f\ell} H_{fi}]. \end{aligned}$$

Let us introduce some basic concepts required for properly describing the main goal. The concept of internal stochastic stability and stabilizability are stated next, where $A \triangleq (A_1, \dots, A_n) \in \mathbb{B}(\mathbb{R}^{n_x})$, $B \triangleq (B_1, \dots, B_n) \in \mathbb{B}(\mathbb{R}^{n_x}, \mathbb{R}^{n_u})$, and $K \triangleq (K_1, \dots, K_n) \in \mathbb{B}(\mathbb{R}^{n_u}, \mathbb{R}^{n_u})$, and for $Q \in \mathbb{H}^n$, $\mathbb{E}_i(Q) \triangleq \sum_{j \in \mathbb{N}} p_{ij} Q_j$. Considering the augmented system (3.61) is stochastic stable, as defined in 3.1.1, the class of the class of admissible controllers is given by $\mathfrak{C} \triangleq \{\mathcal{C}\}$.

Next we redefine the concept of \mathcal{H}_∞ norm of (3.61) concerning outputs $z(k)$ and $r(k)$ adapted from (TODOROV; FRAGOSO; COSTA, 2018). This process is necessary since we aim to provide a solution that is an FDF and a state-feedback controller simultaneously. To fulfill this purpose, it is necessary to redefine the optimization processes and their respective LMIs constraints twice, where the optimization considering the output $z(k)$ refers to the control part of the problem, and the other considering $r(k)$ to take up the FDF side of the problem.

For that, we set $\mathcal{W}_i \triangleq \{\tilde{w} \in l_2^{r+f} : \|\tilde{w}\|_{2i} > 0\}$, where for any signal $g = \{g(k), k = 0, 1, 2, \dots\}$, $\|g\|_{2i}^2 \triangleq \mathbb{E}(\|g(k)\|^2 \mid \theta_0 = i)$. Now we redefine the \mathcal{H}_∞ and \mathcal{H}_2 norms, which will be used to present later on the mixed formulation. We start with the \mathcal{H}_∞ norm definition.

Definition 4 (\mathcal{H}_∞ norms). *Given that $\mathfrak{C} \in \mathcal{C}$, the \mathcal{H}_∞ norm of (3.61) with respect to z is given by*

$$\|\mathcal{G}_c\|_\infty^{(\tilde{w} \mapsto z)} \triangleq \sup_{i \in \mathbb{N}} \sup_{\tilde{w} \in \mathcal{W}_i} \frac{\|z\|_{2i}}{\|\tilde{w}\|_{2i}},$$

and the \mathcal{H}_∞ norm of (3.61) with respect to r by,

$$\|\mathcal{G}_c\|_\infty^{(\tilde{w} \rightarrow r)} \triangleq \sup_{i \in \mathbb{N}} \sup_{\tilde{w} \in \mathcal{W}_i} \frac{\|r\|_{2i}}{\|\tilde{w}\|_{2i}}.$$

Consider the following inequalities for given $\gamma_c > 0$ and $\gamma_r > 0$,

$$\begin{bmatrix} P_i & 0 \\ 0 & \gamma_c^2 I \end{bmatrix} > \sum_{\ell \in \mathbb{M}_i} \phi_{i\ell} \begin{bmatrix} M_{i\ell} & \bullet \\ N_{i\ell} & S_{i\ell} \end{bmatrix}, \quad (3.62)$$

$$\begin{bmatrix} M_{i\ell} & \bullet \\ N_{i\ell} & S_{i\ell} \end{bmatrix} > \begin{bmatrix} \tilde{A}_{i\ell} & \tilde{J}_{i\ell} \\ \tilde{C}_{ci\ell} & 0 \end{bmatrix}' \begin{bmatrix} \mathbb{E}_i(P) & 0 \\ 0 & I \end{bmatrix} \begin{bmatrix} \tilde{A}_{i\ell} & \tilde{J}_{i\ell} \\ \tilde{C}_{ci\ell} & 0 \end{bmatrix}, \quad (3.63)$$

and

$$\begin{bmatrix} \mathfrak{P}_i & 0 \\ 0 & \gamma_r^2 I \end{bmatrix} > \sum_{l \in \mathbb{M}_i} \phi_{il} \begin{bmatrix} \mathfrak{M}_{il} & \bullet \\ \mathfrak{N}_{il} & \mathfrak{S}_{il} \end{bmatrix}, \quad (3.64)$$

$$\begin{bmatrix} \mathfrak{M}_{il} & \bullet \\ \mathfrak{N}_{il} & \mathfrak{S}_{il} \end{bmatrix} > \begin{bmatrix} \tilde{A}_{il} & \tilde{J}_{il} \\ \tilde{C}_{fil} & \tilde{E}_{fil} \end{bmatrix}' \begin{bmatrix} \mathbb{E}_i(\mathfrak{P}) & 0 \\ 0 & I \end{bmatrix} \begin{bmatrix} \tilde{A}_{il} & \tilde{J}_{il} \\ \tilde{C}_{fil} & \tilde{E}_{fil} \end{bmatrix}, \quad (3.65)$$

for all $i \in \mathbb{N}$. The following bounded-real lemma is adapted from (TODOROV; FRAGOSO; COSTA, 2018).

Lemma 7 (Bounded-real Lemma). *If there exists $P \in \mathbb{H}^{2n+}$, $P > 0$, $\mathfrak{P} \in \mathbb{H}^{2n+}$, $\mathfrak{P} > 0$, such that (3.62), (3.63), (3.64), and (3.65) hold, then $\mathfrak{C} \in \mathfrak{C}$, $\|\mathcal{G}_c\|_\infty^{(\tilde{w} \rightarrow z)} < \gamma_c$ and $\|\mathcal{G}_c\|_\infty^{(\tilde{w} \rightarrow r)} < \gamma_r$.*

Therefore the goal is to design $\mathfrak{C} \in \mathfrak{C}$ so that $\|\mathcal{G}_c\|_\infty^{(\tilde{w} \rightarrow z)} < \gamma_c$ and $\|\mathcal{G}_c\|_\infty^{(\tilde{w} \rightarrow r)} < \gamma_r$ for $\tilde{w} \in \mathcal{W}_i$, $i \in \mathbb{N}$. Specifically in this work we focus our efforts in finding

$$\inf_{\mathfrak{C} \in \mathfrak{C}, P, \gamma_r, \gamma_c} \{\gamma_c \beta_c + \gamma_r \beta_r\}: \text{ s. t. (3.62), (3.63), (3.64) and (3.65)} \quad (3.66)$$

hold for a given $\beta_c > 0, \beta_r > 0$. This particular formulation will be useful later on in this paper. We present next the \mathcal{H}_2 norm definition.

Definition 5 (\mathcal{H}_2 norms). *Assume that $\mathfrak{C} \in \mathfrak{C}$. For $\tilde{x}(0) = 0$, define $z^{s,i}$ and $r^{s,i}$, the outputs of (3.61) for the initial condition $\theta(0) = i$ and the input $\tilde{w}(k) = 0$ for $k \geq 1$ and $\tilde{w}(0) = e_s$, where e_s is the s -th vector of the standard basis of \mathbb{R}^s . The \mathcal{H}_2 norms of (3.61) with respect to the outputs z and r are given by*

$$\|\mathcal{G}_c\|_2^{(\tilde{w} \rightarrow z)} = \sqrt{\sum_{s=1}^r \sum_{i=1}^N \mu_i \|z^{s,i}\|_2^2} \quad (3.67)$$

and

$$\|\mathcal{G}_c\|_2^{(\tilde{w} \rightarrow r)} = \sqrt{\sum_{s=1}^r \sum_{i=1}^N \mu_i \|r^{s,i}\|_2^2}, \quad (3.68)$$

where the initial Markov chain state distribution is given by $\mathcal{P}(\theta(0) = i) = \mu_i \geq 0$ for all $i \in \mathbb{N}$.

Considering the strict inequalities,

$$\tilde{Q}_i > \sum_{\ell \in \mathbb{M}_i} \phi_{i\ell} (\tilde{A}'_{i\ell} \mathbb{E}_i(\tilde{Q}) \tilde{A}_{i\ell} + \tilde{C}'_{c i \ell} \tilde{C}_{c i \ell}), \quad i \in \mathbb{N}, \ell \in \mathbb{M}_i, \quad (3.69)$$

and

$$\tilde{\mathfrak{Q}}_i > \sum_{l \in \mathbb{M}_i} \phi_{i l} (\tilde{A}'_{i l} \mathbb{E}_i(\tilde{\mathfrak{Q}}) \tilde{A}_{i l} + \tilde{C}'_{f i l} \tilde{C}_{f i l}), \quad i \in \mathbb{N}, l \in \mathbb{M}_i, \quad (3.70)$$

for $\tilde{Q}_i > 0$ and $\tilde{\mathfrak{Q}}_i > 0$, we have that

$$\left(\|\mathcal{G}_c\|_2^{(\tilde{w} \rightarrow z)} \right)^2 < \sum_{i=1}^N \sum_{\ell \in \mathbb{M}_i} \phi_{i\ell} \mu_i \text{Tr}(\tilde{J}'_{i\ell} \mathbb{E}_i(\tilde{Q}) \tilde{J}_{i\ell}) \quad (3.71)$$

and

$$\left(\|\mathcal{G}_c\|_2^{(\tilde{w} \rightarrow r)} \right)^2 < \sum_{i=1}^N \sum_{\ell \in \mathbb{M}_i} \phi_{i\ell} \mu_i \text{Tr}(\tilde{J}'_{i\ell} \mathbb{E}_i(\tilde{\mathfrak{Q}}) \tilde{J}_{i\ell} + \tilde{E}'_{f i \ell} \tilde{E}_{f i \ell}). \quad (3.72)$$

Following the discussion presented in (COSTA; FRAGOSO; TODOROV, 2015) and (OLIVEIRA; COSTA, 2017a), we get that if the following inequalities for the filter part

$$\sum_{i=1}^N \sum_{\ell \in \mathbb{M}_i} \mu_i \phi_{i\ell} \text{Tr}(W_{i\ell}) < \lambda_r^2, \quad (3.73)$$

$$\begin{bmatrix} W_{i\ell} & \bullet & \bullet \\ \tilde{J}_{i\ell} & \mathbb{E}_i(\tilde{Q})^{-1} & \bullet \\ \tilde{E}_{f i \ell} & 0 & I \end{bmatrix} > 0, \quad (3.74)$$

$$\tilde{Q}_{i\ell} > \sum_{l \in \mathbb{M}_i} \phi_{i l} \tilde{R}_{i l}, \quad (3.75)$$

$$\begin{bmatrix} \tilde{R}_{i\ell} & \bullet & \bullet \\ \tilde{A}_{i\ell} & \mathbb{E}_i(\tilde{Q})^{-1} & \bullet \\ \tilde{C}_{f i \ell} & 0 & I \end{bmatrix} > 0. \quad (3.76)$$

and for the controller side

$$\sum_{i=1}^N \sum_{\ell \in \mathbb{M}_i} \mu_i \phi_{i\ell} \text{Tr}(\mathfrak{W}_{i\ell}) < \lambda_c^2, \quad (3.77)$$

$$\begin{bmatrix} \mathfrak{W}_{i\ell} & \bullet \\ \tilde{J}_{i\ell} & \mathbb{E}_i(\tilde{\mathfrak{Q}})^{-1} \end{bmatrix} > 0, \quad (3.78)$$

$$\tilde{\mathcal{Q}}_{i\ell} > \sum_{\ell \in \mathbb{M}_i} \phi_{i\ell} \tilde{\mathfrak{R}}_{i\ell}, \quad (3.79)$$

$$\begin{bmatrix} \tilde{\mathfrak{R}}_{i\ell} & \bullet & \bullet \\ \tilde{A}_{i\ell} & \mathbb{E}_i(\tilde{\mathfrak{Q}})^{-1} & \bullet \\ \tilde{C}_{ci\ell} & 0 & I \end{bmatrix} > 0. \quad (3.80)$$

hold, then $\mathfrak{C} \in \mathfrak{C}$, $\|\mathcal{G}_c\|_2^{(\tilde{w} \rightarrow z)} < \lambda_c$ and $\|\mathcal{G}_c\|_2^{(\tilde{w} \rightarrow r)} < \lambda_r$. Similarly to the \mathcal{H}_∞ case, the main goal is to design $\mathfrak{C} \in \mathfrak{C}$ so that $\|\mathcal{G}_c\|_2^{(\tilde{w} \rightarrow z)} < \lambda_c$ and $\|\mathcal{G}_c\|_2^{(\tilde{w} \rightarrow r)} < \lambda_r$ for $\tilde{w} \in \mathcal{W}_i$, $i \in \mathbb{N}$. Specifically in this work we focus our efforts in finding

$$\psi = \{W_{i\ell}, Q_i, R_{i\ell}, \mathfrak{W}_{i\ell}, \mathfrak{Q}_i, \mathfrak{R}_{i\ell}, i \in \mathbb{N}, \ell \in \mathbb{M}_i\} \quad (3.81)$$

$$\Delta = \{\psi \text{ such that (3.73)-(3.80) hold}\}$$

$$\inf_{\mathfrak{C} \in \mathfrak{C}, P, \lambda_r, \lambda_c} \{\lambda_c \zeta_c + \lambda_r \zeta_r\} : \text{s. t. } \psi \in \Delta, \quad (3.82)$$

for a given $\zeta_c, \zeta_r > 0$. Similarly to the \mathcal{H}_∞ case, we choose this particular formulation in order to derive some results later on.

3.3.1 \mathcal{H}_∞ Simultaneous Fault Detection and Control Design for MJLS with parameter estimation

The next result presents BMI constraints regarding the controller design (3.83), (3.84), and for the filter design (3.85) and (3.86).

Theorem 10. *There exists an SFDC described as in (3.60) such that $\mathfrak{C} \in \mathfrak{C}$, $\|\mathcal{G}_c\|_\infty^{(\tilde{w} \rightarrow z)} < \gamma_c$, and $\|\mathcal{G}_c\|_\infty^{(\tilde{w} \rightarrow r)} < \gamma_r$ for fixed $\gamma_c > 0$ and $\gamma_r > 0$ if there exist symmetric matrices Z_i , X_i , $M_{i\ell}^{11}$, $M_{i\ell}^{22}$, $S_{i\ell}^{11}$, $S_{i\ell}^{22}$, \mathfrak{Z}_i , \mathfrak{X}_i , $\mathfrak{M}_{i\ell}^{11}$, $\mathfrak{M}_{i\ell}^{22}$, $\mathfrak{S}_{i\ell}^{11}$, $\mathfrak{S}_{i\ell}^{22}$, and the matrices $M_{i\ell}^{21}$, $S_{i\ell}^{21}$, $\mathfrak{M}_{i\ell}^{21}$, $\mathfrak{S}_{i\ell}^{21}$, $N_{i\ell}^{11}$, $N_{i\ell}^{12}$, $N_{i\ell}^{21}$, $N_{i\ell}^{22}$, $\mathfrak{N}_{i\ell}^{11}$, $\mathfrak{N}_{i\ell}^{12}$, $\mathfrak{N}_{i\ell}^{21}$, $\mathfrak{N}_{i\ell}^{22}$, G_ℓ , Γ_ℓ , χ_ℓ , Θ_ℓ , Φ_ℓ , and K_ℓ with compatible dimensions such that inequalities (3.83), (3.84), (3.85), and (3.86) hold $\forall i \in \mathbb{N}, \ell \in \mathbb{M}$. If a feasible solution is obtained, a suitable SFDC is given by $\mathcal{A}_{cl} = -G_\ell^{-1}\Gamma_\ell$, $\mathcal{B}_{cl} = -G_\ell^{-1}\chi_\ell$, $\mathcal{C}_{cl} = K_\ell$, $\mathcal{C}_{fl} = -\Theta_\ell$, $\mathcal{D}_{fl} = -\Phi_\ell$.*

Proof: The proof follows similar reasoning as presented in (OLIVEIRA; COSTA, 2020) and (GONÇALVES; FIORAVANTI; GEROMEL, 2010). We set the structure of matrices P_i and P_i^{-1} of (3.62)-(3.63) as

$$P_i = \begin{bmatrix} X_i & \bullet \\ U_i & \hat{X}_i \end{bmatrix}, \quad P_i^{-1} = \begin{bmatrix} Z_i^{-1} & \bullet \\ V_i & \hat{Y}_i \end{bmatrix}, \quad (3.87)$$

and similarly for matrices \mathfrak{P}_i and \mathfrak{P}_i^{-1} of (3.64)-(3.65), we set

$$\mathfrak{P}_i = \begin{bmatrix} \mathfrak{X}_i & \bullet \\ \mathfrak{U}_i & \hat{\mathfrak{X}}_i \end{bmatrix}, \quad \mathfrak{P}_i^{-1} = \begin{bmatrix} \mathfrak{Z}_i^{-1} & \bullet \\ \mathfrak{V}_i & \hat{\mathfrak{Y}}_i \end{bmatrix}. \quad (3.88)$$

$$\begin{bmatrix} Z_i & \bullet & \bullet & \bullet \\ Z_i & X_i & \bullet & \bullet \\ 0 & 0 & \gamma_c^2 \infty I & \bullet \\ 0 & 0 & 0 & \gamma_c^2 \infty I \end{bmatrix} > \sum_{l \in \mathbb{M}_i} \phi_{il} \begin{bmatrix} M_{il}^{11} & \bullet & \bullet & \bullet \\ M_{il}^{21} & M_{il}^{22} & \bullet & \bullet \\ N_{il}^{11} & N_{il}^{12} & S_{il}^{11} & \bullet \\ N_{il}^{21} & N_{il}^{22} & S_{il}^{21} & S_{il}^{22} \end{bmatrix}, \quad (3.83)$$

$$\begin{bmatrix} M_{il}^{11} & \bullet & \bullet & \bullet & \bullet & \bullet & \bullet \\ M_{il}^{21} & M_{il}^{22} & \bullet & \bullet & \bullet & \bullet & \bullet \\ N_{il}^{11} & N_{il}^{12} & S_{il}^{11} & \bullet & \bullet & \bullet & \bullet \\ N_{il}^{21} & N_{il}^{22} & S_{il}^{21} & S_{il}^{22} & \bullet & \bullet & \bullet \\ \Pi^{5,1} & \mathbb{E}_i(Z)A_i & \mathbb{E}_i(Z)J_i & \mathbb{E}_i(Z)F_i & \mathbb{E}_i(Z) & \bullet & \bullet \\ \Pi^{6,1} & G_\ell A_i + \chi_\ell L_i & G_\ell J_i + \chi_\ell H_{wi} & G_\ell F_i + \chi_\ell H_{fi} & 0 & \Pi^{6,6} & \bullet \\ C_i + D_i K_\ell & C_i & 0 & 0 & 0 & 0 & I \end{bmatrix} > 0, \quad (3.84)$$

$$\begin{aligned} \Pi^{5,1} &= \mathbb{E}_i(Z)(A_i + B_i K_\ell), & \Pi^{6,1} &= G_\ell(A_i + B_i K_\ell) + \Gamma_\ell + \chi_\ell L_i, \\ \Pi^{6,6} &= \text{Her}(G_\ell) + \mathbb{E}_i(Z - X), \end{aligned}$$

$$\begin{bmatrix} \mathfrak{z}_i & \bullet & \bullet & \bullet \\ \mathfrak{z}_i & \mathfrak{x}_i & \bullet & \bullet \\ 0 & 0 & \gamma_r^2 \infty I & \bullet \\ 0 & 0 & 0 & \gamma_r^2 \infty I \end{bmatrix} > \sum_{l \in \mathbb{M}_i} \phi_{il} \begin{bmatrix} \mathfrak{M}_{il}^{11} & \bullet & \bullet & \bullet \\ \mathfrak{M}_{il}^{21} & \mathfrak{M}_{il}^{22} & \bullet & \bullet \\ \mathfrak{N}_{il}^{11} & \mathfrak{N}_{il}^{12} & \mathfrak{S}_{il}^{11} & \bullet \\ \mathfrak{N}_{il}^{21} & \mathfrak{N}_{il}^{22} & \mathfrak{S}_{il}^{21} & \mathfrak{S}_{il}^{22} \end{bmatrix}, \quad (3.85)$$

$$\begin{bmatrix} \mathfrak{M}_{il}^{11} & \bullet & \bullet & \bullet & \bullet & \bullet & \bullet \\ \mathfrak{M}_{il}^{21} & \mathfrak{M}_{il}^{22} & \bullet & \bullet & \bullet & \bullet & \bullet \\ \mathfrak{N}_{il}^{11} & \mathfrak{N}_{il}^{12} & \mathfrak{S}_{il}^{11} & \bullet & \bullet & \bullet & \bullet \\ \mathfrak{N}_{il}^{21} & \mathfrak{N}_{il}^{22} & \mathfrak{S}_{il}^{21} & \mathfrak{S}_{il}^{22} & \bullet & \bullet & \bullet \\ \check{\Pi}^{5,1} & \mathbb{E}_i(\mathfrak{z})A_i & \mathbb{E}_i(\mathfrak{z})J_i & \mathbb{E}_i(\mathfrak{z})F_i & \mathbb{E}_i(\mathfrak{z}) & \bullet & \bullet \\ \check{\Pi}^{6,1} & G_\ell A_i + \chi_\ell L_i & G_\ell J_i + \chi_\ell H_{wi} & G_\ell F_i + \chi_\ell H_{fi} & 0 & \check{\Pi}^{6,6} & \bullet \\ \check{\Pi}^{7,1} & \Phi_\ell L_i & \Phi_\ell H_{wi} & I + \Phi_\ell H_{fi} & 0 & 0 & I \end{bmatrix} > 0. \quad (3.86)$$

$$\begin{aligned} \check{\Pi}^{5,1} &= \mathbb{E}_i(\mathfrak{z})(A_i + B_i K_\ell), & \check{\Pi}^{6,1} &= G_\ell(A_i + B_i K_\ell) + \Gamma_\ell + \chi_\ell L_i, \\ \check{\Pi}^{7,1} &= \Theta_\ell + \Phi_\ell L_i, & \check{\Pi}^{6,6} &= \text{Her}(G_\ell) + \mathbb{E}_i(\mathfrak{z} - \mathfrak{x}). \end{aligned}$$

We also define the matrices τ_i and v_i as

$$\tau_i = \begin{bmatrix} I & I \\ v_i Z_i & 0 \end{bmatrix}, \quad v_i = \begin{bmatrix} I & \mathbb{E}_i(X) \\ 0 & \mathbb{E}_i(U) \end{bmatrix}, \quad (3.89)$$

along with

$$\mathfrak{t}_i = \begin{bmatrix} I & I \\ \mathfrak{v}_i \mathfrak{z}_i & 0 \end{bmatrix}, \quad \mathfrak{u}_i = \begin{bmatrix} I & \mathbb{E}_i(\mathfrak{x}) \\ 0 & \mathbb{E}_i(\mathfrak{u}) \end{bmatrix}. \quad (3.90)$$

By verifying the diagonal blocks of (3.83) and also (3.84), we note that $\text{Her}(G_\ell) > \mathbb{E}_i(X - Z) > 0$ so that G_ℓ is non-singular. Considering the fact that $P_i P_i^{-1} = I$ and $\mathfrak{P}_i \mathfrak{P}_i^{-1} = I$, we rewrite the matrices P_i and P_i^{-1} by setting $U_i = -\hat{X}_i$, and matrices \mathfrak{P}_i and \mathfrak{P}_i^{-1} by setting $\mathfrak{u}_i = -\hat{\mathfrak{x}}_i$, as follows

$$P_i = \begin{bmatrix} X_i & \bullet \\ Z_i - X_i & X_i - Z_i \end{bmatrix}, \quad (3.91)$$

$$P_i^{-1} = \begin{bmatrix} Z_i^{-1} & \bullet \\ Z_i^{-1} & Z_i^{-1} + (X_i - Z_i)^{-1} \end{bmatrix}, \quad (3.92)$$

and

$$\mathfrak{P}_i = \begin{bmatrix} \mathfrak{x}_i & \bullet \\ \mathfrak{z}_i - \mathfrak{x}_i & \mathfrak{x}_i - \mathfrak{z}_i \end{bmatrix}, \quad (3.93)$$

$$\mathfrak{P}_i^{-1} = \begin{bmatrix} \mathfrak{z}_i^{-1} & \bullet \\ \mathfrak{z}_i^{-1} & \mathfrak{z}_i^{-1} + (\mathfrak{x}_i - \mathfrak{z}_i)^{-1} \end{bmatrix}. \quad (3.94)$$

Besides, (3.146) and (3.90) become

$$\tau_i = \begin{bmatrix} I & I \\ I & 0 \end{bmatrix}, \quad v_i = \begin{bmatrix} I & \mathbb{E}_i(X) \\ 0 & \mathbb{E}_i(Z - X) \end{bmatrix}, \quad (3.95)$$

and

$$\mathfrak{t}_i = \begin{bmatrix} I & I \\ I & 0 \end{bmatrix}, \quad \mathfrak{u}_i = \begin{bmatrix} I & \mathbb{E}_i(\mathfrak{x}) \\ 0 & \mathbb{E}_i(\mathfrak{z} - \mathfrak{x}) \end{bmatrix}. \quad (3.96)$$

Since G_ℓ is non-singular, we set $\Gamma_\ell = -G_\ell \mathcal{A}_{cl}$, $\chi_\ell = -G_\ell \mathcal{B}_{cl}$, $K_\ell = \mathcal{C}_{cl}$, $\Theta_\ell = -\mathcal{C}_{fl}$, and $\Phi_\ell = -\mathcal{D}_{fl}$. As presented in (OLIVEIRA; BERNUSSOU; GEROMEL, 1999; GONÇALVES; FIORAVANTI; GEROMEL, 2010), we get that $G_\ell \mathbb{E}_i(X - Z)^{-1} G_\ell^T \geq \text{Her}(G_\ell) + \mathbb{E}_i(Z - X)$ and $G_\ell \mathbb{E}_i(\mathfrak{x} - \mathfrak{z})^{-1} G_\ell^T \geq \text{Her}(G_\ell) + \mathcal{E}_i(\mathfrak{z} - \mathfrak{x})$ so that (3.84) and (3.86) still hold if the diagonal blocks in which $\text{Her}(G_\ell) + \mathbb{E}_i(Z - X)$ and $\text{Her}(G_\ell) + \mathbb{E}_i(\mathfrak{z} - \mathfrak{x})$ appear are substituted by $G_\ell \mathbb{E}_i(X - Z)^{-1} G_\ell^T$ and $G_\ell \mathbb{E}_i(\mathfrak{x} - \mathfrak{z})^{-1} G_\ell^T$, respectively, resulting in

$$\begin{bmatrix} M_{i\ell}^{11} & \bullet & \bullet & \bullet & \bullet & \bullet & \bullet \\ M_{i\ell}^{21} & M_{i\ell}^{22} & \bullet & \bullet & \bullet & \bullet & \bullet \\ N_{i\ell}^{11} & N_{i\ell}^{12} & S_{i\ell}^{11} & \bullet & \bullet & \bullet & \bullet \\ N_{i\ell}^{21} & N_{i\ell}^{22} & S_{i\ell}^{21} & S_{i\ell}^{22} & \bullet & \bullet & \bullet \\ \Xi^{51} & \mathbb{E}_i(Z)A_i & \mathbb{E}_i(Z)J_i & \mathbb{E}_i(Z)F_i & \mathbb{E}_i(Z) & \bullet & \bullet \\ \Xi^{61} & \Xi^{62} & \Xi^{63} & \Xi^{64} & 0 & \Xi^{66} & \bullet \\ C_i + D_i \mathcal{C}_{cl} & C_i & 0 & 0 & 0 & 0 & I \end{bmatrix} > 0, \quad (3.97)$$

and

$$\begin{bmatrix} \mathfrak{M}_{i\ell}^{11} & \bullet & \bullet & \bullet & \bullet & \bullet & \bullet \\ \mathfrak{M}_{i\ell}^{21} & \mathfrak{M}_{i\ell}^{22} & \bullet & \bullet & \bullet & \bullet & \bullet \\ \mathfrak{N}_{i\ell}^{11} & \mathfrak{N}_{i\ell}^{12} & \mathfrak{S}_{i\ell}^{11} & \bullet & \bullet & \bullet & \bullet \\ \mathfrak{N}_{i\ell}^{21} & \mathfrak{N}_{i\ell}^{22} & \mathfrak{S}_{i\ell}^{21} & \mathfrak{S}_{i\ell}^{22} & \bullet & \bullet & \bullet \\ \tilde{\Xi}^{51} & \mathbb{E}_i(\mathfrak{z})A_i & \mathbb{E}_i(\mathfrak{z})J_{wi} & \mathbb{E}_i(\mathfrak{z})F_i & \mathbb{E}_i(\mathfrak{z}) & \bullet & \bullet \\ \Xi^{61} & \Xi^{62} & \Xi^{63} & \Xi^{64} & 0 & \Xi^{66} & \bullet \\ -\mathcal{C}_{fl} - \mathcal{D}_{fl}L_i & -D_{fl}L_i & -D_{fl}H_{wi} & I - D_{fl}H_{fi} & 0 & 0 & I \end{bmatrix} > 0, \quad (3.98)$$

where

$$\begin{aligned} \Xi^{51} &= \mathbb{E}_i(Z)(A_i + B_i \mathcal{C}_{cl}), & \Xi^{61} &= G_\ell(A_i + B_i \mathcal{C}_{cl}) - G_\ell \mathcal{A}_{cl} - G_\ell B_{cl} L_i, \\ \Xi^{62} &= G_\ell A_i - G_\ell B_{cl} L_i, & \Xi^{63} &= G_\ell J_i - G_\ell B_{cl} H_{wi}, & \Xi^{64} &= G_\ell F_i - G_\ell B_{cl} H_{fi}, \\ \Xi^{66} &= G_\ell \mathbb{E}_i(X - Z)^{-1} G_\ell', & \tilde{\Xi}^{51} &= \mathbb{E}_i(\mathfrak{z})(A_i + B_i \mathcal{C}_{cl}), & \tilde{\Xi}^{66} &= G_\ell \mathbb{E}_i(\mathfrak{x} - \mathfrak{z})^{-1} G_\ell'. \end{aligned}$$

By defining the following matrices

$$\Pi_{i\ell} = \begin{bmatrix} \mathbb{E}_i(Z)^{-1} & I \\ 0 & G_\ell^{-T} \mathbb{E}_i(X-Z) \end{bmatrix}, \quad (3.99)$$

and

$$\tilde{\pi}_{i\ell} = \begin{bmatrix} \mathbb{E}_i(\mathfrak{z})^{-1} & I \\ 0 & G_\ell^{-T} \mathbb{E}_i(\mathfrak{x}-\mathfrak{z}) \end{bmatrix}, \quad (3.100)$$

and applying the congruence transformations $\text{diag}(I, I, \Pi_{i\ell}, I)$ and $\text{diag}(I, I, \tilde{\pi}_{i\ell}, I)$ to (3.150) and (3.98), respectively, we get that

$$\begin{bmatrix} \tau'_i M_{i\ell} \tau_i & \bullet & \bullet & \bullet \\ N_{i\ell} \tau_i & S_{i\ell} & \bullet & \bullet \\ v'_i \tilde{A}_{i\ell} \tau_i & v'_i \tilde{J}_{i\ell} & v'_i \mathbb{E}_i(P)^{-1} v_i & \bullet \\ \tilde{C}_{ci\ell} \tau_i & 0 & 0 & I \end{bmatrix} > 0, \quad (3.101)$$

and

$$\begin{bmatrix} \mathfrak{t}'_i \mathfrak{M}_{i\ell} \mathfrak{t}_i & \bullet & \bullet & \bullet \\ \mathfrak{N}_{i\ell} \mathfrak{t}_i & \mathfrak{S}_{i\ell} & \bullet & \bullet \\ \mathfrak{u}'_i \tilde{A}_{i\ell} \mathfrak{t}_i & \mathfrak{u}'_i \tilde{J}_{i\ell} & \mathfrak{u}'_i \mathbb{E}_i(\mathfrak{P})^{-1} \mathfrak{u}_i & \bullet \\ \tilde{C}_{fi\ell} \mathfrak{t}_i & \tilde{E}_{fi\ell} & 0 & I \end{bmatrix} > 0, \quad (3.102)$$

hold, for τ_i , v_i , \mathfrak{t}_i , and \mathfrak{u}_i given as in (3.149) and (3.96). By applying the congruence transformations $\text{diag}(\tau_i^{-1}, I, v^{-1}, I)$ and $\text{diag}(\mathfrak{t}_i^{-1}, I, \mathfrak{u}_i^{-1}, I)$ to (3.152) and (3.102), respectively, and the Schur complement to the resulting inequalities, we get that (3.63) and (3.65) hold. Finally, by noting that (3.83) and (3.85) can be equivalently rewritten as follows

$$\begin{bmatrix} \tau'_i P_i \tau & \bullet \\ 0 & \gamma_c^2 I \end{bmatrix} > \sum_{l \in \mathbb{M}_i} \phi_{il} \begin{bmatrix} \tau'_i M_{i\ell} \tau_i & \bullet \\ N_{i\ell} \tau_i & S_{i\ell} \end{bmatrix}, \quad (3.103)$$

and

$$\begin{bmatrix} \mathfrak{t}'_i \mathfrak{P}_i \mathfrak{t}_i & \bullet \\ 0 & \gamma_r^2 I \end{bmatrix} > \sum_{l \in \mathbb{M}_i} \phi_{il} \begin{bmatrix} \mathfrak{t}'_i \mathfrak{M}_{i\ell} \mathfrak{t}_i & \bullet \\ \mathfrak{N}_{i\ell} \mathfrak{t}_i & \mathfrak{S}_{i\ell} \end{bmatrix}, \quad (3.104)$$

we get, after applying the congruence transformations $\text{diag}(\tau_i^{-1}, I)$ and $\text{diag}(\mathfrak{t}_i^{-1}, I)$ to (3.153) and (3.104), respectively, that (3.62) and (3.64) hold. Thus, since (3.62)-(3.63) and (3.64)-(3.65) hold for the closed-loop system as in (3.61), we get from Lemma 7 that $\mathfrak{C} \in \mathfrak{C}$, $\|\mathcal{G}_c\|_{\tilde{w} \rightarrow z} < \gamma_c$, and $\|\mathcal{G}_c\|_{\tilde{w} \rightarrow r} < \gamma_r$, and the claim follows. ■

3.3.2 \mathcal{H}_2 Simultaneous Fault Detection and Control Design for MJLS with parameter estimation

The next result presents BMI constraints related to the control and filter design of the SFDC system (3.60).

Theorem 11. *There exists an SFDC described as in (3.60) such that $\mathfrak{C} \in \mathfrak{C}$, $\|\mathcal{G}_c\|_2^{(\tilde{w} \rightarrow z)}$*

$$\sum_{i \in \mathbb{N}} \sum_{\ell \in \mathbb{M}_i} \mu_i \phi_{i\ell} \text{Tr}(W_{i\ell}) < \lambda_c^2, \quad (3.105)$$

$$\begin{bmatrix} T_i & \bullet \\ T_i & O_i \end{bmatrix} > \sum_{\ell \in \mathbb{M}_i} \begin{bmatrix} V_{i\ell}^{11} & \bullet \\ V_{i\ell}^{21} & V_{i\ell}^{22} \end{bmatrix}, \quad (3.106)$$

$$\begin{bmatrix} W_{i\ell}^{11} & \bullet & \bullet & \bullet \\ W_{i\ell}^{21} & W_{i\ell}^{22} & \bullet & \bullet \\ \mathbb{E}_i(T)J_i & \mathbb{E}_i(T)F_i & \mathbb{E}_i(T) & \bullet \\ G_\ell J_i + \chi_\ell H_{wi} & G_\ell F_i + \chi_\ell H_{fi} & 0 & \text{Her}(G_\ell) + \mathbb{E}_i(T-O) \end{bmatrix} > 0, \quad (3.107)$$

$$\begin{bmatrix} V_{i\ell}^{11} & \bullet & \bullet & \bullet & \bullet \\ V_{i\ell}^{21} & V_{i\ell}^{22} & \bullet & \bullet & \bullet \\ \mathbb{E}_i(T)(A_i + B_i K_\ell) & \mathbb{E}_i(T)A_i & \mathbb{E}_i(T) & \bullet & \bullet \\ G_\ell(A_i + B_i K_\ell) + \Gamma_\ell + \chi_\ell L_i & G_\ell A_i + \chi_\ell L_i & 0 & \text{Her}(G_\ell) + \mathbb{E}_i(T-O) & \bullet \\ C_i + D_i K_\ell & C_i & 0 & 0 & I \end{bmatrix} > 0, \quad (3.108)$$

$$\sum_{i \in \mathbb{N}} \sum_{\ell \in \mathbb{M}_i} \mu_i \phi_{i\ell} \text{Tr}(\mathfrak{W}_{i\ell}) < \lambda_r^2, \quad (3.109)$$

$$\begin{bmatrix} \mathfrak{T}_i & \bullet \\ \mathfrak{T}_i & \mathfrak{D}_i \end{bmatrix} > \sum_{\ell \in \mathbb{M}_i} \begin{bmatrix} \mathfrak{V}_{i\ell}^{11} & \bullet \\ \mathfrak{V}_{i\ell}^{21} & \mathfrak{V}_{i\ell}^{22} \end{bmatrix}, \quad (3.110)$$

$$\begin{bmatrix} \mathfrak{W}_{i\ell}^{11} & \bullet & \bullet & \bullet & \bullet \\ \mathfrak{W}_{i\ell}^{21} & \mathfrak{W}_{i\ell}^{22} & \bullet & \bullet & \bullet \\ \mathbb{E}_i(\mathfrak{T})J_i & \mathbb{E}_i(\mathfrak{T})F_i & \mathbb{E}_i(\mathfrak{T}) & \bullet & \bullet \\ G_\ell J_i + \chi_\ell H_{wi} & G_\ell F_i + \chi_\ell H_{fi} & 0 & \text{Her}(G_\ell) + \mathbb{E}_i(\mathfrak{T}-\mathfrak{D}) & \bullet \\ \Phi_\ell H_{wi} & I + \Phi_\ell H_{fi} & 0 & 0 & I \end{bmatrix} > 0, \quad (3.111)$$

$$\begin{bmatrix} \mathfrak{V}_{i\ell}^{11} & \bullet & \bullet & \bullet & \bullet \\ \mathfrak{V}_{i\ell}^{21} & \mathfrak{V}_{i\ell}^{22} & \bullet & \bullet & \bullet \\ \mathbb{E}_i(\mathfrak{T})(A_i + B_i K_\ell) & \mathbb{E}_i(\mathfrak{T})A_i & \mathbb{E}_i(\mathfrak{T}) & \bullet & \bullet \\ G_\ell(A_i + B_i K_\ell) + \Gamma_\ell + \chi_\ell L_i & G_\ell A_i + \chi_\ell L_i & 0 & \text{Her}(G_\ell) + \mathbb{E}_i(\mathfrak{T}-\mathfrak{D}) & \bullet \\ \Theta_\ell + \Phi_\ell L_i & \Phi_\ell L_i & 0 & 0 & I \end{bmatrix} > 0. \quad (3.112)$$

$< \lambda_c$, and $\|\mathcal{G}_c\|_2^{(\tilde{w} \rightarrow r)} < \lambda_r$ for fixed $\lambda_c > 0$ and $\lambda_r > 0$ if there exist symmetric matrices $W_{i\ell}^{11}$, $W_{i\ell}^{22}$, T_i , O_i , $V_{i\ell}^{11}$, $V_{i\ell}^{22}$, $\mathfrak{W}_{i\ell}^{11}$, $\mathfrak{W}_{i\ell}^{22}$, \mathfrak{T}_i , \mathfrak{D}_i , $\mathfrak{V}_{i\ell}^{11}$, $\mathfrak{V}_{i\ell}^{22}$ and the matrices $W_{i\ell}^{21}$, $V_{i\ell}^{21}$, $\mathfrak{W}_{i\ell}^{21}$, $\mathfrak{V}_{i\ell}^{21}$, G_ℓ , Γ_ℓ , χ_ℓ , Θ_ℓ , Φ_ℓ , and K_ℓ with compatible dimensions such that inequalities (3.105), (3.106), (3.107), (3.108), (3.109), (3.110), (3.111), and (3.112) hold $\forall i \in \mathbb{N}, \ell \in \mathbb{M}$. If a feasible solution is obtained, a suitable SFDC is given by $\mathcal{A}_{c\ell} = -G_\ell^{-1}\Gamma_\ell$, $\mathcal{B}_{c\ell} = -G_\ell^{-1}\chi_\ell$, $\mathcal{C}_{c\ell} = K_\ell$, $\mathcal{C}_{f\ell} = -\Theta_\ell$, $\mathcal{D}_{f\ell} = -\Phi_\ell$.

Proof: The proof follows the similar reasoning as the one employed in the proof of Theorem 10. Similarly as presented in (GONÇALVES; FIORAVANTI; GEROMEL, 2010), (OLIVEIRA; COSTA, 2020), the structure of matrices \tilde{Q}_i and \tilde{Q}_i^{-1} of (3.73)-(3.76), and $\tilde{\mathfrak{Q}}_i$ and $\tilde{\mathfrak{Q}}_i^{-1}$ of (3.77)-(3.80), are

$$\tilde{Q}_i = \begin{bmatrix} O_i & \bullet \\ \bar{U}_i & \hat{O}_i \end{bmatrix}, \quad \tilde{Q}_i^{-1} = \begin{bmatrix} T_i^{-1} & \bullet \\ \bar{V}_i & \hat{T}_i \end{bmatrix}, \quad (3.113)$$

and

$$\tilde{\mathfrak{Q}}_i = \begin{bmatrix} \mathfrak{D}_i & \bullet \\ \bar{\mathfrak{U}}_i & \hat{\mathfrak{D}}_i \end{bmatrix}, \quad \tilde{\mathfrak{Q}}_i^{-1} = \begin{bmatrix} \mathfrak{T}_i^{-1} & \bullet \\ \bar{\mathfrak{V}}_i & \hat{\mathfrak{T}}_i \end{bmatrix}. \quad (3.114)$$

We also define the matrices η_i and σ_i

$$\eta_i = \begin{bmatrix} I & I \\ \bar{V}_i T_i & 0 \end{bmatrix}, \quad \sigma_i = \begin{bmatrix} I & \mathbb{E}_i(T) \\ 0 & \mathbb{E}_i(\bar{U}) \end{bmatrix}, \quad (3.115)$$

along with \mathbf{n}_i and \mathbf{s}_i ,

$$\mathbf{n}_i = \begin{bmatrix} I & I \\ \bar{\mathfrak{V}}_i \bar{\mathfrak{T}}_i & 0 \end{bmatrix}, \quad \mathbf{s}_i = \begin{bmatrix} I & \mathbb{E}_i(\bar{\mathfrak{T}}) \\ 0 & \mathbb{E}_i(\bar{\mathfrak{U}}) \end{bmatrix}. \quad (3.116)$$

We get from (3.107)-(3.108) as well as (3.111)-(3.112) that G_ℓ is non-singular. By setting $\bar{U}_i = -\hat{O}_i$ and $\bar{\mathfrak{U}}_i = -\hat{\mathfrak{D}}_i$ in (3.158) and (3.114) and using the fact that $\tilde{Q}_i \tilde{Q}_i^{-1} = I$ and $\tilde{\mathfrak{Q}}_i \tilde{\mathfrak{Q}}_i^{-1} = I$, we get that (3.158)-(3.116) can be rewritten as

$$\tilde{Q}_i = \begin{bmatrix} O_i & \bullet \\ T_i - O_i & O_i - T_i \end{bmatrix}, \quad \tilde{Q}_i^{-1} = \begin{bmatrix} T_i^{-1} & \bullet \\ T_i^{-1} & \Upsilon_{1i} \end{bmatrix}, \quad (3.117)$$

where $\Upsilon_{1i} = T_i^{-1} - (O_i - T_i)^{-1}$, and

$$\tilde{\mathfrak{Q}}_i = \begin{bmatrix} \mathfrak{D}_i & \bullet \\ \bar{\mathfrak{T}}_i - \mathfrak{D}_i & \mathfrak{D}_i - \bar{\mathfrak{T}}_i \end{bmatrix}, \quad \tilde{\mathfrak{Q}}_i^{-1} = \begin{bmatrix} \bar{\mathfrak{T}}_i^{-1} & \bullet \\ \bar{\mathfrak{T}}_i^{-1} & \Upsilon_{2i} \end{bmatrix}, \quad (3.118)$$

where $\Upsilon_{2i} = \bar{\mathfrak{T}}_i^{-1} - (\mathfrak{D}_i - \bar{\mathfrak{T}}_i)^{-1}$, along with

$$\eta_i = \begin{bmatrix} I & I \\ I & 0 \end{bmatrix}, \quad \sigma_i = \begin{bmatrix} I & \mathcal{E}_i(T) \\ 0 & \mathcal{E}_i(T-O) \end{bmatrix} \quad (3.119)$$

and

$$\mathbf{n}_i = \begin{bmatrix} I & I \\ I & 0 \end{bmatrix}, \quad \mathbf{s}_i = \begin{bmatrix} I & \mathbb{E}_i(\bar{\mathfrak{T}}) \\ 0 & \mathbb{E}_i(\bar{\mathfrak{T}} - \mathfrak{D}) \end{bmatrix}. \quad (3.120)$$

Recalling the previous reasoning applied in the proof of Theorem 10, we get that $G_\ell \mathbb{E}_i(O - T)^{-1} G'_\ell \geq \text{Her}(G_\ell) + \mathbb{E}_i(T - O)$ and $G_\ell \mathbb{E}_i(\mathfrak{D} - \bar{\mathfrak{T}})^{-1} G'_\ell \geq \text{Her}(G_\ell) + \mathbb{E}_i(\bar{\mathfrak{T}} - \mathfrak{D})$. By performing the change of variables $\Gamma_\ell = -G_\ell \mathcal{A}_{c\ell}$, $\chi_\ell = -G_\ell \mathcal{B}_{c\ell}$, $K_\ell = \mathcal{C}_{c\ell}$, $\Theta_\ell = -\mathcal{C}_{f\ell}$, and $\Phi_\ell = -\mathcal{D}_{f\ell}$, we can rewrite (3.107)-(3.108) and (3.111)-(3.112) as follows

$$\begin{bmatrix} W_{i\ell}^{11} & \bullet & \bullet & \bullet \\ W_{i\ell}^{21} & W_{i\ell}^{22} & \bullet & \bullet \\ \mathbb{E}_i(T) J_i & \mathbb{E}_i(T) F_i & \mathbb{E}_i(T) & \bullet \\ G_\ell [J_i - \mathcal{B}_{c\ell} H_{wi}] & G_\ell [F_i - \mathcal{B}_{c\ell} H_{fi}] & 0 & G_\ell \mathbb{E}_i(O - T)^{-1} G'_\ell \end{bmatrix} > 0, \quad (3.121)$$

and

$$\begin{bmatrix} V_{i\ell}^{11} & \bullet & \bullet & \bullet & \bullet \\ V_{i\ell}^{21} & V_{i\ell}^{22} & \bullet & \bullet & \bullet \\ \mathbb{E}_i(T) A_i (\mathcal{C}_{c\ell}) & \mathbb{E}_i(T) A_i & \mathbb{E}_i(T) & \bullet & \bullet \\ G_\ell \Upsilon_{3i\ell} & G_\ell [A_i - \mathcal{B}_{c\ell} L_i] & 0 & G_\ell \mathbb{E}_i(O - T)^{-1} G'_\ell & \bullet \\ C_i + D_i \mathcal{C}_{c\ell} & C_i & 0 & 0 & I \end{bmatrix} > 0, \quad (3.122)$$

where $A_i(C_c) = A_i + B_i C_{cl}$ and $\Upsilon_{3il} = [A_i(C_{cl}) - \mathcal{A}_{cl} - \mathcal{B}_{cl} L_i]$. Along with

$$\begin{bmatrix} \mathfrak{W}_{i\ell}^{11} & \bullet & \bullet & \bullet & \bullet \\ \mathfrak{W}_{i\ell}^{21} & \mathfrak{W}_{i\ell}^{22} & \bullet & \bullet & \bullet \\ \mathbb{E}_i(\mathfrak{T})J_i & \mathbb{E}_i(\mathfrak{T})F_i & \mathbb{E}_i(\mathfrak{T}) & \bullet & \bullet \\ G_\ell[J_i - \mathcal{B}_{cl}H_{wi}] & G_\ell[F_i - \mathcal{B}_{cl}H_{fi}] & 0 & G_\ell\mathbb{E}_i(\mathfrak{D} - \mathfrak{T})^{-1}G'_\ell & \bullet \\ -\mathcal{D}_{f\ell}H_{wi} & I - \mathcal{D}_{f\ell}H_{fi} & 0 & 0 & I \end{bmatrix} > 0, \quad (3.123)$$

and

$$\begin{bmatrix} \mathfrak{Y}_{i\ell}^{11} & \bullet & \bullet & \bullet & \bullet \\ \mathfrak{Y}_{i\ell}^{21} & \mathfrak{Y}_{i\ell}^{22} & \bullet & \bullet & \bullet \\ \mathbb{E}_i(\mathfrak{T})A_i(C_{cl}) & \mathbb{E}_i(\mathfrak{T})A_i & \mathbb{E}_i(\mathfrak{T}) & \bullet & \bullet \\ G_\ell\Upsilon_{3il} & G_\ell[A_i - \mathcal{B}_{cl}L_i] & 0 & G_\ell\mathbb{E}_i(\mathfrak{D} - \mathfrak{T})^{-1}G'_\ell & \bullet \\ -\mathcal{C}_{f\ell} - \mathcal{D}_{f\ell}L_i & -\mathcal{D}_{f\ell}L_i & 0 & 0 & I \end{bmatrix} > 0. \quad (3.124)$$

By defining the matrices

$$\bar{\Pi}_{i\ell} = \begin{bmatrix} \mathbb{E}_i(T)^{-1} & I \\ 0 & G_\ell^{-T}\mathbb{E}_i(O-T) \end{bmatrix},$$

and

$$\bar{\pi}_{i\ell} = \begin{bmatrix} \mathbb{E}_i(\mathfrak{T})^{-1} & I \\ 0 & G_\ell^{-T}\mathbb{E}_i(\mathfrak{D} - \mathfrak{T}) \end{bmatrix},$$

and applying the congruence transformations $\text{diag}(I_{r+f}, \bar{\Pi}_{i\ell})$ and $\text{diag}(I_{2n}, \bar{\Pi}_{i\ell}, I_q)$ to (3.162) and (3.163) as well as $\text{diag}(I_{r+f}, \bar{\pi}_{i\ell}, I_f)$ and $\text{diag}(I_{2n}, \bar{\pi}_{i\ell}, I_f)$ to (3.123)-(3.124), we get

$$\begin{bmatrix} W_{i\ell} & \bullet \\ \sigma'_i \tilde{J}_{i\ell} & \sigma'_i \mathbb{E}_i(\tilde{Q})^{-1} \sigma_i \end{bmatrix} > 0, \quad (3.125)$$

$$\begin{bmatrix} \eta'_i \tilde{R}_{i\ell} \eta_i & \bullet & \bullet \\ \sigma'_i \tilde{A}_{i\ell} \eta_i & \sigma'_i \mathbb{E}_i(\tilde{Q})^{-1} \sigma_i & \bullet \\ \tilde{C}_{ci\ell} \eta_i & 0 & I \end{bmatrix} > 0, \quad (3.126)$$

and

$$\begin{bmatrix} \mathfrak{W}_{i\ell} & \bullet & \bullet \\ \mathfrak{s}'_i \tilde{J}_{i\ell} & \mathfrak{s}'_i \mathbb{E}_i(\tilde{\mathfrak{Q}})^{-1} \mathfrak{s}_i & \bullet \\ \tilde{E}_{f\ell} & 0 & I \end{bmatrix} > 0, \quad (3.127)$$

$$\begin{bmatrix} \mathfrak{n}'_i \tilde{\mathfrak{R}}_{i\ell} \mathfrak{n}_i & \bullet & \bullet \\ \mathfrak{s}'_i \tilde{A}_{i\ell} \mathfrak{n}_i & \mathfrak{s}'_i \mathbb{E}_i(\tilde{\mathfrak{Q}})^{-1} \mathfrak{s}_i & \bullet \\ \tilde{C}_{fi\ell} \mathfrak{n}_i & 0 & I \end{bmatrix} > 0. \quad (3.128)$$

By applying the congruence transformations $\text{diag}(I, \sigma_i^{-1})$, $\text{diag}(\eta_i^{-1}, \sigma_i^{-1}, I)$, $\text{diag}(I, \mathfrak{s}_i^{-1}, I)$, $\text{diag}(\mathfrak{n}_i^{-1}, \mathfrak{s}_i^{-1}, I)$ to (3.164)-(3.128), we get that (3.74), (3.76), (3.78), and (3.80) hold with the closed-loop matrices of system (3.61). Finally, by noting that (3.106) and (3.110) can be rewritten as follows

$$\eta'_i \tilde{Q}_i \eta_i > \sum_{\ell \in \mathbb{M}_i} \phi_{i\ell} \eta'_i \tilde{R}_{i\ell} \eta_i, \quad (3.129)$$

and

$$\mathbf{n}_i' \tilde{\mathcal{Q}}_i \mathbf{n}_i > \sum_{\ell \in \mathbb{M}_i} \phi_{i\ell} \mathbf{n}_i' \tilde{\mathcal{R}}_{i\ell} \mathbf{n}_i, \quad (3.130)$$

and thus, by noting that (3.105) and (3.109) are equivalent to (3.73) and (3.77), and by applying the congruence transformations η_i^{-1} and \mathbf{n}_i^{-1} to (3.166)-(3.130), respectively, we get that (3.75)-(3.79) are also satisfied. Therefore, considering the discussion presented in Section 3.2, see, for instance, (COSTA; FRAGOSO; TODOROV, 2015) and (OLIVEIRA; COSTA, 2017a), we get that $\mathcal{C} \in \mathfrak{C}$, $\|\mathcal{G}_c\|_2^{(\tilde{w} \rightarrow z)} < \lambda_c$, and $\|\mathcal{G}_c\|_2^{(\tilde{w} \rightarrow r)} < \lambda_r$, and the claim follows. ■

3.3.3 Mixed $\mathcal{H}_2/\mathcal{H}_\infty$ Simultaneous Fault Detection and Control Design for MJLS with parameter estimation

We present now the design of mixed $\mathcal{H}_2/\mathcal{H}_\infty$ SFDC for MJLS with partial information on the jump parameter.

Observing the constraints in Theorems 10 and 11 it is possible to notice that the structure to obtain SFDC is the same, therefore a mixed solution can be formulated.

To increase the overall performance the \mathcal{H}_2 norm will be considered in the controller side of the design due to its equivalence to the LQR controllers, which provide good performance in practical solutions. For the fault detection side, we consider the \mathcal{H}_∞ norm, which provides an FDI with a lower occurrence of false alarms, (ZHONG et al., 2005; PATTON; FRANK; CLARK, 2013).

From the aforementioned discussion, we consider the mixed solution with the control side of the SFDC designed using the BMI conditions for Theorem 11 and the fault detection side obtained using the BMI from Theorem 10. Hence, the new rewritten optimization problem is

$$\phi = \{\mathfrak{Z}_i, \mathfrak{X}_i, \mathfrak{M}_{i\ell}, \mathfrak{N}_{i\ell}, \mathfrak{S}_{i\ell}, W_{i\ell}, V_{i\ell}, T_i, O_i G_\ell, \Gamma_\ell, \chi_\ell, K_\ell, \Theta_\ell, \Phi_\ell\} \quad (3.131)$$

$$\kappa = \{\phi \text{ such that (3.85)-(3.86) and (3.105)-(3.108) hold}$$

$$\inf_{\mathfrak{C} \in \mathfrak{C}, P, \gamma_r, \lambda_c} \{\lambda_c \zeta_c + \gamma_r \beta_r\} : \text{s. t. } \phi \in \kappa. \quad (3.132)$$

for a given $\zeta_c > 0$, $\beta_r > 0$.

Theorem 12. *There exists an SFDC described as in (3.60) such that $\mathfrak{C} \in \mathfrak{C}$, $\|\mathcal{G}_c\|_\infty^{(\tilde{w} \rightarrow r)}$*

$< \gamma_r$, and $\|\mathcal{G}_c\|_2^{(\tilde{w} \rightarrow z)} < \lambda_c$ for fixed, $\gamma_r > 0$, and $\lambda_c > 0$ if there exist symmetric matrices $\mathfrak{Z}_i, \mathfrak{X}_i, \mathfrak{M}_{il}^{11}, \mathfrak{M}_{il}^{22}, \mathfrak{S}_{il}^{11}, \mathfrak{S}_{il}^{22}, W_{il}^{11}, W_{il}^{22}, V_{il}^{11}, V_{il}^{22}, T_i, O_i$ and the matrices $\mathfrak{M}_{il}^{21}, \mathfrak{S}_{il}^{21}, \mathfrak{N}_{il}^{11}, \mathfrak{N}_{il}^{12}, \mathfrak{N}_{il}^{21}, \mathfrak{N}_{il}^{22}, W_{il}^{21}, V_{il}^{21}, G_\ell, \Gamma_\ell, \chi_\ell, \Theta_\ell, \Phi_\ell$, and K_ℓ with compatible dimensions such that inequalities, (3.85), (3.86), (3.105), (3.106), (3.107), and (3.108), hold $\forall i \in \mathbb{N}, \ell \in \mathbb{M}_i$. If a feasible solution is obtained, a suitable fault-compensation controller is given by $\mathcal{A}_{c\ell} = -G_\ell^{-1}\Gamma_\ell, \mathcal{B}_{c\ell} = -G_\ell^{-1}\chi_\ell, \mathcal{C}_{c\ell} = K_\ell, \mathcal{C}_{f\ell} = -\Theta_\ell$, and $D_{f\ell} = -\Phi_\ell$.

Proof: The proof for Theorem 12 is a direct consequence of Theorems 10 and 11. ■

Coordinate Descent Algorithm

As explained at the start of this section the constraints in Theorem 10 and 11 are in the form of Bilinear Matrices Inequalities. Therefore it is necessary to implement an appropriate procedure to solve such a problem. It can be found in the literature several numerical ways of dealing with BMI as, for instance, a combination of line search and a sequence of LMI as presented in (YAN et al., Nov 2019). Although of great interest, an analysis of the techniques to solve the BMI in Theorems 10 and 11 would fall outside the scope of this thesis. Due to that, we will focus on a procedure that is extensively used in the literature known as the Coordinate Descent Algorithm (CDA), as implemented in (SIMON et al., 2011), or (WANG; ZEMOUCHE; RAJAMANI, 2018). The specific approach implemented in the present paper was first introduced in (OLIVEIRA; COSTA, 2020).

By inspection, it is possible to observe that all the non-linearities are "caused" by the state-feedback controller K . A usual workaround for those non-linearities is to fix the state-feedback controller and solve the resulting LMI. Assume that there exists a state-feedback controller K , and apply this controller in the constraints (3.83), (3.84), (3.85), and (3.86) for the \mathcal{H}_∞ case, or (3.105), (3.106), (3.107), (3.108), (3.109), (3.110), (3.111), and (3.112) for the \mathcal{H}_2 case. If a feasible solution is found it may or may not be the optimized solution, due to the choice of the state-feedback controller. The CDA algorithm is described as in Algorithm 2.

Remark 11. Note that the initial condition for K_i can be obtained from the results in (TODOROV; FRAGOSO; COSTA, 2018), which is a state-feedback controller with similar MJLS assumptions. If the first iteration finds a feasible solution then the CDA will eventually converge to a better solution, and the amount of iteration is set using the stop criterion ϵ .

Algorithm 2: Coordinate Descent Algorithm

Input: $K_l, \gamma^{-1}, t_{max}, \epsilon$
Output: $\mathcal{A}_c, \mathcal{B}_c, \mathcal{C}_c, \mathcal{C}_f, \mathcal{D}_f$

- 1 Design stabilizing state-feedback controller (e.g. (TODOROV; FRAGOSO; COSTA, 2018)).
 - 2 Fix K in the LMI constraints for the \mathcal{H}_∞ case or for the \mathcal{H}_2 case, and solve it to obtain the matrices Z_i, \mathfrak{Z}_i , and G_ℓ for the \mathcal{H}_∞ case, or T_i, \mathfrak{T}_i , and G_ℓ for the \mathcal{H}_2 case, or \mathfrak{Z}_i, T_i , and G_ℓ for the mixed case.
 - 3 Fix $Z_i, \mathfrak{Z}_i, G_\ell$ for \mathcal{H}_∞ case, or T_i, \mathfrak{T}_i , and G_ℓ for the \mathcal{H}_2 case, or Z_i, \mathfrak{T}_i , and G_ℓ for the mixed case, and solve the same LMI constraint and now obtain $\mathcal{A}_{cl}, \mathcal{B}_{cl}, \mathcal{C}_{cl}, \mathcal{C}_{f\ell}, \mathcal{D}_{f\ell}$, and the upper bound values γ_c, γ_r for the \mathcal{H}_∞ case and λ_c, λ_r for the \mathcal{H}_2 case.
 - 4 If $\frac{\gamma_c^{t-1} - \gamma_c^t}{\gamma_c^{t-1}} \leq \epsilon$ or $t \leq t_{max}$, go back to step 2.
-

3.3.4 Simulations Results

In the same manner as in the other examples in this chapter we use the coupled tank. The discrete-time domain space-state model is

$$\begin{aligned}
 A_{1,2} &= \begin{bmatrix} -0.0239 & -0.0127 \\ 0.0127 & -0.0285 \end{bmatrix}, & B_{1,2} &= \begin{bmatrix} 0.71 & 0 \\ 0 & 0.71 \end{bmatrix}, \\
 J_{w\ 1,2} &= 0.01B_{1,2}, & J_{f\ 1,2} &= I^{2 \times 2}, \\
 L_1 &= I^{2 \times 2}, & L_2 &= 0^{2 \times 2}, & H_{w\ 1,2} &= 0.1I^{2 \times 2}, & H_{f\ 1,2} &= 0^{2 \times 2}, \\
 C_1 &= I^{2 \times 2}, & C_2 &= 0^{2 \times 2}, & D_1 &= I^{2 \times 2}, & D_2 &= 0^{2 \times 2}.
 \end{aligned}$$

The transition matrix, initial distribution, and ϕ_{kl} are

$$\mathbb{P} = \begin{bmatrix} 0.8 & 0.2 \\ 0.6 & 0.4 \end{bmatrix}, \quad \mu' = \begin{bmatrix} 0.7 \\ 0.3 \end{bmatrix}, \quad \Psi = \begin{bmatrix} 0.7 & 0.3 \\ 0.6 & 0.4 \end{bmatrix}. \quad (3.133)$$

The SFDC obtained using Theorem 10 is

$$\begin{aligned}
 A_{c1} &= \begin{bmatrix} 0.5053 & 0.1653 \\ -0.2767 & 0.4161 \end{bmatrix}, & A_{c2} &= \begin{bmatrix} 0.2048 & 0.0686 \\ -0.1065 & 0.1725 \end{bmatrix}, \\
 B_{c1} &= \begin{bmatrix} -0.8252 & -0.2487 \\ 0.5756 & -0.8252 \end{bmatrix}, & B_{c2} &= \begin{bmatrix} -0.7180 & -0.2263 \\ 0.5173 & -0.7661 \end{bmatrix}, \\
 C_{c1} &= 10^{-4} \begin{bmatrix} -0.1854 & -0.0811 \\ 0.0043 & -0.1406 \end{bmatrix}, & C_{c2} &= 10^{-4} \begin{bmatrix} 0.4957 & 0.3046 \\ -0.0602 & 0.3867 \end{bmatrix}, \\
 C_{f1} &= 10^{-6} \begin{bmatrix} -0.1244 & -0.0451 \\ 0.0547 & -0.1130 \end{bmatrix}, & C_{f2} &= 10^{-6} \begin{bmatrix} -0.5927 & -0.2846 \\ 0.2542 & -0.6101 \end{bmatrix}, \\
 D_{f1} &= 10^{-5} \begin{bmatrix} -0.2573 & -0.0176 \\ -0.0419 & -0.1089 \end{bmatrix}, & D_{f2} &= 10^{-5} \begin{bmatrix} 0.6632 & 0.0647 \\ 0.0588 & 0.3256 \end{bmatrix}.
 \end{aligned}$$

The SFDC obtained using Theorem 11 is

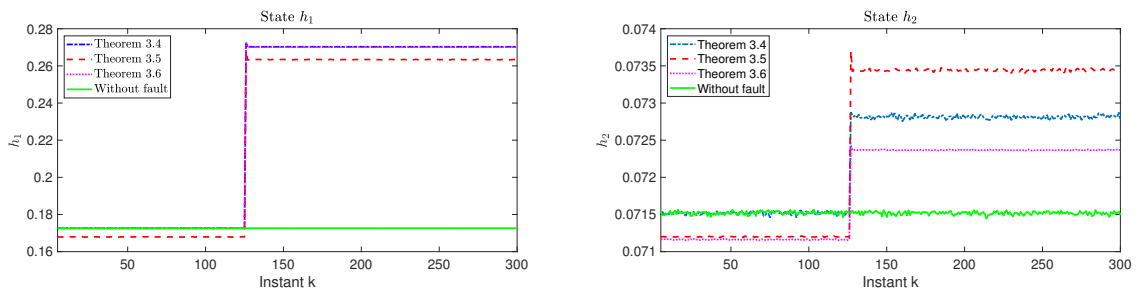
$$\begin{aligned} A_{c1} &= \begin{bmatrix} 0.5929 & 0.0388 \\ 0.0201 & -0.1255 \end{bmatrix}, & A_{c2} &= \begin{bmatrix} -0.5929 & -0.0388 \\ -0.0201 & 0.1255 \end{bmatrix}, \\ B_{c1} &= 10^{-6} \begin{bmatrix} -0.2409 & -0.0079 \\ 0.0093 & -0.3303 \end{bmatrix}, & B_{c2} &= 10^{-6} \begin{bmatrix} 0.3691 & 0.0010 \\ 0.0044 & 0.0364 \end{bmatrix}, \\ C_{c1} &= \begin{bmatrix} 0.8648 & 0.0728 \\ 0.0108 & -0.1349 \end{bmatrix}, & C_{c2} &= \begin{bmatrix} -0.8053 & -0.0366 \\ -0.0460 & 0.2186 \end{bmatrix}, \\ C_{f1} &= 10^{-13} \begin{bmatrix} 0.0748 & -0.0001 \\ 0.0000 & -0.1463 \end{bmatrix}, & C_{f2} &= 10^{-13} \begin{bmatrix} -0.0835 & 0.0001 \\ -0.0000 & 0.1375 \end{bmatrix}, \\ D_{f1} &= \begin{bmatrix} 43.2163 & -0.0000 \\ -0.0000 & 7.5839 \end{bmatrix}, & D_{f2} &= \begin{bmatrix} -33.2163 & 0.0000 \\ 0.0000 & 2.4161 \end{bmatrix}. \end{aligned}$$

For the last, the SFDC obtained using Theorem 12 is

$$\begin{aligned} A_{c1} &= \begin{bmatrix} 0.5929 & 0.0388 \\ 0.0201 & -0.1255 \end{bmatrix}, & A_{c2} &= \begin{bmatrix} -0.5929 & -0.0388 \\ -0.0201 & 0.1255 \end{bmatrix}, \\ B_{c1} &= 10^{-6} \begin{bmatrix} -0.2409 & -0.0079 \\ 0.0093 & -0.3303 \end{bmatrix}, & B_{c2} &= 10^{-6} \begin{bmatrix} 0.3691 & 0.0010 \\ 0.0044 & 0.0364 \end{bmatrix}, \\ C_{c1} &= \begin{bmatrix} 0.8648 & 0.0728 \\ 0.0108 & -0.1349 \end{bmatrix}, & C_{c2} &= \begin{bmatrix} -0.8053 & -0.0366 \\ -0.0460 & 0.2186 \end{bmatrix}, \\ C_{f1} &= 10^{-13} \begin{bmatrix} 0.0748 & -0.0001 \\ 0.0000 & -0.1463 \end{bmatrix}, & C_{f2} &= 10^{-13} \begin{bmatrix} -0.0835 & 0.0001 \\ -0.0000 & 0.1375 \end{bmatrix}, \\ D_{f1} &= \begin{bmatrix} 43.2163 & -0.0000 \\ -0.0000 & 7.5839 \end{bmatrix}, & D_{f2} &= \begin{bmatrix} -33.2163 & 0.0000 \\ 0.0000 & 2.4161 \end{bmatrix}. \end{aligned}$$

3.3.4.1 Monte Carlo Simulation

The same setup from the other examples was also implemented in this simulation. The Monte Carlo simulation with 300 iterations was performed, and the results obtained are shown in the following manner, first we present the output signal obtained using Theorem 10, 11 and, 12, in Figs. 20a, 20b, the average and standard deviation of the control signal obtained using Theorems 10, 11, 12 is presented in Fig. 22a, 22b, and 22c show the residue signals acquired for each case, and the evaluation function in Fig. 23.



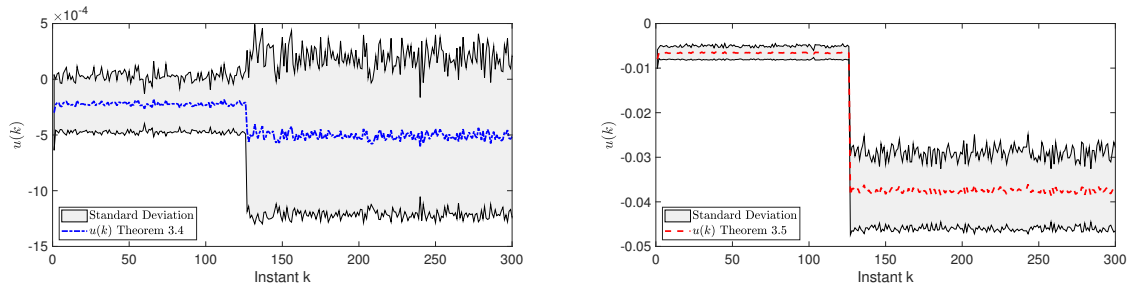
(a) Mean for first output signal obtained using Theorems 10, 11, and 12 . (b) Mean for second output signal obtained using Theorems 10, 11, and 12.

Figure 20: The Mean of the output signals obtained for SFDC designed via Theorem 10(blue curve), 11(red curve), and 12(magenta curve). All three curves were obtained when there is a fault, except for the green curve which represents the states without fault.

Observe that all controllers manage to stabilize the system, even in the presence of

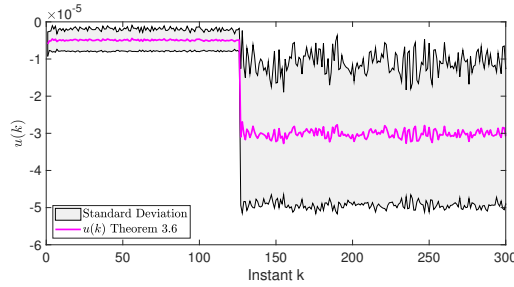
the fault, however, some presented a higher level of steady-state error after the fault, which is expected, since this controller was not designed to mitigate nor accommodate the fault. The important aspect that is observed in Figs. 20a, 20b that all controllers designed simultaneously worked properly.

Now we present Figs. 21a, 21b, 21c which represents the mean and standard deviation for the control signal using Theorems 10, 11, and 12 respectively. Observe that all control



(a) Mean and standard deviation for control signal obtained using Theorem 10.

(b) Mean and standard deviation for control signal obtained using Theorem 11



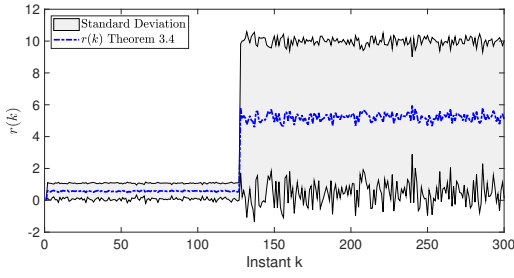
(c) Mean and standard deviation for control signal obtained using Theorem 12

Figure 21: Mean and standard deviation for all control signals acquired using the SFDC designed via Theorems 10(blue curve), 11(red curve), and 12(magenta curve).

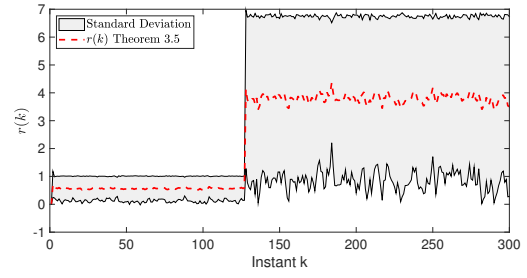
signals presented a proper behavior and standard deviation. Therefore, the controller side of the SFDC works properly.

The residue behavior obtained via Theorems 10, 11, and 12 are presented in Figs. 22a, 22b, and 22c. Regarding the residue signal obtained with Theorems 10, 11, and 12 presented a similar behavior, however, the result obtained using 10 in 22a show a slightly better performance. Observe that the standard deviation for all three approaches is low. Leading to a low chance of false alarms.

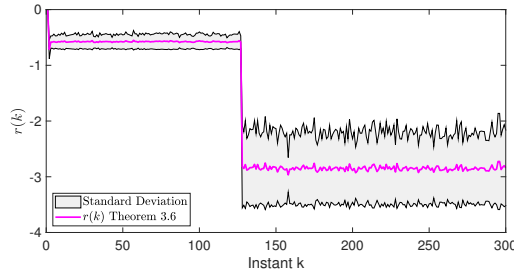
The last result obtained via Monte Carlo simulation is the behavior of the evaluation function for each case. This result is presented in Fig. 23 Fig.23 allows us to state that the results obtained using Theorem 10 presented a better performance, but all the proposed



(a) Mean and standard deviation for residue signal obtained using Theorem 10.



(b) Mean and standard deviation for residue signal obtained using Theorem 11



(c) Mean and standard deviation for residue signal obtained using Theorem 12

Figure 22: Mean and standard deviation for all residue signals acquired using the SFDC designed via Theorems 10(blue curve), 11(red curve), and 12(magenta curve).

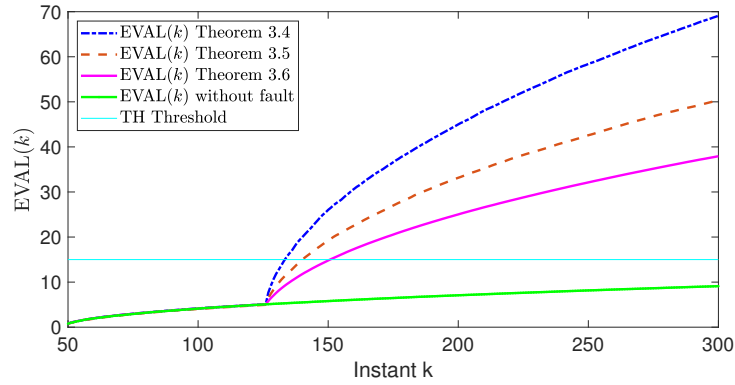


Figure 23: The mean value of the evaluation function signal for three distinct cases, where the blue curve represent the results using Theorem 10, the red curve represent the results obtained via 11, the black curve represents the results through Theorem 12, the green curve portrays the evaluation function signal when there is no fault signal, and the indigo line denotes the threshold TH.

approaches successfully detected the fault, hence, all approaches are viable solution for the FDI problem.

3.4 Fault Accommodation Formulation for MJLS with Parameter Estimation

The Fault Accommodation Control problem is a particular class of FTC, which uses a different approach when compared to the usual FTC in the literature. The majority of FTC approaches consider the occurrence of faults during the design process of a static controller. In the case of FAC, two controllers are working alongside each other where the first one is designed for the nominal conditions while the other one will be active when a fault occurs.

For the FAC problem, we consider the following MJLS formulation

$$\mathcal{G} : \begin{cases} x(k+1) = A_{\theta(k)}x(k) + B_{\theta(k)}u_{\text{Total}}(k) + J_{\theta(k)}w(k) + F_{\theta(k)}f(k), \\ y(k) = C_{\theta(k)}x(k) + D_{\theta(k)}w(k), \\ x(0) = x_0, \end{cases} \quad (3.134)$$

where the vectors $x(k) \in \mathbb{R}^{n_x}$, $y(k) \in \mathbb{R}^{n_p}$, $w(k) \in \mathbb{R}^{n_d}$, $f(k) \in \mathbb{R}^{n_f}$, $u_{\text{Total}}(k) \in \mathbb{R}^{n_u}$ are respectively, the system state, output, exogenous input, fault signal, the control input, and $\theta(k)$ denotes the mode of a Markov chain which is initialized at θ_0 . The nominal control is provided by a state-feedback controller

$$u(k) = -K_{\hat{\theta}(k)}x(k), \quad (3.135)$$

where $x(k) \in \mathbb{R}^{n_x}$ represents the states of system (3.134).

Fig.24 depicts the overall block diagram of the MJLS along with the FAC controllers K_{ℓ} for the nominal one and $K_{c\ell}$ for the faulty ones.

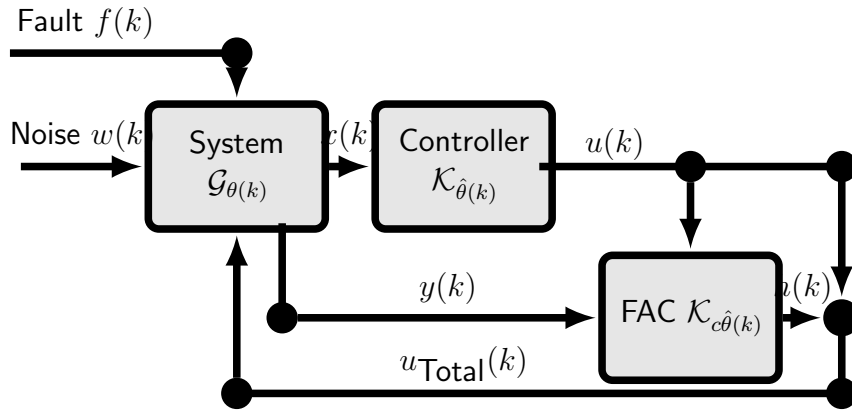


Figure 24: Fault accommodation control scheme diagram under the assumption that the network model is not accessible.

As shown in Fig.24, the signal $u_{\text{total}}(k)$ is the sum of the nominal control signal $u(k)$

and the fault compensation control signal $h(k)$, as in

$$u_{\text{Total}}(k) = u(k) + h(k). \quad (3.136)$$

Consequently, in nominal conditions the signal $h(k)$ is close to zero. In other words, the fault compensation control signal only acts in the presence of a fault as expected.

The FAC controller \mathcal{K}_c is assumed to have the following structure

$$\mathcal{K}_c : \begin{cases} \eta(k+1) = \mathfrak{A}_{\hat{\theta}(k)}\eta(k) + \mathfrak{M}_{\hat{\theta}(k)}u(k) + \mathfrak{B}_{\hat{\theta}(k)}y(k), \\ h(k) = \mathfrak{C}_{\hat{\theta}(k)}\eta(k), \\ \eta(0) = \eta_0, \end{cases} \quad (3.137)$$

where $\eta \in \mathbb{K}^{n_\eta}$ represents the FAC state vector, $u(k)$ and $y(k)$, are respectively, the control signal from the nominal controller and the measured signal from the system. It is of utmost importance to note that the FAC does not depend on the index $\theta(k)$. Instead, it depends solely on the index $\hat{\theta}(k)$, which is one of the novelties of the present work.

As presented in Figure 24 the closed-loop for system (3.134), the state feedback control law (3.135), and the proposed FAC (3.137) can be compactly written as

$$\mathcal{G}_{\text{aug}} : \begin{cases} \bar{x}(k+1) = \bar{A}_{\theta(k)\hat{\theta}(k)}\bar{x}(k) + \bar{J}_{\theta(k)\hat{\theta}(k)}\bar{w}(k), \\ \bar{z}(k) = \bar{C}_{\theta(k)\hat{\theta}(k)}\bar{x}(k) + \bar{D}_{\theta(k)\hat{\theta}(k)}\bar{w}(k), \\ \bar{x}(0) = \eta_0, \end{cases} \quad (3.138)$$

where $\bar{x}(k) = [x(k) \ \eta(k)]$ and $\bar{w}(k) = [w(k) \ f(k)]$, with the augmented matrices given by

$$\bar{A}_{i\ell} = \begin{bmatrix} A_i - B_i K_\ell & B_i \mathfrak{C}_\ell \\ \mathfrak{B}_\ell C_i - \mathfrak{M}_\ell K_\ell & \mathfrak{A}_i \end{bmatrix}, \quad \bar{J}_{i\ell} = \begin{bmatrix} J_i & F_i \\ \mathfrak{B}_\ell D_i & 0 \end{bmatrix}. \quad (3.139)$$

As previously stated, the main purpose of this work is to provide a FAC design, as in (3.137), where the supplementary control signal will accommodate the fault signal. This accommodation for the \mathcal{H}_∞ case is described by the difference $o(k) = F_{\theta(k)}f(k) - B_{\theta(k)}h(k)$, which we desire to be close to zero. From the above, the optimization problem regarding the \mathcal{H}_∞ case can be described as

$$\|\mathcal{G}_{\text{aug}}\|_\infty = \sup_{\|\bar{w}\|_2 \neq 0, \bar{w} \in \mathcal{L}_2} \frac{\|o\|_2}{\|\bar{w}\|_2} < \gamma, \quad \gamma > 0, \quad (3.140)$$

where the augmented matrices $\bar{C}_{i\ell}$ and $\bar{D}_{i\ell}$ are given by

$$\bar{C}_{i\ell} = [0 \ -B_i \mathfrak{C}_\ell], \quad \bar{D}_{i\ell} = [0 \ F_i]. \quad (3.141)$$

The use of the \mathcal{H}_2 norm as a performance criteria is due to the similarities to the LQR controllers, which are known in the literature for its good performance and reliability. Therefore, the optimization problem for the \mathcal{H}_2 case can be described as

$$\|\mathcal{G}_{\text{aug}}\|_2^2 = \sum_{s=1}^m \sum_{i=1}^N \mu_i \|o\|_2^2 < \delta, \quad (3.142)$$

where the augmented matrices are

$$\bar{C}_{i\ell} = [0 \ -B_i \mathfrak{C}_\ell], \quad \bar{D}_{i\ell} = [0 \ F_i].$$

It is important to point out that the controller K_ℓ is obtained beforehand, for instance the controller in (TODOROV; FRAGOSO; COSTA, 2018), but any other controller that guarantees stability in the same condition can be implemented.

3.4.1 \mathcal{H}_∞ Fault Accommodation Control Design for MJLS with Parameter Estimation

Our first main result on the procedures to design the FAC for the \mathcal{H}_∞ norm case is presented in Theorem 13 below.

Theorem 13. *There exist a mode-dependent FAC as described in (3.137) satisfying the constraint (3.140) for some $\gamma > 0$ if there exist symmetric matrices Z_i , X_i , $M_{i\ell}^{11}$, $M_{i\ell}^{22}$, $S_{i\ell}^{11}$, $S_{i\ell}^{22}$ and matrices $M_{i\ell}^{21}$, $N_{i\ell}^{11}$, $N_{i\ell}^{12}$, $N_{i\ell}^{21}$, $N_{i\ell}^{22}$, $S_{i\ell}^{21}$, R_ℓ , \mathfrak{A}_ℓ , \mathfrak{B}_ℓ , \mathfrak{M}_ℓ , and \mathfrak{C}_ℓ with compatible dimensions such that inequalities*

$$\begin{bmatrix} Z_i & \bullet & \bullet & \bullet \\ Z_i & X_i & \bullet & \bullet \\ 0 & 0 & \gamma^2 I & \bullet \\ 0 & 0 & 0 & \gamma^2 I \end{bmatrix} > \sum_{\ell \in \mathbb{M}_i} \phi_{i\ell} \begin{bmatrix} M_{i\ell}^{11} & \bullet & \bullet \\ M_{i\ell}^{21} & M_{i\ell}^{22} & \bullet \\ N_{i\ell}^{11} & N_{i\ell}^{12} & S_{i\ell}^{11} & \bullet \\ N_{i\ell}^{21} & N_{i\ell}^{22} & S_{i\ell}^{21} & S_{i\ell}^{22} \end{bmatrix}, \quad (3.143)$$

$$\begin{bmatrix} M_{i\ell}^{11} & \bullet & \bullet & \bullet & \bullet & \bullet & \bullet \\ M_{i\ell}^{21} & M_{i\ell}^{22} & \bullet & \bullet & \bullet & \bullet & \bullet \\ N_{i\ell}^{11} & N_{i\ell}^{12} & S_{i\ell}^{11} & \bullet & \bullet & \bullet & \bullet \\ N_{i\ell}^{21} & N_{i\ell}^{22} & S_{i\ell}^{21} & S_{i\ell}^{22} & \bullet & \bullet & \bullet \\ \Pi_{i\ell}^{5,1} & \Pi_{i\ell}^{5,2} & \mathcal{E}_i(Z)J_i & \mathcal{E}_i(Z)F_i & \mathcal{E}_i(Z) & \bullet & \bullet \\ \Pi_{i\ell}^{6,1} & \Pi_{i\ell}^{6,2} & R_\ell J_i + R_\ell \mathfrak{B}_\ell D_i & R_\ell F_i & 0 & \Pi_{i\ell}^{6,6} & \bullet \\ -B_i \mathfrak{C}_\ell & 0 & 0 & F_i & 0 & 0 & I \end{bmatrix} < 0, \quad (3.144)$$

with

$$\begin{aligned}\Pi_{i\ell}^{5,1} &= \mathbb{E}_i(Z)A_i - \mathbb{E}_i(Z)B_iK_\ell + \mathbb{E}_i(Z)B_i\mathfrak{C}_\ell, & \Pi_{i\ell}^{5,2} &= \mathbb{E}_i(Z)A_i - \mathbb{E}_i(Z)B_iK_\ell, \\ \Pi_{i\ell}^{6,1} &= R_\ell(A_i - B_iK_\ell + B_i\mathfrak{C}_\ell + \mathfrak{A}_\ell + \mathfrak{B}_\ell C_i - \mathfrak{M}_\ell K_\ell), \\ \Pi_{i\ell}^{6,2} &= R_\ell(A_i - B_iK_\ell + \mathfrak{B}_\ell C_i - \mathfrak{M}_\ell K_\ell), & \Pi_{i\ell}^{6,6} &= \text{Her}(R_\ell) - \mathbb{E}_i(X) + \mathbb{E}_i(Z),\end{aligned}$$

hold for all $i \in \mathbb{K}$ and for all $\ell \in \mathbb{M}_i$.

Proof: The proof is based on the results presented in (OLIVEIRA; COSTA, 2020) and (GONÇALVES; FIORAVANTI; GEROMEL, 2010). We impose as before, the structure of the matrices P_i and P_i^{-1} of (3.10)-(3.11) as

$$P_i = \begin{bmatrix} X_i & \bullet \\ U_i & \hat{X}_i \end{bmatrix}, \quad P_i^{-1} = \begin{bmatrix} Z_i^{-1} & \bullet \\ V_i & \hat{Y}_i \end{bmatrix}. \quad (3.145)$$

Also define the matrices τ_i and v_i as

$$\tau_i = \begin{bmatrix} I & I \\ V_i Z_i & 0 \end{bmatrix}, \quad v_i = \begin{bmatrix} I & \mathbb{E}_i(X) \\ 0 & \mathbb{E}_i(U) \end{bmatrix}. \quad (3.146)$$

Observing that (3.144) is diagonal block, we can also write that $\text{Her}(R_\ell) > \mathbb{E}_i(X - Z) > 0$, and as a by-product R_ℓ is non-singular. Setting $U_i = -\hat{X}_i$, allow us to rewrite the matrices P_i and P_i^{-1} as

$$P_i = \begin{bmatrix} X_i & \bullet \\ Z_i - X_i & X_i - Z_i \end{bmatrix}, \quad (3.147)$$

$$P_i^{-1} = \begin{bmatrix} Z_i^{-1} & \bullet \\ Z_i^{-1} & Z_i^{-1} + (X_i - Z_i)^{-1} \end{bmatrix}. \quad (3.148)$$

Hence, (3.146) are now

$$\tau_i = \begin{bmatrix} I & I \\ I & 0 \end{bmatrix}, \quad v_i = \begin{bmatrix} I & \mathbb{E}_i(X) \\ 0 & \mathbb{E}_i(Z - X) \end{bmatrix}. \quad (3.149)$$

Following the same idea from the proofs provided for the FDF case in Section 3.2. As R_ℓ is non-singular, and using the results presented in (OLIVEIRA; BERNUSSOU; GEROMEL, 1999; GONÇALVES; FIORAVANTI; GEROMEL, 2010), we get that $R_\ell \mathbb{E}_i(X - Z)^{-1} R'_\ell \geq \text{Her}(R_\ell) + \mathbb{E}_i(Z - X)$, so that the constraint (3.144) still hold if the diagonal term $\text{Her}(R_\ell) + \mathbb{E}_i(Z - X)$ is substituted by $R_\ell \mathbb{E}_i(X - Z)^{-1} R'_\ell$, resulting in

$$\begin{bmatrix} M_{i\ell}^{11} & \bullet & \bullet & \bullet & \bullet & \bullet & \bullet \\ M_{i\ell}^{21} & M_{i\ell}^{22} & \bullet & \bullet & \bullet & \bullet & \bullet \\ N_{i\ell}^{11} & N_{i\ell}^{12} & S_{i\ell}^{11} & \bullet & \bullet & \bullet & \bullet \\ N_{i\ell}^{21} & N_{i\ell}^{22} & S_{i\ell}^{21} & S_{i\ell}^{22} & \bullet & \bullet & \bullet \\ \Xi_{i\ell}^{5,1} & \Xi_{i\ell}^{5,2} & \mathbb{E}_i(Z)J_i & \mathbb{E}_i(Z)F_i & \mathbb{E}_i(Z) & \bullet & \bullet \\ \Xi_{i\ell}^{6,1} & \Xi_{i\ell}^{6,2} & \Xi_{i\ell}^{6,3} & \Xi_{i\ell}^{6,4} & 0 & \Xi_{i\ell}^{6,6} & \bullet \\ -B_i\mathfrak{C}_\ell & 0 & 0 & F_i & 0 & 0 & I \end{bmatrix} > 0, \quad (3.150)$$

where

$$\begin{aligned}
\Xi_{i\ell}^{5,1} &= \mathbb{E}_i(Z)A_i - \mathbb{E}_i(Z)B_iK_\ell - \mathbb{E}_i(Z)B_i\mathfrak{C}_\ell, & \Xi_{i\ell}^{5,2} &= \mathbb{E}_i(Z)A_i - \mathbb{E}_i(Z)B_iK_\ell, \\
\Xi_{i\ell}^{6,1} &= R_\ell(A_i - B_iK_\ell + B_i\mathfrak{C}_\ell + \mathfrak{A}_\ell + \mathfrak{B}_\ell C_i - \mathfrak{M}_\ell K_\ell), \\
\Xi_{i\ell}^{6,2} &= R_\ell(A_i - B_iK_i + \mathfrak{B}_\ell C_i - \mathfrak{M}_\ell K_\ell), \\
\Xi_{i\ell}^{6,3} &= R_\ell J_i + R_\ell \mathfrak{B}_\ell D_i, & \Xi_{i\ell}^{6,4} &= R_\ell F_i, & \Xi_{i\ell}^{6,6} &= R_\ell \mathbb{E}_i(X - Z)^{-1} R'_\ell.
\end{aligned}$$

Now defining the matrix $\Pi_{i\ell}$ as

$$\Pi_{i\ell} = \begin{bmatrix} \mathbb{E}_i(Z)^{-1} & I \\ 0 & R_\ell^{-T} \mathbb{E}_i(X - Z) \end{bmatrix}, \quad (3.151)$$

and pre and post multiplying (3.150) by $\text{diag}(I, I, \Pi_{i\ell}, I)$, and its transpose, respectively, we get that

$$\begin{bmatrix} \tau'_i M_{i\ell} \tau_i & \bullet & \bullet & \bullet \\ N_{i\ell} \tau_i & S_{i\ell} & \bullet & \bullet \\ v'_i \bar{A}_{i\ell} \tau_i & v'_i \bar{J}_{i\ell} & v'_i \mathbb{E}_i(P)^{-1} v_i & \bullet \\ \bar{C}_{i\ell} \tau_i & \bar{D}_{i\ell} & 0 & I \end{bmatrix} > 0. \quad (3.152)$$

By pre and post multiplying (3.152) by $\text{diag}(\tau_i^{-1}, I, v_i^{-1}, I)$, and after that using the Schur complement to the resulting constraint, we obtain that (3.11) holds. At last, observing that (3.143) can be rewritten as

$$\begin{bmatrix} \tau'_i P_i \tau & \bullet \\ 0 & \gamma^2 I \end{bmatrix} > \sum_{\ell \in \mathbb{M}_i} \phi_{i\ell} \begin{bmatrix} \tau'_i M_{i\ell} \tau_i & \bullet \\ N_{i\ell} \tau_i & S_{i\ell} \end{bmatrix}, \quad (3.153)$$

we get, after pre and post multiplying (3.153) by $\text{diag}(\tau_i^{-1}, I)$, that constraint (3.10) holds. Since (3.10)-(3.11) hold for the closed-loop system as in (3.138), we get from Lemma 7 that $\|\mathcal{G}_{\text{aug}}\|_\infty < \gamma$, and the claim follows. \blacksquare

Remark 12. Notice that the matrices for the FAC controller in (3.137) and satisfying (3.140) are directly obtained from the solution of the inequalities (3.143), (3.144).

Remark 13. It is necessary to explain that the state feedback controller K_ℓ is given, and designed beforehand using for example the Theorems presented in (TODOROV; FRAGOSO; COSTA, 2018). The nominal controller is not designed using Theorem 13.

3.4.2 \mathcal{H}_2 Fault Accommodation Control Design for MJLS with Parameter Estimation

We present now the design of an FAC for the \mathcal{H}_2 norm case.

Theorem 14. There exists a mode-dependent FAC \mathcal{K}_c as in (3.137) satisfying the constraint (3.142) for some $\delta > 0$ if there exist symmetric matrices $T_i, O_i, W_{i\ell}^{11}, W_{i\ell}^{22}, V_{i\ell}^{11}$,

$V_{i\ell}^{22}$ and matrices $W_{i\ell}^{21}$, $V_{i\ell}^{21}$, R_ℓ , \mathfrak{A}_ℓ , \mathfrak{B}_ℓ , \mathfrak{M}_ℓ , and \mathfrak{C}_ℓ with compatible dimensions such that the inequalities

$$\sum_{i=1}^N \sum_{\ell \in \mathbb{M}_i} \mu_i \phi_{i\ell} \text{Tr} \left(\begin{bmatrix} W_{i\ell}^{11} & \bullet \\ W_{i\ell}^{21} & W_{i\ell}^{22} \end{bmatrix} \right) < \delta^2, \quad (3.154)$$

$$\begin{bmatrix} T_i & \bullet \\ T_i & O_i \end{bmatrix} > \sum_{\ell \in \mathbb{M}_i} \phi_{i\ell} \begin{bmatrix} V_{i\ell}^{11} & \bullet \\ V_{i\ell}^{21} & V_{i\ell}^{22} \end{bmatrix}, \quad (3.155)$$

$$\begin{bmatrix} W_{i\ell}^{11} & \bullet & \bullet & \bullet & \bullet \\ W_{i\ell}^{21} & W_{i\ell}^{22} & \bullet & \bullet & \bullet \\ \mathbb{E}_i(T)J_i & \mathbb{E}_i(T)F_i & \mathbb{E}_i(T) & \bullet & \bullet \\ R_\ell J_i + R_\ell \mathfrak{B}_\ell D_i & R_\ell F_i & 0 & \Theta_{i\ell}^{4,4} & \bullet \\ 0 & F_i & 0 & 0 & I \end{bmatrix} > 0, \quad (3.156)$$

$$\begin{bmatrix} V_{i\ell}^{11} & \bullet & \bullet & \bullet & \bullet \\ V_{i\ell}^{21} & V_{i\ell}^{22} & \bullet & \bullet & \bullet \\ \check{\Theta}_{i\ell}^{3,1} & \check{\Theta}_{i\ell}^{3,2} & \mathcal{E}_i(T) & \bullet & \bullet \\ \check{\Theta}_{i\ell}^{4,1} & \check{\Theta}_{i\ell}^{4,2} & 0 & \check{\Theta}_{i\ell}^{4,4} & \bullet \\ -B_i \mathfrak{C}_\ell & 0 & 0 & 0 & I \end{bmatrix} > 0, \quad (3.157)$$

with

$$\begin{aligned} \Theta_{i\ell}^{4,4} &= \text{Her}(R_\ell) + \mathbb{E}_i(O) - \mathbb{E}_i(T), & \check{\Theta}_{i\ell}^{3,1} &= \mathbb{E}_i(T)(A_i - B_i K_\ell + B_i \mathfrak{C}_\ell), \\ \check{\Theta}_{i\ell}^{3,2} &= \mathbb{E}_i(T)(A_i - B_i K_\ell), & \check{\Theta}_{i\ell}^{4,1} &= R_\ell(A_i - B_i K_\ell + B_i \mathfrak{C}_\ell + \mathfrak{A}_\ell + \mathfrak{B}_\ell C_i - \mathfrak{M}_\ell K_\ell), \\ \check{\Theta}_{i\ell}^{4,2} &= R_\ell(A_i - B_i K_\ell + \mathfrak{B}_\ell C_i - \mathfrak{M}_\ell K_\ell), & \check{\Theta}_{i\ell}^{4,4} &= \text{Her}(R_\ell) + \mathbb{E}_i(O) - \mathbb{E}_i(T), \end{aligned}$$

hold for all $i \in \mathbb{K}$ and for all $\ell \in \mathbb{M}_i$.

Proof: The proof uses a similar scheme as the one of Theorem 13. Consider \bar{Q}_i in (3.16)-(3.19) with the following form

$$\bar{Q}_i = \begin{bmatrix} O_i & \bullet \\ \bar{U}_i & \hat{O}_i \end{bmatrix}, \quad \bar{Q}_i^{-1} = \begin{bmatrix} T_i^{-1} & \bullet \\ \bar{V}_i & \hat{T}_i \end{bmatrix}, \quad (3.158)$$

and define the matrices η_i and σ_i by

$$\eta_i = \begin{bmatrix} I & I \\ \bar{V}_i T_i & 0 \end{bmatrix}, \quad \sigma_i = \begin{bmatrix} I & \mathbb{E}_i(T) \\ 0 & \mathbb{E}_i(\bar{U}) \end{bmatrix}. \quad (3.159)$$

It follows from (3.156)-(3.157) that R_ℓ is non-singular. By imposing $\bar{U}_i = -\hat{O}_i$ and recalling that $\bar{Q}_i \bar{Q}_i^{-1} = I$, we can rewrite (3.158) as

$$\bar{Q}_i = \begin{bmatrix} O_i & \bullet \\ T_i - O_i & O_i - T_i \end{bmatrix}, \quad \bar{Q}_i^{-1} = \begin{bmatrix} T_i^{-1} & \bullet \\ T_i^{-1} & \Upsilon_{1i} \end{bmatrix}, \quad (3.160)$$

where $\Upsilon_{1i} = T_i^{-1} - (O_i - T_i)^{-1}$, and we can also rewrite (3.159) as

$$\nu_i = \begin{bmatrix} I & I \\ I & 0 \end{bmatrix}, \quad \sigma_i = \begin{bmatrix} I & \mathbb{E}_i(T) \\ 0 & \mathbb{E}_i(T - O) \end{bmatrix}. \quad (3.161)$$

Using the same idea applied as in the proof of Theorem 13 we get that $R_\ell \mathbb{E}_i(O - T)^{-1} R_\ell' \geq$

$\text{Her}(R_\ell) + \mathbb{E}_i(T - O)$. Let us rewrite (3.156)-(3.157) as follows

$$\begin{bmatrix} W_{i\ell}^{11} & \bullet & \bullet & \bullet & \bullet \\ W_{i\ell}^{21} & W_{i\ell}^{22} & \bullet & \bullet & \bullet \\ \mathbb{E}_i(T)J_i & \mathbb{E}_i(T)F_i & \mathbb{E}_i(T) & \bullet & \bullet \\ R_\ell J_i - R_\ell \mathfrak{B}_\ell D_i & R_\ell F_i & 0 & T_{33} & \bullet \\ 0 & F_i & 0 & 0 & I \end{bmatrix} > 0, \quad (3.162)$$

$$T_{33} = \text{Her}(R_\ell) + \mathbb{E}_i(O) - \mathbb{E}_i(T),$$

and

$$\begin{bmatrix} V_{i\ell}^{11} & \bullet & \bullet & \bullet & \bullet \\ V_{i\ell}^{21} & V_{i\ell}^{22} & \bullet & \bullet & \bullet \\ \Psi_{i\ell}^{3,1} & \Psi_{i\ell}^{3,2} & \mathbb{E}_i(T) & \bullet & \bullet \\ \Psi_{i\ell}^{4,1} & \Psi_{i\ell}^{4,2} & 0 & R_\ell \mathbb{E}_i(O-T)^{-1} R_\ell' & \bullet \\ -B_i \mathfrak{C}_\ell & 0 & 0 & 0 & I \end{bmatrix} > 0, \quad (3.163)$$

$$\begin{aligned} \Psi_{i\ell}^{3,1} &= \mathbb{E}_i(T)(A_i - B_i K_\ell + B_i \mathfrak{C}_\ell), & \Psi_{i\ell}^{3,2} &= \mathbb{E}_i(T)(A_i - B_i K_\ell), \\ \Psi_{i\ell}^{4,1} &= R_\ell(A_i - B_i K_\ell + B_i \mathfrak{C}_\ell + \mathfrak{A}_\ell + \mathfrak{B}_\ell C_i - \mathfrak{M}_\ell K_\ell), \\ \Psi_{i\ell}^{4,2} &= R_\ell(A_i - B_i K_\ell + B_i + \mathfrak{B}_\ell C_i - \mathfrak{M}_\ell K_\ell). \end{aligned}$$

By defining

$$\bar{\Pi}_{i\ell} = \begin{bmatrix} \mathbb{E}_i(T)^{-1} & I \\ 0 & R_\ell^{-T} \mathbb{E}_i(O-T) \end{bmatrix},$$

pre and post multiplying (3.162) by $\text{diag}(I, I, \bar{\Pi}_{i\ell})$, and (3.163) by $\text{diag}(I, I, \bar{\Pi}_{i\ell}, I)$ we get

$$\begin{bmatrix} W_{i\ell} & \bullet & \bullet \\ \sigma_i' J_{i\ell} & \sigma_i' \mathbb{E}_i(\bar{Q})^{-1} \sigma_i & \bullet \\ \bar{D}_{i\ell} & 0 & I \end{bmatrix} > 0, \quad (3.164)$$

$$\begin{bmatrix} \nu_i' \bar{R}_{i\ell} \nu_i & \bullet & \bullet \\ \sigma_i' \bar{A}_{i\ell} \nu_i & \sigma_i' \mathbb{E}_i(\bar{Q})^{-1} \sigma_i & \bullet \\ \bar{C}_{i\ell} \nu_i & 0 & I \end{bmatrix} > 0. \quad (3.165)$$

By pre and post multiplying (3.164) by $\text{diag}(I, \sigma_i^{-1}, I)$, and (3.165) by $\text{diag}(\nu_i^{-1}, \sigma_i^{-1}, I)$ we get that (3.17), (3.19), hold with the closed-loop matrices of system (3.138). Consequently we can rewrite (3.154) as

$$\nu_i' \bar{Q}_i \nu_i > \sum_{\ell \in \mathbb{M}_i} \phi_{i\ell} \nu_i' \bar{R}_{i\ell} \nu_i. \quad (3.166)$$

Therefore, it is noticeable that (3.154) and (3.16) are equivalent, we can see that (3.18) is also satisfied by pre and pos multiplying (3.166) by ν_i^{-1} . From Lemma 6, $\|\mathcal{G}_{\text{aug}}\|_2 < \delta$, and the claim follows. \blacksquare

Remark: As for the \mathcal{H}_∞ case, the matrices for the FAC controller in (3.137) and satisfying (3.142) are directly obtained from the solution of the inequalities (3.154)-(3.157).

3.4.3 Mixed $\mathcal{H}_2/\mathcal{H}_\infty$ Fault Accommodation Control Design for MJLS with Parameter Estimation

Now we provide the design of mixed $\mathcal{H}_2 / \mathcal{H}_\infty$ FAC for MJLS with partial information on the jump parameter.

By inspecting the BMI constraints provided in Theorems 13 and Theorem 14 we can observe that the structure to solve the FAC problem is similar. This similarity allows us to also obtain a mixed solution.

The main motivation to provide the mixed solution is that the FAC will consider both \mathcal{H}_∞ and \mathcal{H}_2 norms during the design process. On the one hand, a guaranteed \mathcal{H}_∞ norm implies that the closed-loop system is robust against external noise signals. On the other hand, the energy of the control signal is minimized in the \mathcal{H}_2 design approach which is desirable as there is no parallel actuators in the systems.

Bearing in mind this information, we provide the mixed design of a FAC using the BMI conditions for Theorem 13 and 14. Hence, we rewrite the constraints as

$$\phi = \{Z_i, X_i, M_{il}^{11}, M_{il}^{22}, S_{il}^{11}, S_{il}^{22}, M_{il}^{21}, N_{il}^{11}, N_{il}^{12}, N_{il}^{21}, N_{il}^{22}, S_{il}^{21}, T_i, O_i, W_{il}^{11}, \\ W_{il}^{21}, W_{il}^{22}, V_{il}^{11}, V_{il}^{21}, V_{il}^{22} R_\ell, \mathfrak{A}_\ell, \mathfrak{B}_\ell, \mathfrak{M}_\ell, \mathfrak{C}_\ell, i \in \mathbb{N}, \ell \in \mathbb{M}_i\} \quad (3.167)$$

$$\kappa = \{Z_i, X_i, M_{il}^{11}, M_{il}^{22}, S_{il}^{11}, S_{il}^{22}, M_{il}^{21}, N_{il}^{11}, N_{il}^{12}, N_{il}^{21}, N_{il}^{22}, S_{il}^{21}, T_i, O_i, W_{il}^{11}, \\ W_{il}^{21}, W_{il}^{22}, V_{il}^{11}, V_{il}^{21}, V_{il}^{22} R_\ell, \mathfrak{A}_\ell, \mathfrak{B}_\ell, \mathfrak{M}_\ell, \mathfrak{C}_\ell\}_{il} \in \phi \\ (3.143)-(3.144) \text{ and } (3.154)-(3.157) \text{ hold for some } \gamma \text{ and } \delta\} \quad (3.168)$$

in which case, the mixed \mathcal{H}_∞ and \mathcal{H}_2 optimization problem is given by

$$\inf_{\phi \in \kappa} \{\gamma^2 \zeta + \delta^2 \beta\}, \quad (3.169)$$

for given weighting scalars $\zeta > 0, \beta > 0$.

Theorem 15. *There exists a mode-dependent FAC \mathcal{K}_c as in (3.137) such that $\|\mathcal{G}_{aug}\|_\infty < \gamma$ and $\|\mathcal{G}_{aug}\|_2 < \delta$ for given $\gamma > 0$ and $\delta > 0$ if there exist symmetric matrices $Z_i, X_i, M_{il}^{11}, M_{il}^{22}, S_{il}^{11}, S_{il}^{22}, T_i, O_i, W_{il}^{11}, W_{il}^{22}, V_{il}^{11}, V_{il}^{22}$ and the matrices $M_{il}^{21}, N_{il}^{11}, N_{il}^{12}, N_{il}^{21}, N_{il}^{22}, S_{il}^{21}, W_{il}^{21}, V_{il}^{21}, R_\ell, \mathfrak{A}_\ell, \mathfrak{B}_\ell, \mathfrak{M}_\ell,$ and \mathfrak{C}_ℓ with compatible dimensions such that inequalities, (3.143), (3.144), (3.154), (3.155), (3.156) and (3.157) hold for all $i \in \mathbb{N}$ and for all $\ell \in \mathbb{M}_i$.*

Proof: The proof for Theorem 15 is a direct consequence of Theorems 13 and 14. ■

Remark 14. *It is important to mention that the level of conservatism in Theorem 15 is higher in comparison to that of Theorem 13 and Theorem 14, since Theorem 15 considers*

the BMI constraints (3.143)-(3.144) from Theorem 13 and (3.154)-(3.157) from Theorem 14 simultaneously. Note that the number of variables for each theorem is

$$\text{Theorem 13} \rightarrow 10 \times i_{\max} \times \ell_{\max} + 2 \times i_{\max} + 5 \times \ell_{\max} + 1$$

$$\text{Theorem 14} \rightarrow 6 \times i_{\max} \times \ell_{\max} + 2 \times i_{\max} + 5 \times \ell_{\max} + 1$$

$$\text{Theorem 15} \rightarrow 16 \times i_{\max} \times \ell_{\max} + 4 \times i_{\max} + 5 \times \ell_{\max} + 2$$

It is noteworthy that the number of variables in Theorem 15 is not the direct sum of the variables in Theorem 13 and 14, because matrices R_ℓ , \mathfrak{A}_ℓ , \mathfrak{B}_ℓ , \mathfrak{M}_ℓ , and \mathfrak{C}_ℓ , which are the matrices that compose the FAC (3.137), are present in the BMIs constraints of Theorem 13 and 14. Regarding the number of BMI constraints Theorem 13 has $2 \times i_{\max} \times \ell_{\max}$ BMIs, Theorem 14 have $4 \times i_{\max} \times \ell_{\max}$ BMIs, and the number of BMIs in Theorem 15 is the sum of BMIs in Theorems 13 and 14, therefore, the number of BMI is $6 \times i_{\max} \times \ell_{\max}$. Hence, the region of feasible solutions in Theorem 15 is smaller in comparison to the ones for Theorem 13 and Theorem 14, and by consequence increasing the computational effort necessary to solve Theorem 15.

Coordinate Descent Algorithm

As stated previously, the constraints in Theorem 13 and 14 are Bilinear Matrices Inequalities (BMI). For solving these optimization problems with BMI constraints, there are a number of approaches presented in literature, to name a few, (SIMON et al., 2011) or (WANG; ZEMOUCHE; RAJAMANI, 2018). In this paper, we use the Coordinate Descent Algorithm (CDA) for solving the problems which is also used and presented in (OLIVEIRA; COSTA, 2020). The CDA is presented below.

Algorithm 3: Coordinate Descent Algorithm.

- 1 **Input:** K_ℓ , γ , t_{\max} , ϕ .
 - 2 **Output:** \mathfrak{A}_ℓ , \mathfrak{B}_ℓ , \mathfrak{M}_ℓ , \mathfrak{C}_ℓ .
 - 3 **Initialization:**
 - 4 **While:** $\frac{\gamma^{t-1} - \gamma^t}{\gamma^{t-1}} \leq \eta$ or $t \leq t_{\max}$ **do:**
 - 5 **Step 1:** Solve the constraint in Theorem 13 or 14 considering \mathfrak{C}_ℓ as a constant, which can be obtained using (TODOROV; FRAGOSO; COSTA, 2018) . Obtain the values of R_ℓ , and Z_i for the Theorem 13 or R_ℓ T_i for the Theorem 14.
 - 6 **Step 2:** Solve the constraint in Theorem 13 or 14 this time using the values of R_ℓ , and Z_i or R_ℓ , and T_i obtained in Step 1 and \mathfrak{C}_ℓ as a variable. Obtain the value of γ .
-

In the above algorithm, the input ϕ is the stop criteria and t_{\max} is the maximum number of iterations allowed.

Remark 15. *The controller used in the CDA can be obtained using any design approach, but it is recommended to use a controller that is also under the MJLS framework. If the first iteration is feasible, the algorithm will at least keep the same result obtained, or improve the results.*

3.4.4 Simulations Results

For the illustrative example we used the exact same matrices that represent the coupled tank presented in Appendix A. The only necessary addition is the detector matrix information as in

$$\Gamma = \begin{bmatrix} 0.65 & 0.35 \\ 0.75 & 0.25 \end{bmatrix}. \quad (3.170)$$

The fault-compensation controller obtained designed using Theorem 13 is

$$\begin{aligned} \mathfrak{A}_1 &= \begin{bmatrix} 0.0535 & -0.1895 \\ -0.1481 & 0.4341 \end{bmatrix}, & \mathfrak{A}_2 &= \begin{bmatrix} 0.0458 & 0.0214 \\ -0.0254 & 0.0574 \end{bmatrix}, \\ \mathfrak{B}_1 &= \begin{bmatrix} -0.0238 & 0.0539 \\ 0.0542 & -0.1331 \end{bmatrix}, & \mathfrak{B}_2 &= \begin{bmatrix} -0.0239 & 0.0540 \\ 0.0542 & -0.1332 \end{bmatrix}, \\ \mathfrak{M}_1 &= \begin{bmatrix} 0.7693 & -0.4043 \\ -0.2708 & 1.5212 \end{bmatrix}, & \mathfrak{M}_2 &= \begin{bmatrix} 0.0492 & 0.0630 \\ -0.0040 & -0.0587 \end{bmatrix}, \\ \mathfrak{C}_1 &= \begin{bmatrix} 0.0149 & -0.0409 \\ -0.0307 & 0.1017 \end{bmatrix}, & \mathfrak{C}_2 &= \begin{bmatrix} 0.0570 & -0.1254 \\ -0.1222 & 0.3138 \end{bmatrix}. \end{aligned}$$

and the upper bound of the \mathcal{H}_∞ norm value is $\gamma = 2.2$.

The fault-compensation controller obtained designed using Theorem 14 is

$$\begin{aligned} \mathfrak{A}_1 &= \begin{bmatrix} -0.0857 & 0.0121 \\ -0.0129 & -0.0769 \end{bmatrix}, & \mathfrak{A}_2 &= \begin{bmatrix} -0.0995 & 0.0141 \\ -0.0149 & -0.0893 \end{bmatrix}, \\ \mathfrak{B}_1 &= \begin{bmatrix} -0.0293 & 0.0036 \\ -0.0044 & -0.0230 \end{bmatrix}, & \mathfrak{B}_2 &= \begin{bmatrix} -0.0340 & 0.0042 \\ -0.0051 & -0.0267 \end{bmatrix}, \\ \mathfrak{M}_1 &= \begin{bmatrix} 0.1734 & -0.0256 \\ 0.0259 & 0.1620 \end{bmatrix}, & \mathfrak{M}_2 &= \begin{bmatrix} -0.0118 & 0.0091 \\ -0.0083 & -0.0133 \end{bmatrix}, \\ \mathfrak{C}_1 &= \begin{bmatrix} 0.0130 & -0.0007 \\ 0.0006 & 0.0047 \end{bmatrix}, & \mathfrak{C}_2 &= \begin{bmatrix} -0.0130 & 0.0007 \\ -0.0006 & -0.0047 \end{bmatrix}. \end{aligned}$$

and the upper bound of the \mathcal{H}_2 norm value is $\gamma = 1.49$.

3.4.4.1 Monte Carlo Simulation

The simulation setup is the same as in Section 2.4, where the fault is a sinusoidal signal $0.025\sin(k)$, and the system is subjected to a white noise with zero mean and deviation equal to 0.01. The Monte Carlo simulation with 300 rounds was performed.

In this simulation it is presented a comparison between the proposed approaches in Theorem 13, 14 and a nominal solution using solely the state-feedback controller, which

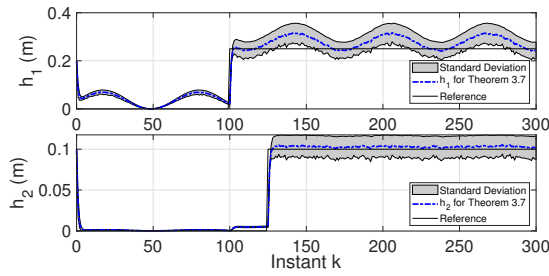
is designed using (TODOROV; FRAGOSO; COSTA, 2018). The results obtained are presented in two distinct sets of graphics, the first set presents the situation when the system is subjected to fault, and the second set is the situation where there is no fault. The sets are organized in the following manner: in Fig. 25a we present the mean and standard deviation for both tank levels h_1 and h_2 obtained using Theorem 13, in Fig. 25b we present the mean and standard deviation for both tank levels h_1 and h_2 obtained using Theorem 14, the third graphic represents the mean and standard deviation for both tank levels h_1 and h_2 obtained using solely the nominal controller, the fourth graphic compares the mean of both previous graphics. The fifth graphic is the mean and standard deviation of the control signal obtained using Theorem 13, the sixth graphic is the mean and standard deviation of the control signal obtained using Theorem 14, the fifth graphic is the mean and standard deviation of the control signal obtained using the nominal controller, and the sixth graphic is the comparison of the fourth and fifth graphics.

In Fig. 25d it is possible to observe that the proposed approaches mitigated the effect of the fault when compared to the nominal approach. Another important aspect is that the standard deviation obtained in all simulation are all similar, which is important since it shows the second-moment stability. As shown in Fig. 25d, the mitigation is noticeable for the approach in Theorems 13, and 14, which was the aim of the approaches. Regarding the control signal, as shown in Fig.25h the control signal presented a discrepancy between the control signal obtained using the Theorems 13, 14 and the nominal controller, however, this difference is not relevant.

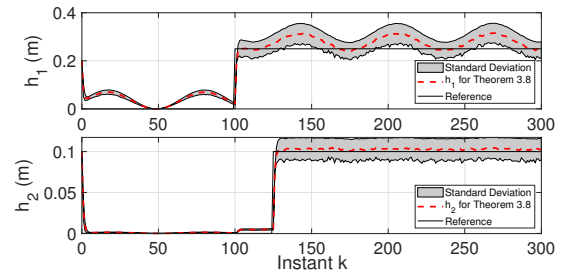
Now for the analysis of the simulation without fault, it is important to observe that the effect of the accommodation controller in the nominal situation was neglectable, which is desirable, since the FAC should not alter the nominal performance. From Fig. 26d we may state that there is no noticeable difference between all three curves, the same can be said regarding the standard deviation. Therefore, the results in Theorems 13, and 14 are suitable solutions for the FAC problem.

3.5 Concluding remarks

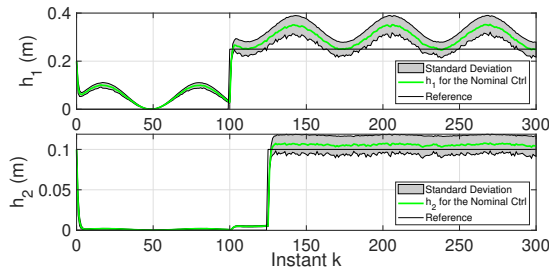
In this chapter we provided the theoretical results to design an FDF and FAC under the MJLS with parameter estimation, furthermore, we also illustrated the viability of the methods presented using some examples. From the results obtained via simulation, we can say that the proposed approach worked as expected. For the next chapter, we introduce the design of the FDF and FAC under the Markov Jump Lur'e Systems.



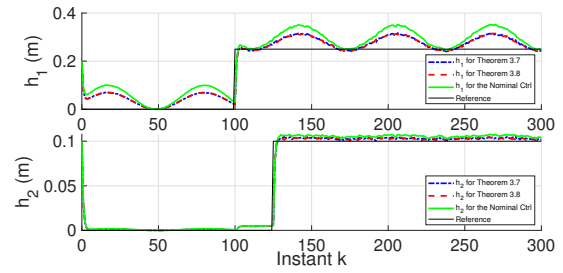
(a) Mean and standard deviation for states sig-1 obtained using Theorem 13.



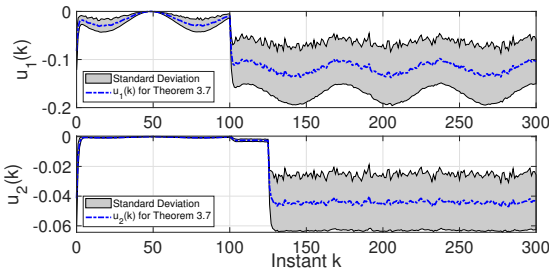
(b) Mean and standard deviation for states sig-1 obtained using Theorem 14.



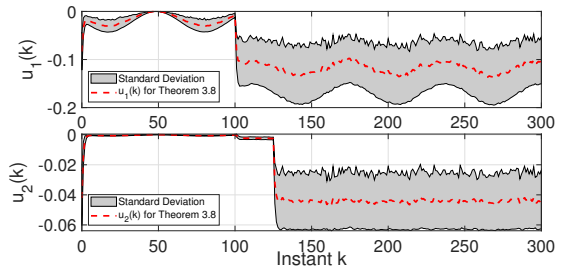
(c) Mean and standard deviation for states sig-1 obtained with the nominal controller.



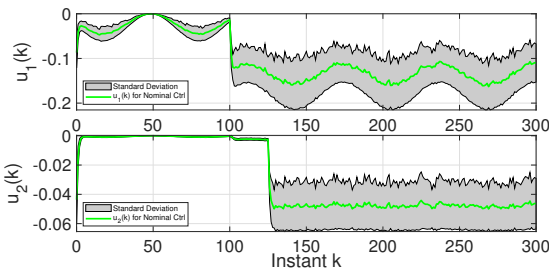
(d) Mean for state signal obtained using Theorem 13, 14 and the nominal controller.



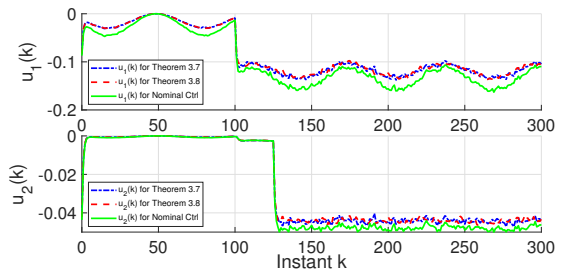
(e) Mean and standard deviation for control signal obtained using Theorem 13.



(f) Mean and standard deviation for control signal obtained using Theorem 14.

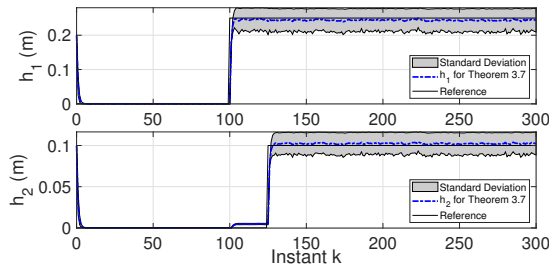


(g) Mean and standard deviation for control signal obtained with the nominal controller.

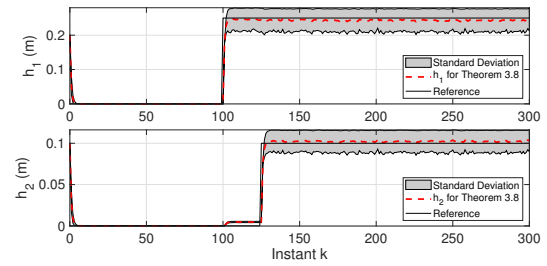


(h) Mean for control signal obtained using Theorem 13, 14 and the nominal controller.

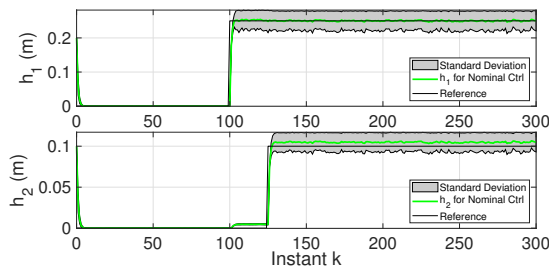
Figure 25: Mean and standard deviation for the states and control signal obtained using the FAC designed via Theorems 13, 14, 15, and the nominal control. These results were obtained via simulation where the system is subjected to an oscillatory fault.



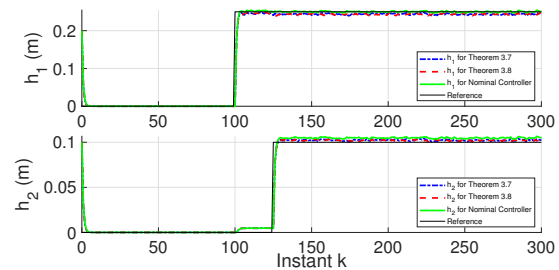
(a) Mean and standard deviation for states signal obtained using Theorem 13.



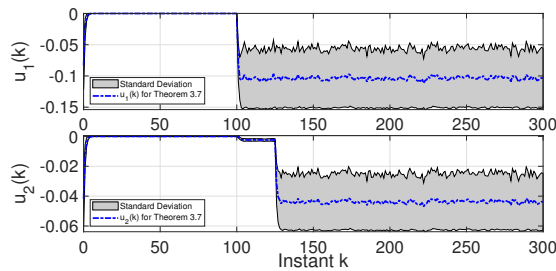
(b) Mean and standard deviation for states signal obtained using Theorem 14.



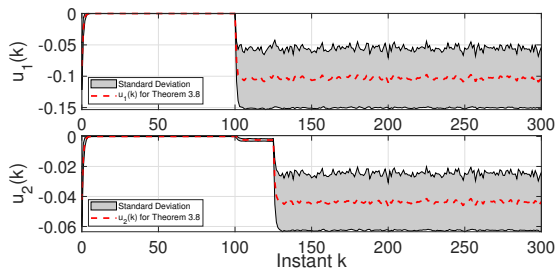
(c) Mean and standard deviation for states signal obtained with the nominal controller.



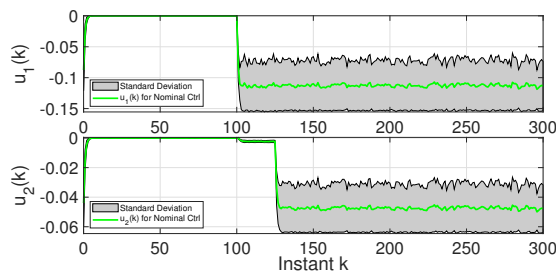
(d) Mean for state signal obtained using Theorems 13, 14 and the nominal controller.



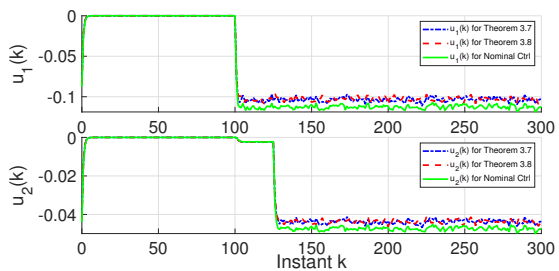
(e) Mean and standard deviation for control signal obtained using Theorem 13.



(f) Mean and standard deviation for control signal obtained using Theorem 14.



(g) Mean and standard deviation for control signal obtained with the nominal controller.



(h) Mean for control signal obtained using Theorems 13, 14, and the nominal controller.

Figure 26: Mean and standard deviation for the states and control signal obtained using the FAC designed via Theorems 13, 14, 15, and the nominal control. These results were obtained via simulation where the system is subjected to an abrupt fault.

4 FDF FOR MARKOVIAN JUMP LUR'E SYSTEMS

As already discussed in the previous chapters all systems are inherently subjected to faults, including communication loss. However, another intrinsic aspect that is present in the majority of the systems is the non-linear behavior. The earlier results presented herein, are based on the premise that it is possible to linearize the system and get a proper model. Yet, in some cases, linearizing the system removes a crucial behavior of the system (JAYAWARDHANA; LOGEMANN; RYAN, 2011). Therefore the use of a proper framework that considers the nonlinear behavior is of utmost importance. For that reason, here we are using the Markovian Jump Lur'e System, which allows us to model the network as in the previous chapter and add the nonlinear behavior at the same time.

The results presented in this chapter were published in the following:

- Subsection 4.2 presented the Fault detection filter for discrete-time Markov jump Lur'e systems, was published and presented in the European Control Conference 2021 (CARVALHO; JAYAWARDHANA; COSTA, 2021).

4.1 Preliminary for Markovian Jump Lur'e Systems

Consider the discrete-time Markov jump Lur'e system as

$$\mathcal{G} : \begin{cases} x(k+1) = A_{\theta(k)}x(k) + G_{\theta(k)}\varphi_{\theta(k)}(p(k)) + J_{\theta(k)}w(k), \\ p(k) = C_{\theta(k)}x(k), \\ z(k) = C_{z\theta(k)}x(k) + H_{\theta(k)}\varphi_{\theta(k)}(p(k)) + D_{\theta(k)}w(k), \end{cases} \quad (4.1)$$

where vectors $x(k) \in \mathbb{R}^{n_x}$, $p(k) \in \mathbb{R}^{n_p}$, $z(k) \in \mathbb{R}^{n_z}$, and $w(k) \in \mathbb{R}^{n_w}$, represent the system states, the output related to the nonlinearity, the system output, and the exogenous input, respectively. We consider that $w(k) \in \mathcal{L}_2$. The term $\varphi(\cdot)$ is considered to be a memoryless non-linearity. Observe that all the terms in (4.1) are dependent on the index $\theta(k)$, which

represents as before the Markov chain jump parameter (ROSS, 2014).

The \mathcal{N} non-linearities $\varphi_i(\cdot)$ are restricted by the following assumptions:

- Assumption I: $\varphi_i(0) = 0$
- Assumption II: for each non-linearity there exist positive definite matrices $\Omega_i \in \mathbb{R}^{n_p \times n_p}$ for all $p \in \mathbb{R}^{n_p}$, $\ell = 1, \dots, n_p$, such that

$$\varphi_{i(\ell)}(p)[\varphi_i(p) - \Omega_i p]_{(\ell)} \leq 0. \quad (4.2)$$

As described in (KHALIL, 2002), the non-linearities $\varphi_i(\cdot)$ satisfy their respective cone bounded sector conditions and are assumed to be decentralized, which allow us to write

$$\text{SC}(\varphi_i(\cdot), p, \Lambda_i) = \varphi_i(p)' \Lambda_i [\varphi_i(p) - \Omega_i p] \leq 0, \quad (4.3)$$

where $\Lambda_i \in \text{diag}(\lambda_{q,i})_{q=1, \dots, n_p} \in \mathbb{R}^{n_p \times n_p}$ are diagonal positive semidefinite matrices, considering (4.2) we can say that (4.3) holds for all $i \in \mathbb{K}$, for all $p \in \mathbb{R}^{n_p}$. As a by product of (4.2) the inequality (4.3) holds for

$$[\Omega_i p]_{\ell} [\varphi_i(p) - \Omega_i p]_{\ell} \leq 0, \quad (4.4)$$

which implies that

$$0 \leq \varphi_i(p)' \Lambda_i \varphi_i(p) \leq \varphi_i(p)' \Lambda_i \Omega_i p \leq p' \Omega_i' \Lambda_i \Omega_i p, \quad \forall p \in \mathbb{R}^{n_p}, \quad (4.5)$$

when Λ_i is a diagonal positive semi definite matrix. Now we present the Mean Square Stable (MSS) definition used throughout this work.

Definition 6. *System (4.1) with $w(k) = 0$ is MSS if, for any initial condition $x(0) = x_0 \in \mathbb{R}^{n_x}$, and initial distribution $\theta(0) = \theta_0 \in \mathbb{K}$,*

$$\lim_{k \rightarrow \infty} \mathbb{E}\{x(k)' x(k) | x_0, \theta_0\} = 0. \quad (4.6)$$

For a detailed discussion, see (COSTA; FRAGOSO, 1993; FRAGOSO; COSTA, 2005).

4.1.1 Candidate Lyapunov function

We define the candidate Lyapunov function as

$$V : \begin{cases} \mathbb{K} \times \mathbb{R}^{n_x} \rightarrow \mathbb{R}, \\ (i, x) \rightarrow x' P_i x + 2(\varphi_i'(C_i x)) \Delta_i \Omega_i C_i x, \end{cases} \quad (4.7)$$

where matrix $P_i \in \mathbb{R}^{n_x \times n_x}$, $\forall i \in \mathbb{K}$ is symmetric positive definite, and the diagonal matrix $\Delta_i \in \mathbb{R}^{n_p \times n_p}$ is positive definite.

Observe that inequality (4.5) allows us to define a lower bound, as in $\underline{v}_i(x) = x'P_i x$, and an upper bound, $\bar{v}_i(x) = x'(P_i + 2C_i'\Omega_i'\Delta_i\Omega_i C_i)x$, for the candidate Lyapunov function. By consequence,

$$\underline{v}_i(x) \leq V(i, x) \leq \bar{v}_i(x), \forall i \in \mathbb{K} \quad (4.8)$$

From the above, we can state that the candidate Lyapunov function possess these properties:

- $V(i, x) \geq 0, \forall x \in \mathbb{R}^{n_x}, i \in \mathbb{K}$, which is guaranteed by the left hand of the inequality (4.8).
- $V(i, x) = 0$ if and only if $x = 0, \forall i \in \mathbb{K}$. This property is guaranteed by imposing that $P_i > 0$ in the inequality (4.8).
- $V(i, x)$ is radially unbounded, $\forall i \in \mathbb{K}$.

The main reason to use this particular Lyapunov function is to allow us to draw results solely under Assumptions I and II. As consequence, it is no longer required any further assumptions regarding the slope of the non-linearity, which is the classical approach for the discrete-time domain Lur'e system, (GONZAGA; JUNGERS; DAAFOUZ, 2012; GONZAGA; COSTA, 2013; GONZAGA; COSTA, 2014).

4.1.2 \mathcal{H}_∞ norm for Markovian Jump Lur'e Systems

Assume that the system (4.1) is MSS and $x_0 = 0$. Its \mathcal{H}_∞ norm (COSTA; MARQUES, 1998) is then given by

$$\|\mathcal{G}\|_\infty = \sup_{0 \neq w \in \mathcal{L}_2, \theta_0 \in \mathbb{K}} \frac{\|z\|_2}{\|w\|_2}. \quad (4.9)$$

An upper bound $\gamma > 0$ for the \mathcal{H}_∞ norm can be acquired by using the following lemma which is based on the stochastic stability constraints presented in (GONZAGA; COSTA, 2013, Theorem 5).

Lemma 8. *Consider that the Assumptions I and II are satisfied. System (4.1) is stochastic stable and the norm constraint $\|\mathcal{G}\|_\infty \leq \gamma$ holds if there exist symmetric $P_i > 0$ and diagonal*

positive semidefnite matrices T_i, W_i, Δ_i such that the following LMI

$$\begin{bmatrix} P_i & \bullet & \bullet & \bullet & \bullet & \bullet \\ (W_i - \Delta_i)\Omega_i C_i & 2T_i & \bullet & \bullet & \bullet & \bullet \\ (\mathbb{E}_i(W) - \mathbb{E}_i(\Delta))\Omega_i C_i A_i & \check{\Pi} & 2\mathbb{E}_i(W) & \bullet & \bullet & \bullet \\ 0 & 0 & \Pi & \gamma^2 I & \bullet & \bullet \\ C_{zi} & H_i & 0 & D_i & I & \bullet \\ \mathbb{E}_i(P)A_i & \mathbb{E}_i(P)G_i & 0 & \mathbb{E}_i(P)J_i & 0 & \mathbb{E}_i(P) \end{bmatrix} \geq 0, \quad (4.10)$$

is satisfied for all $i \in \mathbb{K}$, where $\check{\Pi} = (\mathbb{E}_i(W) - \mathbb{E}_i(\Delta))\Omega_i C_i G_i$, $\Pi = J_i' C_i' \Omega_i (\mathbb{E}_i(W) - \mathbb{E}_i(\Delta))$.

Proof: Let us show that if there are matrices $P_i > 0$ such that (4.10) is satisfied then $\|\mathcal{G}\|_\infty \leq \gamma$. Pre- and post-multiplying (4.10) by $\text{diag}(I, I, I, I, I, \mathbb{E}_i(P)^{-1})$ and applying Schur complement in (4.10), we get that

$$\begin{bmatrix} A_i' \mathbb{E}_i(P) A_i - P_i + C_{zi}' C_{zi} & \bullet & \bullet & \bullet \\ \check{\Pi} & G_i' \mathbb{E}_i(P) G_i + H_i' H_i - 2T_i & \bullet & \bullet \\ (\mathbb{E}_i(\Delta) - \mathbb{E}_i(W))\Omega_i C_i A_i & (\mathbb{E}_i(\Delta) - \mathbb{E}_i(W))\Omega_i C_i G_i & -2\mathbb{E}_i(W) & \bullet \\ J_i' \mathbb{E}_i(P) A_i - D_i' C_{zi} & J_i' \mathbb{E}_i(P) G_i + D_i' H_i & \Pi & \check{\Pi} \end{bmatrix} \leq 0, \quad (4.11)$$

where $\check{\Pi} = G_i' \mathbb{E}_i(P) A_i + \Delta_i \Omega_i C_i - T_i \Omega_i C_i + H_i' C_{zi}$, $\Pi = J_i' C_i' \Omega_i (\mathbb{E}_i(\Delta) - \mathbb{E}_i(W))$, $\check{\Pi} = J_i' \mathbb{E}_i(P) J_i + D_i' D_i - \gamma^2$. Pre- and post-multiplying (4.11) by $[x(k)' \varphi_i(p(k)) \varphi_i(p(k+1)) w(k)]$, and following a routine computation, we obtain

$$\begin{aligned} & x(k+1)' \mathbb{E}_{\theta(k)}(P) x(k+1) + 2\varphi_{\theta(k+1)}(p(k+1))' \mathbb{E}_{\theta(k)}(\Delta) \Omega_{\theta(k+1)} C_{\theta(k+1)} x(k+1) \cdots \\ & + x(k)' P_{\theta(k)} x(k) + 2\varphi_{\theta(k)}(p(k))' \Delta_{\theta(k)} \Omega_{\theta(k)} C_{\theta(k)} x(k) \cdots \\ & - 2\text{SC}(\varphi_{\theta(k+1)}(k+1), p(k+1), \mathbb{E}_{\theta(k)}(W)) \cdots \\ & - 2\text{SC}(\varphi_{\theta(k)}(k), p(k), T_{\theta(k)}) + z(k)' z(k) - \gamma^2 w(k)' w(k) \leq 0. \end{aligned} \quad (4.12)$$

Considering that the σ -field \mathfrak{F}_k is generated by the variables $\{x(l), w(l), \theta(l); l = 0, \dots, k\}$ we get that $x(k+1)' \mathbb{E}_{\theta(k)}(P) x(k+1) = \mathbb{E}(x(k+1)' P_{\theta(k+1)} x(k+1) | \mathfrak{F}_k)$. Hence $\mathbb{E}(x(k+1)' \mathbb{E}_{\theta(k)}(P) x(k+1)) = \mathbb{E}(x(k+1)' P_{\theta(k+1)} x(k+1))$. In what follows, we recall that $\text{SC}(\cdot) \leq 0$ as in (4.3). From (4.12), and summing over k from 0 to \mathbb{T} , we get

$$\begin{aligned} & \sum_{k=0}^{\mathbb{T}} \mathbb{E} \left[x(k+1)' P_{\theta(k+1)} x(k+1) \cdots \right. \\ & + 2\varphi_{\theta(k+1)}(p(k+1))' \Delta_{\theta(k+1)} \Omega_{\theta(k+1)} C_{\theta(k+1)} x(k+1) \cdots \\ & - x(k)' P_{\theta(k)} x(k) - 2\varphi_{\theta(k)}(p(k))' \Delta_{\theta(k)} \theta(k) \Omega_{\theta(k)} C_{\theta(k)} x(k) \cdots \\ & - \underbrace{2\text{SC}(\varphi_{\theta(k+1)}(k+1), p(k+1), W_{\theta(k+1)})}_{\leq 0} - \underbrace{2\text{SC}(\varphi_i(k), p(k), T_{\theta(k)})}_{\leq 0} \cdots \\ & \left. + z(k)' z(k) - \gamma^2 w(k)' w(k) \right] \leq 0. \end{aligned}$$

It follows then that

$$\mathbb{E}(V(\mathbb{T}+1)) - \mathbb{E}(V(\mathbb{T})) + \sum_{k=0}^{\mathbb{T}} \mathbb{E}(\|z(k)\|^2) - \gamma \sum_{k=0}^{\mathbb{T}} \mathbb{E}(\|w(k)\|^2) \leq 0. \quad (4.13)$$

Considering $w(k) = 0$ and recalling that $C'_{zi}C_{zi} > dI$ we obtain from (4.13) that $\sum_{k=0}^{\mathbb{T}} \mathbb{E}(\|x(k)\|^2) \leq \frac{1}{\alpha} \mathbb{E}(V(0))$ and taking the limit as $\mathbb{T} \rightarrow \infty$ yields the stochastic stability property. When $x_0 = 0$, it follows from (4.13) that $\sum_{k=0}^{\mathbb{T}} \mathbb{E}(\|x(k)\|^2) - \gamma \sum_{k=0}^{\mathbb{T}} \mathbb{E}(\|w(k)\|^2) \leq 0$. By taking the limit $\mathbb{T} \rightarrow \infty$, we obtain the desired result. ■

4.2 Fault Detection Filter for Markov Jump Lur'e Systems

The scheme that describes the Fault Detection Filter is presented in Fig. 27. Observing

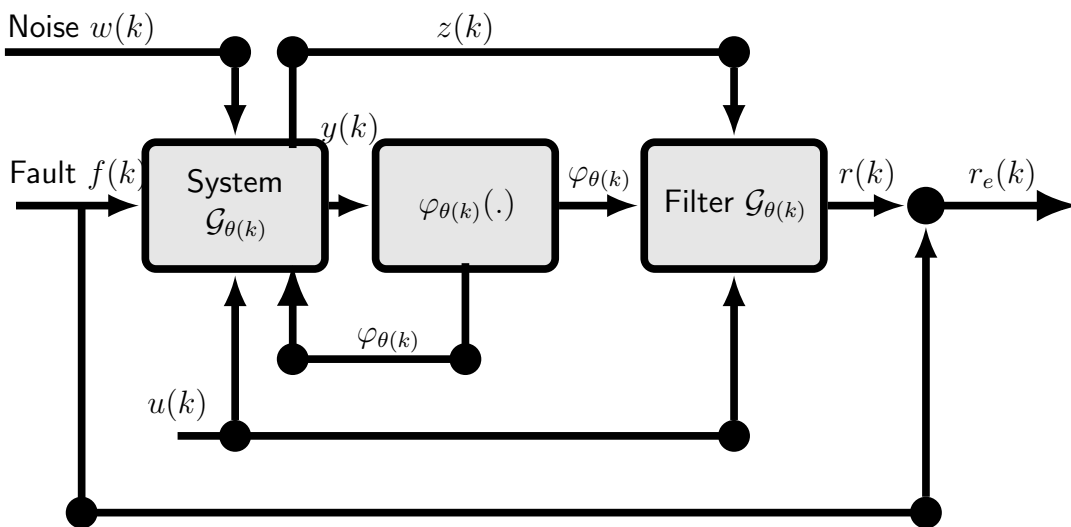


Figure 27: Fault Detection Scheme for Lur'e systems.

the topology in Fig.27 we need to describe the system, control law, and the Fault Detection Filter (FDF), to provide the design of the FDF.

The Markov Jump Lur'e System subject to faults is described as

$$\mathcal{G} : \begin{cases} x(k+1) = A_{\theta(k)}x(k) + B_{\theta(k)}u(k) + G_{\theta(k)}\varphi_{\theta(k)}(y(k)) + J_{\theta(k)}w(k) + F_{\theta(k)}f(k), \\ y(k) = C_{\theta(k)}x(k), \\ z(k) = C_{z\theta(k)}x(k) + H_{\theta(k)}\varphi_{\theta(k)}(y(k)) + D_{\theta(k)}w(k) + E_{\theta(k)}f(k), \end{cases} \quad (4.14)$$

where $x(k) \in \mathbb{R}^{n_x}$ represents the system states, $u(k) \in \mathbb{R}^{n_u}$ represents the control input, $w(k) \in \mathbb{R}^{n_w}$ denotes the exogenous input, $z(k) \in \mathbb{R}^{n_z}$ represents the output signal, and $f(k) \in \mathbb{R}^{n_f}$ denotes the fault signal. We assume that $w(k), f(k) \in \mathcal{L}^2$. Recall that, $\varphi_i(\cdot)$ is under the assumptions I and II in (4.2). The index $\theta(k)$ represents the Markov chain, as described in (4.1).

The control signal is obtained using the state feedback controller

$$\mathcal{K} : \left\{ u(k) = K_{\theta(k)}x(k) + R_{\theta(k)}\varphi_{\theta(k)}(y(k)). \right. \quad (4.15)$$

The main objective in this paper is to design a Fault Detection Filter to generate a residue signal $r(k)$, the FDF is defined as

$$\mathcal{F} : \begin{cases} \eta(k+1) = \mathcal{A}_{\eta\theta(k)}\eta(k) + \mathcal{M}_{\eta\theta(k)}u(k) + \mathcal{B}_{\eta\theta(k)}z(k) + \mathcal{L}_{\eta\theta(k)}\varphi_{\theta(k)}(y(k)), \\ r(k) = \mathcal{C}_{\eta\theta(k)}\eta(k) + \mathcal{D}_{\eta\theta(k)}z(k), \\ \eta(0) = \eta_0, \end{cases} \quad (4.16)$$

where $\eta(k) \in \mathbb{R}^{n_x}$ represents the filter states, $u(k) \in \mathbb{R}^{n_u}$ represents the control input, $r(k) \in \mathbb{R}^{n_r}$ denotes the residue signal, and $f(k) \in \mathbb{R}^{n_f}$ denotes the fault signal.

Considering that $r_e(k) = r(k) - f(k)$, we get the augmented system

$$\mathcal{G}_{\text{aug}} : \begin{cases} x(k+1) = \tilde{A}_{\theta(k)}\tilde{x}(k) + \tilde{G}_{\theta(k)}\tilde{\varphi}_{\theta(k)}(y(k)) + \tilde{J}_{\theta(k)}\tilde{w}(k), \\ y(k) = \tilde{C}_{\theta(k)}\tilde{x}(k), \\ z(k) = \tilde{C}_{z\theta(k)}\tilde{x}(k) + \tilde{H}_{\theta(k)}\tilde{\varphi}_{\theta(k)}(y(k)) + \tilde{D}_{\theta(k)}\tilde{w}(k), \end{cases} \quad (4.17)$$

where $\tilde{x}(k) = [x(k) \ \eta(k)]$, $\tilde{\varphi}_{\theta(k)}(y(k)) = \varphi_{\theta(k)}(y(k))$, $\tilde{w}(k) = [w(k) \ f(k)]$, hence, the augmented matrices that compose system (4.17) are

$$\begin{aligned} \tilde{A}_i &= \begin{bmatrix} A_i + B_i K_i & 0 \\ \mathcal{M}_{\eta_i} K_i + \mathcal{B}_{\eta_i} C_{zi} & \mathcal{A}_{\eta_i} \end{bmatrix}, & \tilde{G}_i &= \begin{bmatrix} B_i R_i + G_i \\ \mathcal{M}_{\eta_i} R_i + \mathcal{L}_{\eta_i} \end{bmatrix}, \\ \tilde{J}_i &= \begin{bmatrix} J_i & F_i \\ \mathcal{B}_{\eta_i} D_i & \mathcal{B}_{\eta_i} E_i \end{bmatrix}, & \tilde{C}_{zi} &= \begin{bmatrix} \mathcal{D}_{\eta_i} C_{zi} & \mathcal{C}_{\eta_i} \end{bmatrix}, \\ \tilde{D}_i &= \begin{bmatrix} \mathcal{D}_{\eta_i} D_i & \mathcal{D}_{\eta_i} E_i - I \end{bmatrix}, & \tilde{H}_i &= \mathcal{D}_{\eta_i} H_i, & \tilde{C}_i &= \begin{bmatrix} C_i & 0 \end{bmatrix}. \end{aligned} \quad (4.18)$$

Define the performance criterion for the \mathcal{H}_∞ norm case as:

$$\|\mathcal{G}_{\text{aug}}\|_\infty = \sup_{\|\tilde{w}\|_2 \neq 0, \tilde{w} \in \mathcal{L}_2} \frac{\|r_e\|_2}{\|\tilde{w}\|_2} < \gamma, \quad (4.19)$$

where the main purpose is to design the FDF as in (4.16) minimizing the \mathcal{H}_∞ gain $\gamma > 0$ for the augmented system (4.17).

$$\begin{bmatrix} Z_i & \bullet & \bullet & \bullet & \bullet & \bullet & \bullet & \bullet & \bullet \\ Z_i & X_i & \bullet & \bullet & \bullet & \bullet & \bullet & \bullet & \bullet \\ (\mathbb{E}_i(W) - \mathbb{E}_i(\Delta))\Omega_i C_i & (\mathbb{E}_i(W) - \mathbb{E}_i(\Delta))\Omega_i C_i & 2T_i & \bullet & \bullet & \bullet & \bullet & \bullet & \bullet \\ \tilde{\Pi} & \tilde{\Pi} & \Pi^{4,3} & 2\mathbb{E}_i(W) & \bullet & \bullet & \bullet & \bullet & \bullet \\ 0 & 0 & 0 & \Pi^{5,4} & \gamma^2 I & \bullet & \bullet & \bullet & \bullet \\ 0 & 0 & 0 & \Pi^{6,4} & 0 & \gamma^2 I & \bullet & \bullet & \bullet \\ \mathcal{D}_{\eta_i} C_{zi} + \mathcal{C}_{\eta_i} & \mathcal{D}_{\eta_i} C_{zi} & \mathcal{D}_{\eta_i} H_i & 0 & \mathcal{D}_{\eta_i} D_i & \mathcal{D}_{\eta_i} E_i - I & I & \bullet & \bullet \\ \mathbb{E}_i(Z)(A_i + B_i K_i) & \mathbb{E}_i(Z)(A_i + B_i K_i) & \Pi^{10,3} & 0 & \mathbb{E}_i(Z)J_i & \mathbb{E}_i(Z)F_i & 0 & \mathbb{E}_i(Z) & \bullet \\ \Pi^{11,1} & \Pi^{11,2} & \Pi^{11,3} & 0 & \Pi^{11,8} & \Pi^{11,9} & 0 & \mathbb{E}_i(Z) & \mathbb{E}_i(X) \end{bmatrix} \geq 0, \quad (4.20)$$

4.2.1 \mathcal{H}_∞ Fault Detection Design for MJS Lur'e Systems

Theorem 16. *Consider that both Assumptions I and II are satisfied. There exists a filter as in (4.16) such that (4.17) is stochastic stable and $\|\mathcal{G}_{aug}\|_\infty \leq \gamma$ if there exist symmetric positive matrices Z_i , X_i , matrices with appropriate size \mathcal{O}_{η_i} , ∇_i , Γ_i , Υ_i , and diagonal positive semidefinite matrices T_i , W_i , $\Delta_i \in \mathbb{R}^{n_y \times n_y}$ such that the LMI constraints (4.20) are satisfied for all $i \in \mathbb{K}$ where*

$$\begin{aligned} \tilde{\Pi} &= (\mathbb{E}_i(W) - \mathbb{E}_i(\Delta))\Omega_i C_i (A_i + B_i K_i), & \Pi^{4,3} &= (\mathbb{E}_i(W) - \mathbb{E}_i(\Delta))\Omega_i C_i (B_i R_i + G_i), \\ \Pi^{5,4} &= J_i' C_i' \Omega_i (\mathbb{E}_i(W) - \mathbb{E}_i(\Delta)), & \Pi^{6,4} &= F_i' C_i' \Omega_i (\mathbb{E}_i(W) - \mathbb{E}_i(\Delta)), \\ \Pi^{10,3} &= \mathbb{E}_i(Z)(B_i R_i + G_i), & \Pi^{11,1} &= \mathbb{E}_i(X)(A_i + B_i K_i) + \Gamma_i K_i + \nabla_i C_{zi} + \mathcal{O}_{\eta_i}, \\ \Pi^{11,2} &= \mathbb{E}_i(X)(A_i + B_i K_i) + \Gamma_i K_i + \nabla_i C_{zi}, & \Pi^{11,3} &= \mathbb{E}_i(X)(B_i R_i + G_i) + \Gamma_i R_i + \Upsilon_i, \\ \Pi^{11,8} &= \mathbb{E}_i(X)J_i + \nabla_i D_i, & \Pi^{11,9} &= \mathbb{E}_i(X)F_i + \nabla_i E_i. \end{aligned}$$

If a feasible solution is obtained, then a suitable FDF is given by $\mathcal{A}_{\eta_i} = \mathbb{E}_i(Z - X)^{-1} \mathcal{O}_{\eta_i}$, $\mathcal{B}_{\eta_i} = \mathbb{E}_i(Z - X)^{-1} \nabla_i$, $\mathcal{M}_{\eta_i} = \mathbb{E}_i(Z - X)^{-1} \Gamma_i$, $\mathcal{L}_{\eta_i} = \mathbb{E}_i(Z - X)^{-1} \Upsilon_i$, \mathcal{C}_{η_i} , and \mathcal{D}_{η_i} .

Proof: Firstly, we introduce the variable substitutions $\mathcal{O}_{\eta_i} = \mathbb{E}_i(Z - X)\mathcal{A}_{\eta_i}$, $\nabla_i = \mathbb{E}_i(Z - X)\mathcal{B}_{\eta_i}$, $\Gamma_i = \mathbb{E}_i(Z - X)\mathcal{M}_{\eta_i}$, and $\Upsilon_i = \mathbb{E}_i(Z - X)\mathcal{L}_{\eta_i}$ in (4.20). Now consider the structure, extracted from (GONÇALVES; FIORAVANTI; GEROMEL, 2011), for P_i , $\mathbb{E}_i(P)$, as

$$P_i = \begin{bmatrix} X_i & U_i \\ U_i' & \hat{X}_i \end{bmatrix}, \quad P_i^{-1} = \begin{bmatrix} Y_i & V_i \\ V_i' & \hat{Y}_i \end{bmatrix}, \quad (4.21)$$

$$\mathbb{E}_i(P) = \begin{bmatrix} \mathbb{E}_i(X) & \mathbb{E}_i(U) \\ \mathbb{E}_i(U)' & \mathbb{E}_i(\hat{U}) \end{bmatrix}, \quad \mathbb{E}_i(P)^{-1} = \begin{bmatrix} R_{1i} & R_{2i} \\ R_{2i}' & R_{3i} \end{bmatrix}. \quad (4.22)$$

We define the matrices α_i and σ_i as

$$\alpha_i = \begin{bmatrix} I & I \\ V_i' Y_i^{-1} & 0 \end{bmatrix}, \quad \sigma_i = \begin{bmatrix} R_{1i}^{-1} & \mathbb{E}_i(X) \\ 0 & \mathbb{E}_i(U)' \end{bmatrix}. \quad (4.23)$$

From (4.21) we get that $U_i = Z_i - X_i$, $V_i = V_i'$, $V_i = Z_i^{-1}$, as well as $R_{1i}^{-1} = \mathbb{E}_i(Z)$, as in (GONÇALVES; FIORAVANTI; GEROMEL, 2010). Therefore, we can write the following

matrices

$$\begin{aligned}
\alpha_i' P_i \alpha_i &= \begin{bmatrix} Z_i & Z_i \\ Z_i & X_i \end{bmatrix}, \quad \sigma_i' \mathbb{E}_i(P) \sigma_i = \begin{bmatrix} \mathbb{E}_i(Z) & \mathbb{E}_i(Z) \\ \mathbb{E}_i(Z) & \mathbb{E}_i(Z) \end{bmatrix}, \\
(\mathbb{E}_i(W) - \mathbb{E}_i(\Delta)) \Omega_i \tilde{C}_i \alpha_i &= [(\mathbb{E}_i(W) - \mathbb{E}_i(\Delta)) \Omega_i C_i \quad (\mathbb{E}_i(W) - \mathbb{E}_i(\Delta)) \Omega_i C_i], \\
(\mathbb{E}_i(W) - \mathbb{E}_i(\Delta)) \Omega_i \tilde{C}_i \tilde{A}_i \alpha_i &= [(\mathbb{E}_i(W) - \mathbb{E}_i(\Delta)) \Omega_i C_i (A_i + B_i K_i) \quad (\mathbb{E}_i(W) - \mathbb{E}_i(\Delta)) \Omega_i C_i (A_i + B_i K_i)], \\
\tilde{C}_{zi} \alpha_i &= [\mathcal{D}_{\eta_i} C_{zi} + C_{\eta_i} \quad \mathcal{D}_{\eta_i} C_{zi}], \quad \sigma_i' \tilde{A}_i \alpha_i = \begin{bmatrix} \mathbb{E}_i(Z) (A_i + B_i K_i) & \mathbb{E}_i(Z) (A_i + B_i K_i) \\ \Pi^{2,1} & \Pi^{2,2} \end{bmatrix}, \\
\Pi^{2,1} &= \mathbb{E}_i(X) (A_i + B_i K_i) + \mathbb{E}_i(U) \mathcal{M}_{\eta_i} K_i + \mathbb{E}_i(U) \mathcal{B}_{\eta_i} C_{zi} + \mathbb{E}_i(U) \mathcal{A}_{\eta_i}, \\
\Pi^{2,2} &= \mathbb{E}_i(X) (A_i + B_i K_i) + \mathbb{E}_i(U) \mathcal{M}_{\eta_i} K_i + \mathbb{E}_i(U) \mathcal{B}_{\eta_i} C_{zi}, \\
(\mathbb{E}_i(W) - \mathbb{E}_i(\Delta)) \Omega_i \tilde{C}_i \tilde{G}_i &= [(\mathbb{E}_i(W) - \mathbb{E}_i(\Delta)) \Omega_i \tilde{C}_i (B_i R_i + G_i)], \quad \tilde{H}_i = \mathcal{D}_{\eta_i} H_i, \\
\sigma_i' \tilde{G}_i &= \begin{bmatrix} \mathbb{E}_i(Z) B_i R_i + \mathbb{E}_i(Z) G_i \\ \mathbb{E}_i(X) (B_i R_i + G_i) + \mathbb{E}_i(U) (\mathcal{M}_{\eta_i} R_i + \mathcal{L}_{\eta_i}) \end{bmatrix}, \quad \tilde{D}_i = [\mathcal{D}_{\eta_i} D_i \quad \mathcal{D}_{\eta_i} E_i - I], \\
\sigma_i' \tilde{J}_i &= \begin{bmatrix} \mathbb{E}_i(Z) J_i & \mathbb{E}_i(Z) F_i \\ \mathbb{E}_i(X) J_i + \mathbb{E}_i(U) \mathcal{B}_{\eta_i} D_i & \mathbb{E}_i(X) F_i + \mathbb{E}_i(U) \mathcal{B}_{\eta_i} E_i \end{bmatrix}.
\end{aligned}$$

From the above LMI, (4.20) can be rewritten as

$$\begin{bmatrix} \alpha_i' P_i \alpha_i & \bullet & \bullet & \bullet & \bullet & \bullet \\ (W_i - \Delta_i) \Omega_i \tilde{C}_i \alpha_i & 2T_i & \bullet & \bullet & \bullet & \bullet \\ (\mathbb{E}_i(W) - \mathbb{E}_i(\Delta)) \Omega_i \tilde{C}_i \tilde{A}_i \alpha_i & \hat{\Pi}_i & 2\mathbb{E}_i(W) & \bullet & \bullet & \bullet \\ 0 & 0 & \Pi_i & \gamma^2 I & \bullet & \bullet \\ \tilde{C}_{zi} \alpha_i & \tilde{H}_i & 0 & \tilde{D}_i & I & \bullet \\ \sigma_i' \tilde{A}_i \alpha_i & \sigma_i' \tilde{G}_i & 0 & \sigma_i' J_i & 0 & \tilde{\Pi} \end{bmatrix} \geq 0, \quad (4.24)$$

where

$$\begin{aligned}
\hat{\Pi}_i &= (\mathbb{E}_i(W) - \mathbb{E}_i(\Delta)) \Omega_i C_i G_i, \quad \Pi_i = \tilde{J}_i' \tilde{C}_i' \Omega_i (\mathbb{E}_i(W) - \mathbb{E}_i(\Delta)), \\
\tilde{\Pi} &= \sigma_i' \mathbb{E}_i(P)^{-1} \sigma_i.
\end{aligned}$$

Pre- and post-multiplying (4.24), respectively, by $\text{diag}(\alpha_i^{-1}, I, I, I, I, I, \sigma_i^{-1})$, and after that pre- and post-multiplying it by $\text{diag}(I, I, I, I, I, I, \mathbb{E}_i(P))$, we get that the LMI constraint (4.20) implies the LMI constraint (4.10). It follows subsequently that (4.17) is stochastic stable and that $\|\mathcal{G}\|_\infty \leq \gamma$. \blacksquare

4.2.2 Simulations Results

For the illustrative simulation for the Lur'e system, we used the classic example of a mass-spring from (KHALIL, 2002). A deeper discussion about the model is presented in Appendix A. The matrices that compose the discretized model of the mass-spring system are

$$\begin{aligned}
A_{1,2} &= \begin{bmatrix} -0.0101 & 0.9588 \\ -0.0160 & -0.0181 \end{bmatrix}, \quad B_{1,2} = \begin{bmatrix} 62.0699 \\ -0.0513 \end{bmatrix}, \quad G_{1,2} = \begin{bmatrix} 0 \\ 0.15 \end{bmatrix}, \quad J_{1,2} = 0.01 \times B_{1,2}, \\
F_{1,2} &= B_{1,2}, \quad C_1 = I^2, \quad C_2 = 0^{2 \times 2}, \quad C_{z1} = I^2, \quad C_{z2} = 0^{2 \times 2},
\end{aligned}$$

$$\begin{aligned}
H_{1,2} &= 0^{2 \times 1}, & D_{1,2} &= 10^{-3} I^{2 \times 1}, & E_{1,2} &= 0^{2 \times 1}, & \Omega_1 &= 0.75, & \Omega_2 &= 0.50, \\
\mathbb{P} &= \begin{bmatrix} 0.8 & 0.2 \\ 0.8 & 0.2 \end{bmatrix}.
\end{aligned} \tag{4.25}$$

The matrices that compose the control law in (4.15) are

$$\begin{aligned}
K_1 &= [-0.0002 \quad -0.0158], & K_2 &= [-0.0368 \quad -0.2877], \\
R_1 &= [5.5373 \times 10^{-03}], & R_2 &= [2.1034e \times 10^{-03}],
\end{aligned}$$

The non-linearity is $\phi(y) = \Omega_i(y)^3$, $i \in [1, 2]$. The noise signal is a white noise in the broad sense, with null mean and standard deviation of 0.1.

The FDF designed using Theorem 16 is

$$\begin{aligned}
\mathcal{A}_{\eta 1} &= \begin{bmatrix} -0.0097 & -0.1416 \\ 0.0001 & 0.0012 \end{bmatrix}, & \mathcal{A}_{\eta 2} &= 10^{-7} \begin{bmatrix} -0.0257 & -0.2720 \\ 0.0007 & 0.0374 \end{bmatrix}, \\
\mathcal{B}_{\eta 1} &= \begin{bmatrix} 1.0522 & 105.2372 \\ -0.0165 & -0.0713 \end{bmatrix}, & \mathcal{B}_{\eta 2} &= \begin{bmatrix} -2.0240 & 2.0240 \\ 0.0172 & -0.0172 \end{bmatrix}, \\
\mathcal{M}_{\eta 1} &= \begin{bmatrix} 6.6740 \\ -0.0034 \end{bmatrix}, & \mathcal{M}_{\eta 2} &= 10^{-6} \begin{bmatrix} -106.1402 \\ 9.7246 \end{bmatrix}, \\
\mathcal{L}_{\eta 1} &= \begin{bmatrix} -19.3626 \\ -0.0282 \end{bmatrix}, & \mathcal{L}_{\eta 2} &= 10^3 \begin{bmatrix} -1.4337 \\ 0.1238 \end{bmatrix}, \\
\mathcal{C}_{\eta 1} &= 10^{-5} [0.0781 \quad -0.1328], & \mathcal{C}_{\eta 2} &= 10^{-5} [0.0170 \quad -0.1342], \\
\mathcal{D}_{\eta 1} &= 10^{-5} [-0.1711 \quad -0.1893], & \mathcal{D}_{\eta 2} &= 10^{-5} [0.1335 \quad -0.1333],
\end{aligned}$$

and the upper bound is $\gamma = 0.92$.

4.2.2.1 Monte Carlo Simulation

Observing the matrices of system (4.25), we consider that the fault in this example represents problems with the actuator. The specific fault signals represent that the actuator performance drops by 10% starting at $t = 125$ s. A Monte Carlo simulation with 300 iterations was performed, and the results are presented in Fig.28, Fig.29, which represent, respectively, the residue signal, and the evaluation function.

In Fig. 28, it can be observed that the FDF designed using Theorem 16 properly reacted to the fault signal as designed. Regarding the residue signal without fault in Fig. 28, when there is no fault signal the residue is close to zero for the entire simulation. It is not completely zero due to the presence of the noise signal $w(k)$ and to the switching behavior from the Markov Jump Systems.

Fig. 29 presents the evaluation function that is represented by the mean and standard deviation. It can be seen from this figure that the designed FDF is able to detect the fault in all cases within the range of [127 132]s. It shows that the designed FDF provides

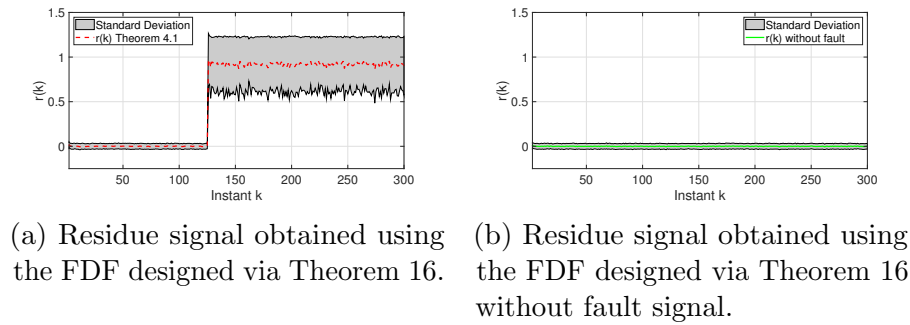


Figure 28: The mean and standard deviation of the residue signal obtained using the FDF designed via Theorem 16.

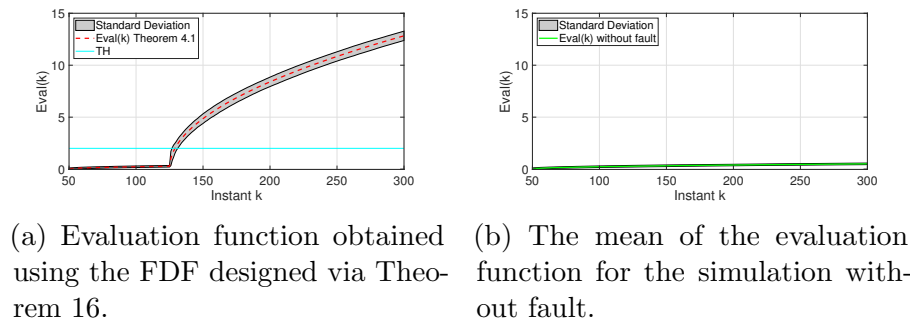


Figure 29: The mean and standard deviation of the evaluation function obtained using the FDF designed via Theorem 16.

a satisfactory level of reliability. The above simulation results show that the proposed method can provide a feasible solution for the fault detection problem.

4.3 Concluding remarks

In this chapter, we presented Lemma 8 and the design of an FDF under the assumption that the nonlinear system is subjected to network communication loss, which was model by using Markov Jump Lur'e Systems. In the next Chapter, we will tackle the FDF and FAC problem from another point of view, based on the linear parameter varying systems instead of the Markov Jump Systems.

5 FDF AND FAC FOR LPV SYSTEMS WITH UNCERTAIN PARAMETERS

This chapter introduces the results regarding the Fault Detection and Fault Accommodation using the Linear Parameter varying as a base. An important premise in this chapter is that the LPV parameter is not directly accessible. To circumvent this issue usually, we implement an estimation process to gather the LPV parameter, when these procedures are implemented normally we assume that the estimation is precise, however, this is not completely true, and in some occasions there will be a discrepancy between the parameter and the estimation. To deal with this imprecision and guarantee the FDF and FAC performance we added this imprecision during the design process using the multi-simplex approach to model an additive noise on the parameter.

The results presented in this chapter were published in the following:

- Subsection 5.2 presented the \mathcal{H}_∞ and \mathcal{H}_2 Gain Scheduled Fault Detection Filter, which was published in IEEE ACCESS October 2021, (CARVALHO et al., 2021b).
- Subsection 5.3 presented the \mathcal{H}_∞ and \mathcal{H}_2 Gain Scheduled Fault Accommodation, which was published and presented in the 4th IFAC Workshop on Linear Parameter Varying systems 2021, (CARVALHO et al., 2021a).

Definition 7. *The unit-simplex Λ_N of dimension $N \in \mathbb{N}$, with $N \geq 2$ is defined as*

$$\Lambda_N = \{\zeta \in \mathbb{R}^N : \sum_{i=1}^N \zeta_i = 1, \zeta_i \geq 0, i = 1, \dots, N\}. \quad (5.1)$$

Definition 8. *The multi-simplex $\Lambda_{m,N}$ is defined as the Cartesian product of m simplexes (as in (5.1)) with dimension of N , that is, $\Lambda_{m,N} = \Lambda_N \times \dots \times \Lambda_N$ with the Cartesian product containing m terms. Thus any $\theta \in \Lambda_{m,N}$ can be decomposed as $\theta = (\theta_1, \theta_2, \dots, \theta_m)$, with $\theta_i = (\theta_{i1}, \theta_{i2}, \dots, \theta_{iN}) \in \Lambda_N$, $i \in \{1, \dots, m\}$.*

Definition 9. *Homogeneous polynomial: For a unit-simplex Λ_N of dimension $N \in \mathbb{N}$, a polynomial $g(\theta)$, $\theta \in \Lambda_N$ is named a homogeneous polynomial of degree $l \in \mathbb{N}$ if all its*

monomials have the same total degree l . As an example, assuming $\theta = [\theta_1, \theta_2] \in \Lambda_2$, and $g(\theta) = \theta_1^3 + \theta_1^2\theta_2 + \theta_1\theta_2^2 + \theta_2^3$, $g(\theta)$ is said to be homogeneous polynomial with a degree of $l = 3$. Define $\mathbb{K}_N^{(l)}$ as the set of N -tuples obtained from all possible combinations of N nonnegative integers k_j , $j = 1, \dots, N$, with sum $k_1 + k_2 + \dots + k_N = l$. A homogeneous polynomial with 0 degree is defined as

$$A(\theta) = \sum_{k \in \mathbb{K}_N^{(l)}} \theta^k A_k, \quad (5.2)$$

where $\theta^k = \theta_1^{k_1} \cdot \theta_2^{k_2} \cdot \dots \cdot \theta_N^{k_N} = \prod_{j=1}^N \theta_j^{k_j}$.

5.1 Preliminary for LPV Systems

Consider the following discrete-time LPV system

$$\mathcal{G} := \begin{cases} x(k+1) = A_{\theta(k)}x(k) + J_{\theta(k)}w(k), \\ z(k) = C_{\theta(k)}x(k) + D_{\theta(k)}w(k), \end{cases}, \quad (5.3)$$

where $x(k) \in \mathbb{R}^{n_x}$ represents the state vector, $w(k) \in \mathbb{R}^{n_w}$ represents the exogenous input, and the $z(k) \in \mathbb{R}^{n_z}$ denotes output signal. We assume that the matrices $A_{\theta(k)}$, $J_{\theta(k)}$, $C_{\theta(k)}$, $D_{\theta(k)}$ in (5.3) depend on the parameter $\theta(k)$ in the affine form as

$$A_{\theta(k)} = A_0 + \sum_{i=1}^m \theta_i(k) A_i, \quad (5.4)$$

where A_0, \dots, A_m are given matrices and $\theta(k) = (\theta_1(k), \dots, \theta_m(k))$ are bounded time-varying parameters satisfying $|\theta_i(k)| \leq t_i$, $t_i \in \mathbb{R}^+$, $i = 1, \dots, m$, $\forall k \geq 0$. Similarly for $J_{\theta(k)}$, $C_{\theta(k)}$, $D_{\theta(k)}$. Observe that the affine form is a particular case of the parameterized form in (5.2) with a degree of 1. Note that if we describe the matrices in (5.3) as polynomials with a degree equal to 0, system (5.3) becomes parameter-independent.

5.1.1 \mathcal{H}_∞ Guaranteed Cost Analysis

In this subsection, we introduce a few concepts that will be important later on regarding the \mathcal{H}_∞ norm. The \mathcal{H}_∞ norm is a classical performance criterion that can be computed using the Bounded Real Lemma (BRL), as proposed in (CAIGNY et al., 2012) for LPV systems. For the system as in (5.3), its \mathcal{H}_∞ norm is defined by

$$\|\mathcal{G}\|_\infty = \sup_{\|w(k)\|_2 \neq 0} \frac{\|z(k)\|_2}{\|w(k)\|_2}, \quad w(k) \in \mathcal{L}_2. \quad (5.5)$$

In the following lemma, based on the conditions from (CAIGNY et al., 2010), we present the Bounded Real Lemma (BRL) for LPV systems where an upper bound for the \mathcal{H}_∞ norm is computed via parameter-dependent LMIs. For the sake of simplicity we set $\theta = \theta(k)$, and $\psi = \theta(k + 1)$.

Lemma 9. *If there exists a symmetric positive definite matrix P_θ , such that*

$$\begin{bmatrix} P_\psi & \bullet & \bullet & \bullet \\ P_\theta A'_\theta & P_\theta & \bullet & \bullet \\ J'_\theta & 0 & \gamma I & \bullet \\ 0 & C_\theta P_\theta & D_\theta & \gamma I \end{bmatrix} > 0, \quad (5.6)$$

holds for all $\theta(k)$, $k \geq 0$, then γ is an upper bound for the \mathcal{H}_∞ norm of system (5.3), that is, $\|\mathcal{G}\|_\infty < \gamma$.

The proof for Lemma 9 can be found in (SOUZA; BARBOSA; NETO, 2006, Lemma 3).

5.1.2 \mathcal{H}_2 Guaranteed Cost Analysis

The \mathcal{H}_2 norm is a performance criterion that is associated with the energy of the impulse response of the system, or in other words,

$$\|\mathcal{G}\|_2 = \limsup_{T \rightarrow \infty} \mathbb{E} \left\{ \frac{1}{T} \sum_{k=0}^T z(k)' z(k) \right\}, \quad (5.7)$$

where T is a positive integer that represents the time horizon and $w(k)$ is a standard white noise (Gaussian zero-mean in which the covariance matrix is equal to the identity matrix) as defined in (BARBOSA; SOUZA; TROFINO, 2002).

Considering an asymptotically stable system in the form (5.3), an upper bound for its \mathcal{H}_2 norm can be obtained by a set of parameter-dependent LMI constraints, as introduced in (CAIGNY et al., 2010) and shown in the following lemma.

Lemma 10. *If there exist symmetric positive definite matrices P_θ , and W_θ , such that*

$$\begin{bmatrix} P_\psi - A_\theta P_\theta A'_\theta & \bullet \\ J'_\theta & I \end{bmatrix} > 0, \quad (5.8)$$

$$\begin{bmatrix} W_\theta - D_\theta D'_\theta & \bullet \\ P_\theta C'_\theta & P_\theta \end{bmatrix} > 0, \quad (5.9)$$

and

$$\text{Tr}(W_\theta) < \lambda^2, \quad (5.10)$$

hold for all $\theta(k)$, $k \geq 0$, then λ is an upper bound for the \mathcal{H}_2 norm of system (5.3), that is, $\|\mathcal{G}\|_2 < \lambda$.

Lemma 10 and its proof are presented in (CAIGNY et al., 2010, Theorem 2).

5.2 Gain Scheduled Fault Detection Formulation

Consider the following LPV discrete-time system

$$\mathcal{G}_f := \begin{cases} x(k+1) = A_{\theta(k)}x(k) + B_{\theta(k)}u(k) + J_{\theta(k)}w(k) + F_{\theta(k)}f(k), \\ y(k) = C_{\theta(k)}x(k) + D_{\theta(k)}w(k) + D_{f\theta(k)}f(k), \end{cases} \quad (5.11)$$

where $x(k) \in \mathbb{R}^{n_x}$ represents the state vector, $u(k) \in \mathbb{R}^{n_u}$ denotes the control input, $w(k) \in \mathbb{R}^{n_w}$ is the exogenous input and $f(k) \in \mathbb{R}^{n_f}$ is the fault signal. We also consider that the signals $w, f \in \mathcal{L}_2$ and recall that the time-varying parameter $\theta(k)$ is bounded as $|\theta_i(k)| \leq t_i$, $t_i \in \mathbb{R}^+$, $i = 1, \dots, m$, $\forall k \geq 0$.

The major component in a Fault Detection and Isolation process is the Fault Detection Filter (FDF), which we can describe as follows

$$\mathcal{F} := \begin{cases} \eta(k+1) = \mathfrak{A}_{\eta\hat{\theta}(k)}\eta(k) + \mathfrak{M}_{\eta\hat{\theta}(k)}u(k) + \mathfrak{B}_{\eta\hat{\theta}(k)}y(k), \\ r(k) = \mathfrak{C}_{\eta\hat{\theta}(k)}\eta(k) + \mathfrak{D}_{\eta\hat{\theta}(k)}y(k), \end{cases} \quad (5.12)$$

where $\eta(k) \in \mathbb{R}^{n_\eta}$ denote the filter state and $r(k) \in \mathbb{R}^{n_r}$ is the residue signal. Note that the FDF (5.12) depends only on the estimated parameter $\hat{\theta}$. We assume that the FDF in (5.12) can be written in the affine form similarly to (5.4), so that the matrices in (5.12) are defined as

$$\mathfrak{A}_{\eta\hat{\theta}(k)} = \mathfrak{A}_{\eta 0} + \sum_{i=1}^m \hat{\theta}_i(k) \mathfrak{A}_{\eta i}, \quad (5.13)$$

Hence, the main focus of this chapter is to design all the matrices in $\mathfrak{A}_{\eta i}$, $\mathfrak{M}_{\eta i}$, $\mathfrak{B}_{\eta i}$, $\mathfrak{C}_{\eta i}$, $\mathfrak{D}_{\eta i}$, $i \in \{1, \dots, m\}$.

5.2.0.1 Parameter under additive uncertainty

One of the major premises of the present chapter is that the time-varying parameters $\theta(k)$ are not directly accessible. Instead, we implement estimation procedures to gather an estimation $\hat{\theta}(k)$ of the time-varying parameter $\theta(k)$, which are not completely precise, meaning that we must assume that $\hat{\theta}(k)$ is an inexact measurement of $\theta(k)$. The design under the assumption of inexact measurements is dealt with a general model described in (LACERDA et al., 2016), (PALMA; MORAIS; OLIVEIRA, 2018), in which we assume that the estimated parameters $\hat{\theta}(k)$ is a sum of the actual parameter $\theta(k)$ with an orthogonal

additive uncertainty $\sigma(k)$, that is

$$\hat{\theta}_i(k) = \theta_i(k) + \sigma_i(k), \quad i = 1, \dots, m \quad (5.14)$$

where $|\sigma_i(k)| \leq d_i$, $d_i \in \mathbb{R}^+$, $i = 1, \dots, m$. Thus, the domain of $(\theta(k), \sigma(k))$ is as displayed in Fig.30.

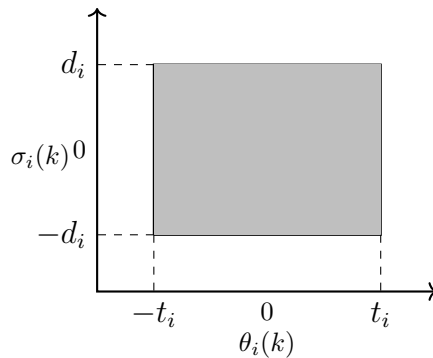


Figure 30: Feasible region for each pair $(\theta_i(k), \sigma_i(k))$, borrowed from (PALMA; MORAIS; OLIVEIRA, 2018).

From the aforementioned discussion, we may define the augmented system which depends on both time-varying parameter $\theta(k)$, $\hat{\theta}(k)$, by taking $e(k) = r(k) - f(k)$, as

$$\mathcal{G}_{aug} := \begin{cases} \tilde{x}(k+1) = \check{A}_{\hat{\theta}(k)\theta(k)} \tilde{x}(k) + \check{J}_{\hat{\theta}(k)\theta(k)} \tilde{w}(k), \\ e(k) = \check{C}_{\hat{\theta}(k)\theta(k)} \tilde{x}(k) + \check{D}_{\hat{\theta}(k)\theta(k)} \tilde{w}(k), \end{cases} \quad (5.15)$$

where we consider the augmented vectors $\tilde{x} = [x'(k) \ \eta'(k)]'$, $\tilde{w} = [u'(k) \ d'(k) \ f'(k)]'$. In order to simplify the visualization of the resulting LMIs, we consider hereafter $\theta = \theta(k)$, and $\hat{\theta} = \hat{\theta}(k)$. The following augmented matrices can be obtained:

$$\begin{aligned} \check{A}_{\hat{\theta}\theta} &= \begin{bmatrix} A_\theta & 0 \\ \mathfrak{B}_{\eta\hat{\theta}} C_\theta & \mathfrak{A}_{\eta\hat{\theta}} \end{bmatrix}, & \check{J}_{\hat{\theta}\theta} &= \begin{bmatrix} B_\theta & J_\theta & F_\theta \\ \mathfrak{M}_{\eta\hat{\theta}} & \mathfrak{B}_{\eta\hat{\theta}} D_\theta & \mathfrak{B}_{\eta\hat{\theta}} D_{f\theta} \end{bmatrix}, \\ \check{C}_{\hat{\theta}\theta} &= [\mathfrak{D}_{\eta\hat{\theta}} C_\theta \ \mathfrak{e}_{\eta\hat{\theta}}], & \check{D}_{\hat{\theta}\theta} &= [0 \ \mathfrak{D}_{\eta\hat{\theta}} D_\theta \ \mathfrak{D}_{\eta\hat{\theta}} D_{f\theta} - I]. \end{aligned}$$

Based on the augmented system as above, we can define the \mathcal{H}_∞ Fault Detection problem as follows.

\mathcal{H}_∞ Fault Detection problem: Given a desired \mathcal{H}_∞ -gain $\gamma > 0$, design the FDF as in (5.12) such that the \mathcal{H}_∞ norm of the augmented system (5.15) satisfies

$$\|\mathcal{G}_{aug}\|_\infty = \sup_{\|\tilde{w}\|_2 \neq 0, \tilde{w} \in \mathcal{L}_2} \frac{\|e\|_2}{\|\tilde{w}\|_2} < \gamma. \quad (5.16)$$

Similarly, we can define the \mathcal{H}_2 Fault Detection problem as follows.

\mathcal{H}_2 **Fault Detection problem:** Given a desired \mathcal{H}_2 -gain $\lambda > 0$, design the FDF as in (5.12) such that the \mathcal{H}_2 norm of the augmented system (5.15) satisfies

$$\|\mathcal{G}_{\text{aug}}\|_2 = \limsup_{T \rightarrow \infty} \mathbb{E} \left\{ \frac{1}{T} \sum_{k=0}^T e(k)' e(k) \right\} < \lambda. \quad (5.17)$$

5.2.0.2 Change of variables

From the discussion presented in the previous sub-sections, a major assumption in this chapter is that the parameter used by the filter is an estimation of the real one affecting the system. To deal with this assumption it is necessary to employ some procedures to design the fault detection filter (5.12). Using, for instance, the procedures given in (LACERDA et al., 2016; BRIAT, 2015), we can perform a variable transformation to deal with this type of parameter subjected to additive uncertainty. These variable transformations, applied to our context can be seen as

$$\alpha_{i1}(k) = \frac{\theta_i(k) + t_i}{2t_i}, \quad \hat{\alpha}_{i1}(k) = \frac{\sigma_i(k) + d_i}{2d_i},$$

and the original parameters are retrieved as

$$\begin{aligned} \theta_i(k) &= 2t_i\alpha_{i1}(k) - t_i, & \sigma_i(k) &= 2d_i\hat{\alpha}_{i1}(k) - d_i, \\ & & i &= 1, \dots, m. \end{aligned}$$

Thus we have that $\alpha_i(k) = (\alpha_{i1}(k), \alpha_{i2}(k))$ and $\hat{\alpha}_i(k) = (\hat{\alpha}_{i1}(k), \hat{\alpha}_{i2}(k))$ belong to the unit-simplex as in (5.1) with $N = 2$, so that $\alpha(k) = (\alpha_1(k), \dots, \alpha_m(k))$ and $\hat{\alpha}(k) = (\hat{\alpha}_1(k), \dots, \hat{\alpha}_m(k))$ belong to the multi-simplex $\Lambda_{m,2} = \Lambda_2 \times \dots \times \Lambda_2$ with m terms. We set $\tilde{\alpha}(k) = (\alpha(k), \hat{\alpha}(k)) \in \Lambda_{m,2} \times \Lambda_{m,2}$, where $\alpha(k)$ is related to $\theta(k)$, and $\hat{\alpha}(k)$ to $\sigma(k)$ (the additive noise time-varying parameter). Notice that the matrices in system (5.3) and in the FDF in (5.12) can be rewritten using the new multi-simplex $\tilde{\alpha}(k)$, following the procedure explained in (LACERDA et al., 2016), which uses the polynomial homogenisation process presented in (OLIVEIRA; BLIMAN; PERES, 2008).

Another assumption made for the numerical procedure is that the parameters are arbitrarily fast in time so that, by consequence, $\theta(k+1)$ is independent from $\theta(k)$.

When using the parser ROLMIP (AGULHARI et al., 2019), associated with YALMIP (LOFBERG, 2004), this procedure is as simple as setting the degrees of the multi-simplex polynomials and the parameter boundaries. Thus for the numerical procedure, this change of variable will be applied to derive the FDF in (5.12).

$$\begin{bmatrix}
\Pi^{1,1} & \bullet & \bullet & \bullet & \bullet & \bullet & \bullet & \bullet \\
\Pi^{2,1} & -W'_{22\theta} + \xi(\text{Her}(\nabla_{\hat{\theta}})) & \bullet & \bullet & \bullet & \bullet & \bullet & \bullet \\
\Pi^{3,1} & \nabla_{\hat{\theta}} + \xi K'_{2\hat{\theta}} & W'_{11\beta} - \text{Her}(K_{1\hat{\theta}}) & \bullet & \bullet & \bullet & \bullet & \bullet \\
\Pi^{4,1} & \nabla_{\hat{\theta}} + \xi \bar{K}'_{\hat{\theta}} & W'_{12\beta} - \bar{K}'_{\hat{\theta}} - K_{2\hat{\theta}} & W'_{22\beta} - \text{Her}(\bar{K}_{\hat{\theta}}) & \bullet & \bullet & \bullet & \bullet \\
\Pi^{5,1} & \xi(K_{2\hat{\theta}}B_{\theta} + \Gamma_{\hat{\theta}})' & B'_{\theta}K'_{1\hat{\theta}} + \Gamma'_{\hat{\theta}} & B'_{\theta}K'_{2\hat{\theta}} + \Gamma'_{\hat{\theta}} & -\gamma^2 I & \bullet & \bullet & \bullet \\
\Pi^{6,1} & \xi(K_{2\hat{\theta}}J_{\theta} + \Omega_{\hat{\theta}}D_{d\theta})' & J'_{\theta}K'_{1\hat{\theta}} + D'_{d\theta}\Omega'_{\hat{\theta}} & J'_{\theta}K'_{2\hat{\theta}} + D'_{d\theta}\Omega'_{\hat{\theta}} & 0 & -\gamma^2 I & \bullet & \bullet \\
\Pi^{7,1} & \xi(K_{2\hat{\theta}}F_{\theta} + \Omega_{\hat{\theta}}D_{f\theta})' & F'_{\theta}K'_{1\hat{\theta}} + D'_{f\theta}\Omega'_{\hat{\theta}} & F'_{\theta}K'_{2\hat{\theta}} + D'_{f\theta}\Omega'_{\hat{\theta}} & 0 & 0 & -\gamma^2 I & \bullet \\
\Pi^{8,1} & \mathfrak{C}_{\eta\hat{\theta}} & 0 & 0 & 0 & \mathfrak{D}_{\eta\hat{\theta}}D_{d\theta} & \mathfrak{D}_{\eta\hat{\theta}}D_{f\theta} - I & -I
\end{bmatrix} < 0, \quad (5.18)$$

5.2.1 Theoretical Results

In this section, we describe the main contributions of this chapter on the design of the fault detection filters for solving the previously defined \mathcal{H}_2 , and \mathcal{H}_{∞} fault detection problems. It is important to stress that the results will be presented in terms of the original parameters $\theta(k)$ and $\hat{\theta}(k)$ to highlight that the derived filter only depends on the measurable parameter $\hat{\theta}(k)$. For the numerical procedure, the change of variable presented in Section 5.2.0.2 should be applied so that we end up with multi-simplex polynomials with the new multi-simplex parameter $\tilde{\alpha} \in \Lambda_{m,2} \times \Lambda_{m,2}$. As before, for the sake of simplicity in what follows we set $\theta = \theta(k)$, $\hat{\theta} = \hat{\theta}(k)$ and $\beta = \theta(k+1)$, and by feasible θ , β , $\hat{\theta}$ we mean that the constraints imposed in Section 5.2 are satisfied.

5.2.1.1 \mathcal{H}_{∞} Fault Detection Filter Design for LPV with uncertain parameter

In the following theorem, we present the design of LPV FDF via LMI to obtain a guaranteed \mathcal{H}_{∞} upper bound of the augmented system in (5.15).

Theorem 17. *For a desired \mathcal{H}_{∞} upper bound $\gamma > 0$, if there exist symmetric positive definite matrices $W_{11\theta}$, and $W_{22\theta}$ and matrices $W_{12\theta}$, $K_{1\hat{\theta}}$, $K_{2\hat{\theta}}$, $\bar{K}_{\hat{\theta}}$, $\Omega_{\hat{\theta}}$, $\nabla_{\hat{\theta}}$, $\Gamma_{\hat{\theta}}$, $\mathfrak{C}_{\eta\hat{\theta}}$, $\mathfrak{D}_{\eta\hat{\theta}}$ with compatible dimensions and a given scalar parameter $\xi \in]-1 \ 1[$ such that (5.18) with*

$$\begin{aligned}
\Pi^{1,1} &= -W_{11\theta} + \xi(\text{Her}(K_{1\hat{\theta}}A_{\theta} + \Omega_{\hat{\theta}}C_{\theta})), \\
\Pi^{2,1} &= -W'_{12\theta} + \xi(\nabla'_{\hat{\theta}} + K_{2\hat{\theta}}A_{\theta} + C'_{\theta}\Omega'_{\hat{\theta}}), \quad \Pi^{3,1} = K_{1\hat{\theta}}A_{\theta} + \Omega'_{\hat{\theta}}C_{\theta} + \xi K'_{1\hat{\theta}}, \\
\Pi^{4,1} &= K_{2\hat{\theta}}A_{\theta} + \Omega'_{\hat{\theta}}C_{\theta} + \xi \bar{K}'_{\hat{\theta}}, \quad \Pi^{5,1} = \xi(K_{1\hat{\theta}}B_{\theta} + \Gamma_{\hat{\theta}})', \\
\Pi^{6,1} &= \xi(K_{1\hat{\theta}}J_{\theta} + \Omega_{\hat{\theta}}D_{d\theta})', \quad \Pi^{7,1} = \xi(K_{1\hat{\theta}}F_{\theta} + \Omega_{\hat{\theta}}D_{f\theta})', \quad \Pi^{8,1} = \mathfrak{D}_{\eta\hat{\theta}}C_{\theta},
\end{aligned}$$

holds for all feasible θ , β , $\hat{\theta}$ then the LPV FDF (5.12) with $\mathfrak{A}_{\eta\hat{\theta}} = \bar{K}_{\hat{\theta}}^{-1}\nabla_{\hat{\theta}}$, $\mathfrak{B}_{\eta\hat{\theta}} = \bar{K}_{\hat{\theta}}^{-1}\Omega_{\hat{\theta}}$, $\mathfrak{M}_{\eta\hat{\theta}} = \bar{K}_{\hat{\theta}}^{-1}\Gamma_{\hat{\theta}}$, $\mathfrak{C}_{\eta\hat{\theta}} = \mathfrak{C}_{\eta\hat{\theta}}$, and $\mathfrak{D}_{\eta\hat{\theta}} = \mathfrak{D}_{\eta\hat{\theta}}$ solves the \mathcal{H}_{∞} fault detection problem (5.16).

Proof: We apply the variable substitutions $\nabla_{\hat{\theta}} = \bar{K}_{\hat{\theta}}\mathfrak{A}_{\eta\hat{\theta}}$, $\Omega_{\hat{\theta}} = \bar{K}_{\hat{\theta}}\mathfrak{B}_{\eta\hat{\theta}}$, $\Gamma_{\hat{\theta}} = \bar{K}_{\hat{\theta}}\mathfrak{M}_{\eta\hat{\theta}}$,

$\mathfrak{C}_{\eta\hat{\theta}} = \mathfrak{C}_{\eta\hat{\theta}}$, and $\mathfrak{D}_{\eta\hat{\theta}} = \mathfrak{D}_{\eta\hat{\theta}}$ in (5.18). Assuming the structure of \mathcal{W}_θ , $\mathcal{K}_{\hat{\theta}}$, as

$$\mathcal{W}_\theta = \begin{bmatrix} W_{11\theta} & W_{12\theta} \\ W'_{12\theta} & W_{22\theta} \end{bmatrix}, \quad \mathcal{K}_{\hat{\theta}} = \begin{bmatrix} K_{1\hat{\theta}} & \bar{K}_{\hat{\theta}} \\ K_{2\hat{\theta}} & \bar{K}_{\hat{\theta}} \end{bmatrix}, \quad (5.19)$$

as well as the augmented matrices in (5.15), the inequality (5.18) can be rewritten as

$$\begin{bmatrix} -\mathcal{W}_\theta + \xi(\text{Her}(\mathcal{K}_{\hat{\theta}}\bar{A}_{\theta\hat{\theta}})) & \bar{A}'_{\theta\hat{\theta}}\mathcal{K}'_{\hat{\theta}} - \xi\mathcal{K}_{\hat{\theta}} & \xi\mathcal{K}_{\hat{\theta}}\bar{J}_{\theta\hat{\theta}} & \bar{C}'_{\theta\hat{\theta}} \\ \mathcal{K}_{\hat{\theta}}\bar{A}_{\theta\hat{\theta}} - \xi\mathcal{K}'_{\hat{\theta}} & -\mathcal{W}_\beta - \mathcal{K}_{\hat{\theta}} - \mathcal{K}'_{\hat{\theta}} & \mathcal{K}_{\hat{\theta}}\bar{J}_{\theta\hat{\theta}} & 0 \\ \xi\bar{J}'_{\theta\hat{\theta}}\mathcal{K}'_{\hat{\theta}} & \bar{J}'_{\theta\hat{\theta}}\mathcal{K}'_{\hat{\theta}} & -\gamma^2 I & \bar{D}'_{\theta\hat{\theta}} \\ \bar{C}_{\theta\hat{\theta}} & 0 & \bar{D}_{\theta\hat{\theta}} & -I \end{bmatrix} < 0. \quad (5.20)$$

Moreover (5.43) can be written as

$$Q_{\theta\hat{\theta}\beta} + U'_{\theta\hat{\theta}}\mathcal{K}'_{\hat{\theta}}V + V'\mathcal{K}_{\hat{\theta}}U_{\theta\hat{\theta}} < 0, \quad (5.21)$$

where

$$\begin{aligned} Q_{\theta\hat{\theta}\beta} &= \begin{bmatrix} -\mathcal{W}_\theta & 0 & 0 & \bar{C}'_{\theta\hat{\theta}} \\ 0 & -\mathcal{W}_\beta & 0 & 0 \\ 0 & 0 & -\gamma^2 I & \bar{D}'_{\theta\hat{\theta}} \\ \bar{C}_{\theta\hat{\theta}} & 0 & \bar{D}_{\theta\hat{\theta}} & -I \end{bmatrix}, \\ U'_{\theta\hat{\theta}} &= \begin{bmatrix} \bar{A}'_{\theta\hat{\theta}} \\ -I \\ \bar{J}'_{\theta\hat{\theta}} \\ 0 \end{bmatrix}, \quad V' = \begin{bmatrix} \xi I \\ I \\ 0 \\ 0 \end{bmatrix}. \end{aligned} \quad (5.22)$$

Now, we pre- and post-multiply the inequality (5.50) by

$$\begin{bmatrix} I & \bar{A}'_{\theta\hat{\theta}} & 0 & 0 \\ 0 & \bar{J}'_{\theta\hat{\theta}} & I & 0 \\ 0 & 0 & 0 & I \end{bmatrix}, \quad (5.23)$$

and its transpose, respectively, and after that applying the Schur complement and using arguments similar to those explained at the end of the proof for Theorem 18 we end up obtaining constraints that are equivalent to those for the bounded real lemma (5.6), concluding the proof. ■

5.2.1.2 \mathcal{H}_2 Fault Detection Filter Design for LPV with uncertain parameter

The next theorem presents the LPV FDF design using an upper bound for the guaranteed cost for the \mathcal{H}_2 norm of the system (5.15).

Theorem 18. *For a desired \mathcal{H}_2 upper bound $\lambda > 0$, if there exist symmetric positive definite matrices $Y_{11\theta}$, $Y_{22\theta}$, M_θ , and matrices $Y_{12\theta}$, $X_{1\hat{\theta}}$, $X_{2\hat{\theta}}$, $\bar{X}_{\hat{\theta}}$, $\Omega_{\hat{\theta}}$, $\nabla_{\hat{\theta}}$, $\Gamma_{\hat{\theta}}$, $\mathfrak{C}_{\eta\hat{\theta}}$, $\mathfrak{D}_{\eta\hat{\theta}}$ with compatible dimensions, and a given scalar parameter $\xi \in]-1, 1[$ such that the following inequalities hold for all feasible θ , β , $\hat{\theta}$, then the LPV FDF (5.12) with $\mathfrak{A}_{\eta\hat{\theta}} = \bar{X}_{\hat{\theta}}^{-1}\nabla_{\hat{\theta}}$, $\mathfrak{B}_{\eta\hat{\theta}} = \bar{X}_{\hat{\theta}}^{-1}\Omega_{\hat{\theta}}$, $\mathfrak{M}_{\eta\hat{\theta}} = \bar{X}_{\hat{\theta}}^{-1}\Gamma_{\hat{\theta}}$, $\mathfrak{C}_{\eta\hat{\theta}} = \mathfrak{C}_{\eta\hat{\theta}}$, and $\mathfrak{D}_{\eta\hat{\theta}} = \mathfrak{D}_{\eta\hat{\theta}}$ solves the \mathcal{H}_2 fault detection problem (5.17).*

$$\text{Tr}(M_\theta) < \lambda^2, \quad (5.24)$$

$$\begin{bmatrix} -Y_{11\theta} + \xi(\text{Her}(X_{1\hat{\theta}}A_\theta + \Omega_{\hat{\theta}}C_\theta)) & \bullet & \bullet & \bullet & \bullet & \bullet & \bullet \\ -Y_{12\theta} + \xi(X_{2\hat{\theta}}A_\theta + \Omega_{\hat{\theta}}C_\theta + \nabla'_{\hat{\theta}}) & -Y_{22\theta} + \xi\text{Her}(\nabla_{\hat{\theta}}) & \bullet & \bullet & \bullet & \bullet & \bullet \\ X_{1\hat{\theta}}A_\theta + \Omega_{\hat{\theta}}C_\theta + \xi X_{1\hat{\theta}} & \nabla_{\hat{\theta}} + \xi X'_{2\hat{\theta}} & Y_{11\beta} - X'_{1\hat{\theta}} - X_{1\hat{\theta}} & \bullet & \bullet & \bullet & \bullet \\ X_{2\hat{\theta}}A_\theta + \Omega_{\hat{\theta}}C_\theta + \xi \bar{X}_{\hat{\theta}} & \nabla_{\hat{\theta}} + \xi \bar{X}'_{\hat{\theta}} & Y'_{12\beta} - X_{2\hat{\theta}} - \bar{X}'_{\hat{\theta}} & Y_{22\beta} - \text{Her}(\bar{X}_{\hat{\theta}}) & \bullet & \bullet & \bullet \\ \xi(B'_\theta X'_{1\hat{\theta}} + \Gamma'_{\hat{\theta}}) & \xi(B'_\theta X'_{2\hat{\theta}} + \Gamma'_{\hat{\theta}}) & B'_\theta X'_{1\hat{\theta}} + \Gamma'_{\hat{\theta}} & B'_\theta X_{2\hat{\theta}} + \Gamma'_{\hat{\theta}} & -I & \bullet & \bullet \\ \xi(J'_\theta X'_{1\hat{\theta}} + D'_{d\theta} \Omega'_{\hat{\theta}}) & \xi(J'_\theta X'_{2\hat{\theta}} + D'_{d\theta} \Omega'_{\hat{\theta}}) & J'_\theta X'_{1\hat{\theta}} + D'_{d\theta} \Omega'_{\hat{\theta}} & J'_\theta X'_{2\hat{\theta}} + D'_{d\theta} \Omega'_{\hat{\theta}} & 0 & -I & \bullet \\ \xi(F'_\theta X'_{1\hat{\theta}} + D'_{f\theta} \Omega'_{\hat{\theta}}) & \xi(F'_\theta X'_{2\hat{\theta}} + D'_{f\theta} \Omega'_{\hat{\theta}}) & F'_\theta X'_{1\hat{\theta}} + D'_{f\theta} \Omega'_{\hat{\theta}} & F'_\theta X'_{2\hat{\theta}} + D'_{f\theta} \Omega'_{\hat{\theta}} & 0 & 0 & -I \end{bmatrix} < 0, \quad (5.25)$$

$$\begin{bmatrix} M_\theta & \bullet & \bullet & \bullet & \bullet & \bullet \\ C'_\theta \mathfrak{D}'_{\eta\hat{\theta}} & Y_{11\theta} & \bullet & \bullet & \bullet & \bullet \\ \mathfrak{C}'_{\eta\hat{\theta}} & Y'_{12\theta} & Y_{22\theta} & \bullet & \bullet & \bullet \\ 0 & 0 & 0 & I & \bullet & \bullet \\ D'_{d\theta} \mathfrak{D}'_{\eta\hat{\theta}} & 0 & 0 & 0 & I & \bullet \\ D'_{f\theta} \mathfrak{D}'_{\eta\hat{\theta}} - I & 0 & 0 & 0 & 0 & I \end{bmatrix} > 0, \quad (5.26)$$

Proof: First, apply the variable substitution $\nabla_{\hat{\theta}} = \bar{X}_{\hat{\theta}} \mathfrak{A}_{\eta\hat{\theta}}$, $\Omega_{\hat{\theta}} = \bar{X}_{\hat{\theta}} \mathfrak{B}_{\eta\hat{\theta}}$, $\Gamma_{\hat{\theta}} = \bar{X}_{\hat{\theta}} \mathfrak{M}_{\eta\hat{\theta}}$, $\mathfrak{C}_{\eta\hat{\theta}} = \mathfrak{C}_{\eta\hat{\theta}}$, and $\mathfrak{D}_{\eta\hat{\theta}} = \mathfrak{D}_{\eta\hat{\theta}}$ in (5.25). Considering the augmented matrices given in (5.15), and the following structures for $X_{\hat{\theta}}$, Y_θ , Y_β ,

$$X_{\hat{\theta}} = \begin{bmatrix} X_{1\hat{\theta}} & \bar{X}_{\hat{\theta}} \\ X_{2\hat{\theta}} & \bar{X}_{\hat{\theta}} \end{bmatrix}, \quad Y_\theta = \begin{bmatrix} Y_{11\theta} & \bullet \\ Y_{21\theta} & Y_{22\theta} \end{bmatrix}, \quad Y_\beta = \begin{bmatrix} Y_{11\beta} & \bullet \\ Y_{21\beta} & Y_{22\beta} \end{bmatrix}, \quad (5.27)$$

we can rewrite the constraint (5.25) as

$$\begin{bmatrix} -Y_\theta + \xi(\text{Her}(X_{\hat{\theta}} \bar{A}_{\theta\hat{\theta}})) & \bar{A}'_{\theta\hat{\theta}} X'_{\hat{\theta}} - \xi X_{\hat{\theta}} & \xi X_{\hat{\theta}} \bar{J}_{\theta\hat{\theta}} \\ \bullet & Y_\beta - \text{Her}(X_{\hat{\theta}}) & X_{\hat{\theta}} \bar{J}_{\theta\hat{\theta}} \\ \bullet & \bullet & -I \end{bmatrix} < 0. \quad (5.28)$$

Rewriting (5.28) we get

$$Q_{\theta\beta} + U'_{\theta\hat{\theta}} X'_{\hat{\theta}} V + V' X_{\hat{\theta}} U_{\theta\hat{\theta}} < 0 \quad (5.29)$$

where

$$Q_{\theta\beta} = \begin{bmatrix} -Y_\theta & 0 & 0 \\ \bullet & Y_\beta & 0 \\ \bullet & \bullet & -I \end{bmatrix}, \quad U_{\theta\hat{\theta}} = [\bar{A}_{\theta\hat{\theta}} \quad -I \quad \bar{J}_{\theta\hat{\theta}}], \quad V = [\xi I \quad I \quad 0].$$

Let the null space for $U_{\theta\hat{\theta}}$ and V be given by

$$\mathcal{N}_U = \begin{bmatrix} I & 0 \\ \bar{A}_{\theta\hat{\theta}} & \bar{J}_{\theta\hat{\theta}} \\ 0 & I \end{bmatrix}, \quad \text{and} \quad \mathcal{N}_V = \begin{bmatrix} -I & 0 \\ \xi I & 0 \\ 0 & I \end{bmatrix}. \quad (5.30)$$

Now, if we pre- and post-multiply (5.28) by \mathcal{N}'_U and \mathcal{N}_U , respectively, and apply twice the Schur complement to the result of this procedure we recover the conditions presented in (5.8) with $P_\theta = Y_\theta^{-1}$ and $P_\psi = Y_\beta^{-1}$. Regarding the constraints (5.26) we consider the same variable substitutions as at the start of the proof. After that, applying twice the Schur complement we obtain the constraint (5.9) with $W_\theta = M_\theta$. ■

5.2.1.3 Mixed $\mathcal{H}_2 / \mathcal{H}_\infty$ Fault Detection Filter Design for LPV with uncertain parameter

In this section, we provide a mixed procedure aiming to improve the FDI performance combining the results for \mathcal{H}_2 and \mathcal{H}_∞ norms introduced earlier in this section. A simple approach to obtain a mixed solution when dealing with LMI constraints to solve both optimization problems simultaneously, for instance, we can consider the following two optimization statements

- (i) Assume a weighting scalar ν , we solve the constraints assuming an objective function of the form

$$g(\lambda, \gamma) = \inf\{\nu\lambda + (1 - \nu)\gamma\}, \quad (5.31)$$

where $\|G_{\text{aug}}\|_2^2 < \lambda$ and $\|G_{\text{aug}}\|_\infty^2 < \gamma$.

- (ii) Given one of the upper bounds of the \mathcal{H}_2 or \mathcal{H}_∞ norms, $\lambda > 0$ or $\gamma > 0$, respectively, we solve the constraints in order to minimize the other upper bound.

Before we introduce the main result of this section, consider the following set of variables

$$\begin{aligned} \psi = \{ & W_{11\theta} > 0, W_{12\theta}, W_{22\theta} > 0, X_{1\hat{\theta}}, X_{2\hat{\theta}}, Y_{11\theta}, K_{1\hat{\theta}}, Y_{12\theta}, Y_{22\theta}, K_{2\hat{\theta}}, \\ & M_\theta > 0, \bar{X}_{\hat{\theta}} = \bar{K}_{\hat{\theta}} > 0, \nabla_{\hat{\theta}}, \Omega_{\hat{\theta}}, \Gamma_{\hat{\theta}}, \mathfrak{C}_{\eta\hat{\theta}}, \mathfrak{D}_{\eta\hat{\theta}} \}, \end{aligned} \quad (5.32)$$

$$\begin{aligned} \psi_1 = \{ & W_{11\theta} > 0, W_{12\theta}, W_{22\theta} > 0, X_{1\hat{\theta}}, X_{2\hat{\theta}}, Y_{11\theta}, K_{1\hat{\theta}}, Y_{12\theta}, Y_{22\theta}, K_{2\hat{\theta}}, \\ & M_\theta > 0, \bar{X}_{\hat{\theta}} = \bar{K}_{\hat{\theta}} > 0, \nabla_{\hat{\theta}}, \Omega_{\hat{\theta}}, \Gamma_{\hat{\theta}}, \mathfrak{C}_{\eta\hat{\theta}}, \mathfrak{D}_{\eta\hat{\theta}} \} \cup \zeta_1 \end{aligned} \quad (5.33)$$

where ζ_1 denotes the set containing λ and γ .

The next theorem provides a sufficient condition for the FDF design for the mixed $\mathcal{H}_2/\mathcal{H}_\infty$ problem.

Theorem 19. *If for a given upper bounds $\lambda > 0$ and $\gamma > 0$ there exist ψ as in (5.32) such that the inequalities (5.18), and (5.24)-(5.26) hold for all feasible $\theta, \beta, \hat{\theta}$, then a suitable LPV FDF as in (5.12) which solves simultaneously the \mathcal{H}_∞ and \mathcal{H}_2 fault detection problems (5.17) and (5.16) is given by $\mathfrak{A}_{\eta\hat{\theta}} = \bar{X}_{\hat{\theta}}^{-1}\nabla_{\hat{\theta}}$, $\mathfrak{B}_{\eta\hat{\theta}} = \bar{X}_{\hat{\theta}}^{-1}\Omega_{\hat{\theta}}$, $\mathfrak{M}_{\eta\hat{\theta}} = \bar{X}_{\hat{\theta}}^{-1}\Gamma_{\hat{\theta}}$, $\mathfrak{C}_{\eta\hat{\theta}} = \mathfrak{C}_{\eta\hat{\theta}}$, and $\mathfrak{D}_{\eta\hat{\theta}} = \mathfrak{D}_{\eta\hat{\theta}}$. Alternatively, one can consider both or one of the upper bounds λ and γ , as variables, and solve the optimization problems in ψ_1 (5.33) according to the stages (i) or (ii).*

Proof: The proof follows directly from the proofs for Theorems 17 and 18. ■

Remark 16. Notice that Theorems 18, 17 and 19 are LMI conditions that provide the system performance regarding the \mathcal{H}_∞ , \mathcal{H}_2 , and $\mathcal{H}_2/\mathcal{H}_\infty$, respectively. Observe that the LMI conditions in (5.24), (5.25), (5.26), and (5.18), are defined as infinite dimensional optimization problem that must be solved. By using the change of variables presented in sub-section 5.2.0.2 and explained at the beginning of this section, we can re-write the LMI optimization problems in terms of the new multi-simplex parameter $\tilde{\alpha} \in \Lambda_{m,2} \times \Lambda_{m,2}$. This sort of optimization problems is hard to deal with but, however, they can be handled by using the modern LMI Parsers as ROLMIP (AGULHARI et al., 2019) and YALMIP (LOFBERG, 2004), which allow us to set polynomial degrees for the optimization variables. This type of polynomial relaxation permits the problem to be rewritten as an analysis of the positivity of homogeneous polynomial matrices (see Definition 9), which is the procedure made by the ROLMIP, and after that the next step is to use a semidefinite programming solver to acquire the solution.

Remark 17. Note that in Theorems 18, 17, and 19 the variables that define if the FDF is in the Robust form or in the Affine form, are $\nabla_{\hat{\theta}}$, $\Omega_{\hat{\theta}}$, $\Gamma_{\hat{\theta}}$, $\mathfrak{C}_{\eta\hat{\theta}}$, $\mathfrak{D}_{\eta\hat{\theta}}$, and $\bar{X}_{\hat{\theta}}$. If the degree of those homogeneous polynomial matrices are set to be 0, the FDF designed will be Robust, meaning that the FDF obtained will be parameter-independent. For a homogeneous polynomial matrices degree equal to 1, the FDF obtained will be in the affine form. Observe that a higher degree of the homogeneous polynomial can be set, leading to the design of FDF with a higher degree. It is important to discuss that it is also allowed to change the degree of the other variables in Theorems 18, 17, and 19, such as $Y_{11\theta}$, $Y_{12\theta}$, $Y_{22\theta}$, M_θ , $W_{11\theta}$, $W_{12\theta}$, and $W_{22\theta}$, with this choice mainly affecting the level of conservatism and the computational effort.

Remark 18. Notice that in Theorems 17 and 18 there are a parameter ξ , the purpose of this particular parameter is to improve the optimization problem results. The simplest way to obtain ξ is to perform a scalar search where $\xi \in [-1 \ 1]$, and use the ξ value of where the upper bound obtained is the lowest.

5.2.2 Simulations Results

As in the previous sections, we are using the coupled-tank model with a fault signal representing an abnormal input on the first tank. The LPV parameter in the tank couple models a flux variation in the connection between tanks. The matrices that compose the system on the LPV formulation is given by

$$A_1 = \begin{bmatrix} -0.0239 & -0.0127 \\ 0.0127 & -0.0285 \end{bmatrix}, \quad A_2 = \begin{bmatrix} 0 & 1 \\ 1 & 0 \end{bmatrix}, \quad B = \begin{bmatrix} 0.71 & 0 \\ 0 & 0.71 \end{bmatrix}, \quad J = \begin{bmatrix} 0.0071 & 0 \\ 0 & 0.0071 \end{bmatrix},$$

$$F = \begin{bmatrix} 0.71 \\ 0 \end{bmatrix}, \quad C = I^{2 \times 2}, \quad D = \begin{bmatrix} 0.01 & 0 \\ 0 & 0.01 \end{bmatrix}, \quad E = \begin{bmatrix} 0 \\ 0 \end{bmatrix}, \quad |\theta(k)| \leq t_i = 0.03,$$

where F has the same structure of the control input matrix B , representing an abnormal input in the first tank, and the matrix E is null since we do not consider that there is a sensor fault during the simulation. Observe that the only matrix that is subjected to LPV is matrix A , representing a variation in the valve that connects both tanks. Regarding the estimation parameter, we need to set a specific value for the range of $\sigma(k)$ beforehand. We can find in the literature some possible ways to obtain this range, see for instance (PALMA; MORAIS; OLIVEIRA, 2018), where a Monte Carlo simulation is performed to obtain this information which is a reliable method to find this range when implementing the FDI. However, since finding the range of $\sigma(k)$ is not the focus of the present chapter, we arbitrarily set the range of $\sigma(k)$ as $|\sigma(k)| \leq d_i = 0.01$. To obtain the estimated parameter $\hat{\theta}$ we implemented the Recursive Least Square (RLS) algorithm (PAULO, 2013; SAYED, 2011). We note that any other adaptive filter algorithms can also be implemented to obtain $\hat{\theta}$, such as \mathcal{H}_∞ adaptive filter algorithm or Least Mean Square-based algorithm.

Remark: Note that the level of reliability in the estimation process is directly connected with the value of $\sigma(k)$, as the less reliable the process the higher the value of $\sigma(k)$ must be.

The parameter $\theta(k)$ behavior is presented in Fig. 31 which we assume to be the

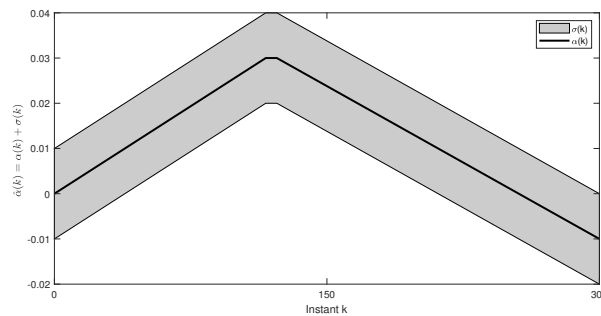


Figure 31: Behavior for the Linear-Parameter variable $\theta(k)$ and $\sigma(k)$.

representation of an imprecision in the valve that interconnects the first tank with the second one.

In the sequence, we present the simulation results given in two distinct parts, the upper bound behavior analysis, and temporal analysis. First, we analyze the obtained values for the upper bounds λ and γ when performing a search in the scalar ξ in the range $]-1 \ 1[$ with 100 steps with the same length. These values for the upper bounds are shown in Fig. 32.

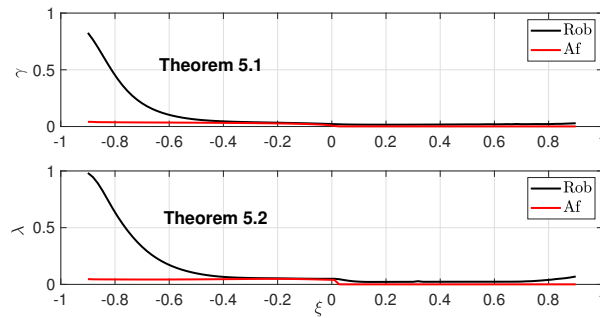


Figure 32: Upper bounds γ and λ behavior for Theorem 17 and 18 when scalar ξ varies. Rob denotes the results using the Robust structure, and Aff represents the results using Affine structure.

Examining the curves in Fig. 32, for the first behavior we can observe is that the values of γ and λ considering the robust form are higher than the affine structure. This is an expected result, mainly due to the less amount of variable in the LMIs that leads to a higher level of conservatism imposed in the optimization problem.

Following a similar procedure, we consider the mixed $\mathcal{H}_2/\mathcal{H}_\infty$ guaranteed costs approach. For that, we assume a fixed upper bound $\gamma = 0.01$ related to the upper bound for \mathcal{H}_∞ and we search for the minimum value of λ , as it was introduced in statement (ii) in Subsection 5.2.1.3. In Fig. 33 we present the obtained values for the upper bound λ given the aforementioned information when the scalar ξ varies in the same interval as previously used.

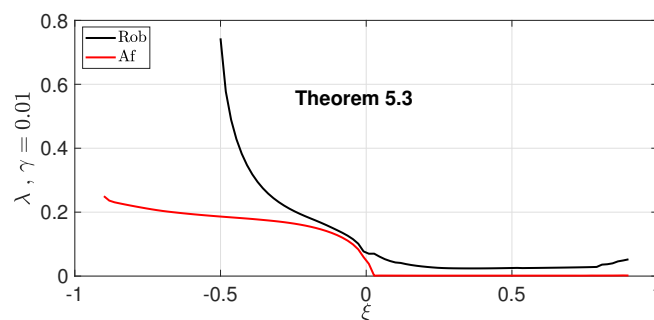


Figure 33: Behavior of the upper bound λ for Theorem 19 when ξ varies and $\gamma = 0.01$. Rob denotes the results using the Robust structure, and Af represents the results using Affine structure.

Looking at the curves shown in Fig. 33 a few statements can be made. Regarding the robust form of the FDF, we see that the first feasible solution for Theorem 18 is provided at $\xi = 0.5$. As expected, the upper bound values are higher considering the

robust structure for the FDF when compared to the affine structure.

Similarly to what we observe in Figs.32 and 33, the higher values obtained for the upper bounds are the ones assuming the Robust form for the FDF in all the studied approaches.

The robust filter obtained using Theorem 17 to provide the upper bounds for the \mathcal{H}_∞ norm is given by

$$\begin{aligned}\mathcal{A}_{\eta_{\text{Rob}}} &= \begin{bmatrix} -1.07 & -87.06 \\ 0.01 & 1.08 \end{bmatrix}, & \mathcal{B}_{\eta_{\text{Rob}}} &= \begin{bmatrix} -1.057 & -82.75 \\ 0.0007 & 1.058 \end{bmatrix}, & \mathcal{M}_{\eta_{\text{Rob}}} &= \begin{bmatrix} -0.47 \\ -0.00 \end{bmatrix}, \\ \mathcal{C}_{\eta_{\text{Rob}}} &= [0.49 \ 38.31], & \mathcal{D}_{\eta_{\text{Rob}}} &= [0.49 \ 38.35].\end{aligned}$$

The affine structure obtained from Theorem 17 to provide upper bounds for the \mathcal{H}_∞ norm is given by

$$\begin{aligned}\mathcal{A}_{\eta_{\text{aff1}}} &= \begin{bmatrix} -0.89 & -70.49 \\ 0.01 & 0.87 \end{bmatrix}, & \mathcal{A}_{\eta_{\text{aff2}}} &= \begin{bmatrix} 0.12 & 4.89 \\ -0.00 & -0.06 \end{bmatrix}, \\ \mathcal{B}_{\eta_{\text{aff1}}} &= \begin{bmatrix} -0.93 & -70.16 \\ -0.00 & 0.89 \end{bmatrix}, & \mathcal{B}_{\eta_{\text{aff2}}} &= \begin{bmatrix} 0.09 & 71.08 \\ -0.00 & -0.91 \end{bmatrix}, \\ \mathcal{M}_{\eta_{\text{aff1}}} &= \begin{bmatrix} -0.75 \\ 0.00 \end{bmatrix}, & \mathcal{M}_{\eta_{\text{aff2}}} &= \begin{bmatrix} -0.71 \\ 0.00 \end{bmatrix}, \\ \mathcal{C}_{\eta_{\text{aff1}}} &= [0.49 \ 38.96], & \mathcal{C}_{\eta_{\text{aff2}}} &= [0.00 \ 0.04], \\ \mathcal{D}_{\eta_{\text{aff1}}} &= [0.49 \ 38.96], & \mathcal{D}_{\eta_{\text{aff2}}} &= [-0.49 \ -38.91].\end{aligned}$$

Regarding the results obtained for the \mathcal{H}_2 norm using Theorem 18, the robust filter is given by

$$\begin{aligned}\mathcal{A}_{\eta_{\text{Rob}}} &= \begin{bmatrix} -1.02 & -10.09 \\ 0.01 & 0.12 \end{bmatrix}, & \mathcal{B}_{\eta_{\text{Rob}}} &= \begin{bmatrix} -1.00 & -10.07 \\ 0.00 & 0.15 \end{bmatrix}, & \mathcal{M}_{\eta_{\text{Rob}}} &= \begin{bmatrix} -0.70 \\ -0.00 \end{bmatrix}, \\ \mathcal{C}_{\eta_{\text{Rob}}} &= [0.49 \ 4.91], & \mathcal{D}_{\eta_{\text{Rob}}} &= [0.49 \ 4.90].\end{aligned}$$

The affine filter obtained with Theorem 18 is given by

$$\begin{aligned}\mathcal{A}_{\eta_{\text{aff1}}} &= \begin{bmatrix} -1.02 & -3.75 \\ 0.01 & 0.05 \end{bmatrix}, & \mathcal{A}_{\eta_{\text{aff2}}} &= \begin{bmatrix} -0.00 & -0.03 \\ 0.00 & -0.01 \end{bmatrix}, \\ \mathcal{B}_{\eta_{\text{aff1}}} &= \begin{bmatrix} -0.99 & -3.99 \\ -0.00 & 0.08 \end{bmatrix}, & \mathcal{B}_{\eta_{\text{aff2}}} &= \begin{bmatrix} 0.00 & 3.97 \\ -0.00 & -0.10 \end{bmatrix}, \\ \mathcal{M}_{\eta_{\text{aff1}}} &= \begin{bmatrix} -0.71 \\ -0.00 \end{bmatrix}, & \mathcal{M}_{\eta_{\text{aff2}}} &= \begin{bmatrix} -0.70 \\ -0.00 \end{bmatrix}, \\ \mathcal{C}_{\eta_{\text{aff1}}} &= [0.49 \ 1.82], & \mathcal{C}_{\eta_{\text{aff2}}} &= [0.00 \ 0.04], \\ \mathcal{D}_{\eta_{\text{aff1}}} &= [0.50 \ 1.95], & \mathcal{D}_{\eta_{\text{aff2}}} &= [-0.49 \ -1.90].\end{aligned}$$

Regarding the mixed $\mathcal{H}_2 / \mathcal{H}_\infty$ results, the robust filter obtained using Theorem 19 is

given by

$$\begin{aligned} \mathcal{A}_{\eta_{\text{rob}}} &= \begin{bmatrix} -1.02 & -12.16 \\ 0.01 & 0.11 \end{bmatrix}, & \mathcal{B}_{\eta_{\text{rob}}} &= \begin{bmatrix} -1.00 & -12.14 \\ 0.00 & 0.14 \end{bmatrix}, & \mathcal{M}_{\eta_{\text{rob}}} &= \begin{bmatrix} -0.71 \\ 0.00 \end{bmatrix}, \\ \mathcal{C}_{\eta_{\text{rob}}} &= \begin{bmatrix} 0.49 & 36.28 \end{bmatrix}, & \mathcal{D}_{\eta_{\text{rob}}} &= \begin{bmatrix} 0.49 & 36.24 \end{bmatrix}. \end{aligned}$$

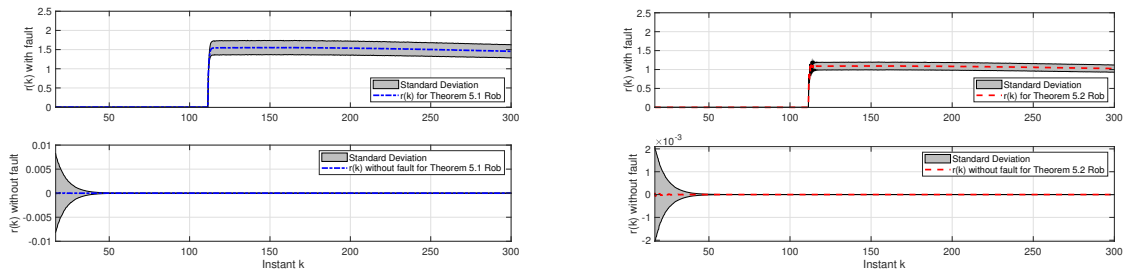
The matrices for the affine structured using Theorem 19 are given by

$$\begin{aligned} \mathcal{A}_{\eta_{\text{aff}_1}} &= \begin{bmatrix} -1.02 & -4.23 \\ 0.01 & -0.00 \end{bmatrix}, & \mathcal{A}_{\eta_{\text{aff}_2}} &= \begin{bmatrix} -0.00 & 1.13 \\ 0.00 & -0.01 \end{bmatrix}, \\ \mathcal{B}_{\eta_{\text{aff}_1}} &= \begin{bmatrix} -1.00 & -3.81 \\ 0.00 & 0.01 \end{bmatrix}, & \mathcal{B}_{\eta_{\text{aff}_2}} &= \begin{bmatrix} -0.00 & 5.04 \\ 0.00 & -0.02 \end{bmatrix}, \\ \mathcal{M}_{\eta_{\text{aff}_1}} &= \begin{bmatrix} -0.71 \\ 0.00 \end{bmatrix}, & \mathcal{M}_{\eta_{\text{aff}_2}} &= \begin{bmatrix} -0.70 \\ -0.00 \end{bmatrix}, \\ \mathcal{C}_{\eta_{\text{aff}_1}} &= \begin{bmatrix} 0.49 & 32.34 \end{bmatrix}, & \mathcal{C}_{\eta_{\text{aff}_2}} &= \begin{bmatrix} 0.00 & -16.76 \end{bmatrix}, \\ \mathcal{D}_{\eta_{\text{aff}_1}} &= \begin{bmatrix} 0.49 & 32.25 \end{bmatrix}, & \mathcal{D}_{\eta_{\text{aff}_2}} &= \begin{bmatrix} -0.50 & -49.21 \end{bmatrix}. \end{aligned}$$

5.2.2.1 Monte Carlo Simulation

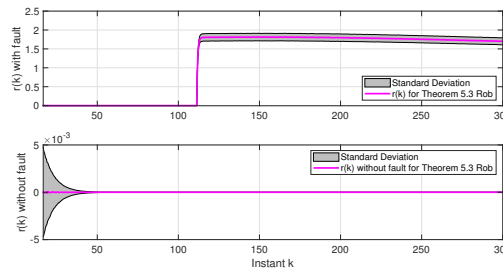
Using the similar setup as defined in the previous section, the major difference is that the network dropout is not accounted for in this simulation, since the designs proposed in this Section do not deal with this particular problem. For instance, matrix C is static. The Monte Carlo simulation with 300 iterations was performed and the results are divided into two classes the Robust, and Affine results. For each class, we provide the following results, the mean and standard deviation of the residue signal obtained using Theorems 17, 18, and 19, and after that the evaluation function for the respective residues.

In Figs. 34a, 34b, 34c , we present some temporal simulations using all the FDF designed using Theorem 17, 18, 19 in the Robust forms. Firstly, we present the residue signal obtained. Observing Figs. 34a, 34b, and 34c, allow us to conclude that all three cases presented a low standard deviation and similar residue signal. The result obtained using Theorem 19 presented a small advantage when compared with the results obtained with Theorems 17 and 18, since it provided the higher values. This information can be verified after the evaluation process, which will be displayed next. In Figs. 35a, 35b and 35c we can see that the interval where the fault was detected was respectively $k = [121 \ 132]$ for Theorem 17, $k = [134 \ 146]$ for Theorem 18, and $k = [119 \ 126]$ for Theorem 19. We can see that the evaluation function for Theorem 19 has a stepper curve and a shorter detection range (7) showing that the FDF designed has a higher performance. As expected the evaluation function when there is no fault is almost null in all cases. Now in Fig. 36 the evaluation function for all the robust cases are presented. We assume that the threshold



(a) Mean and standard deviation for residue signal obtained using Theorem 17.

(b) Mean and standard deviation for residue signal obtained using Theorem 18

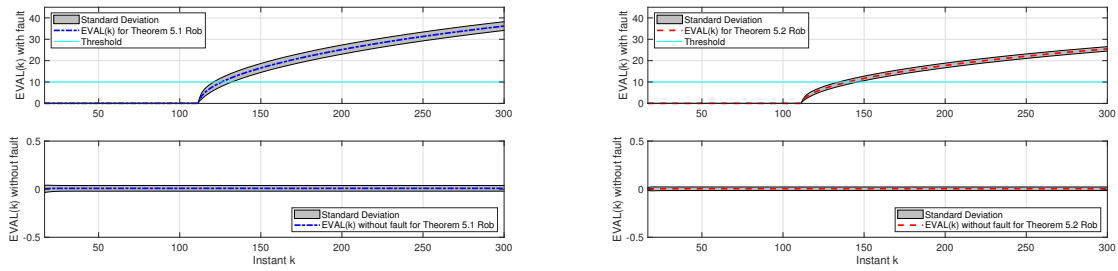


(c) Mean and standard deviation for residue signal obtained using Theorem 19

Figure 34: Mean and standard deviation for the residue signal (with and without fault) obtained using the FDI in the robust form designed via Theorem 17 (blue curve), 18 (red curve), and 19 (magenta curve).

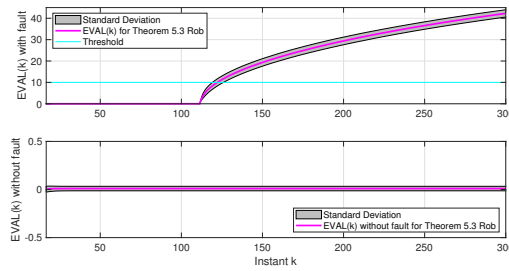
is equal to $TH = 10$. Analyzing Fig.36 we can confirm that the better performance is provided by Theorem 19. But observing all curves we can confirm that all the FDF in the robust form designed using Theorem 17, 18, and 19 are viable solutions for the FDI problem. Another important aspect is that the evaluation function when there is no fault is almost null during the entire simulation, which is different from FDF counterparts in Chapters 2, 3 that consider Markov Jumps.

In Figs. 37a, 37b, 37c , we present some temporal simulations using all the FDF designed using Theorem 17, 18, 19 in the Affine forms. We present now the residue signal gathered during the simulation. Note that in Fig.37a the higher value and the smaller standard deviation, which provide a fast and at the same time reliable detection process. On the other hand, results presented in Fig. 37b the level of reliability is lower since the standard deviation is higher, which may lead to false alarms. This particularity observed in the results in 37b, is expected due to the fact this design is based solely on \mathcal{H}_2 norm, which does not mitigate the exogenous disturbance. Figs. 38a, 38b, and 38c the detection interval are respectively, $k = [120 \ 126]$, $k = [137 \ 156]$, and $k = [122 \ 125]$. Once again, the FDF designed using Theorem 19 provided a better performance, regarding the steepness of the curve and the standard deviation. Besides these performance differences, all three



(a) Mean and standard deviation for evaluation function obtained using Theorem 17.

(b) Mean and standard deviation for evaluation function obtained using Theorem 18



(c) Mean and standard deviation for evaluation function obtained using Theorem 19

Figure 35: Mean and standard deviation for the evaluation function (with and without fault) obtained using the FDI in the robust form designed via Theorem 17 (blue curve), 18 (red curve), and 19(magenta curve).

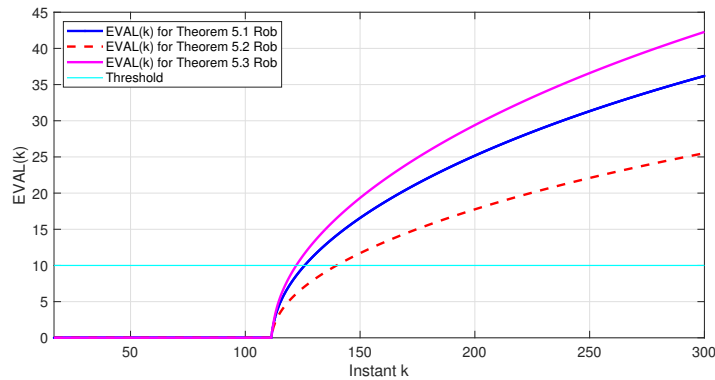
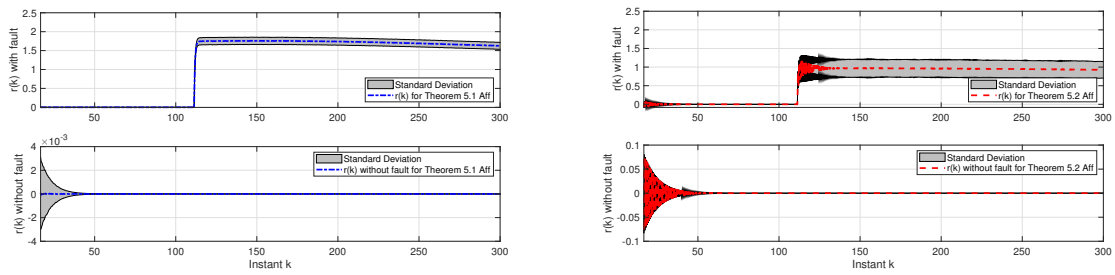


Figure 36: The mean value of the evaluation function signal for three distinct cases, where the blue curve represent the results using Theorem 17, the red curve represent the results obtained via 18, the magenta curve represents the results through Theorem 19, and the cyan line denotes the threshold TH.

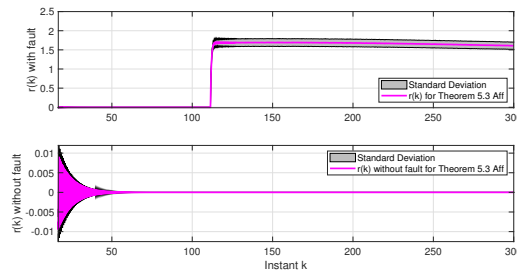
approaches behave as intended.

The evaluation function obtained using the Affine form are presented in Fig.39 As expected the results obtained using Theorem 17 presented the better performance, but closely followed by the results using Theorem 19. All the solutions are seen as viable solutions for the FDI problem, however, the results for Theorem 18 are more prone to



(a) Mean and standard deviation for residue signal obtained using Theorem 17.

(b) Mean and standard deviation for residue signal obtained using Theorem 18



(c) Mean and standard deviation for residue signal obtained using Theorem 19

Figure 37: Mean and standard deviation for the residue signal (with and without fault) obtained using the FDI in the affine form designed via Theorem 17 (blue curve), 18 (red curve), and 19(magenta curve).

false alarms.

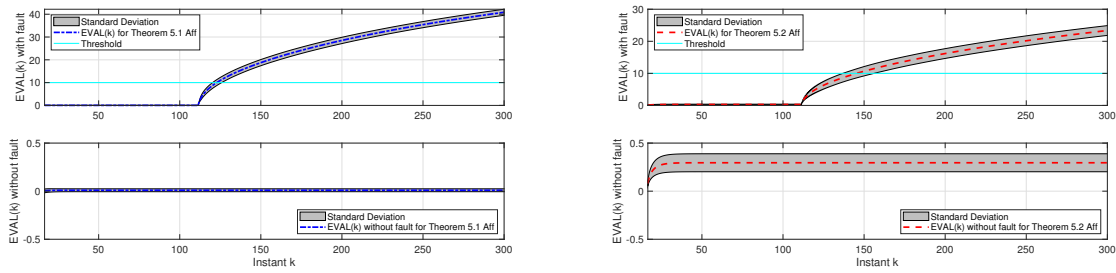
5.3 Gain Scheduled Fault Accommodation Formulation

Consider the following discrete-time linear system, that depends on time-varying parameters

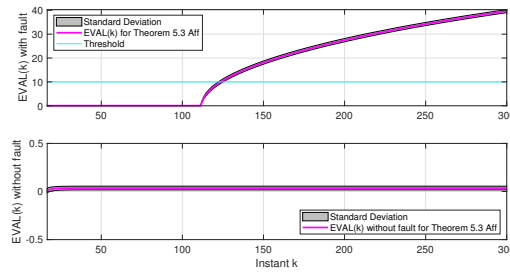
$$\mathcal{G} : \begin{cases} x(k+1) = A_{\theta(k)}x(k) + B_{\theta(k)}u(k) + B_{\theta(k)}h(k) + J_{\theta(k)}w(k) + F_{\theta(k)}f(k), \\ y(k) = C_{\theta(k)}x(k) + D_{\theta(k)}w(k) + D_{f\theta(k)}f(k), \end{cases} \quad (5.34)$$

where $x(k) \in \mathbb{R}^{n_x}$, $u(k) \in \mathbb{R}^{n_u}$, $w(k) \in \mathbb{R}^{n_w}$, and $y(k) \in \mathbb{R}^{n_y}$, are the system states, control input, exogenous input, and the measurement signal, respectively. The fault signal is represented by $f(k) \in \mathbb{R}^{n_f}$. The fault accommodation control signal is denoted by $h(k) \in \mathbb{R}^{n_u}$. It is assumed that the signals $w(k)$, $f(k) \in \mathcal{L}_2$. As defined for the FDF in the previous section, the index $\theta(k)$ represents the same bounded time-varying parameter.

Another particularity presented in the previous section that also remains true here, is that the matrices that compose the system (5.34), are all in the affine form, as described



(a) Mean and standard deviation for evaluation function obtained using Theorem 17. (b) Mean and standard deviation for evaluation function obtained using Theorem 18.



(c) Mean and standard deviation for evaluation function obtained using Theorem 19.

Figure 38: Mean and standard deviation for the evaluation function (with and without fault) obtained using the FDI in the affine form designed via Theorem 17 (blue curve), 18 (red curve), and 19(magenta curve).

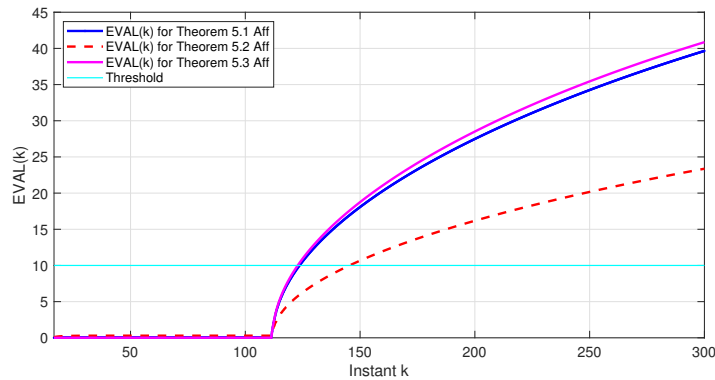


Figure 39: The mean value of the evaluation function signal for three distinct cases, where the blue curve represent the results using Theorem 17, the red curve represent the results obtained via 18, the magenta curve represents the results through Theorem 19, and the indigo line denotes the threshold TH.

in (5.4).

The change of variable presented in Section 5.2.0.2 is also implemented here, since the premise of the time-varying parameter $\theta(k)$ is not precisely known, and the assumption of $\theta(k)$ is contaminated by an additive disturbance $\sigma(k)$, where σ is also a bounded parameter.

Assuming the nominal situation (without fault signal), system (5.34) is controlled by

a state-feedback controller, as in (CAIGNY et al., 2010). Therefore, the nominal control law is described as

$$u(k) = \underbrace{\left(K_0 + \sum_{i=1}^m \hat{\theta}(k)_i K_i \right)}_{=: K_{\hat{\theta}(k)}} x(k). \quad (5.35)$$

Since the problem we tackle in this chapter regards the occurrence of faults, the access of the system states $x(k)$ is unrealistic. Therefore, we assume that the states are estimated using some type of adequate procedure. However, for the sake of simplicity, we are omitting the notation to avoid overcrowding the equations.

The present chapter aims to provide a fault accommodation controller with the main purpose of producing an auxiliary control signal whenever a fault occurs, or no input otherwise. The fault compensation controller can be described by

$$\mathcal{K}_c : \begin{cases} \eta(k+1) = \mathfrak{A}_{\hat{\theta}(k)} \eta(k) + \mathfrak{M}_{\hat{\theta}(k)} u(k) + \mathfrak{B}_{\hat{\theta}(k)} y(k), \\ h(k) = \mathfrak{C}_{\hat{\theta}(k)} \eta(k), \\ \eta(0) = \eta_0, \quad \hat{\theta}(0) = \hat{\theta}_0, \end{cases} \quad (5.36)$$

where $\eta(k) \in \mathbb{R}^{n_\eta}$ represents the FAC signal, $u(k)$ and $y(k)$ are, respectively, the control signal from the regular controller and the measured signal from the system. Note that the nominal controller (5.35), and the Fault Accommodation controller (5.36) depend both only on the estimated LPV parameter $\hat{\theta}(k)$. Therefore, the matrices that compose the FAC (5.36) can be written using the affine form, as in (5.4), where the matrices affinely depend on $\hat{\theta}(k)$. Thus, the system (5.34) depends on the parameter $\theta(k)$, while the state-feedback controller (5.35) and FAC controller (5.36) depend on the parameter $\hat{\theta}(k)$.

The augmented system with the state feedback control law (5.35) and with the FAC (5.36) is given by

$$\mathcal{G}_{\text{aug}} : \begin{cases} \bar{x}(k+1) = \bar{A}_{\theta(k)\hat{\theta}(k)} \bar{x}(k) + \bar{B}_{\theta(k)\hat{\theta}(k)} \bar{w}(k), \\ o(k) = \bar{C}_{\theta(k)\hat{\theta}(k)} \bar{x}(k) + \bar{D}_{\theta(k)\hat{\theta}(k)} \bar{w}(k), \\ \bar{x}_0 = \eta_0, \end{cases} \quad (5.37)$$

where $\bar{x}(k) = [x'(k) \ \eta'(k)]'$ and $\bar{w}(k) = [w'(k) \ f'(k)]'$. To simplify the visualization of the resulting LMIs, we omit the time-dependency in the time-varying parameters by

considering hereafter $\theta = \theta(k)$, and $\hat{\theta} = \hat{\theta}(k)$. The augmented matrices are as follows:

$$\begin{aligned} \bar{A}_{\theta\hat{\theta}} &= \begin{bmatrix} A_\theta - B_\theta K_{\hat{\theta}} & B_\theta \mathfrak{C}_{\hat{\theta}} \\ \mathfrak{B}_{\hat{\theta}} C_\theta - \mathfrak{M}_{\hat{\theta}} K_{\hat{\theta}} & \mathfrak{A}_{\hat{\theta}} \end{bmatrix}, & \bar{B}_{\theta\hat{\theta}} &= \begin{bmatrix} J_\theta & F_\theta \\ \mathfrak{B}_{\hat{\theta}} D_\theta & \mathfrak{B}_{\hat{\theta}} D_{f\theta} \end{bmatrix}, \\ \bar{C}_\theta &= [0 \ -B_\theta \mathfrak{C}_{\hat{\theta}}], & \bar{D}_\theta &= [0 \ F_\theta]. \end{aligned} \quad (5.38)$$

The main goal of this chapter is to design a FAC as presented in (5.36) where the difference $o(k) = F_{\theta(k)} f(k) - B_{\hat{\theta}(k)} h(k)$ is close to zero, meaning that the fault accommodation control signal will suppress the fault signal. Therefore, the optimization problem for the \mathcal{H}_∞ norm is described as

$$\|\mathcal{G}_{\text{aug}}\|_\infty = \sup_{\|\bar{w}\|_2 \neq 0, \bar{w} \in \mathcal{L}_2} \frac{\|o\|_2}{\|\bar{w}\|_2} < \gamma, \quad (5.39)$$

where $\gamma > 0$, as similarly described in (CAIGNY et al., 2010). For the \mathcal{H}_2 norm case, the optimization problem is given by

$$\|\mathcal{G}_{\text{aug}}\|_2 = \limsup_{T \rightarrow \infty} \mathcal{E} \left\{ \frac{1}{T} \sum_{k=0}^T o(k)' o(k) \right\} < \lambda, \quad (5.40)$$

where $\lambda > 0$, T is a positive integer that represents the time horizon, $\bar{w}(k)$ in (5.37) is a standard white noise (Gaussian zero-mean in which the covariance matrix is equal to the identity matrix), and \mathcal{E} represents the expected value operator, see (CAIGNY et al., 2010) for more details.

5.3.1 Theoretical Results

In this section, we present our main results on obtaining a gain-scheduled fault accommodation controllers for LPV systems, having as performance indexes the \mathcal{H}_∞ and \mathcal{H}_2 norms.

It is essential to explain that the results will be presented in terms of the original parameters $\theta(k)$ and $\hat{\theta}(k)$ to feature that the FAC designed depends solely on the measured parameter $\hat{\theta}(k)$. Afterwards, in order to solve the theorems presented in this section, it is imperative the use of the change of variables in sub-section 5.2.0.2 and rewriting all matrices in terms of the multi-simplex parameter $\tilde{\alpha} \in \Lambda_{m,2}$. As previously stated, to easy the notation, we set $\theta = \theta(k)$, $\hat{\theta} = \hat{\theta}(k)$, and $\beta = \theta(k+1)$.

5.3.1.1 \mathcal{H}_∞ Fault Accommodation Control Design

Firstly, we present a theorem for obtaining a gain-scheduled FAC using the \mathcal{H}_∞ norm.

Theorem 20. *If there exist symmetric positive definite matrices $W_{11\theta}$, $W_{22\theta}$ matrices $W_{12\theta}$, $Y_{1\hat{\theta}}$, $Y_{2\hat{\theta}}$, $\check{Y}_{\hat{\theta}}$, $\Omega_{\hat{\theta}}$, $\nabla_{\hat{\theta}}$, $\Gamma_{\hat{\theta}}$, $\mathfrak{C}_{\eta\hat{\theta}}$ with compatible dimensions, and a given scalar parameter $\xi \in [-1 \ 1]$ such that the following inequality*

$$\begin{bmatrix} \Pi^{1,1} & \Pi^{1,2} & \Pi^{1,3} & \Pi^{1,4} & \xi(Y_{1\hat{\theta}}J_\theta + \Omega_{\hat{\theta}}D_\theta) & \xi(\check{Y}_{\hat{\theta}}F_\theta + \Omega_{\hat{\theta}}D_{f\theta}) & 0 \\ \bullet & \Pi^{2,2} & \Pi^{2,3} & \Pi^{2,4} & \xi(Y_{2\hat{\theta}}J_\theta + \Omega_{\hat{\theta}}D_\theta) & \xi(\check{Y}_{\hat{\theta}}F_\theta + \Omega_{\hat{\theta}}D_{f\theta}) & B_\theta \mathfrak{C}_{\eta\hat{\theta}} \\ \bullet & \bullet & \Pi^{3,3} & \Pi^{3,4} & Y_{1\hat{\theta}}J_\theta + \Omega_{\hat{\theta}}D_\theta & \check{Y}_{\hat{\theta}}F_\theta + \Omega_{\hat{\theta}}D_{f\theta} & 0 \\ \bullet & \bullet & \bullet & \Pi^{4,4} & Y_{2\hat{\theta}}J_\theta + \Omega_{\hat{\theta}}D_\theta & \check{Y}_{\hat{\theta}}F_\theta + \Omega_{\hat{\theta}}D_{f\theta} & 0 \\ \bullet & \bullet & \bullet & \bullet & -\gamma^2 I & 0 & 0 \\ \bullet & \bullet & \bullet & \bullet & \bullet & -\gamma^2 I & 0 \\ \bullet & \bullet & \bullet & \bullet & \bullet & \bullet & -I \end{bmatrix} < 0, \quad (5.41)$$

with

$$\begin{aligned} \Pi^{1,1} &= -W_{11\theta} + \xi \text{Her}(Y_{1\hat{\theta}}A_\theta - Y_{1\hat{\theta}}B_\theta K_{\hat{\theta}} + \Omega_{\hat{\theta}}C_\theta - \Gamma_{\hat{\theta}}K_{\hat{\theta}}), \\ \Pi^{1,2} &= -W_{12\theta} + \xi(Y_{1\hat{\theta}}B_\theta \mathfrak{C}_{\eta\hat{\theta}} + \nabla_{\hat{\theta}} + (A'_\theta - K'_{\hat{\theta}}B'_\theta)\check{Y}'_{\hat{\theta}} + C'_\theta \Omega'_{\hat{\theta}} - K'_{\hat{\theta}}\Gamma'_{\hat{\theta}}), \\ \Pi^{1,3} &= (A'_\theta - K'_{\hat{\theta}}B'_\theta)Y'_{1\hat{\theta}} + C'_\theta \Omega'_{\hat{\theta}} - K'_{\hat{\theta}}\Gamma'_{\hat{\theta}} - \xi Y_{1\hat{\theta}}, \\ \Pi^{1,4} &= (A'_\theta - K'_{\hat{\theta}}B'_\theta)Y'_{2\hat{\theta}} + C'_\theta \Omega'_{\hat{\theta}} - K'_{\hat{\theta}}\Gamma'_{\hat{\theta}} - \xi \check{Y}_{\hat{\theta}}, \\ \Pi^{2,2} &= -W_{22\hat{\theta}} + \xi \text{Her}(Y_{1\hat{\theta}}B_\theta \mathfrak{C}_{\eta\hat{\theta}} + \nabla_{\hat{\theta}}), \\ \Pi^{2,3} &= \mathfrak{C}'_{\eta\hat{\theta}}B'_\theta Y'_{1\hat{\theta}} + \nabla'_{\hat{\theta}} - \xi Y_{2\hat{\theta}}, \quad \Pi^{2,4} = \mathfrak{C}'_{\eta\hat{\theta}}B'_\theta Y'_{1\hat{\theta}} + \Gamma'_{\hat{\theta}} - \xi \check{Y}_{\hat{\theta}}, \\ \Pi^{3,3} &= -W_{11\beta} - \text{Her}(Y_{1\hat{\theta}}), \quad \Pi^{3,4} = -W_{12\beta} - \check{Y}_{\hat{\theta}} - Y'_{2\hat{\theta}}, \quad \Pi^{4,4} = -W_{22\beta} - \text{Her}(\check{Y}_{\hat{\theta}}), \end{aligned}$$

holds for all $\theta, \hat{\theta}, \beta$, under the boundaries $|\sigma_i(k)| \leq d_i$, $|\theta_i(k)| \leq t_i$, then a suitable linear parameter-varying FAC, as in (5.36), is given by $\mathfrak{A}_{\eta\hat{\theta}} = \check{Y}_{\hat{\theta}}^{-1}\nabla_{\hat{\theta}}$, $\mathfrak{B}_{\eta\hat{\theta}} = \check{Y}_{\hat{\theta}}^{-1}\Omega_{\hat{\theta}}$, $\mathfrak{M}_{\eta\hat{\theta}} = \check{Y}_{\hat{\theta}}^{-1}\Gamma_{\hat{\theta}}$, and $\mathfrak{C}_{\eta\hat{\theta}}$, and (5.39) is satisfied.

Proof: Consider the augmented matrices in (5.37), and the following structure for \mathbb{W}_θ , \mathbb{W}_β , $\mathbb{Y}_{\hat{\theta}}$

$$\mathbb{W}_\theta = \begin{bmatrix} W_{11\theta} & W_{12\theta} \\ W'_{12\theta} & W_{22\theta} \end{bmatrix}, \quad \mathbb{W}_\beta = \begin{bmatrix} W_{11\beta} & W_{12\beta} \\ W'_{12\beta} & W_{22\beta} \end{bmatrix}, \quad \mathbb{Y}_{\hat{\theta}} = \begin{bmatrix} Y_{1\hat{\theta}} & \check{Y}_{\hat{\theta}} \\ Y_{2\hat{\theta}} & \check{Y}_{\hat{\theta}} \end{bmatrix}. \quad (5.42)$$

From the above, the constraints (5.41) can be rewritten as

$$Q + U'_{\theta\hat{\theta}}\mathbb{Y}'_{\hat{\theta}}V + V'\mathbb{Y}_{\hat{\theta}}U_{\theta\hat{\theta}} < 0, \quad (5.43)$$

where

$$Q = \begin{bmatrix} -\mathbb{W}_\theta & 0 & 0 & \bar{C}'_{\theta\hat{\theta}} \\ 0 & -\mathbb{W}_\beta & 0 & 0 \\ 0 & 0 & -\gamma^2 I & \bar{D}'_{\theta\hat{\theta}} \\ \bar{C}_{\theta\hat{\theta}} & 0 & \bar{D}_{\theta\hat{\theta}} & -I \end{bmatrix}, \quad U_{\theta\hat{\theta}} = [\bar{A}_{\theta\hat{\theta}} \ -I \ \bar{B}_{\theta\hat{\theta}} \ 0], \quad V' = [\xi I \ I \ 0 \ 0]. \quad (5.44)$$

Pre- and post-multiplying (5.43) by

$$\mathcal{B}_{\theta\hat{\theta}} = \begin{bmatrix} I & \bar{A}'_{\theta\hat{\theta}} & 0 & 0 \\ 0 & \bar{B}'_{\theta\hat{\theta}} & I & 0 \\ 0 & 0 & 0 & I \end{bmatrix}, \quad (5.45)$$

and then applying the Schur complement we have that (5.41) implies the constraint in (SOUZA; BARBOSA; NETO, 2006, Lemma 3), which yields (5.39), completing the proof. ■

5.3.1.2 \mathcal{H}_2 Fault Accommodation Control Design

We present as follows a theorem that proposes a FAC having the \mathcal{H}_2 norm as a performance index.

Theorem 21. *If there exist symmetric positive definite matrices $\mathcal{W}_{11\theta}$, $\mathcal{W}_{22\theta}$, M_θ and matrices $\mathcal{W}_{12\theta}$, \check{X}_θ , $X_{1\hat{\theta}}$, $X_{2\hat{\theta}}$, $\Omega_{\hat{\theta}}$, $\nabla_{\hat{\theta}}$, $\Gamma_{\hat{\theta}}$, $\mathfrak{C}_{\eta\hat{\theta}}$ with compatible dimensions, and a given scalar parameter ξ such that the following inequality*

$$\begin{bmatrix} \Psi^{1,1} & \Psi^{1,2} & \Psi^{1,3} & \Psi^{1,4} & \xi(X_{1\hat{\theta}}J_\theta + \Omega_{\hat{\theta}}D_\theta) & \xi(\check{X}_\theta F_\theta + \Omega_{\hat{\theta}}D_{f\theta}) \\ \bullet & \Psi^{2,2} & \Psi^{2,3} & \Psi^{2,4} & \xi(X_{2\hat{\theta}}J_\theta + \Omega_{\hat{\theta}}D_\theta) & \xi(\check{X}_\theta F_\theta + \Omega_{\hat{\theta}}D_{f\theta}) \\ \bullet & \bullet & \Psi^{3,3} & \Psi^{3,4} & X_{1\hat{\theta}}J_\theta + \Omega_{\hat{\theta}}D_\theta & \check{X}_\theta F_\theta + \Omega_{\hat{\theta}}D_{f\theta} \\ \bullet & \bullet & \bullet & \mathcal{W}_{22\theta} - \text{Her}(\check{X}_\theta) & X_{2\hat{\theta}}J_\theta + \Omega_{\hat{\theta}}D_\theta & \check{X}_\theta F_\theta + \Omega_{\hat{\theta}}D_{f\theta} \\ \bullet & \bullet & \bullet & \bullet & -I & 0 \\ \bullet & \bullet & \bullet & \bullet & \bullet & -I \end{bmatrix} < 0, \quad (5.46)$$

with

$$\begin{aligned} \Psi^{1,1} &= -\mathcal{W}_{11\theta} + \xi \text{Her}(X_{1\hat{\theta}}A_\theta - X_{1\hat{\theta}}B_\theta K_{\hat{\theta}} + \Omega_{\hat{\theta}}C_\theta - \Gamma_{\hat{\theta}}K_{\hat{\theta}}), \\ \Psi^{1,2} &= -\mathcal{W}_{12\theta} + \xi(X_{1\hat{\theta}}B_\theta \mathfrak{C}_{\eta\hat{\theta}} + \nabla_{\hat{\theta}} + (A'_\theta - K'_{\hat{\theta}}B'_\theta)\check{X}'_\theta + C'_\theta \Omega'_{\hat{\theta}} - K'_{\hat{\theta}}\Gamma'_{\hat{\theta}}), \\ \Psi^{1,3} &= (A'_\theta - K'_{\hat{\theta}}B'_\theta)X'_{1\hat{\theta}} + C'_\theta \Omega'_{\hat{\theta}} - K'_{\hat{\theta}}\Gamma'_{\hat{\theta}} - \xi X_{1\hat{\theta}}, \\ \Psi^{1,4} &= (A'_\theta - K'_{\hat{\theta}}B'_\theta)X'_{2\hat{\theta}} + C'_\theta \Omega'_{\hat{\theta}} - K'_{\hat{\theta}}\Gamma'_{\hat{\theta}} - \xi \check{X}_\theta, \\ \Psi^{2,2} &= -\mathcal{W}_{22\theta} + \xi \text{Her}(X_{1\hat{\theta}}B_\theta \mathfrak{C}_{\eta\hat{\theta}} + \nabla_{\hat{\theta}}), \quad \Psi^{2,3} = \mathfrak{C}'_{\eta\hat{\theta}}B'_\theta X'_{1\hat{\theta}} + \nabla'_{\hat{\theta}} - \xi X_{2\hat{\theta}}, \\ \Psi^{2,4} &= \mathfrak{C}'_{\eta\hat{\theta}}B'_\theta X'_{1\hat{\theta}} + \Gamma'_{\hat{\theta}} - \xi \check{X}_\theta, \quad \Psi^{3,3} = -\mathcal{W}_{11\beta} - \text{Her}(X_{1\hat{\theta}}), \\ \Psi^{3,4} &= -\mathcal{W}_{12\beta} - \check{X}_\theta - X'_{2\hat{\theta}}, \end{aligned}$$

$$\begin{bmatrix} M_\theta & 0 & B_{\theta\hat{\theta}}\mathfrak{C}_{\eta\hat{\theta}} & 0 & F_\theta \\ \bullet & \mathcal{W}_{11\theta} & \mathcal{W}_{12\theta} & 0 & 0 \\ \bullet & \bullet & \mathcal{W}_{22\theta} & 0 & 0 \\ \bullet & \bullet & \bullet & I & 0 \\ \bullet & \bullet & \bullet & \bullet & I \end{bmatrix} > 0, \quad (5.47)$$

$$\text{Tr}(M_\theta) > \lambda^2, \quad (5.48)$$

holds for all θ , β , $\hat{\theta}$ under the boundaries $|\sigma_i(k)| \leq d_i$, $|\theta_i(k)| \leq t_i$, then a suitable

linear parameter-varying FAC as in (5.36), is given by $\mathfrak{A}_{\eta\hat{\theta}} = \check{X}_{\hat{\theta}}^{-1}\nabla_{\hat{\theta}}$, $\mathfrak{B}_{\eta\hat{\theta}} = \check{X}_{\hat{\theta}}^{-1}\Omega_{\hat{\theta}}$, $\mathfrak{M}_{\eta\hat{\theta}} = \check{X}_{\hat{\theta}}^{-1}\Gamma_{\hat{\theta}}$, and $\mathfrak{C}_{\eta\hat{\theta}}$ which satisfies (5.40).

Proof: Consider the augmented matrices in (5.37), and the following structure for \mathfrak{W}_{θ} , \mathfrak{W}_{β} , $\mathfrak{X}_{\hat{\theta}}$

$$\begin{aligned} \mathfrak{W}_{\theta} &= \begin{bmatrix} W_{11\theta} & W_{12\theta} \\ W'_{12\theta} & W_{22\theta} \end{bmatrix}, & \mathfrak{W}_{\beta} &= \begin{bmatrix} W_{11\beta} & W_{12\beta} \\ W'_{12\beta} & W_{22\beta} \end{bmatrix}, \\ \mathfrak{X}_{\hat{\theta}} &= \begin{bmatrix} X_{1\hat{\theta}} & \check{X}_{\hat{\theta}} \\ X_{2\hat{\theta}} & \check{X}_{\hat{\theta}} \end{bmatrix}. \end{aligned} \quad (5.49)$$

The inequality (5.46) can be rewritten as

$$Q + U'_{\theta\hat{\theta}}\mathfrak{X}'_{\hat{\theta}}V + V'\mathfrak{X}_{\hat{\theta}}U_{\theta\hat{\theta}} < 0, \quad (5.50)$$

where

$$Q = \begin{bmatrix} -\mathfrak{W}_{\theta} & 0 & 0 \\ 0 & -\mathfrak{W}_{\beta} & 0 \\ 0 & 0 & -I \end{bmatrix}, \quad U'_{\theta\hat{\theta}} = \begin{bmatrix} \bar{A}'_{\theta\hat{\theta}} \\ -I \\ \bar{B}'_{\theta\hat{\theta}} \end{bmatrix}, \quad V = \begin{bmatrix} \xi I \\ I \\ 0 \end{bmatrix}. \quad (5.51)$$

Assume the null bases for U and V as

$$\mathcal{N}'_U = \begin{bmatrix} I & \bar{A}'_{\theta\hat{\theta}} & 0 \\ 0 & \bar{B}'_{\theta\hat{\theta}} & 0 \end{bmatrix}, \quad \mathcal{N}'_V = \begin{bmatrix} -I & \xi I & 0 \\ 0 & 0 & I \end{bmatrix}. \quad (5.52)$$

By pre- and post-multiplying (5.50) by \mathcal{N}'_U , and, using the Schur complement twice we obtain the same constraints as presented in (CAIGNY et al., 2010, Theorem 2). The results within (CAIGNY et al., 2010) show that (CAIGNY et al., 2010, Theorem 2) is equivalent to (5.40). Concerning the constraint (5.48), we use the same variable substitution as described at the start of the proof and applying the Schur complement twice we get that the constraint (5.48) is equivalent to the second constraint in (CAIGNY et al., 2010, Theorem 2). This concludes the proof. ■

Coordinate Descent Algorithm

Note that the constraints in Theorem 20 and 21 are BMIs, due to the term $\mathfrak{C}_{\eta\hat{\theta}}$ multiplying other variables in the problems. To solve an optimization problem in the context of BMI forms, we can use, for instance, the Coordinate Descent Algorithm (CDA), as it was applied in (CARVALHO; OLIVEIRA; COSTA, 2020). The algorithm implemented

to solve the constraints in this chapter is given as follows.

Algorithm 4: Coordinate Descent Algorithm.

1 Input: $K_{\hat{\theta}}^0$, γ^0 or λ^0 , t_{\max} , ϕ .

2 Output: $\mathfrak{A}_{\eta\hat{\theta}}$, $\mathfrak{B}_{\eta\hat{\theta}}$, $\mathfrak{M}_{\eta\hat{\theta}}$, $\mathfrak{C}_{\eta\hat{\theta}}$.

3 Initialization:

4 While: $\frac{\gamma^{t-1}-\gamma^t}{\gamma^{t-1}} \leq \phi$ or $t \leq t_{\max}$ **do:**

5 Step 1: Solve the constraint in Theorem 20 or 21 considering $\mathfrak{C}_{\hat{\theta}}$ as a constant, to initialize the algorithm the first value of $\mathfrak{C}_{\eta\hat{\theta}}$ can be set as K which can be obtained using the results in (MONTAGNER et al., 2005). Obtain the values of $Y_{1\hat{\theta}}$, for the Theorem 20 or $X_{1\hat{\theta}}$ for the Theorem 21.

6 Step 2: Solve the constraint in Theorem 20 or 21 this time using the values of $Y_{1\hat{\theta}}$ or $X_{1\hat{\theta}}$ obtained in Step 1 and $\mathfrak{C}_{\eta\hat{\theta}}$ as a variable. Obtain the value of γ^{t+1} for Theorem 20 or λ^{t+1} Theorem 21.

Notice that the inputs $K_{\hat{\theta}}^0$ represent the starting value of $\mathfrak{C}_{\eta\hat{\theta}}$, γ^0 or λ^0 are the input to calculate the stop criteria at the first iteration, ϕ is the stop criteria, and t_{\max} is the maximum number of iterations.

5.3.2 Simulations Results

To illustrate the viability of the proposed approaches, we apply our method to a simple quarter vehicle model system, (NGUYEN; SENAME; DUGARD, 2015). The states vector for the linearized model is $x(k)$ is obtained from the discretization of $x(t) = [z_s \dot{z}_s z_{us} \dot{z}_{us}]$, which represents the displacement for the sprung mass, its variation, the displacement for the mass unsprung, and its variation. The matrices that compose the discrete-time system are

$$A_1 = \begin{bmatrix} 0.99 & 0.01 & 0.00 & 0.00 \\ -0.23 & 0.97 & 0.05 & 0.02 \\ 0.01 & 0.00 & 0.98 & 0.00 \\ 1.75 & 0.17 & -14.42 & 0.81 \end{bmatrix}, \quad A_2 = \begin{bmatrix} 0.99 & 0.00 & 0.00 & 0.00 \\ -0.19 & 0.98 & 0.04 & 0.01 \\ 0.00 & 0.00 & 0.98 & 0.00 \\ 1.75 & 0.17 & -14.42 & 0.81 \end{bmatrix},$$

$$B_1 = \begin{bmatrix} -0.00 \\ -0.017 \\ 0.0006 \\ 0.13 \end{bmatrix}, \quad B_2 = \begin{bmatrix} -0.00 \\ -0.018 \\ 0.00 \\ 0.14 \end{bmatrix}, \quad J = \begin{bmatrix} 0.00 \\ -0.02 \\ 0.00 \\ 0.014 \end{bmatrix}, \quad F = \begin{bmatrix} -0.00 \\ -0.018 \\ 0.00 \\ 0.14 \end{bmatrix},$$

$$C = \begin{bmatrix} 1 & 0 & 0 & 0 \\ 0 & 0 & 1 & 0 \end{bmatrix}, \quad D = \begin{bmatrix} -0.01 \\ 0.10 \end{bmatrix}, \quad D_f = \begin{bmatrix} 0 \\ 0 \end{bmatrix}, \quad \begin{matrix} |\theta(k)| \leq t_i = 0.05, \\ |\sigma(k)| \leq d_i = 0.005 \end{matrix}$$

from where we can see that the time-varying parameter $\theta(k)$ affects the dynamical behavior of the system in A and B , forming a polytope with 2 vertices. In this way, matrices A_1 , B_1 , and A_2 , B_2 represent the vertices of such polytope. The other matrices are not affected by the time-varying parameter, therefore, their degree of dependence on the parameter $\theta(k)$ is 0. Note that, matrix F has the same structure of the control input matrix B , for the purpose of representing an abnormal input. Since in this example we are not

considering the presence of any sensor fault, we have that, D_f is null. We assume that the nominal gain-scheduled state-feedback controllers are obtained using the method described in (MONTAGNER et al., 2005, Lemma 2), where the authors search for such controllers in the context of LPV systems without faults. The resulted controller for the system of this example is

$$K_{\text{aff1}} = [-0.1201 \quad -0.2372 \quad 6.3420 \quad 0.4433] \times 10^4,$$

$$K_{\text{aff2}} = [0.3094 \quad 0.0391 \quad -1.5798 \quad 0.0369] \times 10^4.$$

The range of the disturbance $\sigma(k)$ is defined a priori, and we arbitrarily set its range in $|\sigma(k)| \leq d_i = 0.005$. The value of $\hat{\theta}(k)$ is obtained in a practical situation by implementing a variate of the filter, such as Recursive Least Square (RLS) algorithm (PAULO, 2013; SAYED, 2011).

In the first part of this example, we apply separately Theorems 20 and 21 searching, respectively, for the upper bounds of the \mathcal{H}_∞ and \mathcal{H}_2 norms (γ and λ). For doing so, we perform a search in the scalar ξ in the range $]-0.9 \ 0.9[$ with 10 steps with the same length. A discussion about the ξ range is made in (ROSA; MORAIS; OLIVEIRA, 2018).

Additionally, we consider the affine and robust structures for the FDF, that is, one structure that depends on the estimated parameter with degree 1 and another with degree 0. The upper bounds γ and λ obtained with the aforementioned considerations are shown in Fig. 40. From this figure, note that the scalar search was more effective for the Robust

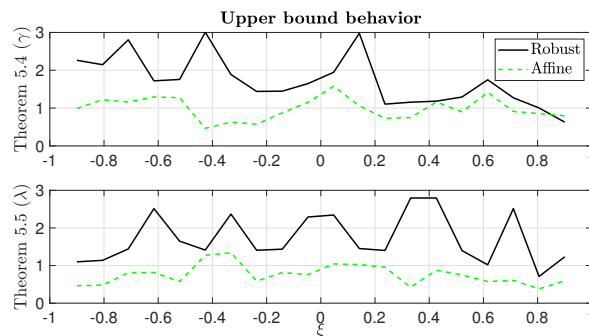


Figure 40: Upper bound behavior for Theorems 20 (\mathcal{H}_∞ norm) and 21 (\mathcal{H}_2 norm) when scalar ξ vary for the Robust, and Affine form.

form than the results obtained using the Affine form. This discrepancy was expected since the Robust form is a more restrict optimization problem, hence, performing the scalar search provides a higher impact on the results for the Robust form. Summing up, the results presented in Fig. 40, shows that the using Affine form in this example provides better results since the upper bound values obtained for both \mathcal{H}_∞ and \mathcal{H}_2 norms are in

general, lower than the values obtained for the Robust form. Therefore, for the temporal simulations, we analyze the results obtained using solely the affine form, which we highlight as follows.

5.3.2.1 Monte Carlo Simulation

Here we implement a Monte Carlos Simulation since the parameter $\hat{\theta}(k)$ has some imprecision, meaning it is not completely deterministic.

The FAC in the affine form obtained applying Theorem 20 with $\xi = -0.6$ is given by

$$\begin{aligned} \mathcal{A}_{\eta_{\text{aff}0}}^{\infty} &= \begin{bmatrix} 0.97 & 0.31 & 0.10 & 0.02 \\ -1.09 & -0.03 & 1.71 & -0.21 \\ 0.09 & 0.31 & 0.53 & 0.06 \\ 1.59 & 1.04 & -24.05 & 0.19 \end{bmatrix}, & \mathcal{B}_{\eta_{\text{aff}0}}^{\infty} &= \begin{bmatrix} 0.31 & 0.03 \\ -0.95 & -0.07 \\ 0.31 & 0.03 \\ 0.73 & 0.49 \end{bmatrix} \\ \mathcal{A}_{\eta_{\text{aff}1}}^{\infty} &= \begin{bmatrix} -0.13 & 3.84 & 7.10 & 0.14 \\ -24.64 & 29.02 & 153.36 & -2.17 \\ 3.21 & -5.35 & -19.71 & 0.13 \\ -92.32 & 453.01 & 596.26 & 26.82 \end{bmatrix}, & \mathcal{B}_{\eta_{\text{aff}1}}^{\infty} &= \begin{bmatrix} 3.65 & 0.36 \\ 31.79 & 3.17 \\ -6.04 & -0.60 \\ 463.43 & 46.33 \end{bmatrix}, \\ \mathcal{M}_{\eta_{\text{aff}0}}^{\infty} &= \begin{bmatrix} 0.00 \\ 0.02 \\ -0.00 \\ 0.11 \end{bmatrix}, & \mathcal{M}_{\eta_{\text{aff}1}}^{\infty} &= \begin{bmatrix} 0.00 \\ 0.02 \\ 0.00 \\ -0.21 \end{bmatrix}, \\ \mathcal{C}_{\eta_{\text{aff}0}}^{\infty} &= [-2.09 \ -0.08 \ 8.54 \ -0.65] 10^4, \\ \mathcal{C}_{\eta_{\text{aff}1}}^{\infty} &= [-0.87 \ -0.105 \ 5.9 \ -0.19] 10^4. \end{aligned}$$

The affine filter obtained with Theorem 21 with $\xi = -0.6$ is given by

$$\begin{aligned} \mathcal{A}_{\eta_{\text{aff}0}}^2 &= \begin{bmatrix} 0.99 & 0.00 & -0.00 & 0.00 \\ -0.47 & 2.11 & -0.77 & 0.15 \\ 0.02 & 0.27 & 0.81 & 0.03 \\ 3.04 & -24.91 & -30.92 & -2.16 \end{bmatrix}, & \mathcal{B}_{\eta_{\text{aff}0}}^2 &= \begin{bmatrix} -0.01 & 0.01 \\ 1.16 & 0.01 \\ 0.26 & -0.01 \\ -25.21 & -0.07 \end{bmatrix}, \\ \mathcal{A}_{\eta_{\text{aff}1}}^2 &= \begin{bmatrix} 1.04 & 0.41 & -0.13 & 0.05 \\ 9.78 & 107.58 & -32.81 & 13.87 \\ -0.27 & -3.46 & 1.79 & -0.45 \\ -79.73 & -846.70 & 225.81 & -109.05 \end{bmatrix}, \\ \mathcal{B}_{\eta_{\text{aff}1}}^2 &= \begin{bmatrix} 0.41 & -0.05 \\ 104.11 & -11.68 \\ -3.77 & 0.39 \\ -807.37 & 91.51 \end{bmatrix}, & \mathcal{M}_{\eta_{\text{aff}0}}^2 &= \begin{bmatrix} -0.00 \\ -0.03 \\ 0.01 \\ 0.19 \end{bmatrix}, \\ \mathcal{M}_{\eta_{\text{aff}1}}^2 &= \begin{bmatrix} 0.00 \\ -0.01 \\ -0.00 \\ 0.02 \end{bmatrix}, & \mathcal{C}_{\eta_{\text{aff}0}}^2 &= [-0.40 \ -0.04 \ 1.27 \ -1.02] 10^3, \\ \mathcal{C}_{\eta_{\text{aff}1}}^2 &= [-2.72 \ -2.44 \ 7.52 \ -2.95] 10^3. \end{aligned}$$

For this example, we consider that the fault signal $f(k)$ represents an oil leak, which reduces the damping capability of the system. Consider that the leak started at $t = 2.5s$, which reduces the damping capability by 20%, and then it gradually lowers until it reaches a reduction of 50%.

We show in Figs. 41 and 42, the respectively results regarding the output and control signals. From Fig.41, it can be seen that the control design based on the Affine form provides a smoother behavior for all three situations of faults. This particular behavior happens mainly due to the lower level of conservatism of the Affine form, and also due

to the parameter variation throughout all the simulation time. Additionally, both FAC approaches provide an accommodation behavior as intended. However, when we compare the FAC approaches with that of the nominal controller, the FAC approaches yield a more aggressive control signal, which is an expected behavior. In summary, the proposed fault accommodation control approaches provided a suitable solution to mitigate the fault signal, and at the same time do not interfere with the controller when there is no fault.

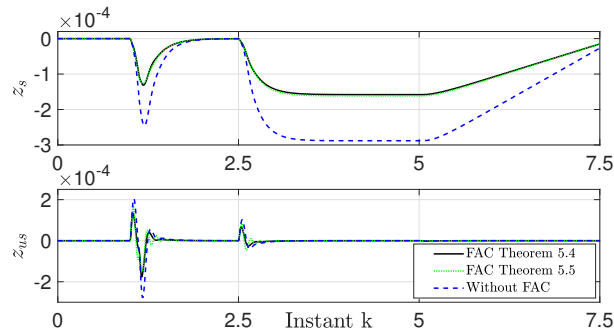


Figure 41: Mean of the states signal obtained using FAC designed in the affine via Theorems 20 (black curve) and 21 (green curve), where the system is subjected to a fault.

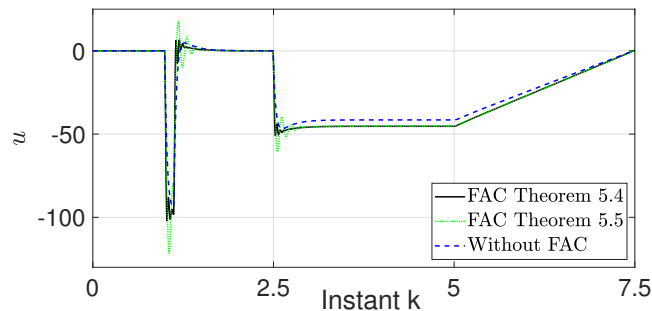


Figure 42: Mean of the control signal obtained using FAC designed in the affine via Theorems 20 (black curve) and 21 (green curve), where the system is subjected to a fault.

5.4 Concluding remarks

In this chapter, we presented the theoretical results obtained for the FDF and FAC using the LPV systems assuming that the parameter is not accessible. Hence, the assumption of the imprecision is incorporated during the FDF and FAC process. We also provided an illustrative example, and the results obtained allow us to state that the proposed methods are viable.

6 CONCLUSIONS

We summarize in a list the main contributions of this thesis and we point out possible topics that can be tackled in the near future based on the results herein.

6.1 Contribution

The main focus of this thesis was the development of procedures to design Fault Detection Filters to be implemented in an FDI scheme, and Fault Accommodation Controller to mitigate the effect of faults on ongoing processes.

- In Chapter 2 we addressed the FDF and FAC design under the assumption that the network that is responsible to transmit the information packet is semi-reliable. To model such behavior, we proposed that the FDF and FAC design was made under the Markovian Jump Linear Systems framework, which allow us to use Markov chains to model the network behavior and its particularities. The main contributions in Chapter 2 were the design of FDF using \mathcal{H}_∞ -norm, \mathcal{H}_2 -norm, \mathcal{H}_- index, Mixed $\mathcal{H}_2/\mathcal{H}_\infty$, and Mixed $\mathcal{H}_-/\mathcal{H}_\infty$ under the MJLS framework (CARVALHO; OLIVEIRA; COSTA, 2018b; CARVALHO; OLIVEIRA; COSTA, 2018a; CARVALHO; OLIVEIRA; COSTA, 2018; CARVALHO et al., May 2021). For the contributions regarding the FAC problem, we proposed the \mathcal{H}_∞ FAC design for MJLS (CARVALHO et al., 2020b).
- In Chapter 3, we kept tackling the FDF and FAC problem from the MJLS point of view but adding the assumption that the network mode is not instantly accessible. This new assumption is important because the idea of the instantaneous access to the network is not realistic from a practical standpoint. To deal with this issue we proposed the use of the MJLS approach which uses Hidden Markov modes to model this inaccessibility. The contributions in Chapter 3, were divided into three sections on FDF, SFDC, and FAC. The results referring to the FDF section were the

design using \mathcal{H}_∞ -norm, \mathcal{H}_2 -norm, and the Mixed $\mathcal{H}_2/\mathcal{H}_\infty$ (CARVALHO; OLIVEIRA; COSTA, 2018c; CARVALHO; OLIVEIRA; COSTA, 2020). The novelty regarding SFDC part is the SFDC design using \mathcal{H}_∞ -norm, \mathcal{H}_2 -norm, and Mixed $\mathcal{H}_2/\mathcal{H}_\infty$ (CARVALHO; OLIVEIRA; COSTA, 2020). The results for the FAC section were the FAC design using \mathcal{H}_∞ -norm, \mathcal{H}_2 -norm, and Mixed $\mathcal{H}_2/\mathcal{H}_\infty$ (CARVALHO et al., 2020a).

- In Chapter 4 we focus our effort on providing an FDF and FAC design where the network behavior was considered and adding the possibility to consider a Lur'e type non-linearity that occurs in the system. This proposition is of utmost importance since all systems are non-linear on some extent, and on some occasion, the use of linearization processes may not provide an adequate solution. Therefore, it is important to put into account those non-linear behaviors to provide a more trustworthy solution for the FDF and FAC designs. The contribution of Chapter 4 was the design of FDF for Lur'e MJS using \mathcal{H}_∞ -norm (CARVALHO; JAYAWARDHANA; COSTA, 2021).
- In Chapter 5 we changed the pace and tackled the FDF and FAC design problem from another point of view, which was achieved using the Linear Parameter Varying framework. Following a parallel idea from Chapter 3, we assumed that the LPV parameter was not directly accessible. Hence, the parameter was estimated, but we assume that the estimated parameter was not precise, meaning that the parameter was contaminated by additive noise. To add the imprecision in the parameter and still guarantee the performance, we proposed the use of the Multi-simplex technique to model an additive noise in the parameter. From the practical point of view, this idea is interesting, since it allows us to implement less sophisticated identification processes to gather the LPV parameter in real-time. The contribution in Chapter 5 were the design of Gain-Scheduled FDF and FAC for LPV systems using the \mathcal{H}_∞ -norm, \mathcal{H}_2 -norm, and Mixed $\mathcal{H}_2/\mathcal{H}_\infty$. The FDF was submitted at IEEE ACCESS and the results regarding the FAC are presented in (CARVALHO et al., 2021a).

6.2 Further Research

There are many routes that we could take after the results proposed in this thesis. Some are closer to the results presented, and others are more exciting and challenging.

- A more direct way to follow the results herein would be to design an FDF and

FAC, under the assumption that network mode is not directly accessible, and also considers that the system presents a non-linear behavior. This would be a direct association of Chapters 3, 4.

- One increment that may be possible is to derive the \mathcal{H}_∞ index LMI constraint for the MJLS under the assumption that the parameter is not directly accessible. And then design the FDF or FAC under these circumstances.
- Another possible follow-up would be the assumption that the Markov chain is not homogeneous and redraw the results presented in Chapter 2. Removing the assumption that the Markov chain is homogeneous imposes some new challenges. A possible way to deal with these new issues would be to use the framework from Chapter 2, and use the techniques from Chapter 5 to model the transition matrix with time-varying parameters. This approach is allowed under the assumptions made presented in (ABERKANE, 2012).
- Another possible path would be the transition from the model-based approach to the data-driven strategy. That would be interesting due to the fact that in some circumstances the data-driven design may be more advantageous when compared with the model-based. Those discrepancies were discussed in the first chapter of this dissertation. This could be achieved by using the approach presented in (NORTMANN; MYLVAGANAM, 2020). (NORTMANN; MYLVAGANAM, 2020) provided an approach to design LPV controller using a data-driven strategy, which can be extended to FDF and FAC design.

REFERENCES

- ABERKANE, S. Bounded real lemma for nonhomogeneous Markovian jump linear systems. **IEEE Transactions on Automatic Control**, IEEE, v. 58, n. 3, p. 797–801, 2012.
- AGULHARI, C. M.; FELIPE, A.; OLIVEIRA, R. C. L. F.; PERES, P. L. D. Algorithm 998: The Robust LMI Parser — A toolbox to construct LMI conditions for uncertain systems. **ACM Transactions on Mathematical Software**, v. 45, n. 3, p. 36:1–36:25, August 2019. (<http://rolmip.github.io>).
- ALAUDDIN, M.; KHAN, F.; IMTIAZ, S.; AHMED, S. A bibliometric review and analysis of data-driven fault detection and diagnosis methods for process systems. **Industrial & Engineering Chemistry Research**, ACS Publications, v. 57, n. 32, p. 10719–10735, 2018.
- ALHELOU, H. H.; GOLSHAN, M. H.; ASKARI-MARNANI, J. Robust sensor fault detection and isolation scheme for interconnected smart power systems in presence of rer and evs using unknown input observer. **International Journal of Electrical Power & Energy Systems**, Elsevier, v. 99, p. 682–694, 2018.
- AOUAOUDA, S.; CHADLI, M.; SHI, P.; KARIMI, H.-R. Discrete-time H_-/H_∞ sensor fault detection observer design for nonlinear systems with parameter uncertainty. **International Journal of Robust and Nonlinear Control**, Wiley Online Library, v. 25, n. 3, p. 339–361, 2015.
- BARBOSA, K. A.; SOUZA, C. E. D.; TROFINO, A. Robust $H_\infty H_2$ filtering for discrete-time uncertain linear systems using parameter-dependent lyapunov functions. In: **Proceedings of the 2002 American Control Conference**. [S.l.: s.n.], 2002. v. 4, p. 3224–3229.
- BENMOUSSA, S.; BOUAMAMA, B. O.; MERZOUKI, R. Bond graph approach for plant fault detection and isolation: Application to intelligent autonomous vehicle. **IEEE Transactions on Automation Science and Engineering**, IEEE, v. 11, n. 2, p. 585–593, 2013.
- BLANKE, M.; STAROSWIECKI, M.; WU, N. E. Concepts and methods in fault-tolerant control. In: IEEE. **2001 American Control Conference**. [S.l.], 2001. v. 4, p. 2606–2620.
- BOLCH, G.; GREINER, S.; MEER, H. D.; TRIVEDI, K. S. **Queueing networks and Markov chains: modeling and performance evaluation with computer science applications**. [S.l.]: John Wiley & Sons, 2006.
- BOYD, S.; GHAOUI, L. E.; FERON, E.; BALAKRISHNAN, V. **Linear matrix inequalities in system and control theory**. [S.l.]: SIAM, 1994.

BOYD, S. P.; VANDENBERGHE, L. **Convex optimization**. [S.l.]: Cambridge university press, 2004.

BRIAT, C. **Linear Parameter-Varying and Time-Delay Systems. Advances in Delays and Dynamics**. [S.l.]: Springer Berlin Heidelberg, 2015.

CAIGNY, J. D.; CAMINO, J. F.; OLIVEIRA, R. C.; PERES, P. L. D.; SWEVERS, J. Gain-scheduled H_2 and H_∞ control of discrete-time polytopic time-varying systems. **IET control theory & applications**, IET, v. 4, n. 3, p. 362–380, 2010.

CAIGNY, J. D.; CAMINO, J. F.; OLIVEIRA, R. C.; PERES, P. L.; SWEVERS, J. Gain-scheduled dynamic output feedback control for discrete-time LPV systems. **International Journal of Robust and Nonlinear Control**, Wiley Online Library, v. 22, n. 5, p. 535–558, 2012.

CARVALHO, L. d. P.; JAYAWARDHANA, B.; COSTA, O. L. d. V. Fault detection filter for discrete-time Markov jump Lur'e systems. **European Control Conference 2021**, v. 2, n. 1, 2021.

CARVALHO, L. D. P.; OLIVEIRA, A. M. D.; COSTA, O. L. D. V. H_2 / H_∞ simultaneous fault detection and control for Markov jump linear systems with partial observation. **IEEE Access**, IEEE, v. 8, p. 11979–11990, 2020.

CARVALHO, L. d. P.; OLIVEIRA, A. M. de; COSTA, O. L. d. V. Fault detection H_2 filter for Markov jump linear systems. **Anais do Congresso da Sociedade Brasileira de Automática**, v. 1, n. 1, 2018.

CARVALHO, L. d. P.; OLIVEIRA, A. M. de; COSTA, O. L. d. V. Robust fault detection H_∞ filter for Markovian jump linear systems. In: IEEE. **2018 European Control Conference (ECC)**. [S.l.], 2018. p. 709–714.

CARVALHO, L. d. P.; OLIVEIRA, A. M. de; COSTA, O. L. d. V. Robust fault detection H_∞ filter for Markovian jump linear systems with partial information on the jump parameter. **9th IFAC Symposium on Robust Control Design (ROCOND), Florianopolis, Brazil**, Elsevier, v. 51, n. 25, p. 202–207, 2018.

CARVALHO, L. d. P.; OLIVEIRA, A. M. de; COSTA, O. L. d. V. Asynchronous fault detection H_2 filter for Markov jump linear systems. **Anais do Congresso da Sociedade Brasileira de Automática**, v. 2, n. 1, 2020.

CARVALHO, L. d. P.; OLIVEIRA, A. Marcorin de; COSTA, O. L. d. V. Mixed fault detection filter for Markovian jump linear systems. **Mathematical Problems in Engineering**, Hindawi, 2018.

CARVALHO, L. d. P.; PALMA, J. M.; ROSA, T. E.; JAYAWARDHANA, B.; COSTA, O. L. d. V. Gain-scheduled controller for fault accommodation in linear parameter varying systems with imprecise measurements. **4th Workshop on Linear Parameter Varying Systems 2021**, v. 2, n. 1, 2021.

CARVALHO, L. d. P.; PALMA, J. M.; ROSA, T. E.; JAYAWARDHANA, B.; COSTA, O. L. d. V. Gain-scheduled fault detection filter for discrete-time LPV systems. **IEEE Access**, IEEE, 2021.

- CARVALHO, L. d. P.; ROSA, T. E.; JAYAWARDHANA, B.; COSTA, O. L. d. V. Fault accommodation controller under Markovian jump linear systems with asynchronous modes. **International Journal of Robust and Nonlinear Control**, Wiley Online Library, v. 30, n. 18, p. 8503–8520, 2020.
- CARVALHO, L. d. P.; ROSA, T. E.; JAYAWARDHANA, B.; COSTA, O. L. d. V. Fault compensation controller for Markovian jump linear systems. **21st IFAC World Congress, Berlin, Germany**, Elsevier, 2020.
- CARVALHO, L. de P.; TORIUMI, F. Y.; ANGÉLICO, B. A.; COSTA, O. L. do V. Model-based fault detection filter for Markovian jump linear systems applied to a control moment gyroscope. **European Journal of Control**, Elsevier, Vol. 59, p. 99–108, May 2021.
- CAUFFRIEZ, L.; GRONDEL, S.; LOSLEVER, P.; AUBRUN, C. Bond graph modeling for fault detection and isolation of a train door mechatronic system. **Control Engineering Practice**, Elsevier, v. 49, p. 212–224, 2016.
- CHADLI, M.; ABDO, A.; DING, S. X. H_2/H_∞ fault detection filter design for discrete-time Takagi-Sugeno fuzzy system. **Automatica**, Elsevier, v. 49, n. 7, p. 1996–2005, 2013.
- CHAMSEDDINE, A.; ZHANG, Y.; RABBATH, C.-A.; APKARIAN, J.; FULFORD, C. Model reference adaptive fault tolerant control of a quadrotor uav. In: **Infotech@Aerospace 2011**. [S.l.: s.n.], 2011. p. 1606.
- CHATTI, N.; OULD-BOUAMAMA, B.; GEHIN, A.-L.; MERZOUKI, R. Signed bond graph for multiple faults diagnosis. **Engineering Applications of Artificial Intelligence**, Elsevier, v. 36, p. 134–147, 2014.
- CHEN, J.; PATTON, J. R. Standard H_∞ filtering formulation of robust fault detection. **IFAC Proceedings Volumes**, Elsevier, v. 33, n. 11, p. 261–266, 2000.
- CHEN, J.; PATTON, R. J. **Robust model-based fault diagnosis for dynamic systems**. [S.l.]: Springer Science & Business Media, 2012. v. 3.
- CHEN, W.; SAIF, M. Fault detection and isolation based on novel unknown input observer design. In: IEEE. **2006 American Control Conference**. [S.l.], 2006. p. 6–pp.
- CHIANG, L. H.; RUSSELL, E. L.; BRAATZ, R. D. **Fault detection and diagnosis in industrial systems**. [S.l.]: Springer Science & Business Media, 2000.
- CHIBANI, A.; CHADLI, M.; SHI, P.; BRAIEK, N. B. Fuzzy fault detection filter design for T-S fuzzy systems in the finite-frequency domain. **IEEE Transactions on Fuzzy Systems**, IEEE, v. 25, n. 5, p. 1051–1061, 2016.
- COSTA, O. L. d. V.; FRAGOSO, M. D. Stability results for discrete-time linear systems with Markovian jumping parameters. **Journal of Mathematical Analysis and Applications**, Elsevier, v. 179, n. 1, p. 154–178, 1993.
- COSTA, O. L. d. V.; FRAGOSO, M. D.; MARQUES, R. P. **Discrete-time Markov jump linear systems**. [S.l.]: Springer Science & Business Media, 2006.

- COSTA, O. L. d. V.; FRAGOSO, M. D.; TODOROV, M. G. A detector-based approach for the H_2 control of Markov jump linear systems with partial information. **IEEE Transactions on Automatic Control**, IEEE, v. 60, n. 5, p. 1219–1234, 2014.
- COSTA, O. L. d. V.; FRAGOSO, M. D.; TODOROV, M. G. A detector-based approach for the H_2 control of Markov jump linear systems with partial information. **IEEE Transactions on Automatic Control**, IEEE, v. 60, n. 5, p. 1219–1234, 2015.
- COSTA, O. L. d. V.; MARQUES, R. P. Mixed H_2/H_∞ -control of discrete-time Markovian jump linear systems. **IEEE Transactions on Automatic Control**, IEEE, v. 43, n. 1, p. 95–100, 1998.
- COSTA, O. L. d. V.; VAL, J. a. B. R. D.; GEROMEL, J. C. A convex programming approach to H_2 control of discrete-time Markovian jump linear systems. **International Journal of Control**, Taylor & Francis, v. 66, n. 4, p. 557–580, 1997.
- DING, S. X. **Data-driven design of fault diagnosis and fault-tolerant control systems**. [S.l.]: Springer, 2014. v. 45.
- DING, S. X. et al. A survey of the application of basic data-driven and model-based methods in process monitoring and fault diagnosis. **IFAC Proceedings Volumes**, Elsevier, v. 44, n. 1, p. 12380–12388, 2011.
- DING, X.; GUO, L.; JEINSCH, T. A characterization of parity space and its application to robust fault detection. **IEEE Transactions on Automatic Control**, IEEE, v. 44, n. 2, p. 337–343, 1999.
- DJEZIRI, M. A.; MERZOUKI, R.; BOUAMAMA, B. O.; DAUPHIN-TANGUY, G. Robust fault diagnosis by using bond graph approach. **IEEE/ASME Transactions on Mechatronics**, IEEE, v. 12, n. 6, p. 599–611, 2007.
- Feedback Instruments Ltd. **FeedBack Coupled Tanks Control Experiments 33-041S (For use with MATLAB)**. 1. ed. Park Road, Crowborough, East Sussex, UK, 2013. Pp. 1-49.
- FIORAVANTI, A. R.; GONÇALVES, A. P. d. C.; GEROMEL, J. C. H_2 filtering of discrete-time Markov jump linear systems through linear matrix inequalities. **International Journal of Control**, Taylor & Francis, v. 81, n. 8, p. 1221–1231, 2008.
- FRAGOSO, M. D.; COSTA, O. L. d. V. A unified approach for stochastic and mean square stability of continuous-time linear systems with Markovian jumping parameters and additive disturbances. **SIAM Journal on Control and Optimization**, SIAM, v. 44, n. 4, p. 1165–1191, 2005.
- FRANK, P. M.; DING, X. Survey of robust residual generation and evaluation methods in observer-based fault detection systems. **Journal of process control**, Elsevier, v. 7, n. 6, p. 403–424, 1997.
- FRANK, S. et al. Hybrid model-based and data-driven fault detection and diagnostics for commercial buildings: Preprint. Disponível em: <https://www.osti.gov/biblio/1290794>.
- GERTLER, J. Analytical redundancy methods in fault detection and isolation-survey and synthesis. **IFAC Proceedings Volumes**, Elsevier, v. 24, n. 6, p. 9–21, 1991.

- GERTLER, J. Fault detection and isolation using parity relations. **Control Engineering Practice**, Elsevier, v. 5, n. 5, p. 653–661, 1997.
- GILBERT, E. N. Capacity of a burst-noise channel. **Bell System Technical Journal**, Wiley Online Library, v. 39, n. 5, p. 1253–1265, 1960.
- GONÇALVES, A. P. d. C.; FIORAVANTI, A. R.; GEROMEL, J. C. Markov jump linear systems and filtering through network transmitted measurements. **Signal Processing**, Elsevier, v. 90, n. 10, p. 2842–2850, 2010.
- GONÇALVES, A. P. d. C.; FIORAVANTI, A. R.; GEROMEL, J. C. Filtering of discrete-time Markov jump linear systems with uncertain transition probabilities. **International Journal of Robust and Nonlinear Control**, Wiley Online Library, v. 21, n. 6, p. 613–624, 2011.
- GONÇALVES, A. P. d. C.; FIORAVANTI, A. R.; GEROMEL, J. C. H_∞ robust and networked control of discrete-time MJLS through LMIs. **Journal of the Franklin Institute**, Elsevier, v. 349, n. 6, p. 2171–2181, 2012.
- GONZAGA, C. A. C.; COSTA, O. L. d. V. Stochastic stability for discrete-time Markov jump Lur'e systems. In: IEEE. **52nd IEEE Conference on Decision and Control**. [S.l.], 2013. p. 5993–5998.
- GONZAGA, C. A. C.; COSTA, O. L. d. V. Stochastic stabilization and induced \mathcal{L}_2 -gain for discrete-time Markov jump Lur'e systems with control saturation. **Automatica**, Elsevier, v. 50, n. 9, p. 2397–2404, 2014.
- GONZAGA, C. A. C.; JUNGERS, M.; DAAFOUZ, J. Stability analysis of discrete-time Lur'e systems. **Automatica**, Elsevier, v. 48, n. 9, p. 2277–2283, 2012.
- HAN, J.; ZHANG, H.; WANG, Y.; SUN, X. Robust fault detection for switched fuzzy systems with unknown input. **IEEE Transactions on Cybernetics**, IEEE, v. 48, n. 11, p. 3056–3066, 2017.
- HAN, K.; FENG, J. Data-driven robust fault tolerant linear quadratic preview control of discrete-time linear systems with completely unknown dynamics. **International Journal of Control**, Taylor & Francis, p. 1–11, 2019.
- ISERMANN, R.; SCHWARZ, R.; STOLZL, S. Fault-tolerant drive-by-wire systems. **IEEE Control Systems**, IEEE, v. 22, n. 5, p. 64–81, 2002.
- JAYAWARDHANA, B.; LOGEMANN, H.; RYAN, E. P. The circle criterion and input-to-state stability. **IEEE Control Systems Magazine**, IEEE, v. 31, n. 4, p. 32–67, 2011.
- JR, G. S.; ADELI, H. System identification in structural engineering. **Scientia Iranica**, Elsevier, v. 19, n. 6, p. 1355–1364, 2012.
- KHALIL, H. K. **Nonlinear systems**. [S.l.]: Prentice Hall Upper Saddle River, NJ, 2002. v. 3.
- KIM, Y.-M. Robust data driven H_∞ control for wind turbine. **Journal of the Franklin Institute**, Elsevier, v. 353, n. 13, p. 3104–3117, 2016.

- KOURTI, T.; NOMIKOS, P.; MACGREGOR, J. F. Analysis, monitoring and fault diagnosis of batch processes using multiblock and multiway pls. **Journal of process control**, Elsevier, v. 5, n. 4, p. 277–284, 1995.
- KULCSÁR, B.; DONG, J.; VERHAEGEN, M. Model-free fault tolerant control approach for linear parameter varying system. **IFAC Proceedings Volumes**, Elsevier, v. 42, n. 8, p. 876–881, 2009.
- LACERDA, M. J.; TOGNETTI, E. S.; OLIVEIRA, R. C.; PERES, P. L. A new approach to handle additive and multiplicative uncertainties in the measurement for LPV filtering. **International Journal of Systems Science**, Taylor & Francis, v. 47, n. 5, p. 1042–1053, 2016.
- LI, X.; KARIMI, H. R.; WANG, Y.; LU, D.; GUO, S. Robust fault estimation and fault-tolerant control for markovian jump systems with general uncertain transition rates. **Journal of the Franklin Institute**, Elsevier, v. 355, n. 8, p. 3508–3540, 2018.
- LOFBERG, J. Yalmip: A toolbox for modeling and optimization in matlab. In: IEEE. **2004 IEEE international conference on robotics and automation (IEEE Cat. No. 04CH37508)**. [S.l.], 2004. p. 284–289.
- LUO, Z.; FANG, H. Fault detection for nonlinear systems with unknown input. **Asian Journal of Control**, Wiley Online Library, v. 15, n. 5, p. 1503–1509, 2013.
- MARZAT, J.; PIET-LAHANIER, H.; DAMONGEOT, F.; WALTER, E. Model-based fault diagnosis for aerospace systems: a survey. **Proceedings of the Institution of Mechanical Engineers, Part G: Journal of aerospace engineering**, SAGE Publications Sage UK: London, England, v. 226, n. 10, p. 1329–1360, 2012.
- MONTAGNER, V.; OLIVEIRA, R. C. L. F.; LEITE, V.; PERES, P. L. D. LMI approach for H_∞ linear parameter-varying state feedback control. **IEE Proceedings-Control Theory and Applications**, IET, v. 152, n. 2, p. 195–201, 2005.
- MONTGOMERY, D. C. **Introduction to statistical quality control**. [S.l.]: John Wiley & Sons, 2007.
- NGUYEN, M. Q.; SENAME, O.; DUGARD, L. An LPV fault tolerant control for semi-active suspension-scheduled by fault estimation. **IFAC-PapersOnLine**, Elsevier, v. 48, n. 21, p. 42–47, 2015.
- NIEMANN, H.; STOUSTRUP, J. Fault diagnosis for non-minimum phase systems using H_∞ optimization. In: IEEE. **American Control Conference, 2001. Proceedings of the 2001**. [S.l.], 2001. v. 6, p. 4432–4436.
- NIIJJAAWAN, N.; NIIJJAAWAN, R. **Modern approach to maintenance in spinning**. [S.l.]: Woodhead Publishing Limited, 2010.
- NORTMANN, B.; MYLVAGANAM, T. Data-Driven control of linear time-varying systems. In: IEEE. **2020 59th IEEE Conference on Decision and Control (CDC)**. [S.l.], 2020. p. 3939–3944.

- ODENDAAL, H. M.; JONES, T. Actuator fault detection and isolation: An optimised parity space approach. **Control Engineering Practice**, Elsevier, v. 26, p. 222–232, 2014.
- OLIVEIRA, A. M. de; COSTA, O. L. d. V. H_2 filtering for discrete-time hidden Markov jump systems. **International Journal of Control**, Taylor & Francis, v. 90, n. 3, p. 599–615, 2017.
- OLIVEIRA, A. M. de; COSTA, O. L. d. V. H_∞ -filtering for Markov jump linear systems with partial information on the jump parameter. **IFAC Journal of Systems and Control**, Elsevier, 2017.
- OLIVEIRA, A. M. de; COSTA, O. L. d. V. Mixed H_2 H_∞ control of hidden Markov jump systems. **International Journal of Robust and Nonlinear Control**, Wiley Online Library, v. 28, n. 4, p. 1261–1280, 2018.
- OLIVEIRA, A. M. de; COSTA, O. L. d. V. An iterative approach for the discrete-time dynamic control of Markov jump linear systems with partial information. **International Journal of Robust and Nonlinear Control**, Wiley Online Library, v. 30, n. 2, p. 495–511, 2020.
- OLIVEIRA, M. C. de; BERNUSSOU, J.; GEROMEL, J. C. A new discrete-time robust stability condition. **Systems & control letters**, Elsevier, v. 37, n. 4, p. 261–265, 1999.
- OLIVEIRA, M. C. de; SKELTON, R. E. Stability tests for constrained linear systems. In: **Perspectives in robust control**. [S.l.]: Springer, 2001. p. 241–257.
- OLIVEIRA, R. C.; BLIMAN, P.-A.; PERES, P. L. Robust LMIs with parameters in multi-simplex: Existence of solutions and applications. In: IEEE. **2008 47th IEEE Conference on Decision and Control, Cancun, Mexico**. [S.l.], 2008. p. 2226–2231.
- ÖREG, Z.; SHIN, H.-S.; TSOURDOS, A. Model identification adaptive control-implementation case studies for a high manoeuvrability aircraft. In: IEEE. **2019 27th Mediterranean Conference on Control and Automation (MED)**. [S.l.], 2019. p. 559–564.
- PALMA, J. M.; MORAIS, C. F.; OLIVEIRA, R. C. L. F. \mathcal{H}_2 gain-scheduled filtering for discrete-time LPV systems using estimated time-varying parameters. In: **Proceedings of the 2018 American Control Conference**. Milwaukee WI, USA: [s.n.], 2018. p. 4367–4372. ISSN 2378-5861.
- PATTON, R. J. Fault-tolerant control: the 1997 situation. **IFAC Fault Detection, Supervision and Safety for Technical Processes, Kingston Upon Hull, UK**, Elsevier, v. 30, n. 18, p. 1029–1051, 1997.
- PATTON, R. J.; CHEN, J. Review of parity space approaches to fault diagnosis for aerospace systems. **Journal of Guidance, Control, and Dynamics**, v. 17, n. 2, p. 278–285, 1994.
- PATTON, R. J.; CHEN, J. Observer-based fault detection and isolation: Robustness and applications. **Control Engineering Practice**, Elsevier, v. 5, n. 5, p. 671–682, 1997.

- PATTON, R. J.; FRANK, P. M.; CLARK, R. N. **Issues of fault diagnosis for dynamic systems**. [S.l.]: Springer Science & Business Media, 2013.
- PAULO, S. D. **Adaptive filtering: algorithms and practical implementation**. [S.l.]: Springer US, 2013.
- PAYA, B.; ESAT, I.; BADI, M. Artificial neural network based fault diagnostics of rotating machinery using wavelet transforms as a preprocessor. **Mechanical systems and signal processing**, Elsevier, v. 11, n. 5, p. 751–765, 1997.
- POTTER, J.; SUMAN, M. **Thresholdless redundancy management with arrays of skewed instruments**. [S.l.: s.n.], 1977.
- RAMBEAUX, F.; HAMELIN, F.; SAUTER, D. Robust residual generation via lmi. **IFAC Proceedings Volumes**, Elsevier, v. 32, n. 2, p. 7920–7925, 1999.
- RICHARD, H. A.; SANDER, M. **Fatigue crack growth**. [S.l.]: Springer, 2016.
- ROSA, T. E.; MORAIS, C. F.; OLIVEIRA, R. C. L. F. New robust LMI synthesis conditions for mixed gain-scheduled reduced-order DOF control of discrete-time LPV systems. **International Journal of Robust and Nonlinear Control**, Wiley Online Library, v. 28, n. 18, p. 6122–6145, 2018.
- ROSS, S. M. **Introduction to Probability Models**. [S.l.]: Academic press, 2014.
- ROTONDO, D. **Advances in gain-scheduling and fault tolerant control techniques**. [S.l.]: Springer, 2017.
- SAMANTA, B.; AL-BALUSHI, K.; AL-ARAIMI, S. Artificial neural networks and support vector machines with genetic algorithm for bearing fault detection. **Engineering applications of artificial intelligence**, Elsevier, v. 16, n. 7-8, p. 657–665, 2003.
- SAMANTARAY, A. K.; MEDJAHHER, K.; BOUAMAMA, B. O.; STAROSWIECKI, M.; DAUPHIN-TANGUY, G. Diagnostic bond graphs for online fault detection and isolation. **Simulation Modelling Practice and Theory**, Elsevier, v. 14, n. 3, p. 237–262, 2006.
- SAYED, A. H. **Adaptive filters**. [S.l.]: John Wiley & Sons, 2011.
- SCHWABACHER, M. A survey of data-driven prognostics. In: **Infotech@ Aerospace**. [S.l.: s.n.], 2005. p. 7002.
- SEILER, P.; SENGUPTA, R. A bounded real lemma for jump systems. **IEEE Transactions on Automatic Control**, IEEE, v. 48, n. 9, p. 1651–1654, 2003.
- SHEWHART, W. A. **Economic control of quality of manufactured product**. [S.l.]: Macmillan And Co Ltd, London, 1931.
- SIMON, E.; R-AYERBE, P.; STOICA, C.; DUMUR, D.; WERTZ, V. LMIs-based coordinate descent method for solving BMIs in control design. **IFAC Proceedings Volumes**, Elsevier, v. 44, n. 1, p. 10180–10186, 2011.
- SOUZA, C. E. de; BARBOSA, K. A.; NETO, A. T. Robust H_∞ filtering for discrete-time linear systems with uncertain time-varying parameters. **IEEE Transactions on Signal processing**, IEEE, v. 54, n. 6, p. 2110–2118, 2006.

SRINIVASAN, K.; DUTTA, P.; TAVAKOLI, A.; LEVIS, P. Understanding the causes of packet delivery success and failure in dense wireless sensor networks. In: **Proceedings of the 4th international conference on Embedded networked sensor systems**. [S.l.: s.n.], 2006. p. 419–420.

TIDRIRI, K.; CHATTI, N.; VERRON, S.; TIPLICA, T. Bridging data-driven and model-based approaches for process fault diagnosis and health monitoring: A review of researches and future challenges. **Annual Reviews in Control**, Elsevier, v. 42, p. 63–81, 2016.

TODOROV, M. G.; FRAGOSO, M. D.; COSTA, O. L. d. V. Detector-based H_∞ results for discrete-time Markov jump linear systems with partial observations. **Automatica**, Elsevier, v. 91, p. 159–172, 2018.

TOHIDI, S. S.; SEDIGH, A. K.; BUZORGNIA, D. Fault tolerant control design using adaptive control allocation based on the pseudo inverse along the null space. **International Journal of Robust and Nonlinear Control**, Wiley Online Library, v. 26, n. 16, p. 3541–3557, 2016.

VENKATASUBRAMANIAN, V.; RENGASWAMY, R.; KAVURI, S. N. A review of process fault detection and diagnosis: Part ii: Qualitative models and search strategies. **Computers & chemical engineering**, Elsevier, v. 27, n. 3, p. 313–326, 2003.

VENKATASUBRAMANIAN, V.; RENGASWAMY, R.; KAVURI, S. N.; YIN, K. A review of process fault detection and diagnosis: Part iii: Process history based methods. **Computers & chemical engineering**, Elsevier, v. 27, n. 3, p. 327–346, 2003.

VENKATASUBRAMANIAN, V.; RENGASWAMY, R.; YIN, K.; KAVURI, S. N. A review of process fault detection and diagnosis: Part i: Quantitative model-based methods. **Computers & chemical engineering**, Elsevier, v. 27, n. 3, p. 293–311, 2003.

VERRON, S.; LI, J.; TIPLICA, T. Fault detection and isolation of faults in a multivariate process with bayesian network. **Journal of Process Control**, Elsevier, v. 20, n. 8, p. 902–911, 2010.

WANG, J.-S.; YANG, G.-H. Data-driven output-feedback fault-tolerant control for unknown dynamic systems with faults changing system dynamics. **Journal of Process Control**, Elsevier, v. 43, p. 10–23, 2016.

WANG, Y.; ZEMOUCHE, A.; RAJAMANI, R. A sequential LMI approach to design a BMI-based multi-objective nonlinear observer. **European Journal of Control**, Elsevier, v. 44, p. 50–57, 2018.

WOLD, S.; ESBENSEN, K.; GELADI, P. Principal component analysis. **Chemometrics and Intelligent Laboratory Systems**, Elsevier, v. 2, n. 1-3, p. 37–52, 1987.

YAN, S.; NGUANG, S. K.; SHEN, M.; ZHANG, G. Event-triggered H_∞ control of networked control systems with distributed transmission delay. **IEEE Transactions on Automatic Control**, IEEE, v. 65, n. 11, p. 495–511, Nov 2019.

YU, J.; RASHID, M. M. A novel dynamic bayesian network-based networked process monitoring approach for fault detection, propagation identification, and root cause diagnosis. **AIChE Journal**, Wiley Online Library, v. 59, n. 7, p. 2348–2365, 2013.

ZAREI, J.; SHOKRI, E. Robust sensor fault detection based on nonlinear unknown input observer. **Measurement**, Elsevier, v. 48, p. 355–367, 2014.

ZHANG, X.; PARISINI, T.; POLYCARPOU, M. M. Adaptive fault-tolerant control of nonlinear uncertain systems: an information-based diagnostic approach. **IEEE Transactions on Automatic Control**, IEEE, v. 49, n. 8, p. 1259–1274, 2004.

ZHANG, Z. Comparison of data-driven and model based methodologies of wind turbine fault detection with scada data. **European Wind Energy Association**, March, 2014.

ZHONG, M.; DING, S. X.; LAM, J.; WANG, H. An LMI approach to design robust fault detection filter for uncertain LTI systems. **Automatica**, Elsevier, v. 39, n. 3, p. 543–550, 2003.

ZHONG, M.; XUE, T.; DING, S. X. A survey on model-based fault diagnosis for linear discrete time-varying systems. **Neurocomputing**, Elsevier, v. 306, p. 51–60, 2018.

ZHONG, M.; YE, H.; SHI, P.; WANG, G. Fault detection for Markovian jump systems. **IET Proceedings-Control Theory and Applications**, IET, v. 152, n. 4, p. 397–402, 2005.

APPENDIX A – NUMERICAL EXAMPLES MODELING AND BASIC RESULTS

Here, we briefly explain and provide the necessary references of the models employed in the simulations throughout this thesis.

A.1 Coupled tank model

The model using in the majority of the examples in the thesis was the coupled tank model, since it is a good benchmark model to test the viability of the approaches, (Feedback Instruments Ltd., 2013). We borrowed the numerical values from the specific educational system. A diagram that represents the structure of the system is presented below, We can describe the dynamic of this system by writing an equation that denotes

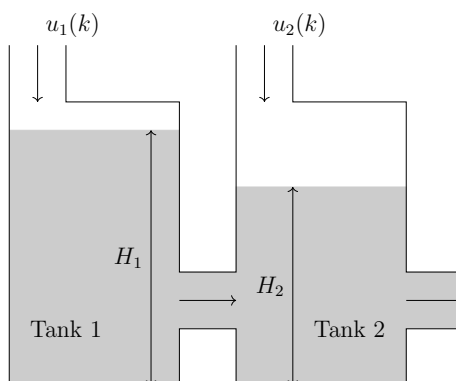


Figure 43: Coupled tank model.

the sum of inputs and output flows on each tank. The height of each tank is determined by the sum of flows which rules the volume on each tank.

$$\sum_{i=1}^p Q_{in_i}(t) - \sum_{j=1}^l Q_{out_j}(t) = A_{cs} \frac{\partial H(t)}{\partial t} \quad (\text{A.1})$$

where A_{cs} represents the area of tanks cross section. The flow output can be written as

$$Q_{out_j}(t) = \alpha\sqrt{2gH(t)} \quad (\text{A.2})$$

where α represent the cross section of the output pipe or the interconnection pipe. Hence, the non-linear system that models the dynamics is

$$\frac{\partial H(t)}{\partial t} = \frac{1}{A_{cs}} \sum_{i=1}^p Q_{in_i}(t) - \frac{1}{A_{cs}} \left(\sum_{j=1}^l \alpha \right) \sqrt{2gH(t)} \quad (\text{A.3})$$

Obtaining the LTI model using Taylor series, considering that the non-linear system is at an equilibrium point. Assuming a specific value of H_0 and Q_{in_0} allow us to write

$$\frac{\partial \hat{H}(t)}{\partial t} = \chi \hat{H}(t) + \Xi \hat{Q}_{in}(t) \quad (\text{A.4})$$

$$\frac{\overbrace{H(t) - H_0}^{\hat{H}(t)}}}{\partial t} = \underbrace{\frac{-\alpha q}{A_{cs}\sqrt{2gH_0}}}_{\chi} \underbrace{(H(t) - H_0)}_{\hat{H}(t)} + \underbrace{\frac{1}{A_{cs}}}_{\Xi} \underbrace{(Q_{in(t)} - Q_{in_0})}_{\hat{Q}_{in}(t)} \quad (\text{A.5})$$

Now considering both tanks, one can write the dynamic equations as

$$\frac{\partial \hat{H}^1(t)}{\partial t} = \frac{Q_{in_1}^1(t)}{A_{cs}} - \frac{\alpha\sqrt{\sqrt{2gH^1(t)}}}{A_{cs}} - \frac{\alpha\sqrt{\sqrt{2g(H^1(t) - H^2(t))}}}{A_{cs}} \quad (\text{A.6})$$

$$\frac{\partial \hat{H}^2(t)}{\partial t} = \frac{Q_{in_2}^1(t)}{A_{cs}} - \frac{\alpha\sqrt{\sqrt{2gH^2(t)}}}{A_{cs}} + \frac{\alpha\sqrt{\sqrt{2g(H^1(t) - H^2(t))}}}{A_{cs}} \quad (\text{A.7})$$

$$(\text{A.8})$$

Considering the state vector as $\bar{H}(t) = [H^1(t) \ H^2(t)]'$. The LTI dynamic matrix A is acquired as

$$A = \frac{1}{A_{cs}} \begin{bmatrix} \frac{\alpha g}{\sqrt{2gH_0^1}} - \frac{\alpha g}{\sqrt{2gH_0^1 - H_0^2}} & -\frac{\alpha g}{\sqrt{2gH_0^1 - H_0^2}} \\ \frac{\alpha g}{\sqrt{2gH_0^1 - H_0^2}} & \frac{\alpha g}{\sqrt{2gH_0^2}} - \frac{\alpha g}{\sqrt{2gH_0^1 - H_0^2}} \end{bmatrix}. \quad (\text{A.9})$$

Now, the parameter values from the educational kit (Feedback Instruments Ltd., 2013) are presented in Table 1.

For the last step, we used a zero order holder with sampling time of 0.05s. The discrete time domain state space model obtained is

$$A = \begin{bmatrix} -0.0239 & -0.0127 \\ 0.0127 & -0.0285 \end{bmatrix} \quad (\text{A.10})$$

g	m/s^2	Gravitational acceleration	9.8
A_{cs}	m^2	Tank cross section area	0.40
α	m^2	Interconnection pipe cross section area	0.01
H_0^1	m^2	height initial condition for the first tank	0.16
H_0^2	m^2	height initial condition for the second tank	0.22

Table 1: Numerical parameter of the coupled tank model.

A.2 Mass-Spring System

For the approaches that consider Markov Jump Lur'e systems a more appropriate example is the mass-spring system from (KHALIL, 2002). A representation of this model is given by Fig. 44 We can write the equation that represents the dynamic of the system

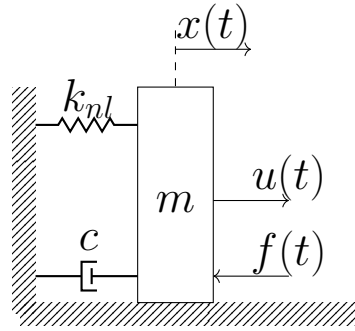


Figure 44: Mass-Spring model, (KHALIL, 2002).

as

$$\ddot{x}(t) + \frac{c}{m}\dot{x}(t) + \frac{k}{m}x(t) + \frac{ka^2}{m}x^3(t) = \frac{u(t)}{m}w(t). \quad (\text{A.11})$$

The parameter descriptions and values are presented in table 2.

m	kg	Block Mass	12
c	Ns/m	Dumper viscous friction coefficient	0.1
k	N/m	Spring elasticity coefficient	0.2
ka^2		Spring non-linear elasticity coefficient	0.9

Table 2: Numerical parameter of the Spring-Mass model.

We can rewrite the equation in the space-state form as,

$$A = \begin{bmatrix} 0 & 1 \\ -\frac{k}{m} & -\frac{c}{m} \end{bmatrix}, \quad G = \begin{bmatrix} 0 \\ \frac{ka^2}{m} \end{bmatrix} \quad (\text{A.12})$$

Using the zero-order holder with a sampling time equal to 5ms, the matrices that

compose the state space system in the discrete time domain are given by,

$$A = \begin{bmatrix} -0.0101 & 0.9588 \\ -0.0160 & -0.0181 \end{bmatrix}, \quad B = \begin{bmatrix} 62.0699 \\ -0.0513 \end{bmatrix}, \quad G = \begin{bmatrix} 0 \\ 0.15 \end{bmatrix}, \quad (\text{A.13})$$

This particular model was used only in the examples in Chapter 4.

A.3 Quarter vehicle

We here use as a numerical example a simple quarter vehicle extracted from (NGUYEN; SENAME; DUGARD, 2015), which represents a quarter vehicle body using a sprung mass (m_s), the wheel and tire are denoted by the unsprung mass (m_{us}). Those components are connected by a spring with a stiffness coefficient k_s , and a semi-active damper. The coefficient k_1 represents the tire stiffness. The states vector for the linearized model is

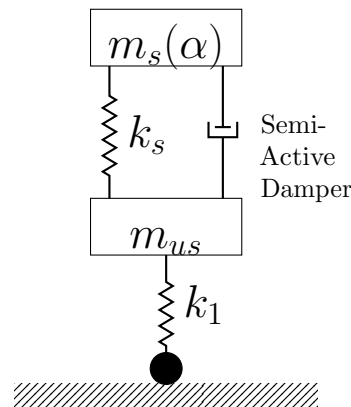


Figure 45: Quarter vehicle model.

$x(k) = [z_s \dot{z}_s z_{us} \dot{z}_{us}]$, which represent the displacement for the sprung mass, its variation, the displacement for the mass unsprung, and its variation. Therefore, the space-state matrices are,

$$A_c = \begin{bmatrix} 0 & 1 & 0 & 0 \\ -\frac{k_s}{m_s(\alpha_k)} & \frac{c_0}{m_s(\alpha_k)} & \frac{k_s}{m_s(\alpha_k)} & \frac{c_0}{m_s(\alpha_k)} \\ 0 & 0 & 0 & 1 \\ \frac{k_s}{m_{us}} & \frac{c_0}{m_{us}} & -\frac{k_s+k_1}{m_{us}} & -\frac{c_0}{m_{us}} \end{bmatrix}, \quad J = \begin{bmatrix} 0 \\ 0 \\ 0 \\ \frac{k_s}{m_{us}} \end{bmatrix},$$

$$B_c = \begin{bmatrix} 0 \\ -\frac{1}{m_s(\alpha_k)} \\ 0 \\ \frac{k_s}{m_{us}} \end{bmatrix}, \quad F = \begin{bmatrix} 0 \\ -\frac{1}{m_s(\alpha_k)} \\ 0 \\ \frac{k_s}{m_{us}} \end{bmatrix}, \quad C = \begin{bmatrix} 1 & 0 \\ 0 & 0 \\ 0 & 1 \\ 0 & 0 \end{bmatrix},$$

$$D_d = 0.01^{2 \times 1}, \quad E_z = 0.01^{2 \times 1}, \quad D_f = 0, \quad \alpha(k) = [-0.050.05].$$

where $m_{us} = 37.5$ denotes the unsprung mass, $k_s = 29500$ represents the stiffness of the semi-damper, $k_1 = 210000$ denotes the stiffness of the tires, and $c_0 = 2850$ damping

coefficient for the semi-damper. The Linear parameter varying in this model will be m_s the sprung mass, which vary linearly between $m_s = [315 \ 285]$. This variation represents a fast decrease in the sprung mass of the vehicle. The discretization time is $T = 0.025\text{s}$.

A.4 Network Packet Loss Modeling

As explained throughout the thesis, one of the main advantages provided by the MJLS framework is the capability of modeling the network packet loss in the network. This procedure is made by setting the transition probability matrix with appropriate structure and values that represent the network behavior. The first step in the network packet loss modeling is the definition of the transition matrix. Firstly, we need to define the amount modes of the system, to simplify the explanation here, we will consider only two modes a nominal mode, and the packet loss mode, by consequence, the transition matrix will be a 2×2 matrix. Another aspect during the definition of the transition matrix is the type of Markov chain that will be implemented. There are plenty of Markov chains that can be used to model a network, each one has its advantages and disadvantages, a few examples Bernoulli model (ROSS, 2014), Gilbert-Elliot model (GILBERT, 1960). A Bernoulli MC is the simplest case of an MC, using this type of MC to model a network will ignore some key behaviors in a network since it only describes a series of Bernoulli trials. To describe some additional behaviors, as the burst communication loss, we can use the Gilbert-Elliot model (GILBERT, 1960). The other part of this procedure is to describe where the packet

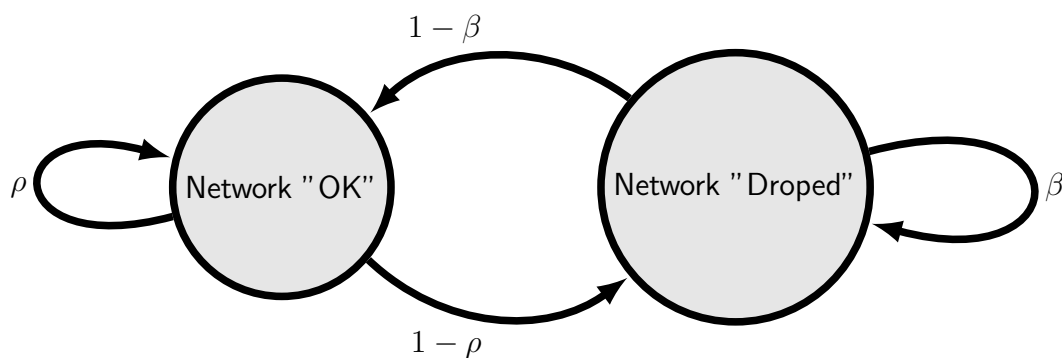


Figure 46: Diagram of the Markov chain for the Gilbert-Elliot model, for the Bernoulli model the variables ρ and β are equal.

loss occurs on the control loop, that is, in the communication between controller and actuator, or between the controller and sensor, or even both cases. What determines the packet loss placement in the control loop is the matrices that switches according to the Markov chain. To model the packet loss between controller and sensor, the matrices that

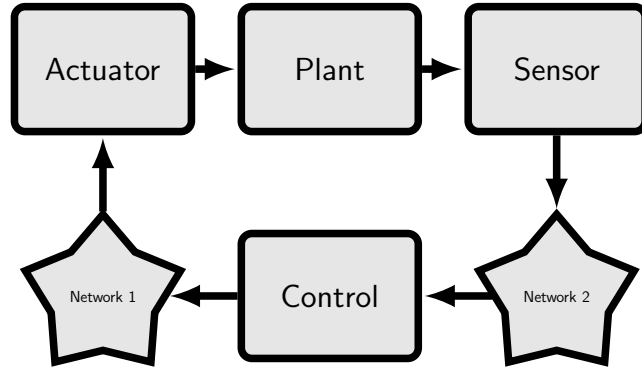


Figure 47: Control loop example.

should switch are C_i , D_i . For the packet loss in the communication between actuator and controller, the matrix is B_i . Regarding the case where we consider all the packet losses, all matrices C_i , D_i , and B_i should switch according to the Markov chain. For the case where all packet losses are considered the transition probability matrix implemented is a Kronecker product of the transition probability matrix from the other two cases, leading to an increased number of modes in the resulting Markov chain.

A.5 Schur Complement

Lemma 11. *The LMI, with the symmetric matrices X e Z*

$$\begin{bmatrix} X & Y' \\ Y & Z \end{bmatrix} > 0 \quad (\text{A.14})$$

holds if and only if the following statements are true

- $\{Z > 0, \quad X > Y'Z^{-1}Y\}$
- $\{X > 0, \quad Z > YX^{-1}Y'\}$

Proof: For the rough sketch of the proof for the necessity, we assume that the statements above are true, hence

$$Q = \begin{bmatrix} X - Y'Z^{-1}Y & 0 \\ 0 & Z \end{bmatrix} > 0 \quad (\text{A.15})$$

defining the non-singular matrix T as

$$T = \begin{bmatrix} I & Y'Z^{-1} \\ 0 & I \end{bmatrix} \quad (\text{A.16})$$

by consequence we get that $TQT' > 0$, since $Q > 0$. This implies that

$$TQT' = \begin{bmatrix} X & Y' \\ Y & Z \end{bmatrix} > 0 \quad (\text{A.17})$$

A detailed discussion about the proof and applications can be obtained in (BOYD; VANDENBERGHE, 2004).

A.6 Bounded Real Lemma

Suppose system

$$G : \begin{cases} x(k+1) = Ax(k) + Bw(k), \\ y(k) = Cx(k) + Dw(k), \end{cases} \quad (\text{A.18})$$

where $w(k) \in \mathbb{R}^m$ represents the exogenous input, and $y(k) \in \mathbb{R}^p$ is the measured output. We can get the \mathcal{H}_∞ norm, considering the Lyapunov function $v(k) = x(k)'Px(k)$, and imposing

$$x(k+1)'Px(k+1) - x(k)Px(k) + y(k)'y(k) - \gamma^2 w(k)w(k) < 0 \quad (\text{A.19})$$

$$\begin{bmatrix} x(k) \\ w(k) \end{bmatrix}' \begin{bmatrix} A'PA - P + C'C & A'PB + C'D \\ B'PA + D'C & B'PB + D'D - \gamma^2 I \end{bmatrix} \begin{bmatrix} x(k) \\ w(k) \end{bmatrix} < 0 \quad (\text{A.20})$$

Matrix A is asymptotically stable and $\|G\|_\infty < \gamma$ if and only if there exists a symmetric matrix $P > 0$ such that

$$\begin{bmatrix} A'PA - P + C'C & A'PB + C'D \\ B'PA + D'C & B'PB + D'D - \gamma^2 I \end{bmatrix} < 0. \quad (\text{A.21})$$

A.7 Finsler Lemma

Considering $w \in \mathbb{R}^n$, $\mathcal{L} \in \mathbb{R}^{n \times n}$ and $\mathcal{B} \in \mathbb{R}^{m \times n}$ with the rank $(\mathcal{B}) < n$ and \mathcal{B}_\perp is a base for a null space, that it $\mathcal{B}\mathcal{B}_\perp = 0$. Therefore, the following statements are equivalent:

- $w'\mathcal{L}w < 0, \forall w \neq 0 : \mathcal{B}w = 0$
- $\mathcal{B}'_\perp \mathcal{L} \mathcal{B}_\perp < 0$
- $\exists \mu \in \mathbb{R} : \mathcal{L} - \mu \mathcal{B}'\mathcal{B} < 0$
- $\exists \mathcal{X} \in \mathbb{R}^{n \times m} : \mathcal{L} + \mathcal{X}\mathcal{B} + \mathcal{B}'\mathcal{X}' < 0$

The proof can be seen in (BOYD et al., 1994; OLIVEIRA; SKELTON, 2001).